CONTENTS

To study the effect of adding Al_2O_3 nanoparticles on the mechanical properties and microstructure of cement mortar

M. R. Arefi [1,*], M. R. Javeri [1], E. Mollaahmadi[1]

[1.] Department of Civil Engineering, Taft Branch, Islamic Azad University, Taft, Iran
[*] arefi@taftiau.ac.ir

Abstract: In this work, research has been done on the compressive, tensile and flexural strength of cement mortar containing Al_2O_3 nanoparticles in the amounts of 1, 3 and 5 percent by weight of cement. The results show that the mechanical properties of samples containing 1 and 3 percent Al_2O_3 nanoparticles are desirable then the ordinary cement mortar. But by increasing Al_2O_3 nanoparticles to 5 percent, the mechanical properties reduce severely. SEM study about the microstructure of cement mortar containing nanoparticles and ordinary cement mortar showed that Al_2O_3 nanoparticles reduces the $CaOH_2$ crystals and fills the pores and increases the density of cement mortar.
[M. R. Arefi, M. R. Javeri, E. Mollaahmadi. **To study the effect of adding Al_2O_3 nanoparticles on the mechanical properties and microstructure of cement mortar**. Life Science Journal. 2011;8(4):613-617] (ISSN:1097-8135). http://www.lifesciencesite.com.

Keywords: Mechanical properties; Al_2O_3 nanoparticles; cement mortar; SEM, microstructure

1. Introduction

By using extensively mineral addition for the improve performance of cement-based materials. Partial replacement of cement with mineral additions improves the performance cement-based materials in fresh and hardened states. In the recent years, using nanoparticles has developed due to its small size possess unique properties such as high specific surface area and high activity. Several reports are present about adding nanoparticles to cement materials, that most of them have focus on the silica nanoparticles.

Ye Qing et al, have shown that adding SiO_2 nanoparticles to hardened cement paste increases the compressive strength and bond strength of paste-aggregate interface more than silica fume addition which means because of SiO_2 nanoparticles due to high specific surface and amount of atoms in the surface has higher chemical reaction area [1].

Wang Baomin and et al showed that adding SiO_2 nanoparticles can improve the microstructure of the cement and result in the increase of freezing resistance with high performance concrete [2].

Mohammad Reza Arefi and et al, have studied the effect of adding SiO_2 particles with different diameters and different amount to the cement mortar. The research results showed that nanoparticles due to higher specific surface area improve the resistance properties and water permeability of cement mortar than the micro-particles. Then, samples consisting nanoparticles, samples with nano-silica large diameters have better effect in improving the mechanical properties. And because of the possibility of increase agglomeration of nanoparticles is more with smaller diameter [3].

Study has been conducted with focus on comparison effect of adding different nanoparticles. For example, study which has compared the addition of TiO_2 nanoparticles with SiO_2, the result shows that the abrasion resistance and flexural fatigue performance of concrete containing TiO_2 nanoparticles is more than the abrasion resistance of concrete containing the same amount of SiO_2 nanoparticles [4, 5]. Also, improving of resistance to chloride penetration for the concrete containing TiO_2 is more than the concrete containing the same amount of SiO_2 [6].

There exists report about the addition of Al_2O_3 nanoparticles to cement-based materials. Ali Nazeri and et al have researched the effect of addition Al_2O_3 nanoparticles with mechanical properties and percentage of water absorbtion of concrete which is cured in water and saturated limewater. Their research results showed that by addition of nanoparticles till two percent improves the mechanical properties and concrete penetration that the amount of this improvement for the sample is more which have cured in limewater [7, 10].

The aim of this study is to research the effect of adding Al_2O_3 nanoparticles to cement mortar and to find optimized percentage of adding nanoparticles and also finding mechanism to improve the mechanical properties of cement mortar.

2. Material and Methods

2.1. Materials and mixture proportions

ASTM C 150 [11] Type II portland cement was used. The Al_2O_3 nanoparticles with average particles size of 20 nm which were purchased from Skyspring Nanomaterials Inc were used. The characteristics of the Al_2O_3 nanoparticles were shown

in Table 1. The superplasticizer (a commercial sulphonated melamine formaldehyde polymer) with relative density of 1.15 was employed to achieve good workability. The content was adjusted for each mixture to ensure that no segregation would occur. Also, the distilled water was used for preparing all mixtures. The fine aggregate was crushed silica sand with a fineness modulus of 2.4, the apparent density of 3.33 gr/cm^3. The sand was graded according to ASTM C33 [12] standard. The largest diameter of these aggregate particles was 4.75mm.

Table 1. Characteristics of nano- Al_2O_3particles

Average particle size	Specific surface area (m^2/g)	Density (g/cm^2)	Purity (%)
20nm	200	0.9	99.9%

The proportions of the mixtures were presented in table 2. The ratio of the water to binder (the cement and Al_2O_3 nanoparticles) was chosen 0.42. In this study the mixtures were prepared with the cement replacement of 1%, 3% and 5% by weight of binder.

Table 2: Mix proportion of samples

Mixture type	Water	Cement	Sand	Nano-Al_2O_3	*SP
*CO	150	360	1800	-	-
1NA	150	356.4	1800	3.6	3.68
3NA	150	349.2	1800	10.8	4.29
5NA	150	342	1800	18	4.9

*CO: Control.
*SP: superplasticizer

2-2- Sample preparation

The high homogenous dispersion of nanoparticles strongly depends on stable suspension preparation. Hence Al_2O_3 nano powder was mixed with the distilled water and stirred for 6-10 hours by rotational speed of 250-300 rpm. At first, the suspension of the Al_2O_3 nanoparticles and the superplasticizer were mixed in the mixer for 30 second, where the cement was added to this mixture simultaneously. Thereafter, the sand, from finest to coarsest, was added gradually to the mixture, and the mixing continued until the complete homogenization of the mixture. Then, the mortar was poured into the standard mold. For tensile test, the briquette specimens with 75×25×25 mm dimension were utilized. The mortar was poured in two layers, both of them compressed by 4 impacts of a steel rod. In order to prepare the specimens of the compressive tests, the mortar was poured into molds to form cubes of size 50×50×50 mm in three layers alternatively, which all layers compressed by 10 impacts of a steel rod. For the flexural test, the mortar was poured into the molds with dimensions of 40×40×160 mm in two layers. Each layer was compacted by 15 impacts of a steel rod. The molded specimens were covered with a plastic layer for 24 hours and then were cured in water at the room temperature up to end of the seventh day. Six specimens were prepared for each test and the average result was reported.

2-3 Test methods

The apparatus made by ELE Company, England was used for performing the mechanical tests. The microstructure of the specimens was studied by the scanning electron microscopy (SEM) Hitachi S-4160. Compressive tests were carried out according to the ASTM C109 [13] and tensile tests were carried out according to the ASTM C190 [14]. Flexural tests were carried out according to ASTM C348 [15].

3. Results and Discussion

3.1. Mechanical properties

Results of compressive strength, tensile strength after curing for seven days is shown in table 3 and figure 1. It can be understood from the table that by adding Al_2O_3 nanoparticles till 3 percent compressive, tensile and flexural strength increases and then by increasing the quantity of nanoparticles to 5 percent, strength reduces less than the ordinary cement mortar. This may be due to the fact that the quantity of nanoparticles present in the mix is higher than the amount required to combine with the liberated lime during the process of hydration, thus leading to excess silica leaching out and causing a deficiency in strength as its replaces part of the cement material and does not contribute to its strength [16].

This issue is because nanoparticles due to their high surface energy have the tendency towards agglomeration. When nanoparticles are over added to the mortar it is not uniformly distributed in cement mortar and due to agglomeration weak areas appear in the cement mortar. Whereas, few amounts of nanoparticles even if not distributed uniformly it increase the strength, this is because that small quantity of nanoparticles agglomeration does not create weak zone [17].

Table 3: Mechanical properties of samples

Mixture no.	Compressive strength at the 7th day		Tensile strength at the 7th day		Flexural strength at the 7th day	
	Target (MPa)	Enhanced extent (%)	Target (MPa)	Enhanced extent (%)	Target (MPa)	Enhanced extent (%)
CO	11.96	-	1.51	-	2.2	-
1NA	17.25	44.23	2.52	66.89	3.25	47.73
3NA	19.54	63.38	2.74	81.46	3.74	70
5NA	10.9	-8.86	1.4	-7.3	2.04	-7.27

The mechanisms of Al_2O_3 nanoparticles that causes the increases of strength of cement mortar it can defined as the Al_2O_3 nanoparticles because of high specific surface area causes the consumption of crystalline $Ca(OH)_2$ which quickly formed during the hydration of cement process and fills the void structure of C-S-H gel and finally the hydrated products are made denser and compact.

In other words, when nanoparticles are uniformly distributed in the cement mortar, each particle is contained in a cube pattern and the distance between nanoparticles can be adjusted. After the beginning of cement hydration process, nanoparticles due to their high activity develops and accelerate the cement hydration and hydrate products of nanoparticles are surrounded as kernel. If the quantity and distance between these nanoparticles is suitable, nanoparticles prevents the growth of $Ca(OH)_2$ crystals [5]. The past research of these researchers show that with excessive increase of nanoparticles quantity, the nanoparticles distance decreases and $Ca(OH)_2$ crystals due to limited space cannot grow enough and finally the crystal quantity is reduced [18]. This factor along with the agglomerated nanoparticles causes the mechanical properties of the sample 5NA is lower than the ordinary mortar sample.

The results show that the addition of Al_2O_3 nanoparticles, increasing amount of tensile and flexural strength is more than compressive strength, which agrees with the research results by Ali Nazeri and et al [7, 8].

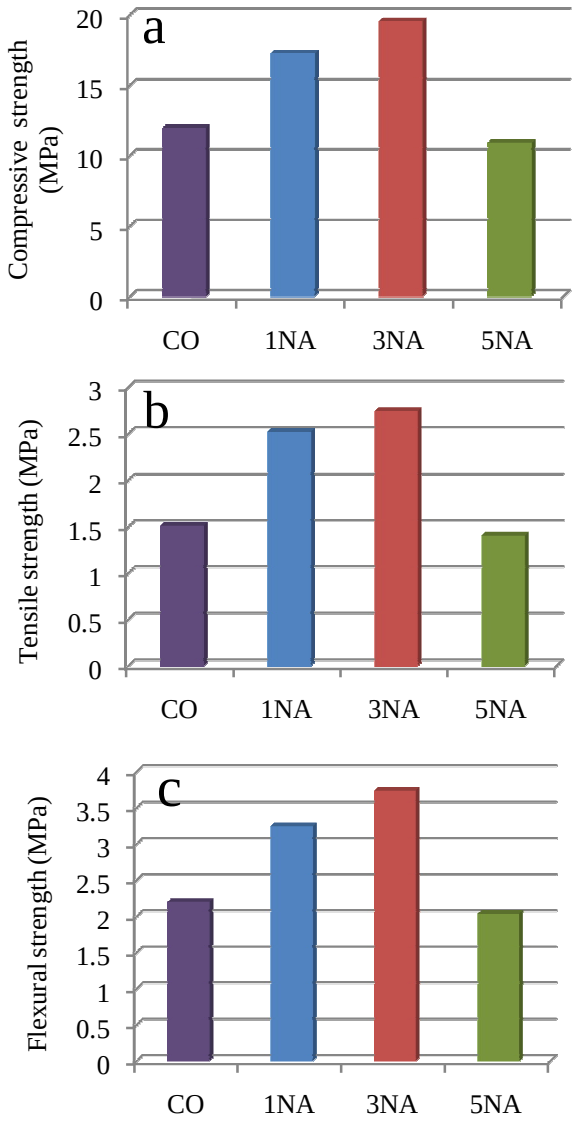

Figure 1. (a) Compressive strength, (b) Tensile strength, and (c) Flexural strength of samples

3.2. Microstructure of samples

To study the mechanism which improves the strength, SEM test has been conducted. The microstructure of samples is shown in figure 2. As shown in the figure, adding Al_2O_3 nanoparticles causes difference in the microstructure samples. In microstructure samples of ordinary cement mortar there exists large crystals of $Ca(OH)_2$. Microstructure of cement mortar is not dense and voids can be seen. As shown in figure 2b, in sample containing 1 percent nanoparticles relative to sample of ordinary cement mortar the structure of cement mortar has become denser and the voids decreased but still large crystals of $Ca(OH)_2$ are observed. But, with increasing quantity of nanoparticles to 3 percent, large crystals of $Ca(OH)_2$ are eliminated and microstructure of cement mortar is completely denser.

As shown in figure 2d, in samples containing 5 percent nanoparticles because of the agglomeration of nanoparticles voids are formed. These microstructures with the reduction of mechanical properties in these samples are appropriate.

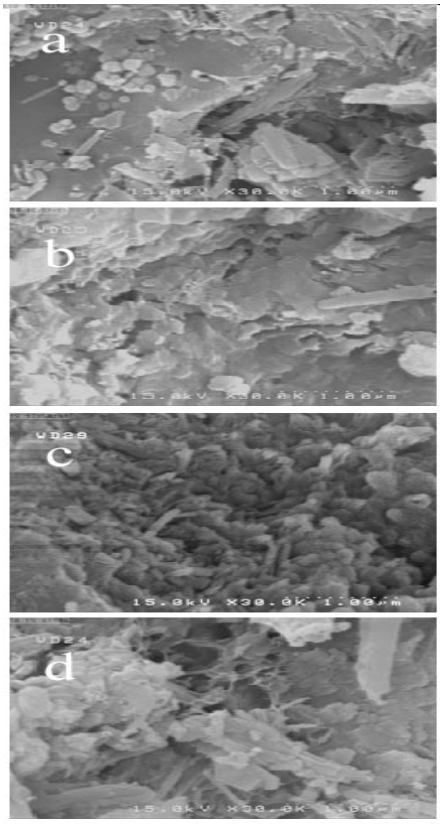

Figure 2. Microstructure of the samples,
a) Sample of CO. b) Sample of 1NA.
c) Sample of 3NA. d) Sample of 5NA

4. Conclusion

With respect to the experimental results of compressive, tensile and flexural strength it is expected that adding of Al_2O_3 nanoparticles to 3 percent weight of cement can act as a filler for strengthening the microstructure of cement and also reduces the quantity and size of $Ca(OH)_2$ crystals and finally structure of hydrated product is compacted and denser. But with the increase of quantity of Al_2O_3 nanoparticles to 5 percent there is decrease in nanoparticles distance and $Ca(OH)_2$ crystal due to limited space cannot grow to appropriate size. This factor along with the agglomerated nanoparticles causes the mechanical properties of the sample 5NA is lower than the ordinary mortar sample.

Corresponding Author:
Mohammad Reza Arefi
Department of Civil Engineering, Taft Branch, Islamic Azad University, Taft, Iran
Member of Young Researchers Club, Islamic Azad University, Yazd, Iran
E-mail: arefi@taftiau.ac.ir

References

1. Ye Qing, Zhang Zenan, Kong Deyu, Chen Rongshen. Influence of nano-SiO2 addition on properties of hardened cement paste as compared with silica fume. Construction and Building Materials 2007; 21: 539–545.
2. Baomin W, Lijiu W, Lai FC. Freezing Resistance of HPC with Nano-SiO2. J Wuhan Univ Technol-Mater(Sci. Ed) 2008;23:85-88.
3. Arefi MR, Javaheri MR, Mollaahmadi E, Zare H, Abdollahi Nejand B, Eskandari M. Silica nanoparticle size effect on mechanical properties and microstructure of cement mortar. Journal of American Science, 2011; 7: 231-238.
4. Li H, Zhang MH, Ou JP. Flexural fatigue performance of concrete containing nano-particles for pavement. Int J Fatigue 2007; 29 : 1292–1301.
5. Li H, Zhang MH, Ou JP. Abrasion resistance of concrete containing nano-particles for pavement. Wear 2006; 260: 1262–1266.
6. Zhang MH, Li H. Pore structure and chloride permeability of concrete containing nano-particles for pavement. Construction and Building Materials 2011; 25: 608–616.
7. Nazari A, Riahi S, Riahi S, Shamekhi SF and Khademno. Influence of Al_2O_3 nanoparticles on the compressive strength and workability of blended concrete. 2010; 6: 6-9.

8. Nazari A, Riahi S, Riahi S, Shamekhi SF and Khademno. Mechanical properties of cement mortar with Al_2O_3 nanoparticles. 2010; 6: 94-97.
9. Nazari A, Riahi S. Al_2O_3 nanoparticles in concrete and different curing media. Energy and Buildings 2011; 43: 1480–1488.
10. Nazari A, Riahi S. Improvement compressive strength of concrete in different curing media by Al2O3 nanoparticles. Materials Science and Engineering A 528 2011:1183–1191.
11. ASTM C150. Standard Specification for Portland cement. American Society for Testing and Materials; 2005.
12. ASTM C33. Standard Specification for Concrete Aggregates. American Society for Testing and Materials; 2007.
13. ASTM C109 / C109M. Standard Test Method for Compressive Strength of Hydraulic Cement Mortars (Using 2-in. or [50-mm] Cube Specimens). American Society for Testing and Materials; 2008.
14. ASTM C190. Method of Test for Tensile Strength of Hydraulic Cement Mortars. American Society for Testing and Materials; 1985.
15. ASTM C348. Standard Test Method for Flexural Strength of Hydraulic-Cement Mortars. American Society for Testing and Materials; 2008.
16. AI-Khalaf MN, Yousift HA.Use of rice husk ash in concrete. Int J Cem Compos Light weight Concr 1984; 6(4):241–248.
17. Li H, Xiao HG, Yuan J, Ou J. Microstructure of cement mortar with nano-particles. Compos: Part B: Eng 2004; 35:185–189.
18. Arefi MR, Mollaahmadi E, Abdollahi Nejand B, Fattah M, High performance self -cleaning cement mortar composite and coats prepared by TiO2 nanoparticles. Submited in Journal of Materials Science.

11/25/2011

Health Promotion program to Improve the Lifestyle of School Children Living in Slum Areas in Helwan Governorate

[1]Sahar A. Sh. Mahmoud., [2] Hanaa A, A. Y, [3] Safaa S, Ismail

[1]Community health Nursing, Faculty of Nursing, Helwan University [2]Community health Nursing ,Faculty of Nursing, Benha University [3]Paediatric nursing, Faculty of nursing, Helwan University

Abstract: The school years are a time when the foundations of a healthy lifestyle are formed and when health promotion programs are likely to have the greatest impact. **The aim** of this study was to evaluate the effect of health promotion program on improving lifestyle of school children living in slum areas. **Design**: A quasi –experimental design was used. **Setting**: The study was conducted at two governmental primary schools in Azbat Elwalda, in Helwan Governorate **Sample**: A stratified multi-stage cluster random sample was used for selection of school children in slum areas ,the total number of governmental primary schools in Azbat Elwalda are (3),two were chosen randomly. One class from fifth grade and one from sixth grade were selected randomly from each school. The total number of children for two schools were 200 (both sexes).**Tools: 3 tools were used 1)** A structured interviewing questionnaire was used to assess students socio-demographic characteristics, students' perception of social and physical environment of school, students' common health problems during the past two years and students' knowledge about healthy life style .These tools were used before and after program. **2)** A physical examination to assess the student from head to toe. **3)** An observational checklist for assessing in and out school's environment. **Results:** the study confirms that diseases of respiratory system had the highest frequencies among the students as follows: less than two fifths for common cold, more than one third for tonsillitis and bronchitis and more than one quarter for influenza. There was difference between before and after program implementation concerning students' health promoting life style, perception of social and physical school environment. The differences were statistically significant for all of variables (P = < 0.001). **Conclusion**: The study concluded that students perception improved toward their social, physical school environment and their knowledge about healthy life style after implementing the health promotion program .This improvement was proved statistically .**Recommendations :** The study recommended that a health promotion program are strongly needed to school children to improve their lifestyle especially school children living in slum areas and the necessity of improving school environmental sanitation for the promotion of students health.

[Sahar A. Sh. Mahmoud., Hanaa A, A. Y, Safaa S, Ismail. **Health Promotion Program to Improve the Lifestyle of School Children Living in Slum Areas in Helwan Governorate]** Life Science Journal, 2011; 8(4): 618-627] (ISSN: 1097-8135). http://www.lifesciencesite.com.

Key words: Slum area, lifestyle, environment, health promotion program, school age children

Introduction

Children are the greatest investment of any community and the main basis for its development. School children constitute a significant and important sector of the population who are constantly growing and developing. This basic dynamic character accounts for their increased vitality and vulnerability and requires specific health promotion in relation to seeking health and using various resources to attain optimum health **(Sherman et al., 2002).**

In Egypt population of the age from 6-12 are 7.4464 million. School students in Egypt are influenced by the general problem of childhood, high density in classes (70 student / class), environmental pollution and educational stress as many are forced to operate in two shifts in a day (**WHO, 2004**).

The environments in which children live affect their health. In developing countries recognized risk factors; are lack of sanitation, poor water supply, poor food safety and air pollution **(Tallinn, 2008).**

Slums are those areas which are characterized by insecure residual status, poor structural quality of house, overcrowding, inadequate access to safe water and sanitation. Therefore, slum dwellers are more vulnerable to infections which results in deterioration of their nutritional status (**Bisai et al , 2009**).

Health promotion in schools can improve children's health and well-being. Among the most effective programmes are those that promote healthy eating and physical activity. School children of slum areas are exposed to many health risks mainly related to their lifestyles, behaviours and environmental factors which they have an impact on health-related quality. Health risks such as childhood overweight and obesity and type 2 diabetes mellitus. Lifestyles are probably the most important determinants of changes in health status **(Stewart- Brown, 2006).**

The school nurses take a leadership role in serving as the coordinator of all school programs .In order to be effective in assisting students to meet their optimal

potential in the classroom, the school nurse needs to have knowledge of current trends and practices in medical/nursing care and have open systems of communication to coordinate care **(Edwards,2006).**

Magnitude of the Problem

People living in slum areas are more likely to suffer from improper housing, poor socioeconomic characteristics, environmental pollution and absence of infrastructure and basic services**.** High health problems for children run riot in slum areas, **(Metwally & Olsen; 2005 & Peace 2010)**

In Egypt, the school aged children particularly in slum areas are vulnerable to a range of health risks that may affect them immediately as infectious diseases, malnutrition, accidents or sexually transmitted diseases and in the future as cardiovascular diseases and cancers. These risks may originate as a result of the life style and health status. School health programs are vital part of public health services and education. The school health nurse is the first responsible person to teach children about disease, hygiene, risk reduction, sexuality and decision making. The school nurse must be sensitive to dynamic nature of this stage, in order to prevent disease, protect them from accidents and promote health through health education about nutrition, exercise, hygienic measures, and healthful environment**.**

Aim of the study

This study was carried out to evaluate the effect of health promotion program on improving the lifestyle of school children living in slum areas in Helwan Governorate through**:**

- Assessing school children health promoting needs regarding their life style.
-Assessing in and out school's environment.
-Developing and implementing health promotion program based on the previously detected needs of school children toward their life style.
-Evaluating the degree of the school children improvement toward their health promoting life style.

Hypothesis:

A health promotion program will improve student's perception toward their physical, social, school environment and also improve their lifestyle in both two schools in slum areas.

Subject and Methods

Design:

A quasi experimental design was used to conduct the study.

Setting :

The study was conducted at two governmental primary schools in Azbat Elwalda, Helwan namely: Asmaa Bent Abo Baker and Naguib Mahfouz**.**

Sample:

A stratified multi-stage cluster random sample was used for selection of school children in slums areas.

First stage: The total numbers of governmental primary schools in Azbat Elwalda is (3), two were chosen randomly for the conduction of the study.

Second stage: One class from fifth grade and one from sixth grade were selected randomly from each school.

Third stage: All school children in the selected classrooms were taken, the total numbers of children for the two schools were 200 (both sexes) according to certain criteria:

1- Their aged ranged between 10-12 years, which are considered as preadolescents and health promotion program will have great benefit for maintenance of their health.

2- They got acceptance letter from their parents to participate in the study.

Tools of the study:

For data collection three tools were used:

The first tool was a structured interview questionnaire developed by the researchers after reviewing of related literature, it consisted of 3 parts:

Part I: Students' socio -demographic characteristics, which include: age, sex, and class grade, and family characteristics as parent's level of education, marital status, occupation, family size and family type.

Part II : This part is a set of questions covering twelve major areas pertaining to students' common health problems during the past two years as regards nervous system (visual disturbance, eye inflammation & headache), respiratory problems (common cold, bronchitis, asthma, influenza, tonsillitis, pneumonia & TB),skin disease (eczema, scab, acne & warts), gastrointestinal problems (diarrhoea, constipation & food poisoning), school accident (wound & fracture), circulatory problems (rheumatic fever & cardiac problems), back pain ,teeth problems, and diabetes mellitus.

Part III: This part deals with students' perception regarding:

-Social school environment using a tool adopted from **Mclellan** (**1999)**.

It includes seven items, which explored students' perception toward teacher support, peers support,

educational achievement, school schedule, school curriculum, and school health services.
-Physical school environment using a sheet constructed by the (**General Health Insurance, and WHO (2001)**. It included items related to safety of school, personal hygiene, environment, and items related sanitation of school environment.
Part IV: Included student's lifestyle Profile according to **(Cookfair, 2008)**.This tool is covering five major areas. Self health responsibility, eating habits and nutrition awareness, physical activity, stress management and environment safety. These tools were used before program implementation which parts III and IV were used before and after the program.

Scoring system:

This tool included 5 items: related to health self responsibility contained 18 sentences, (total score = 36), eating habits 13 sentences (total score= 26), physical activity 7 sentences, (total score =14), stress management contained 14 sentences, (total score =28), environmental sensitivity contained 12 sentences (total score = 24). The students responses were scored as follows, always = 2, sometimes =1, and never = 0.The investigator categorized students perceptions as satisfied when the score is 75% or more, and unsatisfied if less than 75%.

The second tool was a physical examination which included physical examination sheet **(Fuller & Schaller, 2005)** to assess the student from head to toe, measure weight and height and personal hygiene. Body Mass Index (BMI) was used to determine the degree of obesity. According to **Dudek, (2003)** scale BMI is divided into three categories >20 is considered underweight, 20->26 is considered normal, 26->30 is considered overweight or obese.

The third tool was an observational checklist. It included two main parts:
Part I: Assessing school environment, it included items related to school place, design, playground, classroom, water supply, water closets, waste disposal and canteen (buffet). The investigator scored the outcomes as present or not present
Part II- Assessing out school's environment, it included items related to building construction, street vendors, sufficient street width, garbage disposal, sewage disposal, insect and rodents and animals excreta.

Statistical Design:

Collected data were categorized, coded, entered and analyzed using the statistical Package for social sciences (SPSS) version 12.0. The analyses carried out included descriptive statistics. The level of statistical significance was set at p-value < 0.01

Field work:

Official letters from the Faculty of Nursing, Helwan University were forwarded to the Ministry of Education with the aim of the study to obtain their permission to visit the schools and conduct the study.

After approval of the Ministry of Education, official letters were addressed to the directors of the schools. Each director was informed about the time and date of data collection.

Each student was interviewed individually after explaining the purpose and method of the study and obtaining his / her approval to participate in the study with confidentiality.

Content validity of the tools was tested by a panel of five experts in community health nursing field, pediatric health nursing and corrections were done accordingly based on their responses.

A pilot study was conducted on 20 students, who were excluded from the main study sample, to test the applicability of the tools. The necessary modifications were done accordingly.

The health promoting life style program was developed based on review of related literature and assessment tools (pretest).

Data were collected during the period from October, 2009, to March 2010

Time plan was established and the students were organized into 6 groups (30-35 students).

The program in a school day starts from 8 .00 a.m. to 2 .00 p.m. Each group of students attended 6 sessions. The duration of each session was 20-45 minutes according to the presented items. Each session was followed by a summary of the essential healthy life style items discussed.

Ethical consideration:

Consent to participate in the study was obtained from parents of school children.

Confidentiality was assured to all children of the study.

The health promotion program construction. Contained 3 phases:
Phase I: Preparatory phase was done by using the assessment tools after being revised and tested for general information about healthy life style, In relation to student's self health responsibility, as eating habits, nutrition awareness, physical activity, stress management and environmental safety.
Phase II: Developing and implementing the program .The general objective of the program was to improve the lifestyle of school children living in slums areas in Helwan Governorate. The program contents covered the following major area: general information about healthy life style, in relation to students' self-health responsibility, eating habits, nutrition awareness,

physical activity, stress management and environmental safety.

The methods used were lectures, discussions, brainstorming, demonstration and re-demonstration. Data show and handouts were used as teaching media,

Phase 3: Evaluation was done to measure the difference between pre-post test.

3. Results

Figures (1, 2): show the frequency distribution of schools, and class grades among the sample; 50.5% of school children were from Naguib Mahfouz School. In relation to class grade, 52.5%of children were in 5th grade while 47.5% were in 6th grade.

Table (1): classifies the socio-demographic characteristics of school children. The table reveals that the school girls were prevalent more than males in both schools (61.5%). Concerning parents' education, only 2.0% and 7.0% of fathers and mothers had university education respectively. In relation to father occupation more than half of fathers (52.5%) were workers, while 37.0% were officers. More than half (57.0%) of mothers were housewives while 43.0% were workers. As regards family size, 59.0%were <4, while 41.0% were ≥4. Concerning family type, only 14.0% of families were single parent (dead), while 50.0% were extended families.

Table (2): demonstrates that 22.5% of the students health problems were visual disturbance, 20.5% of students complain from eye inflammation, and 16.0% from headache. Diseases of respiratory system had the highest frequencies among the students as follows: 38.5% for common cold, 34.0 % for tonsillitis, 32.5 % for bronchitis, 29.5 % for influenza, 11.5 % for asthma, and an equal percentage of 11.0 % for T.B. and 9.0% for pneumonia. As regards skin diseases, the table shows that acne was found among 18.0 % of students, followed by eczema 12.5 %, then wart 8.5 %. Scab had the lowest prevalence 2.5% among students.

In relation to gastrointestinal problems, stomach pain was prevalent among 28.0 % of students, followed by diarrhea 23.0 %and constipation 13.5 % .Food poisoning was found among 1.5% of students. Hepatitis A was found among 17.0% of students.

In relation to school accidents, more than one quarter 27.5 % of the students in the study sample reported wounds as accident in school, back pain among 30.0%. Regarding to circulatory diseases, minority of them (2.0%) complain from rheumatic fever and cardiac problems (2.0%) and the diabetes mellitus (4.5%).

In relation to teeth problems, results of the present study showed that 27% of the students in the two schools complained from teeth problems.

Table (3): shows the mean score of before and after program changes in promoting life style among students. In relation to self health responsibilities, the mean was 21.2±2.0 before program increased to 28.2± 1.54 after program and the difference was statistically significant (t= 25.5.p=<0.001).The mean nutritional awareness was 9.2+ 1.8 before program increased to 18.2± 2.4 and there was a statistically significant difference (t= 35.5 at p= <0.001) . In relation to the mean of physical activity it was 2.7 ± 1.0, pre-program, which increased to 8 .2± 3.2 after program and there was a significant difference (t= 13.5 at p= <0.001). The mean of stress management was 15.9± 1.6 before program, which increased to 20.5 ± 2.6 after program. As regards to the mean environmental safety, it was 13.8 ±1.7 pre-program and increased to 23.2±1.3 with a statistically significant difference (t=15.8at p= <0.001).

Table (4): shows the mean score of students' perception of school environment and health promoting life style before and after the program. The table reveals change in student's perception of social and physical school environment after program implementation. The improvement or changes were statistically significant for all variables (P = < 0.001). As well, the total student's knowledge about health promoting life style improved after implementation of the program, (p< 0.001).

Table (5): displays mean score of student's perception of physical school environment according to the two selected schools. The mean score for Asmaa Bent Abo Baker was 39.5 ± 2.1 and for Nagiub Mahfouz school 33.9 ± 2.3 with highly significant difference (P=<0.001). However, there were no statistically significant differences in other variables.

Table (6): shows the correlation between promoting life style knowledge and students' common health problems. There was a highly statistically significant correlation between life style and student health problems.

Table (7): indicates that (33.5%) of students were under weight. The majority (81.5%) of the students had tooth decay, 48% complained from rhinitis, 36.5%had dandruff and 15% are wearing eye glasses. Regarding skin condition 5% had acne. Concerning personal hygiene for 40% of the students, personal hygiene was good.

Table (8): describes the school environment of students of the studied sample. The studied two schools were not away from noise and dusty places, canteens were not clean and no proper food preservation, no dry and clean water closets, no collection of refuse in baskets. In classes students' number was more than 30 students, while there was suitable classroom light, sanitary water supply and medical clinics. Only one school had neither sufficient classroom ventilation nor sufficient playground area.

Table (9): Reveals that in both schools slum environment had unsafe cluster of building, there were

vendors in the streets around schools and garbage was collected and thrown down in the streets. Out of both schools environment had no sanitary sewage systems, and insects and rodents spread in the street .In one of the two schools there were no sufficient street width. Animals excreta were collects and thrown down in the street around only one school.

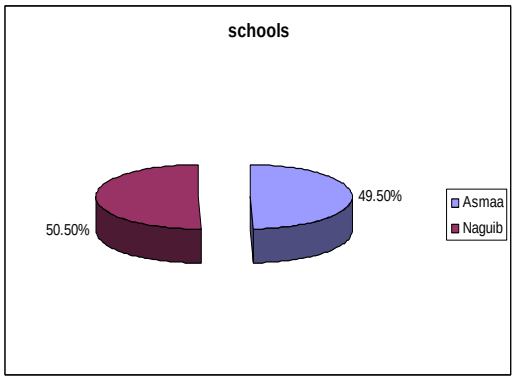

Figure (1) : Frequency distribution of schools among sample

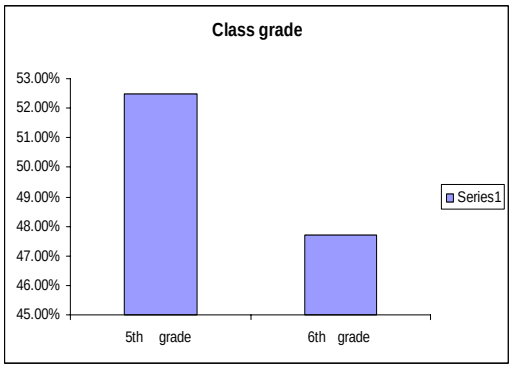

Figure (2): Frequency distribution among study sample related to class grade

Table (1): Students' socio-demographic characteristics.

Variable	No	%
Students' sex:		
-Male	77	38.5
-Female	123	61.5
Fathers education :		
- Illiterate	95	47.50
- Read and write	68	34.00
- Secondary education	33	16.50
- High education	4	2.00
Fathers occupation :		
- Workers	105	52.50
- Officer	74	37.00
- Retired	21	10.50
Mothers education :		
- Illiterate	58	29.00
-Read and write	66	33.00
- Secondary education	62	31.00
- High education	14	7.00
Mothers occupation:		
- Workers	86	43.00
- Housewives	114	57.00
Family size :		
<4	118	59.00
>4	82	41.00
Family types :		
- Nuclear	72	36.00
- Extended	100	50.00
- Single parent (dead)	28	14.00

Table (2): Shows distribution of students according to their self reported common health problems during the past two years.

Common Health Problems	No	%
Nervous system diseases :		
- Visual disturbance	45	22.50
- Eye inflammation	41	20.50
- Headache	32	16.00
Respiratory diseases :		
- Common cold	77	38.50
-Bronchitis	65	32.50
Asthma	23	11.50
- Influenza	59	29.50
- Tonsillitis-	68	34.00
-Pneumonia	18	9.00
T.B	22	11.00
Skin diseases:		
- Eczema .	25	12.50
- Scab	5	2.50
-Acne	36	18.00
-Warts.	17	8.50
Gastrointestinal problems :		
- Stomach pain-	56	28.00
- Diarrhea.	46	23.00
- Constipation.-	27	13.50
- Food poisoning.-	3	1.50
Hepatitis A.	34	17.00
School accidents :		
- Wound.	55	27.50
- Fracture	7	3.50
Circulatory diseases :		
-Rheumatic fever.	4	2.00
-Cardiac problems	4	2.00
Back pain.	60	30.00
Teeth problems	54	27.00
Diabetes mellitus	9	4.50

Table (3) : Mean score of student life style before & after implementation of the program.

Variables	Pre			Post			Paired t-test	
	Mean	±	SD	Mean	±	SD	T- test	P-value
Self health responsibility.	21.193	±	2.001	28.215	±	1.542	25.465	<0.001*
Eating habits nutrition awareness	9.249	±	1.822	18.245	±	2.354	35.456	<0.001*
Physical activity .	2.690	±	0.959	8.224	±	3.240	13.546	<0.001*
Stress management.	15.888	±	1.561	20.549	±	2.645	19.564	<0.001*
Environmental safety.	13.751	±	1.667	23.244	±	1.250	15.840	<0.001*
Total	66.376	±	4.217	89.914	±	10.236	29.922	<0.001

T: paired t-test Statistically significant at p<0.05

Table (4) : Mean score of students' perception of school environment &health promoting life style before & after the program.

Variables		Range			Mean	±	SD	Paired t-test	
								T- test	P-value
Students' perception of social school environment	Pre	22.000	-	34.000	27.751	±	2.365	35.542	<0.001*
	Post	34.00		47.00	45.872	±	5.635		
Students' perception of physical school environment	Pre	29.000	-	45.000	39.020	±	3.455	-29.609	<0.001*
	Post	40.73	-	55.746	49.853	±	4.268		
Total student knowledge about healthy life style	Pre	57.00	-	77.00	66.376	±	4.217	-29.922	<0.001*
	Post	70.00	-	121.00	89.914	±	10.236		

Table (5) : Mean score of students perception of social , physical school environment and total students health promoting life style according to the two selected schools.

Variables	School						
	Asmaa Bent Abo Baker			Naguib Mahfouz			Paired t-test	
	Mean	±	SD	Mean	±	SD	T-test	P-value
Students' perception of social school environment	27.207	±	2.204	27.288	±	2.599	0.168	0.867
Students' perception of physical school environment	39.472	±	2.081	33.956	±	2.256	12.581	<0.001*
Total student knowledge about healthy life style	66.849	±	4.409	66.111	±	4.179	0.846	0.400

Table (6): Correlation between promoting life style knowledge and students common health problems

Correlation between Knowledge and Problems	
R	P-value
0.622	<0.001*

Table (7): Distribution of students' health condition

Students' health Condition	No	%
Body Mass Index (BMI):		
- Under weight	67	33.5
- Normal weight	120	60
- Over weight	13	6.5
Hair:		
- Dandruff	73	36.5
- Nits-pediculosis	14	7
Eye:		
- Inflammation of eyelids	15	7.5
- Wearing eye glasses	30	15
- Visual measurement disorder	14	7
Ears:		
- Wax	2	1
- Discharge	3	1.5
Nose:		
- Rhinitis	96	48
Mouth:		
- Lips dry & cracked	41	20.5
- Tooth decay	163	81.5
Skin:		
- Acne	10	5
- Warts	0	0
Personal hygiene:		
-Good	80	40
- Poor	120	60

Table (8): Distribution of studied schools regarding their environment

School Environment	No	%
Place away from noise and dusty place	0	0
No. of students in the class:-		
- < 30	0	0
- 30+	2	100
Sufficient classroom area /students number	1	50
Good classroom ventilation	1	50
Good classroom light	2	100
Canteen clean and has proper food preservation	0	0
Presence of sanitary water supply	2	100
Water closets :		
- Dry and clean	0	0
- Sufficient water closets / children number	1	50
Waste disposal :		
-Collection of refuse in baskets	0	0
Sufficient playground area	1	50
Existence of medical clinic	2	100

Table (9): Distribution of studied Schools regarding their slums environment (n=2).

Slums Environment (Around the School)	No	%
Building construction:		
Safe and healthy building construction	0	0
Unsafe cluster of building	2	100
Street vendors:		
Present around the school	2	100
Not Present around the school	0	0
Sufficient wide streets :		
Yes	0	0
No	1	50
Garbage disposal:		
Collected and thrown down in special places	0	0
Collected and thrown down in the street	2	100
Sewage disposal:		
Sanitary sewage system	0	0
Cesspool	2	100
Streets free from insects and rodents:		
Yes	2	100
No	0	0
Animals excreta:		
Collected and thrown down in special places	0	0
Collected and thrown down in the street	1	50

4. Discussion

The health promoting school aims to achieving healthy life styles for the total school population by developing supportive environment conductive to the promotion of health (**Scriven & Orme ,1996**).

Socio demographic characteristics of the present study indicate that more than half of children were in 5th grade, while less than half were in 6th grade (Figure, 2). This study was in agreement with **Abd-Elhaleem (2004),** who reported that two thirds of children were in different levels of education, especially primary schools.

The present study result showed that the school girls were more prevalent than males in both schools (Table 1). This study was disagreement with **Sedik (2002**), who reported that males were more than females in school children especially in primary schools.

In relation to parents; education the study indicated that few of fathers and mothers had university education in both schools. In relation to father's occupation, more than half of fathers were workers, while more than one third was officers. As for mother's occupation less than three fifths were housewives while the rest of them were workers, (Table, 1). The present study was in agreement with **Elsamaloty (2000),** who reported in his study that percent of illiteracy between family parents increased due to poverty and low of socio-economic standard. As well **Abd-Elhaleem (2004)** found that the majority of fathers and mothers had technical works, they were sellers also the majority of mothers were housewives.

The assessment of student's health problems in this study revealed that less than one quarter complained from visual disturbances slightly more than one fifth of students complained either from eye inflammation or headache. Diseases of respiratory system were reported by more than one third of them who complained from common cold, while approximately one third had tonsillitis, bronchitis, and more than one quarter had influenza, and minorities of them complained from asthma, pneumonia and TB (table 2). These results were in agreement with **Radwan (2005),** who reported that gradual progressive decrease in visual acuity during the school years especially eye inflammation and headache had been noted. Additionally the previous results were in consistence with a study carried out by **Viswanathan (2006),** who stated that respiratory illness especially common cold, bronchitis, asthma, influenza, tonsillitis, pneumonia and TB were present in 17.2 % of the studied school age children at slums areas of Chennai. These health problems could be attributed unsafe school environment and slums environment in which the students live.

In relation to gastrointestinal problems, the findings of this study showed that more than one quarter of students had stomach pain followed by diarrhea, than constipation. Less than one fifth complained from hepatitis A, and the minority of them complained of food poisoning (Table,2).These results were in agreement with a study carried out by **Cohen(2003),** who reported that almost half of a total of 858 school age children were sick due to gastrointestinal problems especially stomach pain, diarrhoea, constipation and 17 % of affected children have been suffering from hepatitis A.

In relation to teeth problems, results of the present study showed that more than one quarter of the students in the two schools complained from teeth problems. This result was disagreement with **Rosdad (2004),** who reported that the school age children have the highest prevalence of teeth problems. Similarly **Abd El Aziz (2005),** noted that tooth decay is due to inadequate knowledge about the importance of regular washing of teeth and its risk factors. The gastro intestinal problems may be due to eating contaminated street food, which the students buy from street vendors around school.

Findings of this study showed that less than one fifth of students in both schools complained from acne, while more than teeth from eczema, and minorities of them from warts and scab (Table2).In accordance, **Edemon (2002)** mentioned that acne is the major skin problem in children affecting 7% of them. Acne starts with increased sebum production stimulated by androgens during puberty. However **Ghobashi and Mandie (2006)** noted that, poor personal hygiene with lack of bathing and cleanliness are the most common

causes of skin problems especially eczema, scab, and warts among school children in Egypt.

Regarding school accidents, more than one quarter of the students in this study sample reported wounds as accident in schools (Table 2).This finding was in agreement with the **General Health Insurance and WHO (2001),** which found the most common accidents related injuries between school children in Egypt are wounds and fractures due to unacceptable school environment as overcrowding of students in playground, unsafe sports equipment and broken stairs. Other school children complain wasback pain as revealed in this study was common among less than one third of students in the two schools. In accordance **Mohamed (2001)** clarified that back pain started among school children when they were 11 years of age. This back pain may be from carrying a heavy books bag.

Regarding circulatory diseases, in the present study few of them complained from rheumatic fever and cardiac problems (Table 2). These finding were disagreement with **Mosa (2005),** who reported in his study in Cairo that circulatory disease complaints were most prevalent among school children.

In relation to diabetes mellitus, a minority of students under study complained from it (table 2). In this respect, **Bartklw (2006)** noted that, the prevalence of diabetes mellitus among US children has jumped for approximately 4%.

According to the research hypotheses:

In this study results there were statistically significant associations between before and after promoting life style program implementation in relation to self health responsibility ,eating habits, nutrition awareness, physical activity, stress management, and environmental safety (Table 3) . These results were in agreement with **Mclellan (2002),** who found that students had negative perceptions towards their promoting life style and self health responsibility, eating habits, physical activity, stress management and environmental safety.

In relation to student's perception toward school environment and total student health promoting life style, the improvement or changes were statistically significant for all of variables (P< 0.001). As well total students' health promoting life style improved after application of the program (Table 4). In a similar study, **Mclellan (2002),** found that students had negative perceptions towards their social school environment, physical school environment and students knowledge about healthy life style.

The relation between student's perception of social and physical school environment and total students health promoting life style was investigated in this study. In relation to student's perception of physical school environment the mean of their perception in Asmaa Bent Abo Baker School was 39.5± 2. 1 and school in Nagib Mahfouz it was 33.9 ±2.256. There was highly statistically significance difference ($p < 0.001$) between the two schools, while there was no statistically significant difference between the two schools and total students' knowledge about healthy life style (Table 5). The present study result was to some extent in agreement with **Elsamaloty (2000),** who reported that the students had negative perception towards their social and physical school environment and healthy promoting life style.

As regards the correlation between promoting life style knowledge and students common health problems, there was a highly statistically significant correlation between life style and student health problems (Table 6).In accordance, **Machle and Olckle (2007)** mentioned that the common health problems in schools in developing countries are due to unsanitary school environment, faulty habits of children, lowered body resistance, and more susceptibility to infection due to malnutrition and poor living conditions of the school children.

Concerning the students' health conditions, results of this study revealed that one third of students were under weight. The majority of the students had tooth decay, less than half had rhinitis, more than one third had dandruff and less than one fifth are wearing eye glasses (Table 7). The present study finding were disagreement with **Ahmadi and Tehrani (2009),** who found that the prevalence of obesity, overweight and underweight represented 9.7 %,4.4 % and 0.57% respectively. The poor health condition of the students may be due to the low literacy level prevailing among the slums parents, their lack of knowledge and practices about good nutrition; and their poor socio-economic status.

Findings of this study showed that the environments of the studied two schools were not away from noise and dusty places, canteens weren't clean and no proper food preservation, no dry and clean water closets, no collection of refuse in baskets. In classes students' number was more than 30 students, while there was suitable classroom light, sanitary water supply and medical clinics. Only one school had neither sufficient classroom ventilation nor sufficient playground area (Table 8). Poor environment conditions, sufficient water closets /children number were associated with a wide range of health conditions, leading to respiratory infection, asthma and injuries.

Concerning the environmental observation of slums area around school's under study, this study results revealed that slum environment had unsafe cluster of buildings, there were vendors in the street around schools and garbage was collected and thrown down in the streets. Slums area around both studied schools had no sanitary sewage systems, insects and

rodents spread in the street. There were no wide streets and animals' excreta are collected and thrown in the streets around only one school (Table 9). These results agreed with **EL-Shiekh (2005)** who reported that more than half of the sample had no sewage systems. The household wastes disposed through cesspool. The health risks of uncontrolled solid wastes are most serious that contribute to spreading of infectious diseases such as diarrheal diseases. They are likely to be exposed to uncontrolled waste in the streets. Collection of garbage causes rodent and insect vectors that transmit a collection of viruses and disease including hepatitis. Pollutants are everywhere, eating street food is dangerous. Street vendors are selling newly-cooked foods that lure the palate or taste buds of bystanders. The selling foods may be contaminated and cause food poising. Food Poisoning can cause fatal effects or even death to students who are at risk when eating street food.

Conclusion:

The study concluded that student's perception improved towards their social, physical school environment and their knowledge about healthy life style after implementing the health promotion program .This improvement was proved statistically.

Recommendations:

Based on the results of this study the following recommendations are suggestion:

1-A health promotion program are strongly needed to school children to improve their lifestyle especially school children living in slum areas, it should include the following:

-Monitoring school children health status and periodic check up to early detecting of any health problems and providing management.

-Health life style of children such as (self-health responsibility, eating habits and nutrition awareness, physical activity and stress management) should be introduced through education in primary schools.

2-The necessity of improving school environmental sanitation for the promotion of student's health.

Corresponding author

Sahar A. Sh. Mahmoud

Community health Nursing, Faculty of Nursing,

Helwan University.

References:

Abd El-Aziz, A. (2005): Health promotion, educational program for primary school children in slums area. Doctors Thesis, Faculty of Nursing, Ain Shams University. pp. 121-135.

Abd-Elhaleem, N. (2004): Social repercussion of the phenomena of street children, homelessness, health examination on need and resource. The National Planning Institute PP.20-45.

Ahmadi, E. & Tehrani ,A., (2009): Prevalence of obesity : Overweight and underweight among elementary school children in Southern Iran. American Journal of Applied Sciences, 7 (11): 1439-1442.

Bartklw, T. (2006): Standard weight table and food composition.2006, Available at; www. WHO.com.

Bisai, S., K. Bose, & Dikshit S. (2009) : Under-nutrition among children aged 3-6 years in Midnapore Town, India .The Internet Journal of Biological Anthropology.2:2

Cookfair,J. (2008)l sing Process and Practice in the community, ,St .Louis, Mosby pp 80-83

Cohen, (2003): Health education for all enabling school age children for healthy living Hygiene, 3(x1): 17-27

Dudek,(2003): The body Mass index (BMI) 23.8.058-basis of BMI and classification of overweight and obesity,

Edwards, L. , (2006): The school nurse's role in school-based clinics. Journal of School Health; 57(4) : 157-9,

Edemon, A. (2002): Health promotion through the life span3rd ed, Mosby Yearbook, U.S.A .pp. 499-539**.**

Elsamaloty , A. (2000) : Deviant behaviour of children homeless : Study of the culture of stranded house knowledge, Cairo University.

EL-Shiekh, O. (2005): Assessment of home environment and its relation to the child health in rural areas in Alexandria, Master Degree of Community Health Nursing, Faculty of Nursing , Alexandria University

Ghobashi, **C, & Mandie , R (2006):** Health promotion throughout the life span.(4th ed,) . U.S.A Mosby Year Book. :.pp 511-554.

Machle, W.& Olckle,P.(2007) : School based health promotion : The physician as advocate, Canad Med Assoc .J. 156 (5): 1301-1305**.**

Mclellan ,K. (1999): Health behaviour and the school environment in new South Wales ,Australia : V.9.8,Social Science Medicine, a (8): .611-619.

Mclellan , K. (2002): Depression measurement. Ph. D. Western Psychiatric Institute and Clinic, University of Pittsburgh, U.S.A.

Metwally, K & Olsen,M. (2005): Health Elementary Schools, (9th ed,) Mosby, Philadelphia. Chapter 4 .

Mohamed, M. (2001): Health perceptions and behaviours of school age boys and girls, in nursing care of infants and children (5th ed), Philadelphia Mosby: pp. 77:86

Mosa, M. (2005): Social merge children, the rate among homelessness. Ph.D Thesis, Faculty of Social Services, Mansura University (1st ed), Egypt, PP 17-40

Radwan, H. (2005): Health assessment a nursing approach,(3rd ed), Lippinpott . **Rosdad , p . (2004**) : Hand book of community nursing ,(2nd ed), saint Louis, London pp. 136=140.

Rosdad , p . (2004) : Hand book of community nursing ,(2nd ed), saint Louis, London pp. 136=140.

Peace, T. (2010) : Challenges of urban- slum primary children in attaining quality education in Uganda ,Available at http://sgs.mak.ac.ug/conference/index.php q=keynotes**.**

Scriven, A.,& Orme, J. (1996): Health promotion professional**, (**1st ed), London MacMillan Press : pp. 129-156.

Sedik A. (2002): Experiences in homeless children in Egypt, Cairo Centre to Protect Right of Children.

Stewart-Brown, S. (2006): What is the evidence on school health promotion in improving health or preventing disease and, specifically, what is the effectiveness of the health promoting schools approach? Copenhagen: WHO Regional Office for Europe Health Evidence Network report : Available at : http://www.euro.who.int/document/e88185.pdf,

Sherman , J., Honegger, S., & Givern (2002) : Comparative indicators of education in the United States and other countries:5(2). 1-8

Tallinn, C. (2008): Health systems for health and wealth. Copenhagen, WHO Regional Office for ,Available Europe, (http://www.who.int/document/e91438.pdf,p2-3

Viswanathan , M. (2006):Prevailing health problems in primary school children and role of school children and role of school nurse in El-Wayely Zone in Cairo Master Thesis Faculty of Nursing , Ain Shams University, pp 109-120.

General Health Insurance and WHO.(2001) : The health education of adolescents in the E.M.R.O. Seri 1: 1-42.

WHO. (2004): E.M.R.O Network of health promoting, Tech paper, ser 1.

11/20/2011

Pre-B Cell Colony-Enhancing Factor as a Marker of Erosions in Rheumatoid Arthritis Patients

Dina S. Al-Zifzaf[1], Eman A. Kaddah[1,] **Samah** A. El Bakri[2], Amer Abd ElZaher[2] and Rania Abo- Shady[3]

[1]Physical Medicine, Rheumatology and Rehabilitation Department, Ain Shams University, Cairo, Egypt
[2]Internal Medicine Department, Ain Shams University, Cairo, Egypt
[3]Clinical Pathology Department, Ain Shams University, Cairo, Egypt.
drdyassin@gmail.com

Abstract: Objective: Our objective in this study was to evaluate pre-B cell enhancing factor (PBEF)/ Visfatin as a disease marker of rheumatoid arthritis, studying its serum level, clinical significance, association with activity and radiographic joint damage. Methods: 28 patients diagnosed according to the 2010 American College of Rheumatology criteria for RA were enrolled in the study. They underwent clinical and laboratory assessment. Radiographic assessment was done and Larsen score was calculated. Anti-CCP3 IgG antibodies were determined using semiquantitative ELISA and Serum PBEF was determined using ELISA and statistical analysis of the results was performed. Results: There was a significant rise in both anti-CCP and serum PBEF levels in RA patients versus controls. PBEF serum levels were significantly higher among patients with erosions as compared to patients without detectable erosions. Serum PBEF showed a significant decrease among patients with severe activity as compared to patients with moderate activity. Using the Ranked Sperman Correlation test, we did not find any significant correlation between age of patients, disease duration, BMI, HAQ, VAS or the DAS 28 with the level of PBEF. The test validity characters for discrimination of erosions in RA for serum PBEF showed 53.8 % specificity, 86.7% sensitivity and 71.4% efficacy. Conclusion: PBEF has a role in the pathogenesis of RA and could be considered as a disease marker in RA and a marker of radiographic bone damage. Further studies are needed to determine the possibility of PBEF as a potential therapeutic target in early RA to prevent erosions.
[Dina S. Al-Zifzaf, Eman A. Kaddah, Samah A. El Bakri, Amer Abd ElZaher and Rania Abo- Shady **Pre-B Cell Colony-Enhancing Factor as a Marker of Erosions in Rheumatoid Arthritis Patients**. Life Science Journal. 2011; 8(4):628-634] (ISSN: 1097-8135). http://www.lifesciencesite.com.

Keywords: Pre-B cell colony-enhancing factor/ Visfatin, erosions, Rheumatoid arthritis**.**

1. Introduction

Rheumatoid arthritis (RA) is a chronic autoimmune disease characterized by systemic inflammatory and destructive joint lesions that are manifested by the involvement of joints, various organs and systems into the pathological process [1].

Failure to diagnose or treat a patient with RA at the early stages of the disease increases the risk of progression to persistent joint inflammation and damage. On the other hand, aggressively treating patients with mild arthritis, which probably will not evolve to erosive forms is also damaging. It exposes such patients to risk without proven benefits and represents the opposite of effective early treatment. Therefore, early diagnosis of those patients who will progress to more severe forms and consequently will require therapy that is more aggressive is essential [2].

It has been suggested that age at disease onset and/or patients' age have influence on disease activity and clinical outcome [3]. Furthermore, female gender, DRB1*04 alleles and the presence of anti-CCP antibodies at baseline were reported to be the most important predictors of radiographic progression. However, the utility of these parameters in clinical practice is limited by their relatively low positive predictive value [4].

Some authors stated that positive antibodies against cyclic citrullinated peptides (anti-CCP) correlated with both the radiological joint damage score and inflammatory parameters in early and established RA, indicating that anti-CCP could serve as a diagnostic tool and predict structural joint damage and thus they proposed that anti-CCP positive patients should receive aggressive therapeutic intervention [5].

Pre-B cell colony-enhancing factor (PBEF), also known as Visfatin, is a 52-kDa protein found in living species from bacteria to humans. PBEF has shown both nuclear and cytoplasmic expression. Within the cell, it functions as a nicotinamide phosphoribosyl transferase, the rate-limiting step in a salvage pathway of nicotinamide adenine dinucleotide (NAD) biosynthesis. By virtue of this role, it can regulate cellular levels of NAD and so affect not only cellular energetics but also NAD-dependent enzymes such as sirtuins. It has been shown to be an adipokine expressed by fat cells and exerts a number of insulin mimetic effects [6].

PBEF was added to a growing list of adipocytokines with potent effects on immunity and inflammation in addition to their metabolic activities [7]. In CD14 (+) monocytes, PBEF induces the production of IL-1beta, TNF-alpha, and IL-6. Moreover, it increases the surface expression of co-stimulatory molecules CD54, CD40 and CD80. PBEF-stimulated monocytes show augmented FITC-dextran uptake and an enhanced capacity to induce alloproliferative responses in human lymphocytes [8]. PBEF is induced by inflammation and immune activation. It enhances B cell differentiation, initiation of cytokines and matrix metalloproteinases and inhibits neutrophil apoptosis thus playing a key role in persistence of inflammation [9].

Though it lacks a signal peptide, PBEF is released by a variety of cells, and elevated levels can be found in the systemic circulation of patients with various inflammatory diseases. Its expression is up regulated in a variety of acute and chronic inflammatory diseases including rheumatoid arthritis, sepsis, acute lung injury, inflammatory bowel disease, and myocardial infarction [6]. A study on experimental animals proved that inhibition of PBEF markedly reduced inflammation, arthritis severity and cartilage damage in a collagen-induced arthritis model. They postulated that pharmacologic inhibition of PBEF led to reduced levels of intracellular NAD in inflammatory cells and decreased production of TNF-alpha and IL-6 by such cells with clinical effects comparable to those of a TNF-alpha inhibitor in a murine arthritis model [10]. Information about the connection between PBEF and disease activity in RA patients is conflicting and little is known about its role in radiographic joint damage.

The aim of this study was to evaluate pre-B cell enhancing factor (PBEF)/ Visfatin as a disease marker in RA by studying its serum level, clinical significance, association with activity and establishing it as a potential marker of radiographic joint damage in patients with rheumatoid arthritis. Consequently, we aimed at identifying PBEF as a potential therapeutic target in RA patients with erosive joint damage.

2. Patients and Methods:

Twenty-eight patients suffering from rheumatoid arthritis diagnosed according to the 2010 American College of Rheumatology criteria for RA [11], attending the Rheumatology and Rehabilitation outpatient clinic and the Rheumatology outpatient clinic of Internal Medicine Department of Ain Shams University Hospital were included in this study. Thirteen age-matched healthy individuals served as the control group. Patients gave informed consents to participate in the study. None of the patients and controls had diabetes mellitus.

Every patient included in this study was subjected to the following:

1. Full history taking with particular attention to disease duration, duration of morning stiffness, and activities of daily living.
2. Thorough clinical examination with particular attention paid to general examination and examination for extra-articular manifestations. As well as, complete musculoskeletal examination of all joints.
3. All patients underwent disease activity evaluation by the 28 joint Disease Activity Score (DAS-28). Patients with score $\leq$ 3.2 were classified as having inactive disease, scores of >3.2 - $\leq$ 5.1 were classified as having moderately active disease while > 5.1 denoted very active disease [12].
4. Pain was assessed by a 0-100 mm horizontal visual analogue scale (VAS). Zero indicated no pain while 100 indicated the worst intolerable pain.
5. Functional disability was evaluated using the Health Assessment Questionnaire (HAQ) to calculate the disability index (DI). The eight categories assessed by the DI are 1) dressing and grooming, 2) arising, 3) eating, 4) walking, 5) hygiene, 6) reach, 7) grip, and 8) common daily activities. The difficulty during each of these acts was assessed as follows: zero= without any difficulty, one=with some difficulty, two=with much difficulty and three=unable to do, then the sum of the categories scores is calculated and divided by the number of categories. This gives a score in the 0-3 range [13].
6. Laboratory investigations:

Sample collection:

- Two ml of venous blood were collected in EDTA-vacutainers for complete blood count.
- Two ml of blood were collected in plain vacutainers for analysis of CRP, Anti-CCP and PBEF.

Methods:

a. Complete blood picture (using Coulter counter).
b. Semi-quantitative measurement of C-reactive protein (CRP) by Latex agglutination assay (Teco Diagnostics, USA).
c. Erythrocyte sedimentation rate (ESR) by Westegren Blot technique.
d. Anti-CCP3 IgG antibodies (anti-Cyclic Citrullinated Peptide 3) were assessed using semiquantitative ELISA (INOVA DIAGNOSTICS, Inc. San Diego, USA). Validity of test results (Anti-CCP): High Positive control OD had to be > 1.0 while Negative control < 0.2 and low Positive

control OD had to be > 0.25 or more than twice the Negative control.

Calculation of Anti-CCP3 IgG: Sample value = sample OD/CCP3 IgG low positive OD x CCp3 IgG low positive control (units). Interpretation of results of anti –CCP: the sample is classified as negative if < 20 units and positive if ≥ 20 units.

e.Serum PBEF (Visfatin) assessment was determined using ELISA, based on the principle of Competitive Enzyme Immunoassay (RayBio,Inc. Norcross, GA). After incubation of the plate with anti-PBEF antibody, both biotinylated PBEF peptide and peptide standard or targeted peptide in samples interacted competitively with the PBEF antibody. Uncompeted (bound) biotinylated PBEF peptide then interacted with Streptavidin horse radish peroxidase (SA-HRP) which catalyzed a color development reaction that was measured at 450nm. The intensity of colorimetric signal was inversely proportional to the amount of PBEF peptide in the standard or samples.

7. Postero-anterior radiographs of hands, wrists, and forefeet were taken at inclusion in the study and on the day of sample collection. Joint destruction was classified by comparison with standard reference films according to the Larsen-Dale index [14]. The joints assessed for this index are the wrists, all metacarpo-phalangeal joints (=10), all proximal interphalangeal joints (=8), both first interphalangeal joints in the hands (=2), metatarso-phalangeal joints II-V (=8), and both first interphalangeal joints in the feet (=2). Thus, 32 joints are scored in all. The degree of erosive damage is the most decisive criterion in grading and the finding of at least one definite erosion in the radiographs was sufficient to consider the patient as having erosive disease. The Larsen score is the total sum of the grading in all 32 joints, with a range of 0-200. The x rays were read by two independent readers.

8. Statistical analysis:

IBM SPSS statistics (V. 19.0, IBM Corp., USA, 2010) was used for data analysis. Data were expressed as Mean ± SD for quantitative parametric measures.

The following tests were done:

1. Comparison between two independent mean groups for parametric data using Student t test.
2. Comparison between two independent groups for non-parametric data using Wilcoxon Rank Sum test.
3. Ranked Sperman correlation test to study the possible association between each two variables among each group for non-parameteric data. The probability of error at 0.05 was considered sig., while at 0.01 and 0.001 are highly sig. Diagnostic validity test including sensitivity, specificity, negative and positive predictive values were calculated.

3. Results

This study included 28 patients; 23 females (82.1%) and five males (17.9%). All patients fulfilled the ACR criteria for diagnosis of RA [11].

There was no significant difference between patients and controls as regards age, sex ratio or BMI. All patients were receiving methotrexate treatment in the range of 15-22 mg/ week as well as folic acid and NSAIDs upon need. Rheumatoid factor was positive in all 28 patients. The mean disability index as determined by the HAQ ranged from 0.25 to 2.88 with a mean of 1.15 ± 0.7.The outcome of clinical and laboratory evaluation of studied patients is shown in table 1.

Table (1): clinical and laboratory data of RA patients included in the study

Variable	Min.	Max.	Mean	SD
Age (years)	22	60	42.3	9.4
Disease duration (years)	0.17	24	6.6	5.57
Morning stiffness duration (minutes)	5	60	30.7	19.7
BMI (kg/m^2)	18	30	26.7	3.03
VAS pain score	10	90	46.4	21.6
Number of swollen joints	0	10	2.8	3.3
Number of tender joints	0	24	10.6	6.5
ESR 1st hr (mm/hr)	20	85	48.4	14.3
CRP(mg/dl)	3	96	49.4	38.9

*ESR: Erythrocyte sedimentation rate *CRP: C-reactive protein *SD: Standard deviation

Evaluation of disease activity using the DAS-28 score revealed a mean score of 5.35 ± 1.19. There were thirteen patients (46.4%) with moderately active disease with a mean DAS-28 score of 4.3 ± 0.5 and fifteen patients (53.6%) had very active disease with a mean DAS-28 score of 6.28 ± 0.7.

Radiological evaluation of patients revealed Larsen score ranging from 6 to 129 with a mean of 59.17 ± 32.8. Patients without erosions evident in their x-rays were 13 (46.4%) with a Larsen score ranging from 6 to 38, the mean being 34.5 ± 9.0. Patients with erosive disease were 15 (53.6%) with

Larsen score ranging from 40 to 129, the mean being 80.6 ± 30.7.

In the healthy controls, the anti-CCP ranged from 5.2-10.6 IU/ml with a mean of 8.12± 2.13.The mean level of anti-CCP antibodies in the serum of RA patients was 92.69 ± 112.9 IU/ml. The mean level of PBEF in the control group was 5.8 ± 8.8 pg/ml, while in rheumatoid patients it was 59.8 ± 109.2 pg/ml. There was a significant difference between both anti-CCP and serum PBEF levels in patients and controls (Table 2).

Table (2): Comparison between the RA patients and the control group as regard the serum anti-CCP and serum PBEF level.

		No.	Mean	SD	z	p	Sig.
Anti-CCP IU/ml	Controls	13	8.12	2.13	-0.9	<0.05	S
	Patients	28	92.68	112.9			
PBEF pg/ml	Controls	13	5.8	8.8	-3.188	< 0.001	HS
	Patients	28	59.8	109.2			

*CCP: Cyclic citrullinated peptides *PBEF: pre-B cell enhancing factor *sig.: Significance

Comparison between patients with erosions (15 patients), and patients with no evidence of erosions (13 patients) as regards age, BMI, ESR, DAS and anti-CCP levels revealed no significant difference. On the other hand, PBEF serum levels showed a significant difference between the two groups (Table3).

Table (3): Serum anti-CCP and PBEF levels in RA patients with and without erosive lesions.

	EROSION	n	Mean	SD	Z	p	Sig.
Anti_CCP IU/ml	Negative	13	89.3	116.1	0	>0.05	NS
	Positive	15	95.8	114.1			
PBEF pg/ml	Negative	13	20.8	23.9	-2.22	<0.05	S
	Positive	15	93.5	140.9			

*CCP: Cyclic citrullinated peptides *PBEF: pre-B cell enhancing factor *sig.: Significance

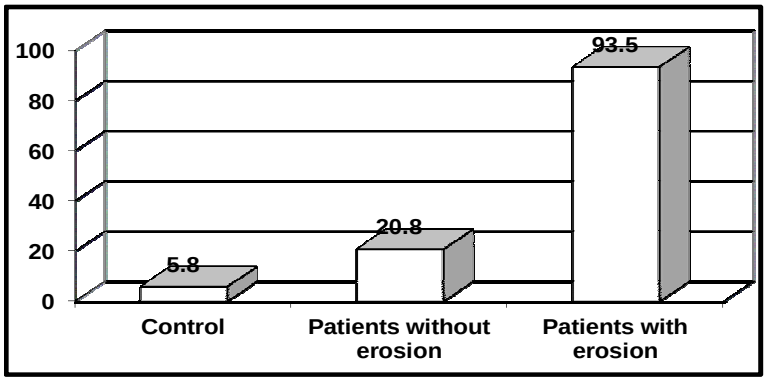

Figure (1): Comparison between control, RA patients without and with erosion as regards mean values of PBEF (pg/ml)

The HAQ score revealed a highly significant rise among patients with severe activity (p= 0.00). Serum PBEF showed a significant decrease (p=0.03) among patients with severe activity (22.7 ± 20.8 pg/ml) as compared to patients with moderate activity (102.5 ± 150.2 pg/ml).

Using the Ranked Sperman Correlation test, we did not find any significant correlation between age of patients, disease duration, BMI, HAQ, VAS or the DAS 28 with the level of PBEF.

The test validity characters for discrimination of RA patients from controls for serum PBEF at the best cut off value of 1.8 pg/ml showed 53.8 % specificity, 85.7% sensitivity and 75.6% efficacy (Fig. 2).

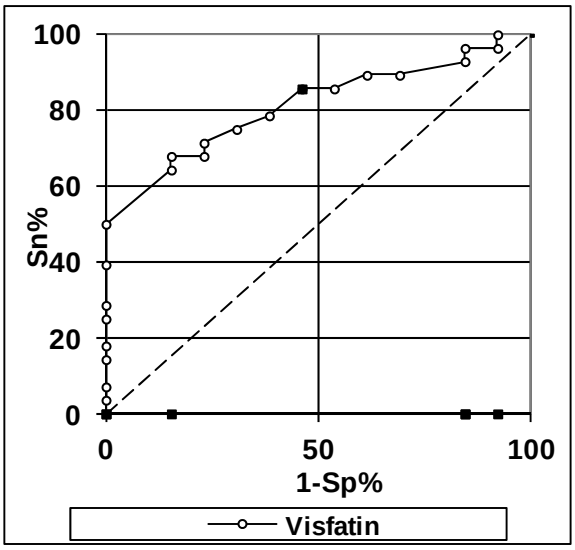

AUC	
PBEF	0.836

*AUC: Area under the curve

Figure (2): ROC curve analysis showing the diagnostic performance of PBEF in discriminating patients with RA from controls

The test validity characters for discrimination of erosions in RA for serum PBEF at the best cut off value of 8 pg/ml showed 53.8 % specificity, 86.7% sensitivity and 71.4% efficacy (Fig. 3).

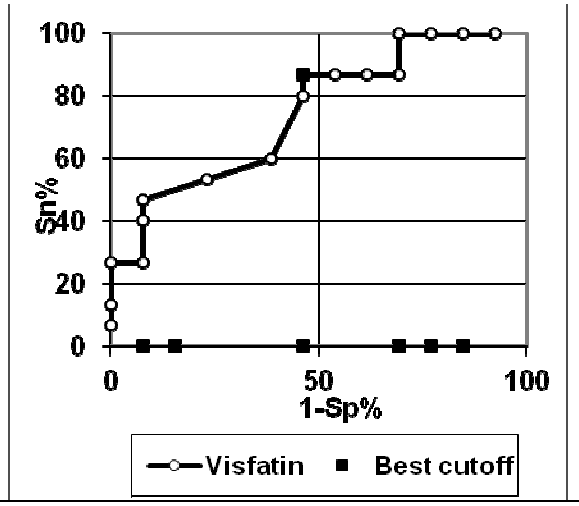

AUC	
PBEF	0.675
PBEF	0.496

Figure (3): ROC curve analysis showing the diagnostic performance of PBEF in discriminating RA patients with erosion from those without erosions

4. Discussion

As current predictors of joint destruction in rheumatoid arthritis have low specificity, serological biomarkers reflecting bone and cartilage destruction have been proposed as tools in assessing prognosis of this disease [15].

Anti-citrullinated peptide antibodies (ACPAs) are established as useful predictors of radiographic

progression in rheumatoid arthritis (RA). Other markers as anti-mutated citrullinated vimentin (anti-MCV), increased urinary levels of C-terminal cross-linked telopeptide of type II collagen (U-CTX-II), an increased urinary total pyridinoline/total deoxypyridinoline (U-PYD/DPD) ratio were independently associated with a higher risk for progression of bone erosion in RA [15, 16].

Pre B-cell colony enhancing factor (PBEF)/ Visfatin was reported to be an adipocytokine having proinflammatory and immunomodulating properties**.** However, the pathological role and clinical relevance of PBEF in the setting of RA are still unclear [17].

In this study, serum PBEF levels in RA patients were significantly higher than controls (z= -3.19, $p< 0.001$). Similar results were reported by several authors [9,18, 19]. Moreover, further research added that this adipocytokine was up regulated in synovial fluid of RA patients and demonstrated synovial fibroblasts as the major PBEF-producing cells in the rheumatoid synovium [17, 20].

No significant correlations between PBEF concentrations and the age of patients at the time of the study or disease duration were detected. These results were consistent with what was previously reported by some authors [21]. In disagreement with our findings, a recent study reported that PBEF concentrations correlated significantly with disease duration, which in their case could be due to progression of the disease over the time with increased bone erosions [9].

Serum levels of PBEF did not correlate with body mass index (BMI) in our series of patients with active RA in contrast to the case in non-RA subjects with wide range of BMI. These findings were in agreement with other research on RA patients [9, 19, 21]. This denotes that PBEF is an adipocytokine whose production in RA patients does not solely relate to the BMI but also to the disease process as part of the systemic inflammation and bone destruction suggesting a role for PBEF in the pathogenesis of RA.

In this study, we found that serum levels of PBEF did not correlate with parameters of disease activity whether clinical or laboratory markers of inflammation such as CRP or ESR levels. These findings differ from another study that reported that PBEF was correlated with serum markers of inflammation as well as clinical disease activity scores [17]. On the other hand, our results were in agreement with other groups reporting no significant correlation between PBEF levels and ESR, CRP levels or DAS 28 [19, 21]. Interestingly, our results showed a significant decrease of serum levels of PBEF in the group of RA patients with severe activity (mean $\pm$ SD = 22.7 $\pm$ 20.8 pg/ml) in comparison to the group of patients with moderate activity (mean $\pm$ SD= 102.5 $\pm$ 150.2 pg/ml). Such findings are somehow unexpected. However, they may be explained by depletion of PBEF in patients' sera due to its accumulation in the active joints synovial fluid and its predominant expression at sites of invasion into cartilage [17]. It is also possible that in patients with RA in the presence of the high inflammatory burden, PBEF secretion might be negatively influenced by other adipokines or other factors as part of a compensatory mechanism that aims to maintain a normal homeostasis in these patients.

To establish if RA patients with radiographic damage had greater concentrations of PBEF than those without erosions, we divided patients into two groups; group I included patients with erosions while group II included those without erosions according to Larsen score. A significant increase in PBEF serum levels was noticed in patients with erosive disease in comparison to those without (mean $\pm$ SD = 93.5 $\pm$ 140.9 and 20.8 $\pm$ 23.9 pg/ml respectively). In addition, a sensitivity analysis revealed 86.7% sensitivity of PBEF for discrimination of erosions. Influenced by this high sensitivity, we can speculate that PBEF is associated with radiographic damage in RA patients. Such results were in accordance with the findings reported in 2009 that PBEF concentrations were associated with higher Larsen scores, and this association remained significant after adjustment for age, race, sex, disease duration, BMI, and inflammation [9]. These findings suggest a role for PBEF as a mediator of joint damage in RA. Such results are supported by experimental animal research that suggested that PBEF modulated inflammatory responses and radiographic joint damage in animal models [10]. The mechanism by which PBEF plays a destructive role in joints of RA patients is through activation of the transcription factors NF-kB and activator protein 1 and induction of IL-6, IL-8, MMP-1 and MMP-3 in RA synovial fibroblasts (RASFs) as well as IL-6 and TNF alpha in monocytes of these patients [17].

Conclusion:

Due to its evident role in the pathogenesis of RA, Pre-B cell colony-enhancing factor/ Visfatin could be considered a useful disease marker in RA and a marker of bone destruction and radiographic damage. Further studies are needed to determine the possibility of PBEF as a potential therapeutic target in early RA to prevent erosions.

Conflict of interest statement

The authors have no conflict of interest to declare.

Corresponding author:
Dina S. Al-Zifzaf.
Associate professor of Physical medicine, rheumatology and rehabilitation
Faculty of medicine- Ain Shams University, Cairo, Egypt.
drdyassin@gmail.com

References

[1] Deciduas NV, Guseva IA and Karateev DE. (2010). Clinical and immunological aspects of early-stage rheumatoid arthritis. Ter Arkh.; 82(5): 71-7.
[2] Mota LM, Laurindo IM and Santos Neto LL. (2010). Early rheumatoid arthritis: concepts. Rev Assoc Med Bras; 56(2): 227-9.
[3] Pawłowska J, Smoleńska Z and Daca A, *et al.* (2011). Older age of rheumatoid arthritis onset is associated with higher activation status of peripheral blood CD4 (+) T cells and disease activity. Clin Exp Immunol.; 163(2): 157-64.
[4] Sanmartí R, Gómez-Centeno A and Ercilla G, *et al.* (2007). Prognostic factors of radiographic progression in early rheumatoid arthritis: a two year prospective study after a structured therapeutic strategy using DMARDs and very low doses of glucocorticoids. Clin Rheumatol., 26(7): 1111-8.
[5] Kim Y, Choi B and Cheon H, *et al.* (2009). B cell activation factor (BAFF) is a novel adipokine that links obesity and inflammation. Exp Mol Med.; 41: 208-16.
[6] Luk T, Malam Z, and Marshall J. (2008). Pre-B cell colony enhancing factor (PBEF)/visfatin: a novel media innate immunity. J Leucoc Biol.; 83(4): 804-16.
[7] Fukuhara A, Matsuda M and Nishizawa M, *et al.* (2005).Visfatin: a protein secreted by visceral fatthat mimics the effects of insulin.Science; 307: 426-30.
[8] Moschen AR, Kaser A and Enrich B, *et al.* (2007). Visfatin, an adipocytokine with proinflammatory and immunomodulating properties. J Immunol.; 178(3): 1748-58.
[9] Rho YH, Solus J and Sokka T, *et al.* (2009). Adipocytokines are associated with radiographic joint damage in rheumatoid arthritis. Arthritis Rheum.; 60(7): 1906-14.
[10] Busso N, Karababa M and Nobile M, *et al.* (2008). Pharmacological inhibition of nicotinamide phosphoribosyl-transferase/visfatin enzymatic activity identifies a new inflammatory pathway linked to NAD. Plos One; 3: 2267.
[11] Aletaha D, Neogi T and Silman A J, *et al.* (2010). Rheumatology/European League Against an American College of 2010 Rheumatoid arthritis classification criteria: Rheumatism collaborative initiative. Ann Rheum Dis.; 69: 1580-1588.
[12] Prevoo MLL, van't Hof MA and Kuper HH, *et al.* (1995). Modified disease activity scores that include twenty eight joint counts. Arthritis Rheum., 38: 44-8.
[13] Ekdahl C, Eberhardt K and Andersson I, *et al.* (1988). Assessing disability in patients with rheumatoid arthritis. Scand J Rheumatol.; 17:263-71.
[14] Larsen A, Dale K and Eek M. (1977). Radiographic evaluation of rheumatoid arthritis and related conditions by standard reference films. Acta Radiol Diagn.; 18: 481-91.
[15] Syversen SW, Goll GL and van der Heijde D, *et al.* (2010). Prediction of radiographic progression in rheumatoid arthritis and the role of antibodies against mutated citrullinated vimentin: results from a 10-year prospective study. Ann Rheum Dis.; 69(2):345-51.
[16] Hashimoto J, Garnero P and van der Heijde D, *et al.* (2009). A combination of biochemical markers of cartilage and bone turnover, radiographic damage and body mass index to predict the progression of joint destruction in patients with rheumatoid arthritis treated with disease-modifying anti-rheumatic drugs. Mod Rheumatol. ; 19(3): 273-82
[17] Brentano F, Schorr O and Ospelt C, *et al.* (2007). Pre-B cell colony-enhancing factor/visfatin, a new marker of inflammation in rheumatoid arthritis with proinflammatory and matrix-degrading activities. Arthritis Rheum.,56(9): 2829-39.
[18] Otero M, Lago R and Gomez R, *et al.* (2006). Change in plasma level of fat-derived hormonesadiponectin, leptin, resistinand visfatin in patients with rheumatoid arthritis. Ann Rheum Dis. ;65:1198-201.
[19] Senolt L, Kryštůfková O and Hulejová H, *et al.* (2011). The level of serum visfatin (PBEF) is associated with total number of B cells in patients with rheumatoid arthritis and decreases following B cell depletion therapy**.** Cytokine. Apr 25. (Epub ahead of print).
[20] Nowell M, Richards P and Fielding C, *et al.* (2006). Regulation of pre-B cell colony enhancing factor by STAT 3-dependent interleukin- 6 trans signaling: implications in the pathogenesis of rheumatoid arthritis. Arthritis Rheum.; 54; 2084-95.
[21] Gonzalez-Gay M, Vazquez-Rodriguez T and Garcia-Unzueta M, *et al.* (2010). Visfatin is not associated with inflammation or metabolic syndrome in patients with severe rheumatoid arthritis undergoing anti-TNF-a therapy. Clin Exp Rheumatol; 28: 56-62.

11/11/2011

Provably Secure Password-based Three-party Key Exchange Protocol with Computation Efficiency

Jih-Ming Fu[1], Jeng-Ping Lin[2], Ren-Chiun Wang[3*]

1 Department of Computer Science & Information Engineering, Cheng Shiu University, No.840, Chengcing Rd., Niaosong Dist., Kaohsiung City 83347, Taiwan (R.O.C.)
2 Department of Commerce Technology & Management, Chihlee Institute of Technology, 313, Sec. 1, Wunhua Rd., Banciao District, New Taipei City, 22050 Taiwan, R.O.C
3 Project Resource Division, Institute for Information Industry
rcwang@icst.org.tw

Abstract: Going along with the rapid development of web technologies, people can make a great quantity of service requests to service providers using mobile devices anytime and anywhere. However, the service requester and the service providers may not trust each other and they may locate at different domain. They require a communal trusted third party to help them establish a shared session key for secure communications. It is so-called three-party key exchange. Recently, many password-based three-party key exchange protocols were proposed against various well-known security threats. In those protocols, to prevent the password guessing attack, a widely used way is to employ public-key and/or symmetric-key cryptosystems to protect the exchanged messages. As we known, the encrypted and decrypted operations in a public-key cryptosystem are time-consuming. In this paper, we propose a password-based three-party key exchange protocol with the computation-efficiency without using public-key systems. Finally, we prove the security of the proposed protocol in the random oracle model.

[Jih-Ming Fu, Jeng-Ping Lin, Ren-Chiun Wang. **Provably Secure Password-based Three-party Key Exchange Protocol with Computation Efficiency.** Life Science Journal. 2012;8(4):635-643] (ISSN:1097-8135). http://www.lifesciencesite.com.

Keywords: cryptography; discrete logarithm problem; on-line undetectable password guessing attack; three-party key exchange.

1. Introduction

Today, people have many opportunities to obtain services or resources from application servers by using their mobile devices through the Internet. However, both of the clients and the servers may be distributed over different network domains and do not win the trust each other. A secure mechanism has to make sure that the identity of the clients and the server can be authenticated each other and the communications are secure against an unauthorized user from eavesdropping the delivery contents[1-2,5]. The client and the application server require a communal trusted third party[3-4,17].

Password is widely employed to construct a secure key exchange protocol since password-based protocols are easily to be developed and to be maintained. However, users have to worry about whether their passwords (have low entropies) have been guessed or not. The password guessing attacks can be divided into three kinds[11-12]:

1) **On-line detectable guessing attack.** Attacker can enumerate all the candidature passwords and pick up one from the list. Then the attacker sends the chosen password to connect the server and verifies the server's response in on-line. Most password-based protocols can prevent this attack by the server limits the fail times.
2) **On-line undetectable guessing attack.** Attacker can enumerate all the candidature passwords and pick up one from the list. Then the attacker sends the chosen password to connect the server and verifies the server's response in on-line. Since the server cannot discriminate whether the request is malicious or honest, therefore the server always replies a honest response. The attacker can catch this chance to guess the password until the password is correctly obtained[23].
3) **Off-line guessing attack.** Since the communicated channel is open, any eavesdropper can collect all the communications. Then the attacker can enumerate all the candidature passwords to launch the attack off-line until a hit is obtained without the help of the server.

Many password-based three-party key exchange protocols were proposed and addressed

to overcome the above guessing attacks by using the concept of public-key and symmetric-key techniques[10-11,19-20,26]. For enhancing the efficiency dramatically, in 2007, Lu and Cao proposed a simple three-party key exchange protocol[21] without using the server's public key. Unfortunately, Lu-Cao's key exchange protocol suffered from the unknown key sharing[1], the on-line undetectable guessing, and the impersonation attacks[12,15,18,23]. For guaranteeing the quality of communication services, low communication and computation cost is required in a three-party key exchange protocol. In 2009, Huang[16] proposed an efficiency-enhanced password-based three-party key exchange protocol. Huang claimed that the proposed protocol is also more efficient than Lu-Cao's protocol and can be applied in practice. However, Huang's protocol is still not secure against the on-line undetectable guessing attack[25].

We propose a provably secure password-based three-party key exchange protocol to withstand various well-known security threats by using the random oracle model[3,11,22]. Compared with the related protocols [10-11,20], our proposed protocol is computation-efficient.

In the next section, we first give a notation of security. In Section 3, we propose a novel three-party key exchange protocol. In Section 4, we analyze the security of the proposed protocol. In Section 5, we analyze the efficiency among our proposed protocol and the related protocols. Finally, we conclude this paper in Section 6.

4) An unknown key-sharing attack on a key exchange protocol which provides the key confirmation property is an attack whereby an entity A believes that she shares a session key with the communicated entity B. Unfortunately, it is fact that if the entity B mistakenly believes that the session key is instead shared with another entity E, where $E \neq A$. A secure key exchange protocol should be against this threat[6,8].

2. Notations of Security

We first define some hard mathematical problems and security of a password-based three-party protocol.

2.1 Hard Problems

1) **Definition 1. Discrete Logarithm Problem (DLP).** Given two elements g and g^a, it is computationally infeasible to find a, where p is a large prime number, g is a generator with order q in $GF(p)$ and $a \in Z_q^*$.

2) **Definition 2. Computational Diffie-Hellman Problem (CDHP).** Given three elements g, g^a, and g^b, it is computationally infeasible to calculate g^{ab}, where p is a large prime number, g is a generator with order q in $GF(p)$ and both of a and $b \in Z_q^*$.

3) **Definition 3. Decisional Diffie-Hellman Problem (DDHP).** Given four elements g, g^a, g^b, and g^c, it is difficult to decide whether c mod q is equal ab mod q, where p is a large prime number, g is a generator with order q in $GF(p)$ and all of a, b and $c \in Z_q^*$.

2.2 Security Definitions

The concrete security of a three party-based protocol is built up both the property of the session key indistinguishability and the protection of the password[7,22]. In a password-based protocol, an on-line detectable guessing attack[14] is inherent and is inevitable. However, this attack can be prevented by locking the account after some reasonable failed attempts in most password-based protocols. A more dangerous attack is the off-line guessing attack after an adversary copies a transcript of executions in a password-based protocol. The mission of a password-based protocol is to rule out the off-line guessing attack and to limit the adversary only to the on-line detectable guessing attack. For thwarting the online detectable guessing attack, the service requesters' requests are required to be authenticated for the operations of the trusted server from distinguishing malicious attempts from real requests. Also, for deterring the on-line undetectable and the off-line guessing attacks, the proposed protocol has to live up to the requirement of attackers that they may pick up the correct password but cannot verify their guessing from the eavesdropped messages.

We denote the proposed protocol, a service requester C_A and a service provider $C_B \in \hat{C} = \{C_1, ..., C_{NC}\}$ and a trusted server S. Each service requester C_A and a service provider $C_B \in \hat{C}$ hold memorial passwords pw_A and pw_B, and the server S maintains a password table $<P_1, ..., P_{NC}>$. We also assume that an adversary AD who controls all the communications that take place by C_A^i, C_B^j and S is a probabilistic machine, where we denote that C_A^i is the ith instance of the service requester C_A and C_B^j is the jth instance of the service provider C_B. AD can interact with all the participants (C_A, C_B, S) through the following oracle queries.

1) Execute(C_A^i, C_B^j), Execute(C_A^i, S), Execute(C_B^j, S): We use this query to model passive attacks where an attacker can eavesdrop all the communications between the instances (C_A^i, C_B^j)

and between the instances (C_A^i, S), and (C_B^j, S) respectively.

2)SendClient(C_A^i, m): We use this query to model an active attack against that the attacker sends a message m to a participant C_A at the ith instance. Then query outputs the result of C_A from receiving the message m to generate.

3)SendServer(m): We use this query to model an active attack against that the attacker sends a message m to the server S. Then query outputs the result of S from receiving the message m to generate.

4)Reveal(C_A^i): We use this query to model an active attack against the known-key attack at the ith instance C_A. The query says that if the instance does not accept the session key, the output is $\perp$; otherwise, the output is the real session key.

5)Corrupt(C_A): We use this query to allow that an attacker AD can corrupt the complete internal state of an entity C_A.

6)Test(C_A^i): If an attacker AD queries this oracle and no session key for $C_A^i \in \hat{C}$ is accepted, this oracle outputs $\perp$; otherwise, the oracle flips a coin b. If $b = 1$, returns the real session key; if $b = 0$; returns a random key which has the same key with the real session key.

The security definition of the proposed protocol depends on the partnership and freshness of oracles, where the partnership of the oracles is defined using the session identifiers *sids* and the partnership is defined to restrict the adversary's Reveal and Corrupt queries. If the partnership is not accepted by the oracles, the adversary is trying to guess the session key.

1)Partnership: We say that two oracles C_A^i and C_B^j are partners, if and only if both of the oracles have accepted the same session key with the same session identifier and they have agreed on the same set of exchanging messages. Besides C_A^i and C_B^j, no other oracles have accepted with the same session identifier.

2)Freshness: We say that two oracles C_A^i and C_B^j are fresh if and only if the oracle C_A^i has accepted another partner oracle C_B^j, the oracle C_B^j has accepted another partner oracle C_A^i, and all the oracles C_A^i and C_B^j have not been sent a Reveal query a Corrupt query.

3)Session key security: We use the standard semantic security notation to model this property[22]. The security of session key is defined that the adversary who wants to discriminate a real key from a random one in the game G is indistinguishable, where the game played between the adversary AD and a collections of U_x^i oracles. The players $U_x \in \hat{C}$ and S and instances $i \in \{1, ..., N_I\}$. AD runs the game G with the following stages.

- Stage 1: AD is allowed to send the queries (Execute, SendClient, SendServer, Reveal and Corrupt) in the game.
- Stage 2: During the game G, at some point, AD can choose a fresh session and end a Test query to one of the fresh oracles C_A^i and C_B^j for the testing. Depending on the unbiased coin b, AD is given ether the actual session key K or a random one from the session key distribution.
- Stage 3: AD can continue to send the queries to the oracles Execute, SendClient, SndServer, Reveal and Corrupt for its choice. However, AD is restricted to send the Reveal and Corrupt queries to the oracles for its test session.
- Stage 4: Eventually, AD winds up the game simulation and decides to output its guess bit b'.

The success of AD from breaking the protocol in the game depends on passwords which are drawn from a dictionary D and is measured in terms of the advantage of AD from distinguishing whether the received value is the real key or a random one. Let $Adv_{P,D}^{G,AD}(k, q_{fake\text{-}C})$ be the advantage of AD and the advantage function be be defined as follows.

$$Adv_{P,D}^{G,AD}(k,q_{fake\text{-}C})=|Pr[b'\text{-}b]\text{-}q_{fake\text{-}C}/N\text{–}1/2*(N\text{-}q_{fake\text{-}C})| \quad (1)$$

where k is a security parameter, N denotes the size of the dictionary D and $q_{fake\text{-}C}$ denotes the number of attempts of the adversary from faking the client. After $q_{fake\text{-}C}$ times of faking the client, the intuition of the formulation is that the advantage of the adversary from finding the correct password and from faking the session key successfully should have the probability at most $q_{fake\text{-}C}/N$. The rest of non-successful faking cases could have the successful probability 1/2.

Password protection: An adversary may try to guess the password of a valid client and verify its guess through the interaction with the server or the client or from the intercepted messages. We require that the protocol has to provide the explicit authentication of a client's request for thwarting the online detectable guessing attack in which the server can do some actions such that the limitation of invalid request attempts cannot exceed the pre-defined threshold. Security against the adversary from launching the off-line guessing and the online undetectable guessing attacks, the protocol should not provide any advantageous information to outsiders or to a curious partner to verify its guess.

Definition 4. We say that a password-based

three-party key exchange protocol is secure in our model when the following requirements are satisfied:

1) Validity: Among three oracles (C_A^i, C_B^j, S), the oracles (C_A^i, C_B^j) accept the same session key in the absence of an active adversary.

2) Session key indistinguishability: For all probabilistic, the advantage of the adversary AD is negligible within a polynomial time.

3) Explicit authentication: As the above mentioned, the protocol should make sure that the explicit authentication of two communicated parties is done for being against the online detectable guessing attacks.

4) Password protection: As the above mentioned, the protocol should not provide any advantageous information to outsiders or to a curious partner to verify its guess for being against the off-line guessing and the undetectable online guessing attacks.

3. Our Proposed Protocol

In our protocol, we define $h_1()$ and $h_2()$ are secure cryptographic one-way hash functions and we will model the functions as random oracles in the security proof. The other parameters are introduced as follows:

A. The system selects a large prime number p, where (p - 1) has a prime factor q.

B. Let g be a generator with order q in $GF(p)$.

C. *TS* denotes the trusted third party.

D. A and B denote two communicated parties.

E. pw_A and pw_B denote the passwords that A shared with *TS* and B shared with *TS*, respectively.

F. $\oplus$ denotes an exclusive OR operation.

G. For simplicity, all the exponentiation operations are under the modular p such as g^x mod $p \rightarrow g^x$.

1) Request that initiator A selects a random number x, calculates $R_A = g^x \oplus h_1(pw_A, A, B, sid)$, and sends ($A$, *sid*, R_A) to the responder B, where the *sid* denotes the session identity.

2) Upon receiving the request, B also selects a random number y, calculates $R_B = g^y \oplus h_1(pw_B, A, B, sid)$, and sends ($B$, R_B) with A's request to the trusted server *TS*.

3)(a) Upon receiving (A, B, *sid*, R_A, R_B), *TS* employs the passwords pw_A and pw_B to extract the exchanged information g^x and g^y, respectively. Then T selects three random numbers (z_1, z_2, z_3) and calculates (a, b, c, d), where $a = g^{xz_1}$, $b = g^{yz_1}$, $c = g^{z_2}$, and $d = g^{z_3}$.

(b) *TS* sends (A, *sid*, Z_{A1}, Z_{A2}) and (B, *sid*, Z_{B1}, Z_{B2}) to A and B in parallel, where $Z_{A1} = b \oplus h_1(pw_A+1, A, B, sid)$, $Z_{A2} = c \oplus h_1(pw_A+2, A, B, sid)$, $Z_{B1} = a \oplus h_1(pw_B+1, A, B, sid)$, and $Z_{B2} = d \oplus h_1(pw_B+2, A, B, sid)$.

4) Do in parallel

(a) Upon receiving (B, *sid*, Z_{B1}, Z_{B2}), B employs $h_1(pw_B+1, A, B, sid)$ and $h_1(pw_B+2, A, B, sid)$ to recover a and d. B then calculates the session key $K = h_2(A, B, sid, a^y)$, $S_{B1} = h_1(A, B, sid, K)$ and $S_{B2} = h_1(A, B, sid, d^y, a)$. B sends S_{B1} to A and S_{B2} to *TS* for identifying the validation of its identity and the session key.

(b) Upon receiving (A, *sid*, Z_{A1}, Z_{A2}), A employs $h_1(pw_A+1, A, B, sid)$ and $h_1(pw_A+2, A, B, sid)$ to recover b and c. A then calculates the session key $K = h_2(A, B, sid, b^x)$, $S_{A1} = h_1(A, B, sid, K+1)$ and $S_{A2} = h_1(A, B, sid, c^x, b)$. A sends S_{B1} to B and S_{A2} to *TS* for identifying the validation of its identity and the session key.

5) Do in parallel

(a) Both of A and B can authenticate each other by checking the validation of S_{B1} and S_{A1} and believe that the owned session key is fresh.

(b) Upon receiving A and B's responses, *TS* can check the validation of S_{B2} and S_{A2}. If any of the conditions does not hold, *TS* will return "*connection failure*" message to the corresponding parties and increase the fail times by one. We introduce the proposed protocol in Figure 1.

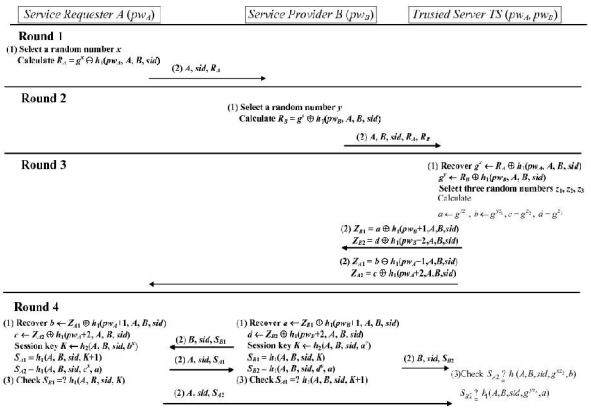

Figure 1. The proposed protocol

4. Security Analysis

In this section, we analyze that the proposed protocol is secure against some well-known attacks. Before our analysis, we first assume that the following mathematical problems are hard to be solved[9,13].

4.1 Analysis

1) **Session Key Security.**

(a) Even if $a = g^{xz_1}$ and $b = g^{yz_1}$ are known by an adversary, based on the difficulty of the CDHP, the adversary cannot derive the session key $K = g^{xyz_1}$ except the parties A and B.

(b) Based on the properties of one-way hash function and the exclusive-OR operator, the adversary is useless to derive (g^x, b, g^y, a) without the knowledge of A and B's passwords. The reason is that the extracted values cannot be verified. The adversary wants to discriminate (g^x, b, g^y, a) from (R_A, R_B, Z_{A1}, Z_{B1}), the probability of obtaining the session key K is equivalent to solve the CDHP on (Z_{A1}, S_{A1}, Z_{B1}, S_{B1}).

2)**Replay Attack.** An adversary who wants to imitate the requester A can resend the used messages ($R_A = g^x \oplus h_1(pw_A, A, B, sid)$) to B or to TS and expect to obtain some useful information from TS such as ($Z_{A1} = g^{yz_1} \oplus h_1(pw_A+1, A, B, sid)$, $Z_{A2} = g^{z_2} \oplus h_1(pw_A+2, A, B, sid)$). Based on the CDHP assumption, the adversary not only cannot derive new session key $K = g^{xyz_1}$ without the knowledge of the ephemeral keys x, but also cannot win the trust of TS without the knowledge of the passwords pw_A since g^{z_2} is encrypted using the password pw_A.

3)**Impersonation Attack.** In Round 3 of our proposed protocol, when someone sends the exchanged messages to TS, TS always returns the messages (Z_{A1}, Z_{A2}, Z_{B1}, Z_{B2}) back. The adversary can catch this chance to launch the attack. Note that TS waits the responses in Round 4. Since all the exchanged messages must be encrypted using the password independently, the adversary cannot know whether the guessed password is correct or not and also cannot judge whether the received message S_{B1} and the computed results (S_{A1}, S_{A2}) are correct or not. Based on the difficult of the CDHP, this way is blocked.

4)**Password Guessing Attack.**

(a) On-line detectable guessing attack. In current systems, there is a standard mechanism to defeat this attack. The solution is that the remote server logs and counts the number of trial failures. If the number is larger than the pre-defined threshold values, the server stops the connection. This concept can be applied to our protocol since TS verifies whether A and B's responses (S_{A2}, S_{B2}) are correct or not in Round 4 and records the failure times.

(b) On-line undetectable guessing attack. To launch the attack successfully, the attacker has to get some useful information in advance for manipulating the data and verifying their guess on TS's response (or B's response). The attack cannot work on our protocol since all the requests have to be sent to TS and TS will wait the feedbacks from both of A and B. It implies that any trial process will be detected by TS. The attack fails.

(c) Off-line guessing attack. All the exchanged messages are encrypted using the passwords independently. The goal of the adversary is to guess the password and to verify the correctness on the intercepted messages. Based on the difficult of the CDHP, the adversary cannot employ the guessed password and derive messages to obtain any results on the messages (S_{A1}, S_{A2}, S_{B1}, S_{B2}) in Round 4.

5)**Forward/Backward Secrecy.**

(a) In each session, A, B and TS select their ephemeral keys (x, y, z_1, z_2) to construct ($R_A = g^x \oplus h_1(pwA, A, B, sid)$, $R_B = g^y \oplus h_1(pw_B, A, B, sid)$, $z_{A1} = b \oplus h_1(pwA+1, A, B, sid)$, $z_{B1} = a \oplus h_1(pw_B+1, A, B, sid)$). Based on the difficult of the CDHP, the adversary cannot calculate the session key $K = h_2(A, B, sid, g^{xyz_1})$ in all the sessions even if the passwords are guessed correctly. The property of the forward secrecy is provided.

(b) Even if one of the used session key $K = h_2(A, B, sid, g^{xyz_1})$ is compromised by the adversary, the adversary cannot obtain any useful information on the corresponding messages. For instance, the adversary may guess the password to get $g^{x'}$ and $g^{yz_1'}$. Based on the difficult of the CDHP, the adversary cannot verify the guessed password. As the above mentioned, without the knowledge of the password, the adversary cannot launch any attacks. Hence, the backward secrecy is also kept in our protocol.

Theorem 1. We claim that the proposed password-based three-party key exchange protocol is secure in the random oracle model if the CDHP is hard.

Proof. We then give the detailed proof in the appendix.

5. Efficiency Analysis

In this section, we analyze the computation cost of a service requester because the requester could use personal mobile devices to obtain the desirable services. Also, as introduced in[24], we can learn a relationship as follows: the time of one modular exponentiation is faster 5/3 times than the time of one public-key en/decryption operation, the time of one modular multiplication computation is faster 240 times than the time of one modular exponentiation operation, and the

time of one one-way hash function operation is faster 600 times than the time of one modular exponentiation.

In Round 1, A calculates $R_A = g^x \oplus h_1(pwA, A, B, sid)$. The cost is one modular exponentiation plus one hash function operation. In Round 4, A recovers $b = Z_{A1} \oplus h\_1(pwA+1, A, B, sid)$ and $c = Z_{A2} \oplus h_1(pwA+2, A, B, sid)$. The cost is two hash function operations. Then A calculates the session key $K = h_2(A, B, sid, b^x)$, $S_{A1} = h_1(A, B, sid, K+1)$ and $S_{A2} = h_1(A, B, sid, c^x, a)$. The cost is two modular exponentiation plus 4 hash function operations. By the above, the computation cost of A is 3 modular exponentiations plus 6 hash function operations.

In the communication cost, we denote that:

1) Message Step denotes that one entity has sent data to the communicated party.

2) Communication Round means that if the sent data are independent between each message steps, one or more message steps can be integrated into the same communication round due to the sent data can be performed in parallel. The burden of the communication cost can be reduced.

We summarize the results in Table 1 and we can see that our protocol is more efficient than the related protocols[10-11,16,20-21].

Table 1. Comparisons of the Computation Cost At Requester Side and the Communication Cost

	Our	Lu-Cao[21]*3	Huang[16]*4	Chien-Wu[11]	Chen *et al.*[10]*	Lo-Yeh[20]
T_{EXP}	3	4	2	2	3	3
T_{MUL}	0	2	0	0	0	0
T_H	7	3	4	4	4*1	4*1
T_{PKC}	0	0	0	1	1*2	1*2
T_{SYM}	0	0	0	0	1	1
Total(T_{MUL})	722.8	963.2	481.6	881.6	1121.6+1T_{SYM}	1121.6+1T_{SYM}
Rounds/Steps	4/8	5/5	5/5	4/4	5/5	4/6

T_{EXP} denotes the time of one modular exponentiation operation; T_{MUL} denotes the time of one modular multiplication computation; T_H denotes the time of one hash function operation; T_{PKC} denotes the time of one public-key en/decryption operation; T_{SYM} denotes the time of one symmetric-key en/decryption operation;

*: the protocol has been proven that the on-line undetectable guessing attack still exists[20].

*1: the computation cost of pseudo-random hash function is similar to the cost of one-way trapdoor hash function.

*2: the computation cost of one-way trapdoor function is similar to the cost of public key en/decryption.

*3: The protocol which is not secure against the unknown key sharing, the on-line undetectable guessing, and the impersonation attacks has been proven by[12,15,18,23].

*4: Wu had have shown that the protocol is not secure against the on-line undetectable guessing attack[25].

5. Conclusions

In this paper, we have proposed a provably secure password-based three-party key exchange protocol to overcome some well known security threats. Compared with the related protocols, the computation efficiency is still kept in our proposed protocol.

Correspondence:
Ren-Chiun Wang
E-mail: rcwang@icst.org.tw

References

1. M. Abdalla, E. Bresson, O. Chevassut, B. MÖoller, D. Pointcheval, Strong Password-Based Authentication in TLS using the Three-Party Group Diffie-Hellman Protocol, International Journal of Security and Networks. 2007, 2(3/4):284-296.
2. M. Abdalla, D. Catalano, C. Chevalier, D. Pointcheval, Efficient Two-Party Password-Based Key Exchange Protocols in the UC Framework, in: Topics in Cryptology - CT-RSA 2008, LNCS 4964, 2008, 335-351.
3. M. Abdalla, P.-A. Fouque, D. Pointcheval, Password-Based Authenticated Key Exchange in the Three-Party Setting, in: Public Key Cryptography - PKC 2005, LNCS 3386, 2005, 65-84.
4. M. Abdalla, P.-A. Fouque, D. Pointcheval, Password-Based Authenticated Key Exchange in the Three-Party Setting, IEE Proceedings, 2006, 153 (1):27-39.
5. M. Abdalla, D. Pointcheval, A Scalable Password-based Group Key Exchange Protocol in the Standard Model, in: Advances in Cryptology - ASIACRYPT 2006, LNCS 4284, 2006, 332-347.
6. J. Baek, K. Kim, Remarks on the unknown key-share attacks, IEICE Trans. on Fundamentals, 2000, E83-A(12):2766-2769.
7. M. Bellare, P. Rogaway, Provably secure

session key distribution the three party case, in: Proc. of the 27th ACM Annual Symposium on the Theory of Computing, 1995, 57-66.

8. S. Blake-Wilson, A. Menezes, Unknown key-share attacks on the stationto-station (STS) protocol, in: Public Key Cryptography (PKC '99) Proceedings, LNCS 1560, 1999, 154-170.
9. S. Boneh, B. Lynn, H. Shacham, Short Signatures from theWeil Pairing, in: Advances in Cryptology - ASIACRYPT 2001, LNCS 2284, 2001, 514-532.
10. H.-B. Chen, T.-H. Chen, W.-B. Lee, C.-C. Chang, Security enhancement for a three-party encrypted key exchange protocol against undetectable on-line password guessing attacks, Computer Standards & Interfaces, 2008, 30(1-2):95-99.
11. H.-Y. Chien, T.-C. Wu, Provably secure password-based three-party key exchange with optimal message steps, The Computer Journal, 2009, 52(6):646-655.
12. H.-R. Chung, W.-C. Ku, Three weaknesses in a simple three-party key exchange protocol, Information Sciences, 2008, 178(1):220-229.
13. W. Diffiee, M. Hellman, New directions in cryptology, IEEE Transations on Information Theory, 1976, IT-22(6):644-654.
14. Y. Ding, P. Horster, Undetected on-line password guessing attacks, ACM Operating Systems Review, 1995, 29(4):77-86.
15. Guo, Z. Li, Y. Mu, X. Zhang, Cryptanalysis of simple three-party key exchange protocol, Computers & Security, 2008, 27(1-2):16-21.
16. H.-F. Huang, A simple three-party password-based key exchange protocol, International Journal of Communication Systems, 2009, 22(7):857-862.
17. W.-S. Juang, Efficient three-party key exchange using smart cards, IEEE Trans. on Consumer Electronics, 2004, 50(2):619-624.
18. H.-S. Kim, J.-Y. Choi, Enhanced password-based simple three-party key exchange protocol, Computers & Electrical Engineering, 2009, 35(1):107{114.
19. T.-F. Lee, J.-L. Liu, M.-J. Sung, S.-B. Yang, C.-M. Chen, Communication-efficient three-party protocols for authentication and key agreement, Computers & Mathematics with Applications, 2009, 58(4):641-648.
20. N.-W. Lo, K.-H. Yeh, Cryptanalysis of two three-party encrypted key exchange protocols, Computer Standards & Interfaces, 2009. 31(6):1167-1174.
21. R. Lu, Z. Cao, Simple three-party key exchange protocol, Computers & Security, 2007, 26(1):94-97.
22. D. P. M. Bellare, P. Rogaway, Authenticated and key exchange secure against dictionary attacks, Advances in Cryptology - EUROCRYPT 2000, LNCS 1807, 2000, 139-155.
23. R. C.-W. Phan, W.-C. Yau, B.-M. Goi, Cryptanalysis of simple threeparty key exchange protocol (S-3PAKE), Information Sciences, 2008, 178(13):2849-2856.
24. B. Schneier, Applied cryptography, 2nd edition, John Wiley & Sons Inc., 1996.
25. S. Wu, Weakness of a three-party password-based authenticated key exchange protocol, Report 2009/535, CryptEAr (Nov. 2009). URL http://eprint.iacr.org/2009/535.pdf
26. E.-J. Yoon, K.-Y. Yoo, Improving the novel three-party encrypted key exchange protocol, Computer Standards & Interfaces, 2008, 30(5):309-314.

Appendix

A. Security Proof

We prove that our protocol provides the session key

indistinguishability property in the random oracle model under the CDHP assumption.

Proof. We use a contradiction way to prove it. We assume that an adversary AD can gain a non-negligible advantage to distinguish the test key in the game and AD can construct a breaker AD" to solve the CDHP problem, where the advantage of AD from differentiating the real session key from a random key as follows:

$Adv_{P,D}^{G,AD}(k,q_{fake\text{-}C})=|Pr[b'\text{-}b]\text{-}q_{fake\text{-}C}/N\text{–}1/2*(N\text{-}q_{fake\text{-}C})|$.

We suppose that an oracle C_A has accepted the session key of the form $K = h_2(A, B, sid, g^{xyz_1})$ with another fresh and partnership oracle C_B. We say that AD is successful if AD picks an oracle C_A or C_B to ask a Test query and can output the bit guess correctly. Thus, we have $Pr[AD\ succeeds] = q_{fake\text{-}C}/N + 1/2 * (N - q_{fake\text{-}C})/N + \eta(k)$, where $\eta(k)$ is non-negligible.

Let Q_h be the event that $h_1()$ or $h_2()$ has been

queried on (A, B, sid, g^{xyz_1}) by AD or some oracles. Then Pr[AD succeeds] = $q_{fake\text{-}C}/N$ + Pr[AD succeeds | Q_h] * Pr[Q_h] + Pr[AD succeeds | $\overline{Q_h}$] * Pr[$\overline{Q_h}$]. Since $h_1()$ and $h_2()$ are random oracles and C_A and C_B are fresh oracles, it implies Pr[AD succeeds | $\overline{Q_h}$] = 1/2. Hence, $q_{fake\text{-}C}/N + 1/2 * (N - q_{fake\text{-}C})/N + \eta(k) \le q_{fake\text{-}C}/N + 1/2 * (N - q_{fake\text{-}C})/N$ + Pr[Q_h]. We then have Pr[Q_h] $\ge \eta(k)$.

The adversary AD selects a fresh oracle C_A which has accepted a session key. Then the probability of $h_2()$ being queried on (A, B, sid, g^{xyz_1}) by AD or some oracles other than C_A and C_B is non-negligible. As mentioned before, we have assumed that AD constructs a breaker AD" which can solve the CDHP with non-negligible probability. The task of AD" is that: Given $X = g^x$ and $Y = g^y$, AD" outputs g^{xy}, where x and y are chosen randomly.

AD" executes the following process:

1. Randomly select C_A and C_B from $\hat{C} = \{C_1, C_2, ..., C_{NC}\}$ and instances u and i from $\{1, 2, ..., N_I\}$, where N_C and N_I denote the number of service requesters and service providers and the instances per entity. Note that all these parameters are polynomial on the security parameter.
2. Determine two oracles C_A^u and C_B^v who are partnership.
3. Guess that AD will choose one of C_A^u and C_B^v who have accepted the session to ask its Test query after AD decides to terminate the game.

Given the challenge ($X^* = g^x$, $Y^* = g^y$) to AD", AD" sets the public parameters as (g, p). AD" also maintains the lists L_{h1} and L_{h2} for the random oracles $h_1()$ and $h_2()$ queries, L_{Send} for the communicated transcripts, and L_{Key} for the corresponding keys of each session. AD" selects the passwords pw for each C_A and $C_B \in \{C_1, C_2, ..., C_{NC}\}$ at random and lets $pw_{\hat{C}}$ be the password file of TS.

During the game, AD will ask some queries to AD". The answers are given as follows:

1. Hash query: AD" randomly responses $h_1()$ and $h_2()$ queries which are like real random oracles do, and records all the inputs and the corresponding outputs in L_{h1} and L_{h2}, respectively.
2. Corrupt(C) query: If C is one of C_A and C_B, AD" gives up; otherwise, AD" answers all the internal state of C to AD.
3. SendClient(C_X^i, m) query:

(a) If ($C_X = C_A$) && ($i = u$) && ($m = start$), then AD" sets $N_X = X^*$ and responds the protocol says $\{CA, sid, N_X \oplus h_1(pw_{C_A}, C_A, C_B, sid)\}$. Finally, the oracle records the responsive transcript and the random exponent (?) in the L_{Send} list and ($h_1(pw_{C_A}, C_A, C_B, sid)$, ($pw_{C_A}, C_A, C_B, sid$)) in the L_{h1} list, where ? denotes the corresponding exponent of X^* and is unknown.

(b) If ($C_X = C_B$) && ($i = v$) && (m has the form of (C_A, sid, $N_X \oplus h_1(pw_{C_A}, C_A, C_B, sid)$), then AD" sets $N_Y = Y^*$ and responds the protocol says $\{C_A, C_B, sid, N_X \oplus h_1(pw_{C_A}, C_A, C_B, sid), N_Y \oplus h_1(pw_{C_B}, C_A, C_B, sid)\}$. Finally, AD" records the responsive transcript and the random exponents (?) in the L_{Send} list and ($h_1(pw_{C_B}, C_A, C_B, sid)$, ($pw_{C_B}, C_A, C_B, sid$)) in the L_{h1} list, where ? denotes the corresponding exponent of Y^* and is unknown.

(c) If ($C_X \in \{C_1, C_2, ..., C_{NC}\}$) && ($m$ has the form of ("start", $C_Y \in \{C_1, C_2, ..., C_{NC}\}$ && $C_Y \neq C_X$)), then AD" selects an integer x' at random, calculates $X^* = g^{x'}$, and responds with the transcript $\{C_X, sid, X^* \oplus h_1(pw_{C_X}, C_X, C_Y, sid)\}$. Finally, AD" records the transcript and the randomly secret exponent x' in its L_{Send} and L_{h1} lists.

(d) If ($C_X \in \{C_1, C_2, ..., C_{NC}\}$) && ($m$ has the form of (C_Y, sid, $Y^* \oplus h_1(pw_{C_Y}, C_Y, C_X, sid)$), then AD" selects an integer x' at random, calculates $X^* = g^{x'}$, and responds with the transcript $\{C_Y, C_X, sid, Y^* \oplus h_1(pw_{C_Y}, C_Y, C_X, sid), X^* \oplus h_1(pw_{C_X}, C_X, C_Y, sid)\}$. Finally, AD" records the transcript and the randomly secret exponent x' in its L_{Send} list.

(e) If ($C_X = C_A \in \{C_1, C_2, ..., C_{NC}\}$) && ($m$ has the form of (C_X, sid, Z_{C_X1}, Z_{C_X2}) for $C_Y = C_B \in \{C_1, C_2, ..., C_{NC}\}$), then AD" consults its L_{Send} list by using sid to find a matched entry. If the matched entry can be found, AD" extracts the local value from L_{Send} to recover the received data and to calculate K, S_{C_X1} and S_{C_X2}. AD" responds with the transcript $\{C_X, sid, S_{C_X1}, S_{C_X2}\}$. Finally, AD" records corresponding data in its L_{Send}, L_{h1}, L_{h2} and L_{Key} lists respectively. Otherwise, AD" responses with error messages.

(f) If ($C_X \in \{C_1, C_2, ..., C_{NC}\}$) && ($m$ has the

form of (C_X, *sid*, S_{C_X1})), then AD" consults its L_{Send} list by using *sid* to find a matched entry. If the matched entry can be found, AD" extracts the local values from L_{h1}, L_{h2} and L_{Key} lists and uses them to verify S_{C_X1}. If the verification does not hold, AD" gives up; AD" records corresponding data in its L_{Send} list.

(g) AD" responses with error messages for all the other cases.

4. SendServer(*m*) query:

(a) If (C_X and $C_Y \in \{C_1, C_2, ..., C_{NC}\}$) && (*m* has the form of ("start", C_X, C_Y, *sid*, $X^* \oplus h_1(pw_{C_X}, C_X, C_Y, sid)$, $Y^* \oplus h_1(pw_{C_Y}, C_Y, C_X, sid)$)), then AD" uses pw_{C_X} and pw_{C_Y} to recover the received data. AD" selects three integers z_1, z_2 and z_3 at random and responds with the transcript {C_X, *sid*, Z_{C_X1}, Z_{C_X2}} and {C_Y, *sid*, Z_{C_Y1}, Z_{C_Y2}}. Finally, AD records all the transcripts and the randomly secret exponents z_1, z_2 and z_3 in its L_{Send} list, L_{h1} list and L_{Key} list respectively.

(b) If ($C_X \in \{C_1, C_2, ..., C_{NC}\}$) && (*m* has the form of (C_X, *sid*, S_{C_X2} for C_Y) $\in \{C_1, C_2, ..., C_{NC}\}$), then AD" consults its L_{Send} list by using *sid* to find a matched entry. If the matched entry can be found, AD" extracts the local values from L_{h1}, L_{h2} and L_{Key} lists and uses them to verify S_{C_X2}. If the verification does not hold, AD" responds an error message to C_Y and records corresponding data in its L_{Send} list.

(c) AD" responses with error messages for all the other cases.

Reveal(C_X^i) query: After receiving the query, AD" consults the records in the list of L_{Key} and reveals all the internal state and the session keys.

AD then answers its guess and requires AD" to searches its L_{h1} and L_{h2} list for the entry, where the entry has the input of the form (C_X, C_Y, *sid*, (*recovered data*)^{secretexponent}) for some *K*. Finally, AD" outputs *K* as the Diffie-Hellman key of C_X and C_Y. There are the two possible results for the above experiment:

1. AD" gives up if AD does not make its queries where C_A^u or C_B^v has accepted their session.
2. If AD does make its queries, then C_A^u or C_B^v will accept their session and hold the key formed $h_2(C_A, C_B, sid, (recovered\ data)^{secretexponent})$. It is the fact that the session key g^{xyz_1} is unknown to AD", AD" cannot calculate this key actually.

AD" will search its L_{h1} and L_{h2} lists for the entry and certainly wins its experiment if Case 2 does happen really. Hence, the probability of AD" outputting the correct value on $g^{xyz_1} \bmod p$ is: $\Pr[Q_h]/(N_C^2 N_I^2)\} \geq \eta(k) /(N_C^2 N_I^2)$, where the probability is non-negligible and the result contradicts our CDHP assumption. Hence, we can conclude that $\eta(k)$ must be negligible and is the advantage of $Adv_{P,D}^{G,AD}(k, q_{fake\text{-}C})$. The theorem is proven. □

11/20/2011

Optimal Library Inventory System Using EMID Technology

Sung-Tsun Shih[1], Chin-Ming Hsu[2], Chian-Yi Chao[3]

[1]Department of Electronic Engineering, Cheng Shiu University, Kaohsiung, Taiwan
[2]Department of Information Technology, Kao Yuan University, Kaohsiung, Taiwan
[3]Department of Electronic Engineering, Kao Yuan University, Kaohsiung, Taiwan
stshih@csu.edu.tw

Abstract: This paper proposes an optimal library inventory system which is based on electromagnetic identification (EMID) technology with the advantages of using electromagnetic (EM) tag and radio frequency identification (RFID) tag. The proposed system is constructed by four processes, including deciding the tag type, finding the optimal tag location for a book, testing the tag readability for multi-layer bookshelves, and connecting a couple of multi-layer bookshelves with multiplexers and updating the tag reading status in the database of the computer terminal. The proposed system is tested at the library of Cheng Shiu University in Taiwan. The quality and quantity of one-side and two-side of antennas applied in reading EMID tags with different time intervals and locations have been tested in the study. According to the experimental results, the designed library inventory system can authenticate the location of a book automatically and can benefit administrating librarians with the capabilities of decreasing the library inventory processing time and reducing the possibility of the books being misplaced.
[Sung-Tsun Shih, Chin-Ming Hsu, Chian-Yi Chao. **Optimal Library Inventory System Using EMID Technology.** Life Science Journal. 2011;8(4):644-649] (ISSN:1097-8135). http://www.lifesciencesite.com.

Keywords: Library Inventory; electromagnetic identification (EMID); radio frequency identification (RFID).

1. Introduction

Traditionally, library inventory work is a time-consuming and labor-exhausting task because librarians need to keep numerous resources such as books and magazines on their tracks correctly [1]. In order to be well maintained, a library generally would halt their service work for a week or a period of time to search all bookshelves in the library for examining whether the resources are put at their locations or not. This implies that the library inventory work not only includes check-in and check-out but also includes keeping the resources at actual locations [2]. Most of time, however, some resources would be either misplaced or stolen. With the development of information technology, many libraries have adopted barcode-label and electromagnetic (EM)-strip technologies for managing abundant books in the library inventory process. A barcode label with unique identification on a book provides check-in/out management capability while the electromagnetic strip of the book supports the anti-theft capability. The librarian would stick the barcode label and EM strips on the book and apply the computer system with the barcode and magnetization scanner to read the book information and adding/deleting the magnetization on the book. However, the barcode labels could be only stuck on the book with one time, manually scanned, and easily damaged; the EM strips don't support resource identification capability [3].

In recent years, in order to overcome the weaknesses mentioned above, the wireless radio frequency identification (RFID) technology has replaced the barcode label and magnetic strip with identification and anti-theft detection capabilities in the library inventory management [4-5]. The fundamental components of a typical RFID system consist of antennas, readers, and tags. The reader firstly sends the wireless radio signal which is then received by the antenna. When the tag perceives the radio signal, it returns the electromagnetic wave back to the reader [6]. Compared with using barcodes in the library inventory management, a RFID tag could be read more than ten-thousand times and could support more convenient and efficient advantages on check-out and return processes.

In the past decade, many universities, such as Cornell Uni., USA [7], Myongji Uni., Korea [8], Uni. of Auckland, New Zealand [9], and City Uni. of New York, USA [10], have done a lot of efforts on their library database managements. At Cornell Uni., the technology of a research library's digital collection would offer information seekers a powerful and easy way to search across existing collections and to retrieve integrated sets of results. At Myongji Uni. (MIU), a metadata system is designed and implemented for MJU library collections, which allows users to search all library materials using one user interface. At Uni. of Auckland, a digital library project is developed and aims at enhancing the IT infrastructure, strategic planning and designing a digitization policy. As for the City Uni. of New York, the library constructs the software usability measurement inventory (SUMI) criteria to evaluate their library database system.

In the reviewing some references applying RFID technology in the library inventory managements, Kern [11] described a RFID-based library inventory system which is used for book identification, for self-checkout, for anti-theft control, for inventory control, and for sorting and conveying of library books and AV materials. Chun, Hwang, and Lee [12] proposed an RFID tag search protocol which would protect the privacy of mobile reader holders and is secure enough to against all known major attacks in RFID systems. Sue and Lo [13] applied the RFID technology in a smart book-locating system which has two location modes – single book mode and book list mode. The single book mode provides users to find the bookshelf containing the desired book which was misplaced. The book list mode offers a corresponding list of the bookshelves and the misplaced books in the wrong bookshelves. Golding and Tennant [14] investigated the factors that may affect the read rate of an inventory reader in a library. The investigated factors were read distance, tag location, number of sweeps and sweep direction. Wang [15] studied the RFID-based methodology and approaches that support library services and management, including sensor gate control, circulation, inventory, searches and utilization statistics. The study also discussed barriers, challenges and future work about RFID applications in libraries and concluded that RFID-based technology would improve digital archives and digital humanities in library systems.

Zhang and Shi [16] and Bin Abdullah, etc. [17] are two literatures related to self services of library management systems. Zhang and Shi strongly pointed out that the necessity of the new RFID technology of self-service book borrowing and returning system in library, which would replace the barcode technology and accelerate the library's self-service process. Bin Abdullah, etc. developed an integrated the RFID system with graphical user interface (GUI) at the host PC. The study aims to develop an automatic library shelf management system to assist the librarians for more efficient shelf management to find any misplaced books on the library shelf. In addition, in the reviewing some other RFID related literatures [18-20], two comments were made: (1) such intelligent plan may not meet the library demand because the system have to consider library internal disturbances such as metal, motion communication electric wave, and wireless network electric wave, which could affect the RFID operation; (2) the proposed inventory system have to be convenient to all readers.

As mentioned above and driven by the advanced ubiquitous computing technology, in this study, the authors proposes an optimal library inventory system which is based on electromagnetic identification (EMID) technology with the advantages of using electromagnetic (EM) tag and radio frequency identification (RFID) tag. This paper is organized as follows. Section 2 describes the proposed optimal library inventory system based on EMID technology. The experimental results are shown in Section 3. Finally, the conclusions and Discussions are summarized in Section 4.

2. Optimal Library Inventory Technology

Figure 1 illustrates the flow chart of the optimal library inventory technology which includes four steps: deciding the tag type, finding the optimal tag location for a book, testing the tag readability for multi-layer bookshelves, and connecting couple of multi-layer bookshelves with multiplexers and updating the tag reading status in the database of the computer terminal.

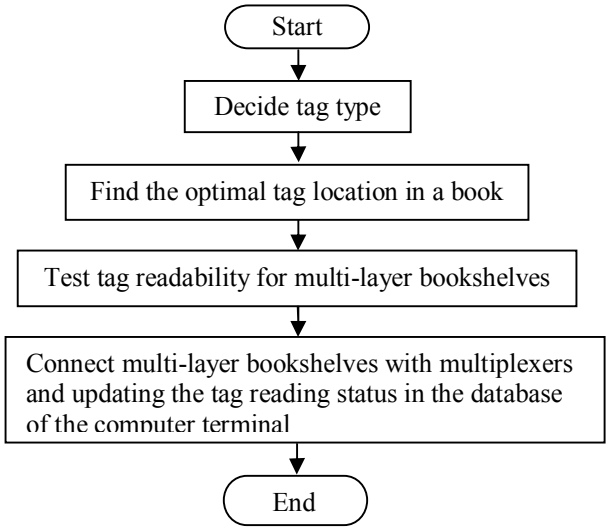

Figure 1. Flow chart of optimal library inventory technology.

2.1. Deciding Tag Type

In this study, embedded electromagnetic identification (EMID) security strips, as shown in Figure 2, are used for securing and managing the stocks on the library bookshelves. This kind of tags combines the technology of electromagnetic (EM) strips with security advantage and radio frequency identification (RFID) tags with managing distribution advantage. A typical EM long strip tag doesn't have storing information capability; it can only secure library articles by sensing (attaching and eliminating) the electromagnetic signal on the EM long strip tag. As for the RFID strip tag, it uses the antenna and radio frequency chip to store the identification information. However, its size usually is too large to be applied in the library bookshelves management.

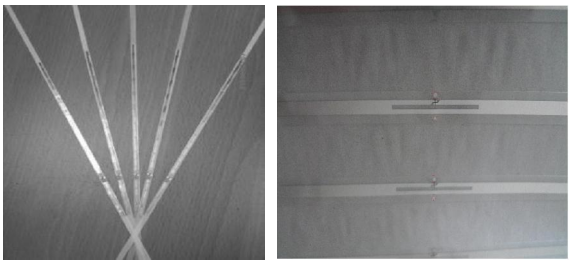

(a) (b)

Figure 2. Embedded electromagnetic identification (EMID) security strips; (a) front side; (b) back side.

2.2. Finding Optimal Tag Location

Figure 3 is the picture of a bookshelf with the width and height of 90 and 19 cm, respectively. Three places, labeled as A, B and C in Figure 3, are used to find the optimal tag location. The place A is located on the left hand side of the bookshelf; the place B is located on the middle of the bookshelf; the place C is located either on the 30 cm from the distance of left and right hand sides of the bookshelf.

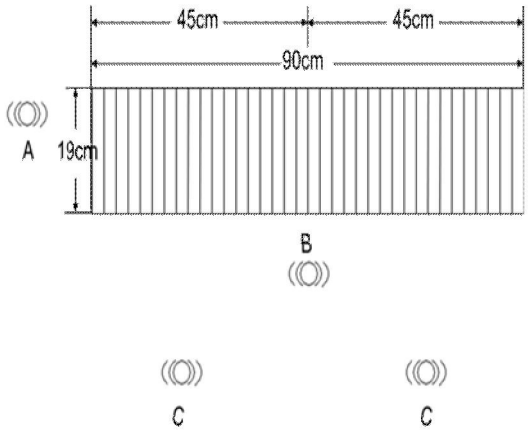

Figure 3. Tag location.

2.3. Testing Tag Readability

Figure 4 illustrates the EMID reader (antenna) locations on the bookshelves. As shown in Figure 4(a) one EMID reader is put on the center of the one-sided bookshelf; the other EMID reader is put on the middle part of two-sided bookshelves. The spine of every book is attached an EMID tag strip as illustrated in Figure 5.

2.4. Connecting Multi-Layer Bookshelves

Figure 6 shows antenna's locations in a multi-layer bookshelf. Figure 7 illustrates the structure of connecting multi-layer bookshelves in a library by using multiplexers. As given in Figure 7, the library computer terminal through multiplexers and readers obtains antenna's signals by rolling every EMID tag. After the computer obtained the EMID tag signal, the database of the computer will authenticate the location of the book. This indicates that whether the book is on the bookshelf or not and the library inventory work can be done automatically.

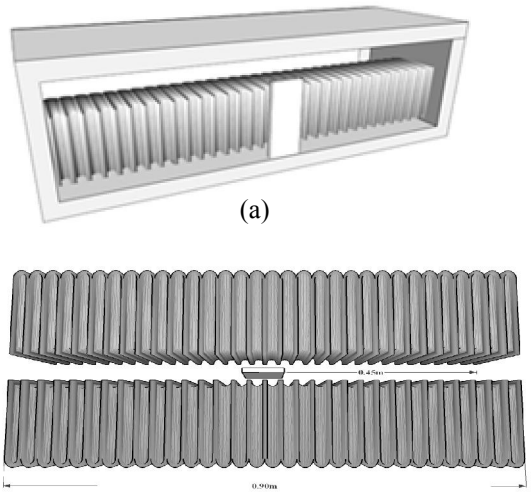

(a)

(b)

Figure 4. Tag Readability; (a) one-sided bookshelf; (b) two-sided bookshelves.

Figure 5. EMID tag strip location in the book.

Figure 6. Antenna locations in multi-layer bookshelves.

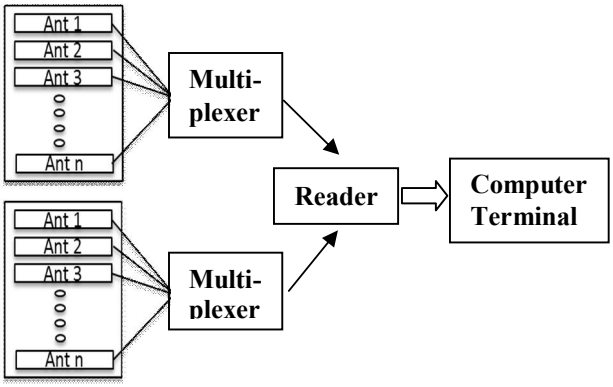

Figure 7. Connection of multi-layer bookshelves.

3. Results

In order to minimize the disturbance while under testing, the proposed system is experimented at night during the library closing time interval. Based on the polling inquiry methodology, the system would automatically read every EMID tag individually by switching different multiplexers gradually. On the other side, the user interface of the computer terminal would show the reading status of each EMID tag and the read data is then stored in the database of the computer terminal.

Table 1 shows the reading rate of EMID tags located at A, B, and C places as shown in Figure 3. From Table 1, the reading rate of 30 EMID tag strips at the location A, B, and C are 50%, 100%, and 100%, respectively. This implies that either location B or C gets better reading rate. Table 2 gives the reading rate of 25 EMID tag strips with different measuring time for one-sided bookshelf. From Table 2, the reading rate of 25 EMID tag strips with the time interval of 1, 3, and 5 minutes are 60%, 88%, and 100%, respectively. This implies that measuring time with 5 minute interval gets the best reading rate. Table 3 illustrates the reading rate of 30 EMID tag strips with different measuring time for two-sided bookshelves. From Table 3, the reading rate of 30 EMID tag strips with the time interval of 1, 3, and 5 minutes are 56.6%, 80%, and 93.3%, respectively. This implies that measuring time with 5 minute interval gets the best reading rate.

Figure 8 shows the user interfaces of reading EMID tag strips and administrator's database management in Chinese at the computer part of the system where the user interface and database are built by C++ codes. There are six main functions shown on the screen of Figure 8(a), including book number, EMID tag number, reading times, starting time, current time, and antenna number. As for Figure 8(b), there are five main functions shown on the screen, including EMID tag number, book title, author's name, publisher, and reading status. According to the experimental results, the proposed system with easy operations allows the library administrator can know whether a book is on the bookshelf or not by checking the screen of Figure 8(b) and can accomplish library inventory work efficiently and effectively.

(a)

(b)

Figure 8. User interfaces for managing stocks in library; (a) reading EMID tag; (b) book database management.

Table 1. Reading rate for different RFID tag locations

EMID Tag Quantity	Location	Reading Quantity	Reading Rate (%)
30	A	15	50%
	B	30	100%
	C	30	100%

Table 2. Reading rate for one side bookshelf

EMID Tag Quantity	Time Interval(Min.)	Reading Quantity	Reading Rate (%)
25	1	15	60%
	3	23	88%
	5	25	100%

Table 3. Reading rate for two side bookshelves

EMID Tag Quantity	Time Interval(Min.)	Reading Quantity	Reading Rate (%)
30	1	17	56.6%
	3	24	80%
	5	28	93.3%

4. Conclusions and Discussions

An optimal library inventory system based on EMID technology has been proposed in this study. The main contribution of the proposed system is to improve traditional human labor-based library inventory methodology by decreasing the library inventory processing time and reducing the possibility of the books being misplaced. Compared to the exiting methods, the proposed system supports three distinctive advantages: (1) Using EMID strip tag with the characteristics of small size and high confidentiality can prevent it from being destroyed easily; (2) From the experimental results, the optimal tag reading status can be obtained by finding the best distance between two tags, the best location of a tag in a book, the optimal time interval for reading a tag accurately, and the best tag quantity for a bookshelf; (3) the number of EMID tag readers are minimized by using multiplexers and two-side antennas.

This work can be practically upgraded by considering the trade-offs of the quality and quantity of one-side and two-side of antennas applied in reading EMID tag with different time intervals. In addition, whether the location of the EMID tag in a book is confidential and readable is also another important factor to be considered.

Acknowledgements:

The authors would like to thank the company of Taiwan-EAS-Technology and the library of Cheng Shiu University supporting the EMID tags and measuring environment for us to carry out the experimental tests.

Corresponding Author:
Dr. Sung-Tsun Shih
Department of Electronic Engineering,
Cheng Shiu University,
Kaohsiung , Taiwan, R.O.C.
E-mail: stshih@csu.edu.tw

References

1. C. P. Zhu, Z. Wang, J. X. Deng, H. Gu, M.L. Shan, Q. B. Han, H. Z. Yu, S. Zhang. Design of an Intelligent Book Conveyor based on RFID. The 2nd International Conference on Information Science and Engineering, 2010; 1993 – 1996.
2. T.M.W. Shamsudin, M.J.E. Salami, W. Martono. RFID-Based Intelligent Bookcs Shelving System. The 1st Annual RFID Eurasia, 2007; 1–5.
3. C. W. Chou. The Application of Radio Frequency Identification Technology to the Library Real-Time Storage Processing. Department of Engineering Science, National Cheng-Kung University. July, 2006.
4. M.S. Selamat, B.Y. Majlis. Challenges in Implementing RFID Tag in a Conventional Library. IEEE International Conference on Semiconductor Electronics, 2006; 258 – 262.
5. F. Cheng. Research for application of RFID in library. International Conference On Computer and Communication Technologies in Agriculture Engineering, 2010; 1:262 – 264.
6. J. W. Choi, D. I. Oh, I. Y. Song. R-LIM: an Affordable Library Search System Based on RFID. International Conference on Hybrid Information Technology, 2006; 1: 103 – 108.
7. K. Calhoun. Integrated framework for discovering digital library collections. Journal of Zhejiang University: Science, 2005; 6(11):1318-1326.
8. H. H. Kim. Myongji University digital library project: Implementing a KORMARC/EAD integrated system. Electronic Library, 2003; 21(4): 367-374.
9. R. Holley. Developing a digitisation framework for your organisation. Electronic Library, 2004; 22(6): 518-522.
10. A. Oulanov, E.J.Y. Pajarillo. Usability evaluation of the City University of New York CUNY+ database. Electronic Library, 2001; 19(2): 84-91.
11. C. Kern. Radio-frequency-identification for security and media circulation in libraries. Electronic Library, 2004; 22(4): 317-324.
12. J. Y. Chun, J. Y. Hwang, D. H. Lee. RFID tag search protocol preserving privacy of mobile reader holders. IEICE Electronics Express, 2011; 8(2): 50-56.
13. K. L. Sue, Y. M. Lo. BLOCS: A Smart Book-Locating System Based on RFID in Libraries. International Conference on Service Systems and Service Management. 2007; 1 – 6.
14. P. Golding, V. Tennant. Performance characterisation for two radio frequency identification inventory readers within a

university library environment. International Journal of Radio Frequency Identification Technology and Applications, Special Issue on RFID-Enhanced Technology Intelligence and Management, 2011; 3(1-2):107-123.
15. S. C. Yu. RFID implementation and benefits in libraries. Electronic Library, 2007; 25(1): 54-64.
16. D. Zhang, X. Shi. Self-service management platform design for library based on RFID. The 2nd International Conference on Artificial Intelligence, Management Science and Electronic Commerce, 2011; 7237 – 7240.
17. A.T. Bin Abdullah, I.B. Ismail, A.B. Ibrahim, M.Z. Hakim Bin Noor. Library shelf management system using RFID technology. IEEE International Conference on System Engineering and Technology, 2011; 215 – 218.
18. P. Golding, V. Tennant. Work in Progress: Performance and Reliability of Radio Frequency Identification (RFID) Library System. International Conference on Multimedia and Ubiquitous Engineering, 2007; 1143 – 1146.
19. I. Ehrenberg, C. Floerkemeier, and S. Sarma. Inventory Management with an RFID-equipped Mobile Robot. IEEE Conference on CASE, 2007; 1020 – 1026.
20. P.Y. Lau, K.K.-O. Yung and E.K.-N. Yung. A Low-Cost Printed CP Patch Antenna for RFID Smart Bookshelf in Library. IEEE Trans. Industrial Electronics, 2010; 5:1583-1589.

10/19/2011

The Cranial Nerves of *Mabuya quinquetaeniata* III: Nervus Trigeminus

*Abdel-Kader, T. G.; Ali, R. S. and Ibrahim, N. M.

Department of Zoology, Faculty of Science, Helwan University, Cairo, Egypt
*tgabdelkader@yahoo.com

Abstract: The present study deals with the nervus trigeminus of *Mabuya quinquetaeniata*. The results showed that the nervus trigeminus has one root, and two separate ganglia, a maxillomandibular ganglion and an ophthalmic one. The maxillomandibular ganglion is continuous with the ophthalmic ganglion. The lateral part of the ventromedial division of the trigeminal root gives off the anguli oris nerve and nerves to the adductor mandibularis externus and the pseudotemporalis muscles. The constrictor dorsalis nerve innervates the protractor pterygoideus, levator pterygoideus, and depressor palpbrae inferioris muscles. It has no anastomosis with ramus palatinus of the nervus facialis. The ramus frontalis is connected with the lacrimal plexus. The ramus nasalis anastomoses with the ethmoidal ganglion and divides into its to rami lateralis and medialis nasi within the nasal capsule. The ramus maxillaris gives off lacrimal and temporal branches in the postorbital region. In the orbital region, it is termed infraorbital nerve and gives off a nerve to the Harderian gland, the supralabial gland and the upper teeth. It fuses with the ramus palatinus lateralis of the nervus facialis. It receives an anastomosing branch from the ramus palatines medialis and fuses with the ramus palatines intermedialis for a short distance. It carries ganglionic cells at the point of fusion. It enters the maxilla as superior alveolar nerve and gives off nerve to the narial muscles. The ramus mandibularis gives off nerves to the pseudotemporalis and pterygomandibularis muscles. It gives off the ramus cutaneous recurrens and then enters the primordial canal as the inferior alveolar nerve, where it gives off a mixed nerve and a sensory one and then receives the chorda tympani (N.VII). The mixed nerve (the inferior alveolar nerve + chorda tympani) gives rise to the rami intermandibularis oralis, intermandibularis medius (ramus paralingualis) and intermandibularis caudalis. The ramus intermandibularis medius is connected with the ramus lingualis lateralis (N.XII). The ramus intermandibularis caudalis gives motor fibres to the intermandibularis muscle.
[Abdel-Kader, T. G.; Ali, R. S. and Ibrahim, N. M. **The Cranial Nerves of *Mabuya quinquetaeniata* III: Nervus Trigeminus]** Life Science Journal, 2011; 8(4):650-669] (ISSN: 1097-8135). http://www.lifesciencesite.com.

Key Words: *Mabuya*, Cranial nerves, Nervus trigeminus

1. Introduction

The neuroanatomy of reptiles is one of the important subjects of herpetology. The neuroanatomical characters are very important not only phylogenetically but also systematically, functionally, and behaviourally. Despite of these important characters, the cranial nerves of reptiles in general and those of lizards in particular have not received adequate interest by investigators. The first valuable work was that of Fischer (1852). This work though of an early date, is still useful for the investigators.

The nervus trigeminus is one of the mixed general nerves that carries both sensory and motor fibres. The distribution of these fibres shows a contradiction in different species. Among reptiles, not only, the origin of (number of roots), ganglia and branches of this nerve vary among different species, but also, the types of fibers carried by it and its distribution.

The nervus trigeminus was studied in *Varanus bivittatus* by Watkinson (1906), *Anolis carolinensis* by Willard (1915), *Ctenosaura pectinata* by Oelrich (1956) and *Chalcides ocellatus* by Soliman and Hegazy (1969).

Also, Mostafa (1990a) gave an account on the nervus trigeminus of *Acanthodactylus opheodurus*. In addition, Dakrory (1994, 2011) presented a detailed study on the cranial nerves of the limbless lizard *Deplometopon zarudnyi* and *Uromastyx aegyptius*, respectively. Abdel-kader (2005) gave a detailed study on the cranial nerves of the blind snake *Leptotyphlops cairi*.

It is obvious from this brief review that studies on the cranial nerves in general and the nervus trigeminus particularly in the family Scincidae are very few compared to the huge number of species in this family. This stimulated us to study the cranial nerves of *Mabuya quinquetaeniata*. The study also aims to analyze the fibre components of the nervus trigeminus and to show the relation between it and the other cranial structures.

2. Material and Methods

The heads of two young specimens of *Mabuya quinquetaeniata* were decalcified using EDTA solution then mounted and embedded in paraffin wax and serially sectioned transversely at 12 µm thick. The serial sections were stained with Malory's Triple Stain (Pantin, 1946).

The transverse sections were drawn with the help of a projector microscope. From these drawings an accurate graphic reconstruction for the nervus trigeminus was made, together with the nervus facialis in a lateral view. In order to show the relations of the nerves to the different parts of the head, several sections were photomicrographed.

3. Results

In *Mabuya quinquetaeniata*, the nervus trigeminus originates from the lateral side of the medulla oblongata by one stout root (Figs. 1& 2, RO.V). The trigeminal root runs forwards, within the cranial cavity passing medial to the lower edge of the auditory capsule, lateral to the medulla oblongata and ventral to the trochlear nerve. Thereafter, the trigeminal root leaves the cranial cavity through incisura prootica. This incisura (Fig. 3, IP) is located ventral to the anterior edge of the auditory capsule (AC) and dorsolateral to the lateral edge of the basisphenoid bone (BSP). The incisura prootica is separated from the facial foramen by the prefacial commissure. During its exit from the cranial cavity, the root of the nervus trigeminus (Figs. 1 & 3) divides into two divisions: a dorsolateral sensory division (DLD.RO.V) and a ventromedial mixed one (VMD.RO.V).

The dorsolateral sensory division extends anterolaterally to enter the maxillomandibular ganglion from its ventral side. This ganglion (Figs. 3, 4 & 6, G.MM) lies in the incisura prootica ventromedial to the anterior edge of the auditory capsule (AC), medial to the adductor mandibularis externus muscle (M.ADME), dorsal to the ventromedial division of the trigeminal root (VMD.RO.V) and lateral to the nervus trochlearis (N.IV). The maxillomandibular ganglion is a round-shaped structure as it appears in the serial transverse sections, its anterior end is continuous with the posterior part of the ophthalmic ganglion (Fig. 1). The ganglion receives a fine branch from the lateral part of the ventromedial division (Fig. 1, R.CM.LP.VMD.RO.V +G.MM). From the lateral side of the maxillomandibular ganglion arises the ramus maxillaris (R.MX) dorsolaterally and the ramus mandibularis (R.MN) ventrolaterally (Figs. 1, & 4).

The ventromedial division (Figs. 1 & 3) extends anterolaterally passing ventromedial and then, ventral to the dorsolateral division and divides into two parts; a medial part (MP.VMD.RO.V) and a lateral one (LP.VMD.RO.V). The medial part, which represents the ramus ophthalmic profundus (Figs. 1 & 4, R.OPH), runs forwards passing ventromedial to the dorsolateral division then to the maxillomandibular ganglion and medial to the lateral part. Shortly forwards it continues being surrounded by the anterior part of the maxillomandibular ganglion. Just at the anterior end of the latter ganglion, it enters the ophthalmic ganglion (Figs. 1 & 5, G.OPH). This ganglion is oval in shape and its posterior end is confluent with the anterior end of the maxillomandibular ganglion. The ophthalmic ganglion (Fig. 5, G.OPH) lies extracranially being ventrolateral to the cranial wall, ventral to the nervus trochlearis (N.IV), dorsal to the protractor pterygoideus muscle (M.PPT) and medial to the pseudotemporalis muscle (M.PST). From the anterior end of the ganglion, the ramus ophthalamicus profundus originates as one trunk (Fig. 1, R.OPH).

The lateral part of the ventromedial division (Figs. 1 & 3, LP.VMD.RO.V) extends forwards passing lateral to the medial part and ventral to the maxillomandibular ganglion. Here, it gives off a dorsal fine branch to the latter ganglion as previously mentioned (Fig. 1, R.CM.LP.VMD.RO.V+G.MM). This part runs anterolaterally passing ventral to the maxillomandibular ganglion, lateral to the medial part of the ventromedial division, dorsal to the protractor pterygoideus muscle and medial to the adductor mandibularis externus muscle. Here, it gives off a medial nerve which represents the constrictor dorsalis nerve (Figs. 1 & 6, N.CD). Shortly after that, the main lateral part of the ventromedial division continues giving off a dorsal nerve to the adductor mandibularis externus muscle (Fig. 1, N.ADME) and a fine nerve which fuses with the ramus mandibularis (Fig. 1, R.CM.LP.VMD.RO.V+MN). The remainder of this part divides into a dorsal nerve and a ventral one. The dorsal nerve represents the anguli oris nerve (Figs. 1 & 6, N.AO) while the ventral nerve enters the pseudotemporalis muscle (Fig. 1, N.PST).

Anguli Oris Nerve

From the lateral part of the ventromedial division of the nervus trigeminus. After its origin, it passes medial to the adductor mandibularis externus muscle and lateral to the maxillomandibular ganglion (Figs. 1 & 6, N.AO). Here, the anguli oris nerve divides into two nerves. The two nerves run anterodorsally passing dorsal to the protractor pterygoideus muscle and ventrolateral to the maxillomandibular ganglion. Thereafter, they pass lateral to the levator pterygoideus muscle, ventral to the ramus maxillaris of the nervus trigeminus and medial to the adductor mandibularis externus muscle (Fig. 7, N.AO). Shortly anterior, one of the two nerves enters the levator pterygoideus muscle to end between its fibres (Fig. 1, N.LPT). The other nerve continues its course forwards passing ventral to the ramus maxillaris and medial to the adductor mandibularis externus muscle. After a long anterior

course, it gives off a dorsal fine branch to the adductor mandibularis externus muscle (Fig. 1, N.ADME). Anterior to the origin of the previous branch, the main nerve extends forwards till it enters the posterior orbital region. Here, it divides into a lateral nerve and a medial one. The lateral nerve (Fig. 1, N.CU+SLG) ramifies and ends in the skin and the supralabial glands. The medial one extends anteromedially to end in the supralabial glands (Fig. 1, N.SLG).

Constrictor Dorsalis Nerve (NV4)

This nerve arises from the lateral part of the ventromedial division of the trigeminal root as previously mentioned (Figs. 1 & 6, N.CD). This nerve runs forwards, for a short distance, passing ventral to the maxillomandibular ganglion and lateral to medial part of ventromedial division. Here, it gives off a ventral nerve which extends forwards to enter the protractor pterygoideus muscle (Fig. 1, N.PPT).

The constrictor dorsalis nerve runs forwards ventral to the maxillomandibular ganglion then to the ophthalmic ganglion and dorsal to the protractor pterygoideus muscle. Thereafter, it continues extending ventromedial to the levator pterygoideus muscle and dorsal to the protractor pterygoideus muscle. Here, it gives off a dorsal nerve to the former muscle where it terminates (Fig. 1, N.LPT). Anterior to the origin of the previous nerve, the main nerve runs forwards for a long distance to enter the depressor palpbrae inferioris muscle, where it ramifies and ends between its fibres (Figs. 1, N.DPI).

Ramus Ophthalmicus Profundus

The ramus ophthalmicus profundus originates from the dorsomedial part of the anterior end of the ophthalmic ganglion as one trunk as previously mentioned (Figs. 1 & 6, R.OPH). It runs anteriorly for a distance and then divides into its two main rami: (Figs. 1 & 7) a dorsolateral ramus frontalis (R.FR) and a ventromedial ramus nasalis (R.NA).

Ramus Frontalis

Anterior to its separation from the ramus ophthalmicus profundus, the ramus frontalis (Figs. 1 & 7, R.FR) extends forwards in the dorsal direction passing dorsolateral to the ramus nasalis, ventrolateral to the membranous cranial wall and dorsomedial to the depressor palpbrae inferioris muscle. Thereafter, the ramus frontalis continues anteriorly extending dorsal to the latter muscle, medial to the levator pterygoideus muscle, lateral to the membranous cranial wall and dorsolateral to the ramus nasalis. More forwards and just posterior to the orbit, the ramus frontalis shifts dorsally passing lateral to the membranous cranial wall and medial to the adductor mandibularis externus muscle (Fig. 8, R.FR). Just ventral to the frontal bone, the ramus frontalis gives off several branches which run somewhat posterior and anastomose with the lacrimal plexus (Fig. 1, R.CM.FR+LCP). Thereafter, the ramus frontalis enters the orbital region and gives off a lateral branch. This branch extends forwards passing ventral to the frontal bone and gives off another lateral branch to the skin of the upper eye lid (Fig. 1, N.CU). The main lateral branch runs anteriorly in the lateral direction to end in the lacrimal gland (Fig. 1, N.LCG). Afterwards, the ramus frontalis runs anteriorly medial to the lacrimal gland and lateral to the cranial membranous wall giving off two successive branches to the skin of the upper eye lid (Fig. 1, Nn.CU). Thereafter, it gives off two successive branches to the meninges inside the cranial cavity (Fig. 1, Nn.ME). More anteriorly, the ramus frontalis gives off several successive branches to the skin of the upper eye lid (Fig. 1, Nn.CU). After a long anterior course, it gives off successive branches to the skin dorsal to the mid line region (dorsal to the nasal bone) and terminates in this region (Fig. 1, Nn.CU).

Ramus Nasalis

Anterior to its separation from the ramus ophthalmicus profundus, the ramus nasalis (Figs. 1& 7, R.NA) runs anteriorly passing dorsal to the depressor palpbrae inferioris muscle, ventral to the membranous cranial wall and ventromedial to the ramus frontalis. Thereafter, it passes dorsal to the bursalis muscle, ventromedial to both ramus frontalis and nervus trochlearis. Here, it gives a ventromedial branch, which is the radix ciliaris longa (Figs. 1 & 7, RCL). This runs anteriorly to enter the ciliary ganglion from its dorsolateral side (Fig. 1, G.CIL).

Anterior to the origin of the radix ciliaris longa, the ramus nasalis continues forwards passing dorsal to the bursalis muscle, lateral to both the rectus superior muscle and the ramus superior of the nervus oculomotorius and ventromedial to the nervus trochlearis. More forwards, the ramus nasalis passes medial to the rectus lateralis muscle, dorsal to the bursalis muscle and ventral and then lateral to the rectus superior muscle and the ramus superior of the nervus oculomotorius. Thereafter, it passes medial to the eye ball, ventral to the rectus superior muscle, lateral to the rectus medialis muscle and dorsal to the nervus opticus. More anteriorly, the ramus nasalis continues passing medial to the eyeball, ventromedial to the rectus superior muscle, ventral to the nervus trochlearis and lateral to the rectus medialis muscle. At the anterior half of the orbital region, the ramus nasalis continues forwards passing ventral to the medial edge of the obliquus superior muscle, dorsal

to the rectus medialis muscle and medial to the eyeball. More forwards, this ramus passes medial to Harder´s gland and lateral to the obliquus superior muscle. Reaching the anterior orbital region, the ramus nasalis passes medial to Harder´s gland and lateral to the interorbital septum. Entering the orbitonasal region, the ramus nasalis continues anteriorly passing ventromedial to sphenethmoidal commissure, lateral to the interorbital septum, medial to the eyeball and dorsolateral to the origin of the obliquus inferior muscle. Shortly anterior, the ramus nasalis gives off a dorsal branch to the blood vessel (Fig. 1, N.BV). Shortly after that, the ramus nasalis gives off a lateral cutaneous branch. This branch (Fig. 1, N.CU) pierces the prefrontal bone and ramifies and terminates in the skin in front of the eyeball (Fig. 1, Nn.CU). Immediately anterior to the origin of the previously described branch, the main ramus nasalis receives an anastomosing branch from the ethmoidal ganglion of the nervus facialis (Figs. 1 & 9, R.CM.NA+G.ET). At the point of connection with the ramus nasalis, the communicating branch carries few ganglionic cells. These cells represent a small dorsal part of the ethmoidal ganglion (Fig. 9, GC). Anterior to the connection, the ramus nasalis enters the nasal region passing through the foramen olfactorium evehens. After a long anterior course, the ramus nasalis divides intracapsularly into its two rami: the ramus medialis nasi (Figs. 1 & 10, R.MNA) and the ramus lateralis nasi (Figs. 1 & 10, R.LNA). There are a few ganglionic cells at the point of the division (Fig. 1, GC).

Ramus Medialis Nasi

Anterior to its separation from the ramus nasalis, the ramus medialis nasi (Figs. 1 & 10, R.MNA) extends, medial to the ramus lateralis nasi (R.LNA), ventromedial to the parietotectal cartilage (PTC) and lateral to the olfactory bulb (OL.BU). After a long anterior intracapsular course, this ramus shifts its course to pass dorsomedial to the olfactory epithelium and ventromedial to the parietotectal cartilage. More anteriorly, the ramus medialis nasi runs medial to the olfactory epithelium and lateral to the internasal septum. Thereafter, this ramus continues forwards passing medial to the olfactory epithelium (OL.EP), lateral to the internasal septum (S.IN) and dorsolateral to the septomaxillary bone (SMX). More forwards, it passes through a canal in the latter bone (Fig. 11, R.MNA). After a long anterior course and just opposite to the anterior end of the vomeronasal organ, the ramus medialis nasi leaves the septomaxillary canal and continues forwards passing ventromedial to the vestibule of the olfactory organ. More and more forwards, this ramus leaves the nasal capsule through the foramen apicale (Fig. 12, F.APC). Anterior to this foramen, the ramus medialis nasi runs anteriorly passing dorsal to the premaxillary bone and lateral to the nasal bone giving off three successive branches, to the blood vessels (Fig. 1, Nn.BV) and the teeth (Fig. 1, N.TE). After a short anterior course, the ramus medialis nasi seperates into two rami; one dorsal to the other: the ramus premaxillaris superior (Fig. 1, R.PMXS) dorsally and the ramus premaxillaris inferior (Fig. 1, R.PMXI) ventrally.

Ramus Premaxillaris Superior

The ramus premaxillaris superior (Fig. 1, R.PMXS) runs anteriorly in the dorsal direction, till it reaches the anterior extremity of the snout. During that, it gives off several branches to the skin at the ventral rim of the nasal capsule (Fig. 1, Nn.CU). Finally, this ramus terminates in the skin covering the anterior extremity of the snout.

Ramus Premaxillaris Inferior

The ramus premaxillaris inferior (Fig. 1, R.PMXI) runs forwards medial to the anterior part of the nasal capsule and dorsal to the premaxillary bone. After a short distance, it gives rise to six nerves to the skin of the anterior region of the nasal capsule (Fig. 1, Nn.CU). Thereafter, the remaining of this ramus ramifies and ends in the skin of the lips and the anterior edge of the snout (Fig. 1, Nn.CU).

Ramus Lateralis Nasi

After the separation of the ramus lateralis nasi from the ramus nasalis (Figs. 1 & 10, R.LNA), it passes lateral to the ramus medialis nasi, dorsal to the olfactory epithelium and ventral to the parietotectal cartilage. After a long anterior course in this position, the ramus lateralis nasi pierces the parietotectal cartilage to become dorsal to its lateral margin. Thereafter, the ramus lateralis nasi runs anterolateraly being lateral to the parietotectal cartilage and dorsomedial to the nasal gland (Fig. 13, R.LNA). After a short distance, it gives off a dorsal branch which runs dorsal to the pareitotectal cartilage and divides giving off two divisions; one lateral to the other. Both divisions pierce the nasal bone to give off several branches to the skin above the cranium medially and above the nostril laterally (Fig. 1, Nn.CU). The ventral branch arises from the ramus lateralis nasi and enters the nasal gland from its dorsal side. Thereafter, this ramus gives off a small lateral branch to innervate the skin lateral to the nasal gland (Fig. 1, Nn.CU). While the ramus lateralis nasi passing through the gland follicles, it gives off many fine branches innervating the nasal gland (Fig. 1, Nn.NAG). After a long anterior course, it leaves the nasal gland from its anterior end and turns laterally to

end in the skin lateral to the nasal region as many fine branches (Fig. 1, Nn.CU). Finally, this ramus ends as fine nerves in the narial muscle (Fig. 1, Nn.NR).

Ramus Maxillaris (N.V2)

The ramus maxillaris (Figs. 1 & 4, R.MX) originates from the dorsolateral corner of the maxillomandibular ganglion. It extends anterolaterally, in the dorsal direction, passing ventral to the levator pterygoideus muscle, medial to the adductor mandibularis externus muscle and dorsal to both the ramus mandibularis and the anguli oris nerve. Thereafter, it continues passing lateral to both the levator pterygoideus muscle and the posterior end of the pseudotemporalis muscle (Fig. 5, R.MX). After a long anterior distance in this position, it gives off two successive branches. These two branches represent the rami lacrimalis (Figs. 1 & 8, R.LC) and temporalis (Figs. 1 & 8, R.TM).

Ramus Lacrimalis

After its separation from the ramus maxillaris, the ramus lacrimalis (Figs. 1 & 8, R.LC) runs anteriorly passing medial to the adductor mandibularis externus muscle (M.ADME), lateral to the levator pterygoideus muscle (M.LPT) and dorsal to both the ramus temporalis (R.TM) and the ramus maxillaris (R.MX). More forwards, the ramus lacrimalis passes dorsomedial to the adductor mandibularis externus muscle, ventrolateral to both the levator pterygoideus muscle and the ramus frontalis of the nervus trigeminus and dorsal to the ramus temporalis. Thereafter, the ramus lacrimalis passes dorsomedial to the ramus temporalis and ventrolateral to the lacrimal gland. Here, it gives off a branch which joins another branch from the ramus frontalis for a short distance and then separate again into two branches; one passes posteriorly to join the lacrimal plexus (Fig. 1, R.CM.LC+LCP) and the other ends in the skin of this region (Fig. 1, N.CU). Shortly after that, the ramus lacrimalis gives off another cutaneous branch for the skin (Fig. 1, N.CU). Shortly anterior, it anastomoses with the ramus frontalis of the nervus trigeminus through a fine branch (Fig. 1, R.CM.FR+LC). Anterior to the origin of this branch, the ramus lacrimalis gives off another branch for the skin. Finally, it ends as two fine nerves in the lacrimal gland (Fig. 1, Nn.LCG).

Ramus Temporalis

After its separation from the ramus maxillaris, the ramus temporalis (Figs. 1 & 8, R.TM) passes dorsomedial to the adductor mandibularis externus muscle (M.ADME), dorsal to the ramus maxillaris (R.MX), ventral to the ramus lacrimalis (R.LC). Thereafter, this ramus passes dorsal to the adductor mandibularis externus muscle, ventral to the lacrimal gland and ventrolateral to the eyeball. More forwards, the ramus temporalis passes dorsal to the adductor mandibularis externus muscle and lateral to the eyeball. Here, it gives off three successive branches to the skin lateral to the eyeball (Fig. 1, Nn.CU). After that, it runs in the ventrolateral direction passing lateral to the eyeball giving off a lateral branch which ramifies and distributes on the skin lateral to the eyeball (Fig. 1, N.CU). Finally, the ramus temporalis continues anteriorly giving rise to many successive branches to the skin lateral to the eyeball (Fig. 1, Nn.CU).

Anterior to the origin of the previously described branches, the ramus maxillaris continues forwards passing in the ventromedial direction till it enters the orbital region as the infraorbital nerve. In the orbital region, the infraorbital nerve (Figs. 1 & 14, N.IO) runs anteriorly passing lateral to the eyeball, medial to the adductor mandibularis externus muscle and dorsal to the anguli oris nerve. Thereafter, it continues forwards passing dorsal to the anterior end of the pterygoid bone, dorsolateral to the depressor palpbrae inferioris muscle and ventrolateral to the eyeball. Here, it gives off a fine branch for the skin just posterior to the eye (Fig. 1, N.CU). Shortly after that, it receives an anastomosing branch from the ramus palatinus lateralis of the nervus facialis (Figs. 1 & 15, R.CM.IO+PAL). Here, the infraorbital nerve carries few ganglionic cells. Shortly anterior, this nerve continues passing ventrolateral to the eye ball and dorsal to the depressor palpbrae inferioris muscle. Here, it gives off four successive branches to the skin of the lower eyelid (Fig. 1, Nn.CU). Thereafter, the infraorbital nerve continues anteriorly passing ventral to the eyeball and medial to the jugal bone giving rise to lateral and medial branches. The lateral branch extends anterolaterally to end in the skin of the lower eyelid (Fig. 1, N.CU). The medial branch extends anterodorsally to enter and end in Harder′s gland (Fig. 1, N.HDG). Anterior to the origin of the previous branches, the infraorbital nerve gives off two or three successive branches for the skin of the check and the lower eyelid and the teeth (Fig. 1, Nn.CU+TE). After a forward course, the infraorbital nerve gives off a ventral branch, which ramifies and ends in the palatal epithelium medial to the dental lamina (Fig. 1, N.EP). Another two branches arise from the nerve and pass to the palatal epithelium (Fig. 1, Nn.EP). Shortly forwards, the infraorbital nerve receives a large branch from the medial palatine ramus (Figs. 1 & 16, R.CM.IO+PAM). The infraorbital nerve carries few ganglionic cells at the point of this fusion. The infraorbital nerve gives off a branch for the duct of Harder′s gland (Fig. 1, N.HDG).

Reaching the orbitonasal region, the infraorbital nerve continues anteriorly passing lateral to the palatal process of the palatine and dorsal to the medial end of the palatal process of the maxilla. Here, it receives the intermediate palatine ramus forming a common nerve (Figs. 1 & 17, CO.N). Anterior to this connection, the common nerve enters the nasal region passing dorsal to the palatal process of the maxilla, ventrolateral to the nasal duct and ventromedial to the prefrontal bone. Here, the common nerve separates into the infraorbital nerve (Figs. 1 & 18, N.IO) laterally and the ramus palatinus intermedialis (Figs. 1 & 18, R.PAI) ventromedially. The infraorbital nerve runs forwards passing dorsal to the palatal process of the maxilla, ventromedial to the cartilage ectocapsularis, ventrolateral to the olfactory chamber and dorsolateral to the ramus palatinus intermedialis. Shortly anterior, it gives off a lateral branch, which penetrates the maxilla and ramifies in the check and the upper lip (Fig. 1, N.CU).

The main nerve runs forwards passing medial to the previously described branch giving rise to a fine nerve which penetrates the maxillary bone laterally to end in the skin of the check lateral to the maxilla (Fig. 1, N.CU). Shortly forwards, the infraorbital nerve enters the maxillary bone through the superior alveolar foramen as the superior alveolar nerve.

The superior alveolar nerve (Figs. 1 & 19, N.SAV) extends anteriorly within the maxillary bone giving rise to a lateral branch. This branch extends anterolaterally leaving the maxilla. Lateral to the latter bone, it ramifies and ends in the skin covering the bone laterally (Fig. 1, N.CU). Shortly forwards, the main nerve divides into two branches, one lateral and the other medial. The lateral branch leaves the maxilla laterally to end in the skin covering its lateral side (Fig. 1, N.CU). The medial branch runs anterolaterally to leave the maxillary bone. Lateral to the latter bone, this branch divides into a ventral and a dorsal nerve. Both nerves run forwards lateral to the maxilla and ramify to innervate the skin lateral to the maxillary and premaxillary bones and posteroventral, ventral and anteroventral to the nostril (Fig. 1, Nn.CU). The medial branch gives off a medial nerve to the narial muscles (Fig. 1, N.NR).

Ramus Mandibularis (N.V3)

The ramus mandibularis (Figs. 1, 4 & 6, R.MN) arises from the ventromedial side of the maxillomandibular ganglion and runs anteroventrally receiving a branch from the lateral part of the ventrolateral division of the trigeminal root. Anterior to this connection, the ramus mandibularis gives off a ventral branch for the pterygomandibularis muscle (Fig. 1, N.PTM). Thereafter, the ramus mandibularis runs anteriorly passing dorsolateral and then lateral to the protractor pterygoideus muscle, ventrolateral to the maxillomandibular ganglion and medial to the adductor mandibularis externus muscle. Here, it gives off a ventral branch for the pseudotemporalis muscle (Fig. 1, N.PST).

Anterior to the origin of the pseudotemporalis nerve, the ramus mandibularis passes medial to the adductor mandibularis externus muscle, ventrolateral to the levator pterygoideus muscle and dorsolateral to the pterygomandibularis muscle. Thereafter, the ramus mandibularis continues anteriorly running medial to the adductor mandibularis externus muscle and lateral to the pterygomandibularis muscle. Here, the ramus mandibularis gives rise to a ventral nerve; the ramus cutaneous recurrens (Figs. 1 & 20, R.CUR). This ramus passes posteriorly running through a foramen excavated in the supra-angular bone of the mandible (Fig. 20, R.CUR). Thereafter, the ramus cutaneous recurrens passes ventral to the adductor mandibularis externus muscle and lateral to the supra-angular bone. More postriorly, the ramus cutaneous recurrens extends posterodorsally passing lateral to the adductor mandibularis externus muscle. Finally, it ends in the skin covering the lateral side of the latter muscle as fine branches (Fig. 1).

Anterior to the origin of the ramus cutaneous recurrens, the ramus mandibularis continues anteriorly in the ventral direction passing ventromedial to the adductor mandibularis externus muscle, lateral to the pterygomandibularis muscle and dorsal to the mandible. Thereafter, the ramus mandibularis passes ventromedial to the adductor mandibularis externus muscle, ventrolateral to the pseudotemporalis muscle and dorsolateral to the mandible. More anteriorly, the ramus mandibularis enters the primordial canal (Fig. 21, PRC) of the mandible through the primordial fossa (Fig. 21, PRF) as the inferior alveolar nerve (Fig. 21, N.IAV). This nerve extends forwards inside this canal giving off a ventromedial mixed; sensory and motor branch (Fig. 1, N.MI). This branch runs anteriorly passing ventral to Meckel's cartilage and after a short course anteriorly, it leaves the primordial canal through a foramen excavated in the ventromedial side of the angular bone. After its exit, this branch runs anteriorly, passing dorsolateral to the intermandibularis muscle and ventromedial to the mandible. Thereafter, it penetrates the latter muscle giving off two lateral branches to it (Fig. 1, Nn.IM). More anteriorly, the main branch runs ventral to the intermandibularis muscle giving off a medial branch to the intermandibularis muscle (Fig. 1, N.IM). The main branch continues forwards passing ventral to the intermandibularis muscle to terminate in the skin lateral and ventrolateral to the mandible and ventral to the latter muscle (Fig. 1, N.CU).

Shortly anterior, the inferior alveolar nerve gives off a lateral branch (Fig. 1, N.CU+ILG). After a long course inside the primordial canal, this branch leaves it through a foramen excavated in the ventrolateral side of the dentary bone. Ventrolateral to the bone, this branch extends forwards giving off a lateral branch to the infralabial gland (Fig. 1, N.ILG). Shortly forwards, the main branch gives off a lateral nerve to the skin of the lower lip (Fig. 1, N.CU). Thereafter, the main branch continues its anterior course giving rise to several cutaneous branches to the skin lateral to the infralabial gland (Fig. 1, Nn.CU). The main branch, finally achieves its final distribution in the infralabial gland (Fig. 1, N.ILG).

Anterior to the origin of the previously described branches, the inferior alveolar nerve continues forwards passing lateral to both Meckel's cartilage and chorda tympani of the facial nerve. Thereafter, the main nerve continues passing ventromedial to the chorda tympani (Fig. 22, CT&N.IAV). After a short course anteriorly, the chorda tympani fuses with the inferior alveolar nerve forming a mixed nerve (Figs. 1 & 15, N.MI). The mixed nerve carries few ganglionic cells at the point of fusion; these cells represent the mandibular ganglion (Fig. 1, G.MN).

After a long anterior course within the primordial canal, the mixed nerve (inferior alveolar nerve and the chorda tympani nerve) gives rise to a large branch; the ramus intermandibularis caudalis.

Ramus Intermandibularis Caudalis

After its separation from the mixed nerve, the ramus intermandibularis caudalis (Figs. 1 & 23, R.IMC) runs forwards inside the primordial canal, in the ventromedial direction till it leaves the canal through a foramen in the angular bone (Fig. 23, R.IMC). After its emergence, this ramus extends anteriorly passing ventrolateral to intermandibularis muscle and medial to the mandible. Here, the ramus intermandibularis caudalis gives off a posterior branch. This branch extends backwards medial and ventral to the mandible, where it ramifies into numerous fine nerves to the skin of this region (Fig. 1, N.CU). After that, the main ramus gives off two nerves which enter the intermandibularis muscle, where they ramify and end between its fibres (Fig. 1, Nn.IM). Thereafter, the ramus intermandibularis caudalis continues forwards being ventromedial to the dentary bone until it reaches the anterior extremity of the lower jaw. During this course, it gives off eight successive nerves to the skin covering the dentary bone ventrally and laterally (Fig. 1, Nn.CU). Finally, the remainder of the ramus intermandibularis caudalis ramifies and terminates in the skin of the anterior extremity of the lower jaw (Fig. 1, Nn.CU).

Anterior to the origin of the ramus intermandibularis caudalis, the mixed nerve gives off a medial branch (Figs. 1 & 24, Rr.IMO+IMM). This branch runs forwards within the primordial canal till it leaves this canal through a foramen in the dentary bone (Fig. 24). After its exit, this branch extends forwards for a short distance and then divides into two large branches: a lateral ramus intermandibularis oralis (Figs. 1 & 25, R.IMO) and a medial ramus intermandibularis medius (Figs. 1 & 25, R.IMM).

Ramus Intermandibularis Oralis

The ramus intermandibularis oralis runs anteriorly in the dorsomedial direction passing medial to the mandible and lateral to the lingual gland. It gives many fine branches (about eight branches) to the lingual gland (Fig. 1, Nn.LGG) and two branches to the epithelium lining the corner of the mouth (Fig. 1, Nn.EP). Afterwards, this ramus extends in the dorsomedial direction, giving off several branches to the epithelium lining the corner of the mouth and the dental lamina (Fig. 1, Nn.CU+DE). Finally, this ramus ends as fine nerves in the taste buds and the epithelium lining the corner of the mouth (Fig. 1, Nn.TB+EP).

Ramus Intermandibularis Medius

The ramus intermandibularis medius or ramus paralingualis (Figs. 1 & 25, R.IMM), runs posteriorly in the dorsolateral direction passing lateral, then, dorsal to the intermandibularis muscle till it fuses with the ramus lingulalis lateralis of the nervus hypoglossus (Fig. 1). The fibres of this ramus are carried to their final fate by the rami of the nervus hypoglossus. From the above description, it is clear that, the fibres of the chorda tympani carried by the inferior alveolar nerve are more or less divided into two portions; one portion incorporates with the intermandibularis oralis, while the other portion combines with the intermandibularis medius or the ramus paralingualis.

After seperation of the ramus intermandibularis medius and the ramus intermandibularis oralis from the inferior alveolar nerve, the latter continues anteriorly inside the primordial canal (Fig. 25, N.IAV). After a long anterior course on this canal, it gives off a lateral branch. This branch (Fig. 1, N.CU+ILG) runs anteriorly and divides into two nerves; one lateral to the other. The lateral nerve runs anteriorly leaving the canal through a foramen in the dentary bone to end in the skin lateral to the latter bone (Fig. 1, N.CU). The medial nerve runs anteriorly through the canal giving off a lateral branch. This branch runs anteriorly to end in the

infralabial gland (Fig. 1, N.ILG). The medial nerve continues anteriorly till it leavs the canal passing ventral then lateral to the infralabial gland and finally terminates in the skin lateral to the gland.

Anterior to the origin of the previously described branch, the inferior alveolar nerve continues inside the primordial canal for a long course (Figs. 18 & 19, N.IAV). After this course, it gives off a fine lateral branch. This lateral branch runs anteriorly passing lateral to the inferior alveolar nerve. After a long distance anteriorly, this branch leaves the canal through a foramen in the dentary bone. This branch terminates in the skin lateral to the latter bone (Fig. 1, N.CU). More anteriorly, the inferior alveolar nerve gives off two lateral branches which leave the primordial canal through the same foramen in the dentary bone to innervate the skin lateral to it (Fig. 1, Nn.CU). After a long forwards course, the inferior alveolar nerve leaves the canal through a foramen in the dentary bone and divides into a dosolateral branch and ventromedial one (Fig. 1). The dorsolateral branch extends anteriorly and branches to innervate in the most anterior infralabial gland and the skin covering this region (Figs. 1, N.CU+ILG). The ventromedial branch runs forwards and ramifies in the skin of the lower jaw at its anterior tip (Fig. 1).

4. Discussion

In this study, the nervus trigeminus of *Mabuya quinquetaeniata* arises by one root. This root shows a distinct separation into two divisions. This is the common condition among lacertilians as in *Chalcides ocellatus* (Soliman and Hegazy, 1969), *Tarentola mauritanica* (Soliman and Mostafa, 1984), *Acanthodactylus opheodurus* (Mostafa, 1990a), in *Agama pallida* and *Ptyodactylus hasselquistii* (Abdel-Kader, 1990*), Diplometopon zarudnyi* (Dakrory, 1994), *Acanthodactylus boskianus* (El-Ghareeb, 1997), *Agama sinaita* (Ramadan, 2009) and *Uromastyx aegyptius* (Dakrory, 2011). However, the nervus trigeminus separates into three roots in *Anolis carolinensis* (Willard, 1915). On the other hand, in some ophidians, the nervus trigeminus originates by two separate roots in both *Eryx jaculus* and *Cerastes vipera* (Hegazy, 1976) and *Spalerosophis diadema* (Mostafa, 1990b). However, three roots were found in *Psammophis sibilans* (Hegazy, 1976) and in *Natrix tessellate* (Dakrory and Mahgoub, 2005). A single trigeminal root was found in *leptotyphlops cairi* (Abdel-Kader, 2005) and in *Telescopus dhara* (Abdel-Kader, 2006).

In birds, the nervus trigeminus arises by two separate roots in *Upupa epops*, and by a single root in both *Passer domesticus* and *Streptopelia senegalensis* (Soliman *et al*., 1986). Also, it arises by a single root in *Gallinula chloropus* (Abdel-Kader, 2000) and in *Merops albicillis* (Abdel-Kader and Fathy, 2002).

In mammals, the nervus trigeminus arises by two separate roots; a large sensory root and a small motor root (Qurinig, 1950; Weichert, 1958; Gasser and Wise, 1972). Earlier, Bandy (1932) reported the existence of an accessory sensory root for the nervus trigeminus in mammals. This root was referred to as an intermediate root which was described in man (Jannetta and Rand, 1966; Vidić and Stefanatus, 1969) and in dog (Augustine *et al*., 1971).

In this study, the protractor pterygoideus, levator pterygoideus and depressor palpebrae inferioris muscles represent the constrictor dorsalis muscles. According to Edgeworth (1935), a depressor palpebrae inferioris muscle is found in lacertilians and crocodilians. However, Lakjer (1926) and Brock (1938) said that a depressor palpebrae inferioris muscle is absent in the geckos. In ophidians, the depressor palpebrae inferioris muscle is commonly lacking (Underwood, 1970; Haas, 1964 & 1968; Hegazy, 1976; Mostafa, 1990b). Also, this muscle is absent in Chelonia (Soliman, 1964).

Regarding reptiles, the constrictor dorsalis muscles are commonly present. However, these muscle are absent in Chelonia (Lakjer, 1926; Poglayen- Neuwall, 1953a; Soliman, 1964). The constrictor dorsalis muscles are present in Plagoistomi, Teleostomi and Saurapsida but absent in Holocephali, Dipnoi, Amphibia and Mammalia (Edgeworth, 1935).

In *Mabuya quinquetaeniata* studied, the constrictor dorsalis nerve is an extension of the motor trigeminal root. This condition is common in the ophidians and is quite different from what was found in majority of lacertilians so far described. Among most lacertilians, the constrictor dorsalis nerve arises directly from the trigeminal (maxillo-mandibular) ganglion (Polglayen-Neuwall, 1954; Soliman and Mostafa, 1984; Abdel-Kader, 1990). On the other hand, the constrictor dorsalis nerve is an extension of the motor trigeminal root in *Chalcides ocellatus* (Soliman and Hegazy, 1969), *Acanthodactylus opheodurus* (Mostafa, 1990a), *Ptyodactylus hasselquistii* (Abdel-Kader, 1990) and in *Diplometopon zarudyi* (Dakrory, 1994). Also, Among ophidians, the constrictor dorsalis nerve is an extension of the motor trigeminal root as present in *Psammophis sibilans*, *Eryx jaculus* and *Cerastes vipera* (Hegazy, 1976) in *Spaleorsophis diadema* (Mostafa, 1990b) and in *Leptotyphlops cairi* (Abdel-Kader, 2005). In *Elaphe obseleta*, however, the constrictor dorsalis nerve or the pterygoid division as termed by Auen and Langebartel (1977) arises as a stalk from the ventral surface of the trigeminal ganglion.

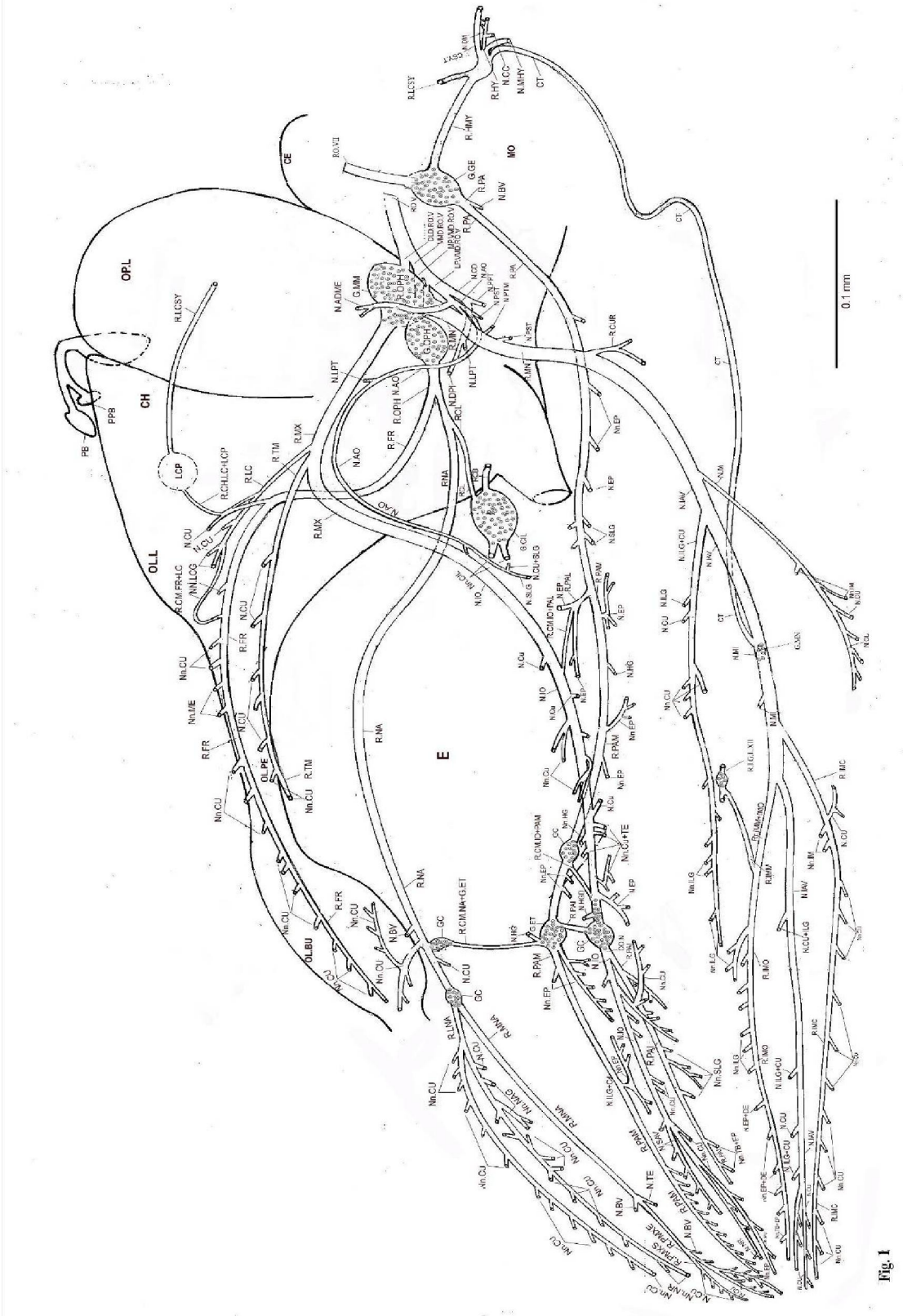

Fig. 1: Graphic reconstruction of the nervi trigeminus and facialis in a lateral view.

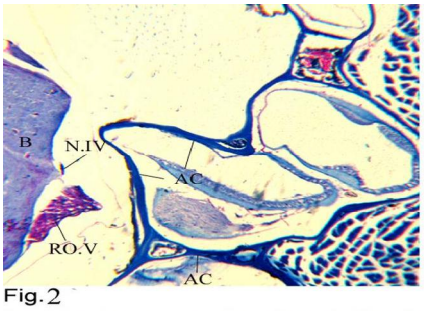

Fig. 2

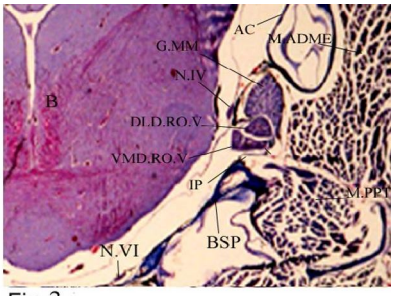

Fig. 3

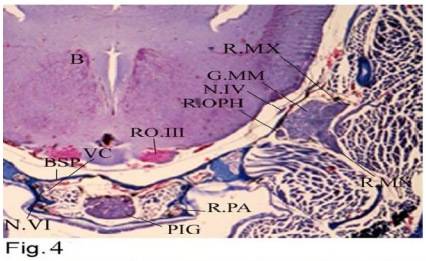

Fig. 4

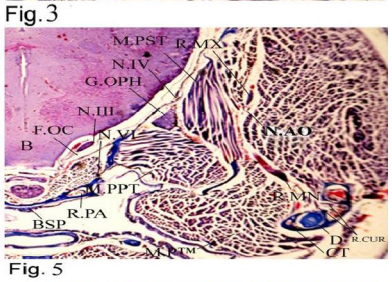

Fig. 5

Fig. 6

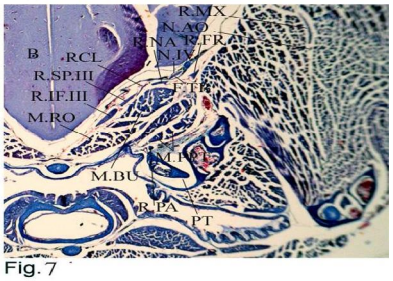

Fig. 7

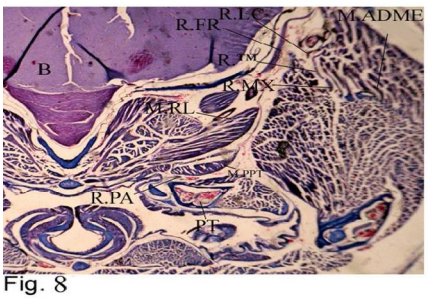

Fig. 8

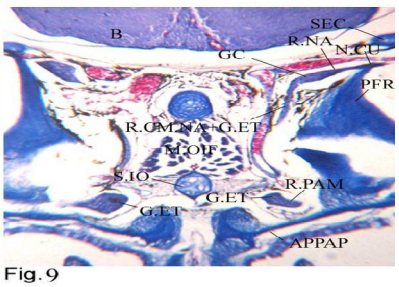

Fig. 9

Fig. 2: Photomicrograph of a part of a transverse section passing through the otic region showing the the origin of the nervus trigeminus from the brain.

Fig. 3: Photomicrograph of a part of a transverse section passing through the anterior part of the otic region showing the division of the trigeminal root into the dorsolateral and the ventromedial divisions, the maxillomandibular ganglion.

Fig. 4: Photomicrograph of a part of a transverse section passing through the postorbital region showing the origin of the rami maxillaris and mandibularis of the nervus trigeminus from the maxillomandibular ganglion and the ramus palatinus of the nervus facialis passing through the vidian canal.

Fig. 5: Photomicrograph of a part of a transverse section passing through the postorbital region showing the position of the ophthalmic profundus ganglion. The course of the rami maxillaris and mandibularis of the nervus trigeminus and the passage of the ramus cutaneus recurrens through the mandible. It also demonstrates the the passage of the ramus palatinus of the nervus facialis through vidian canal within the basisphenoid bone.

Fig. 6: Photomicrograph of a part of a transverse section passing through the anterior part of the otic region showing the maxillomandibular ganglion, the ophthalmic profundus ramus, the constrictor dorsalis and anguli oris nerves. It also demonstrates the origin of the ramus mandibularis from the maxillomandibular ganglion.

Fig. 7: Photomicrograph of a part of a transverse section passing through the postorbital region showing the course of the rami frontalis and nasalis. It also illustrates the radix ciliaris longa, the ramus maxillaris and the anguli oris nerve.

Fig. 8: Photomicrograph of a part of a transverse section passing through the postorbital region showing the passage of the rami frontalis, maxillaris, lacrimalis and temporalis.

Fig. 9: Photomicrograph of a part of a transverse section passing through the orbitonasal region illucidating the ethmoidal ganglion, the ramus nasalis and the communicating branch in-between.

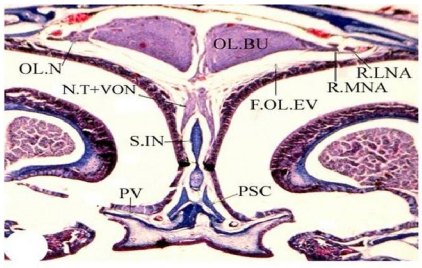

Fig.10

Fig.11

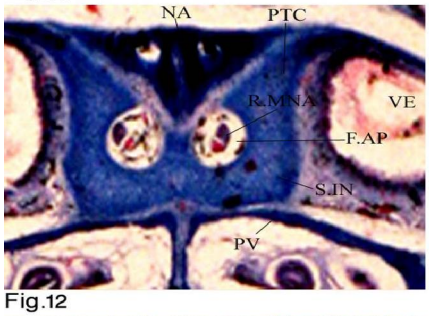

Fig.12

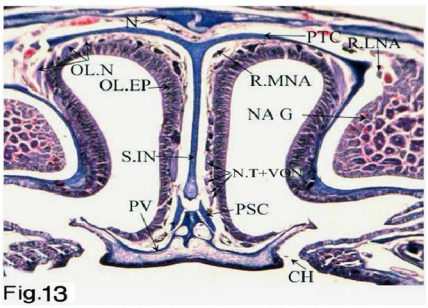

Fig.13

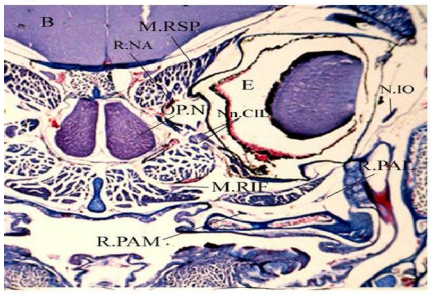

Fig. 14

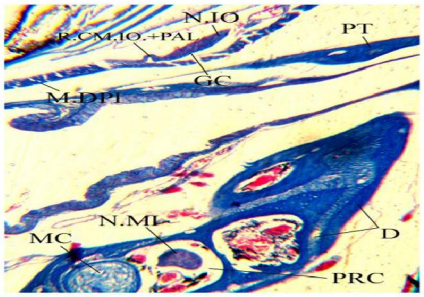

Fig. 15

Fig. 16

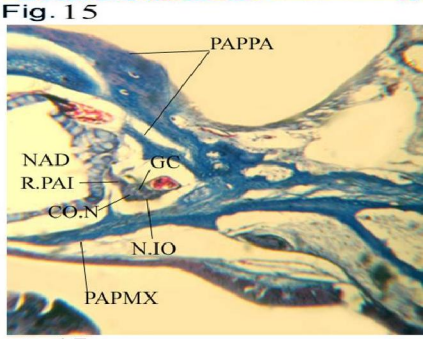

Fig. 17

Fig. 10: Photomicrograph of a part of a transverse section of the olfactory region showing the position of rami medialis and lateralis nasi.

Fig. 11: Photomicrograph of a part of a transverse section passing through the olfactory region showing the course of the ramus naslais of the nervus trigeminus in a bony cana of the septomaxillary bone.

Fig. 12: Photomicrograph of a part of a transverse section passing through the olfactory region showing the ramus medialis nasi passing through the foramen apicale.

Fig 13: Photomicrograph of a part of a transverse section passing through the olfactory region showing the position of each of the rami medialis and lateralis nasi.

Fig. 14: Photomicrograph of a part of a transverse section passing through the orbital region showing the position of the infraorbital nerve and the rami palatinus lateralis and medialis.

Fig. 15: Photomicrograph of a part of a transverse section passing through the orbital region showing the fusion of the infraorbital nerve and the ramus palatinus lateralis. It also illucidates the passage of the mixed nerve (ramus mandibularis and chorda tympani) through the primordial canal of the mandible.

Fig. 16: Photomicrograph of a part of a transverse section passing through the orbitonasal region showing the communication between the infraorbital nerve and the ramus palatinus medialis.

Fig. 17: Photomicrograph of a part of a transverse section passing through the orbitonasal region showing the fusion of the infraorbital nerve and the ramus palatinus intermedialis.

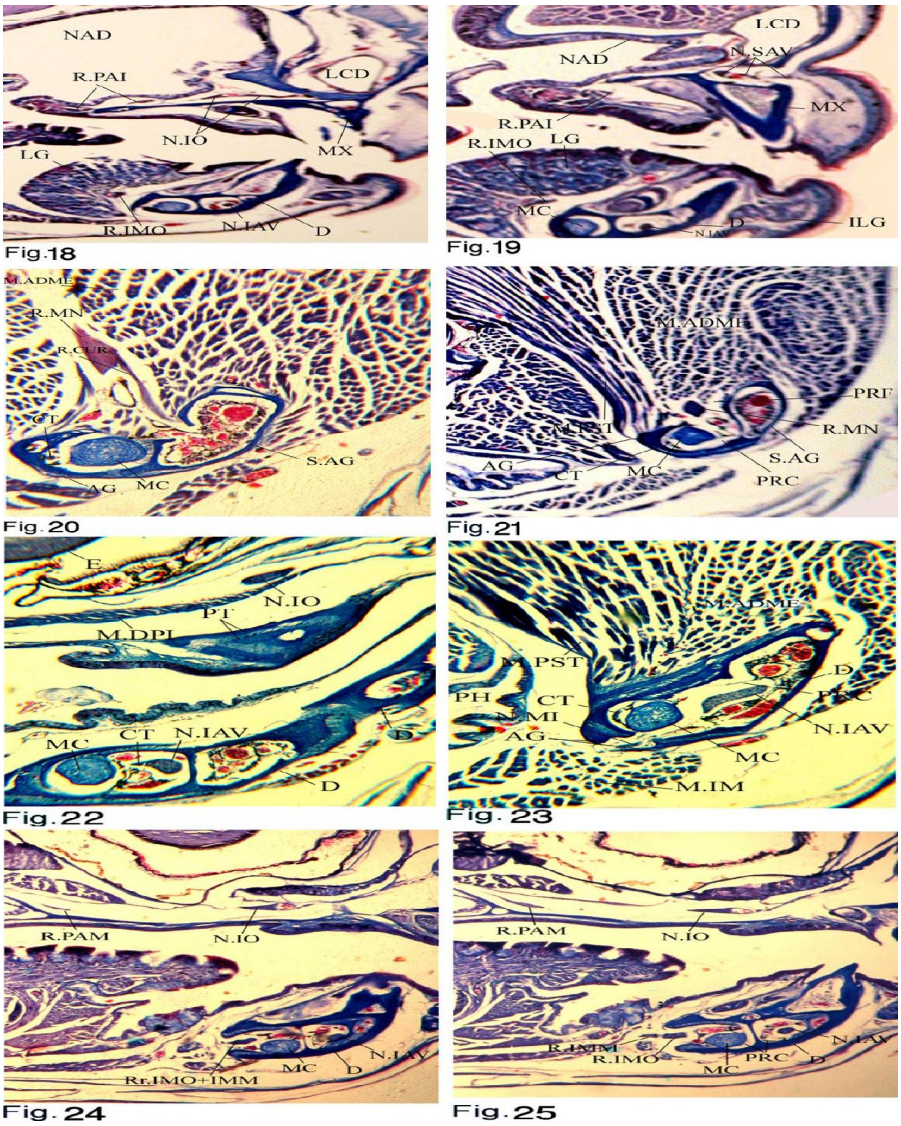

Fig. 18: Photomicrograph of a part of a transverse section passing through the olfactory region showing the infraorbital nerve passing through the maxilla and the intermediate palatine ramus passing to the supralabial gland. It also illucidates the inferior alveolar nerve passing through the primordial canal and position of the ramus intermandibularis oralis.

Fig. 19: Photomicrograph of a part of a transverse section passing through the olfactory region showing both the superior alveolar nerve passing through the maxilla and the position of the intermediate palatine ramus. It also demonstrates the inferior alveolar nerve passing through the primordial canal and the position of the ramus intermandibularis oralis.

Fig. 20: Photomicrograph of part of transverse section passing through the postorbital region showing the origin of the ramus cutaneous recurrens from the ramus mandibularis and its passage through the mandible.

Fig. 21: Photomicrograph of a part of a transverse section passing through the postorbital region showing the entrance of the ramus mandibularis into the primordial canal through the primordial fossa. It also illucidates the passage of the chorda tympani through the same canal.

Fig. 22: Photomicrograph of a part of a transverse section passing through the orbital region showing the position of the infraorbital nerve and the position of both the inferior alveolar nerve and the chorda tympani.

Fig. 23: Photomicrograph of a part of a transverse section passing through the orbital region showing the mixed nerve in the primordial canal giving off the ramus intermanibularis caudalis, the latter leaves the mandible. It also shows the position of the chorda tympani inside the canal.

Fig. 24: Photomicrograph of a part of a transverse section passing through the orbital region showing the origin of the rami intermandibularis oralis and medius, as one nerve, from the ramus mandibularis and their exit from the primordial canal. It also demonstrates the position of the infraorbital nerve and the medial palatine ramus.

Fig. 25: Photomicrograph of a part of a transverse section passing through the orbital region showing the separation of the rami intermandibularis oralis and medius. It also illustrates the position of the infraorbital nerve and the medial palatine ramus.

The absence of the constrictor dorsalis muscles in Chelonia leads to the absence of the constrictor dorsalis nerve as stated by Lakjer (1926), Poglayen-Neuwall (1953b) and Soliman (1964). However, Hoffmann (1890) described a nerve arising from the trigeminal trunk to innervate such muscles in *Chelone*; a case which was denied by Soliman (1964) dealing with the same chelonid.

In this study, there is one constrictor dorsalis nerve to innervate the three constrictor dorsalis muscles. This was found in *Hatteria* (Poglayen-Neuwall, 1954), in *Agama pallida* (Soliman *et al*., 1984; Abdel-Kader, 1990), *Diplometopon zarudnyi* (Dakrory, 1994), *Acanthodactylus boskianus* (El-Ghareeb, 1997) and in *Leptotyphlops cairi* (Abdel-Kader, 2005). However, in Lacertilia, the constrictor dorsalis nerve is represented by two branches in *Tarentola mauritanica* (Poglayen-Neuwall, 1954; Soliman and Mostafa, 1984) and in *Acanthodactylus opheodurus* (Mostafa, 1990a).

In the present study, there is no anastomosis between the constrictor dorsalis nerve and the ramus palatinus of the nervus facialis. This case was also described in gecko *Ptyodactylus hasselquistii* (Abdel-Kader, 1990). On the other hand, this anastomosis was mentioned by many authors in several lacertilians and ophidians. Among Lacertilia, this was described in *Chalcides ocellatus* (Soliman and Hegazy, 1969), *Tarentola mauritanica* (Poglayen-Neuwall, 1954; Soliman and Mostafa, 1984), *Acanthodactylus opheodurus* (Mostafa, 1990a), *Agama pallida* (Abdel-Kader, 1990) and in *Diplometopon zarudnyi* (Dakrory, 1994). About ophidians, the connection between the constrictor dorsalis nerve and the ramus palatinus of the nervus facialis was described by Hegazy (1976) in *Psammophis sibilans*, *Eryx jaculus* and *Cerastes vipera,* by Mostafa (1990b) in *Spaleorsophis diadema* and by Abdel-Kader (2005) in *Leptotyphlops cairi*.

In *Mabuya quinquetaeniata* studied, the trigeminal ganglion is represented by two ganglia; the maxillomandibular and the ophthalmic profundus ganglia. This is the common case in reptiles. Among lizards, this condition was described by Polglayen-Neuwall (1954), Soliman and Mostafa (1984), Abdel-Kader (1990), El-Ghareeb (1997) and by Ramadan (2009). In addition, this case was reported in snakes by Haas (1964 & 1968), Hegazy (1976) and Mostafa (1990b) and by Shiino (1914) in the crocodilian *Crocodilus*.

In other reptiles, the trigeminal ganglion is represented by a single mass; the Gasserian ganglion. This case present in chelonians as recorded by Polglayen-Neuwall (1953a & b) and Soliman (1964) and in the amphisbaenian *Diplometopon zarudnyi* (Dakrory, 1994).

In the present study, the maxillomandibular and the ophthalmic ganglia are connected with each other and are located extracranially. This case was mentioned in *Tarentola mauritanica* (Soliman and Mostafa, 1984), *Agama pallida* and *Ptyodactylus hasselquistii* (Abdel-Kader, 1990), *Diplometopon zarudnyi* (Dakrory, 1994), in *Acanthodactylus boskianus* (El-Ghareeb, 1997) and in *Uromastyx aegyptius* (Dakrory, 2011). However, in *Chalcides ocellatus* (Soliman and Hegazy, 1969), the maxillomandibular ganglion lies intracranially. In Chelonia, the trigeminal ganglion located intracranially in chelonians studied by Polglayen-Neuwall (1953b). In *Chedydra serpentine*, Soliman (1964) said that the posteromedial part of the trigeminal ganglion is located intracranially, while its anterolateral part lies extracranially. In Ophidia, the maxillomandibular and the ophthalmic ganglia are connected with each other and are located intracranially. This was recorded by Hegazy (1976) in *Psammophis sibilans*, *Eryx jaculus* and *Cerastes vipera,* by Mostafa (1990b) in *Spalerosophis diadema.* In some other cases, there is a fusion occures between the trigeminal and geniculate ganglia. This fusion was recorded in *Liotyphlps albirostris* and *Anomalepis aspinosus* (Haas, 1964 & 1968, respectively) and in *Leptotyphlops cairi* (Abdel-Kader, 2005).

In the present study, the trigeminal ganglia (maxillomandibular and ophthalmic) give off three main rami; the ophthalmicus profundus, maxillaris and mandibularis. This was the condition observed in *Chalcides ocellatus* (Soliman and Hegazy, 1969), *Acanthodactylus opheodurus* (Mostafa, 1990a), *Ptyodactylus hasselquistii* (Abdel-Kader, 1990) and in the amphisbaenian *Diplometopon zarudnyi* (Dakrory, 1994). This case, however, is quite different from what was found in the majority of lacertilians so far described, where the constrictor dorsalis nerve arises from the trigeminal ganglion (Poglayen-Neuwall, 1954; Soliman and Mostafa, 1984; Abdel-kader, 1990). In Ophidia, the trigeminal ganglia also give off the same three rami. This case was observed by many authors (Pringle, 1954; Hegazy, 1976; Auen and Langebartel, 1977; Mostafa, 1990b; Dakrory and Mahgoub, 2005; Abdel-Kader, 2005). The condition observed in *Mabuya quinquetaeniata* studied was also mentioned by Hegazy (1976) and Mostafa (1990b) in the ophidians.

In the present study, the anguli oris nerve arises from the main lateral part of the ventromedial division of the nervus trigeminus. This nerve carries both motor and sensory fibres; the motor component passes to the adductor mandibularis extenus and the

levator pterygoideus muscles. The sensory fibres are carried to the skin at the angle of the mouth. This agrees with the finding of Poglayen-Neuwall (1954) in all the lizards she studied, Soliman and Mostafa (1984) in *Tarentola mauritanica*, Abdel-Kader (1990) in *Ptyodactylus hasselquistii* and Dakrory (1994) in *Diplometopon zarudnyi*. On the other hand, the anguli oris nerve innervates in addition to the adductor externus muscle, the pseudotemporalis muscle in *Chalcides ocellatus* (Soliman and Hegazy, 1969), *Agama pallida* (Soliman *et al*., 1984; Abdel-Kader, 1990) and in *Acanthodactylus opheodurus* (Mostafa, 1990a).

In Ophidia, there is a branch given by the ramus mandibularis to the adductor externus muscle, it may be homologous to the anguli oris nerve as it carries both motor and sensory fibres. This was described by Hegazy (1976) in *Psammophis sibilans*, *Eryx jaculus* and *Cerastes vipera*, by Mostafa (1990b) in *Spalerosophis diadema* and by Abdel-Kader (2005) in *Leptotyphlops cairi*. However, the anguli oris nerve arises from ramus maxillaris in *Dermochelys coriacea* and from the trigeminal ganglion itself in Chelonia (poglayen-Neuwall, 1953 a & b).

In this study, the ramus ophthalmicus profundus arises from the anterior end of the ophthalmic ganglion as a separate branch, and then it divides into two rami; the ramus frontalis and the ramus nasalis. This case was mentioned among Lacertilia in *Diplometopon zardunyi* (Dakrory, 1994). This condition was recorded in most ophidians as in *Psammophis sibilans*, *Eryx jaculus* and *Cerastes vipera* (Hegazy, 1976), *Elaphe obsolete* and *Thamnophis ordinoides* (Auen and Langerbartel, 1977), *Spalerosophis diadema* (Mostafa, 1990b), *Natrix tessellata* (Dakrory and Mahgoub, 2005) and in *Leptotyphlops cairi* (Abdel-Kader, 2005). However, in most lacertialians, the ramus ophthalmicus arises as two separate rami; frontalis and nasalis (Soliman and Hegazy, 1969; Soliman and Mostafa, 1984; Mostafa, 1990a; Abdel-Kader, 1990; El-Ghareeb, 1997).

In the present study, the ramus frontalis is in connection with the lateral cranial sympathetic ramus through the lacrimal plexus. This is the case mentioned in all the lacertilians so far described (Underwood, 1970; Soliman and Mostafa, 1984; Mostafa, 1990a; Dakrory, 1994; Ramadan, 2009). On the other hand, in the Agamid *Uromastyx aegyptius* (Dakrory, 2011) the connection is described with the ophthalmic ganglion and not with the ramus frontalis.

In this study, the ramus nasalis anastomoses once with the medial palatine ramus of the nervus facialis in the orbitonasal region where the latter carries the ethmoidal ganglion. Howevere, in Chelonia, there is no connection between the ramus nasalis and the ramus palatinus of the nervus facialis in the anterior orbital region (Soliman, 1964). The same result was found in *Diplometepopon zarudnyi* (Dakrory, 1994). On the other hand, in *Chalcides ocellatus* (Soliman and Hegazy, 1969) and *Acanthodactylus opheodurus* (Mostafa, 1990a), there are two anastomosis; where the medial palatine ramus is connected with both the ramus nasalis and the ramus medialis nasi (ramus premaxillaris inferior). The anastomosis between the ramus medailis nasi and the ramus maxillaris recorded in the amphisbaenian *Diplometopon zarudnyi* (Dakrory, 1994) was not recorded in the present study. Among ophidians, the latter connection was reported in *Eryx jaculus* and *Cerastes vipera* by Hegazy (1976) and in snake *leptotyphlops cairi* (Abdel-kader, 2005).

Concerning Reptilia, Underwood (1970) stated that the connection between the ramus nasalis and the medial palatine ramus is a common character among Lacertilia. This connection was mentioned by Soliman and Hegazy (1969), Soliman and Mostafa (1984), Mostafa (1990a), Abdel-Kader (1990), Dakrory (1994) and El-Ghareeb (1997). Concerning Ophidia, such anastomosis was found in *Psammophis sibilians*, *Eryx jaculus* and *Cerastes vipeira* (Hegazy, 1976), *Spalerosophis diadema* (Mostafa, 1990b) and in *Leptotyphlops cairi* (Abdel-Kader, 2005).

In the present study, the ramus nasalis divides into two main branches; the ramus lateralis nasi and the ramus medialis nasi. This division occures in the nasal capsule "intracapsullarly" and the ramus lateralis nasi emerges from the nasal capsule through the foramen epiphaniale. This agrees with the condition found in *Cordylus cordylus* (Van Pletzen, 1946), *Chalcides ocellatus* (Soliman and Hegazy, 1969), *Tarentola mauritanica* (Soliman and Mostafa, 1984), *Acanthodactylus opheodeurus* (Mostafa, 1990a), *Ptyodactylus hasselquistii* (Abdel-Kader, 1990), *Diplometopon zarudnyi* (Dakrory, 1994) and *Acanthodactylus boskianus* (El-Ghareeb, 1997). In *Rhampholeon platyceps* (Frank, 1951), *Microsaura pumila* (Engelbrecht, 1951), *Agama pallida* (Abdel-kader, 1990), *Agama sinaita* (Ramadan, 2009) and in *Uromastyx aegyptius* (Dakrory, 2011) the division is extracapsullar and the ramus lateralis nasi does not enter the nasal capsule and therefore the foramen epiphaniale is absent. The same was found in *Agama atra* and *Agama hispida* (Malan, 1946). However, Barry (1953) stated that the ramus nasalis in *Agama hispida* neither spilt into its two known branches nor enters the nasal capsule. On the other hand, Eyal-Giladi (1964) reported that, in *Agama stellio*, the ramus nasalis divides extracapsular and the ramus lateralis nasi leaves the nasal capsule through the foramen epiphaniale. This agrees very well with the

condition found in *Calotes versicolor* (Ramaswami, 1946).

In Ophidia, the ramus nasalis divids extracapsullary and the ramus lateralis nasi enters the cavity of the nasal capsule and then leaves it through the foramen epiphaniale. This found in Liotyphlops albirostris (Haas, 1964), *Psammophis sibilans*, *Eryx jaculus* and *Cerastes vipeira* (Hegazy, 1976), *Spalerosophis diadema* (Mostafa, 1990b) and in *Leptotyphlops cairi* (Abdel-Kader, 2005). On the other hand, in *Causus rhombeatus* (Pringle, 1954) and *Natrix tessellata* (Dakrory and Mahgoub, 2005) the division of the ramus nasalis into its two main branches is extracapsular but the ramus lateralis nasi does not enter the cavity of the nasal capsule.

Among Chelonia, the ramus nasalis divides intracapsular in *Emys lutaria* and the ramus lateralis nasi emerges from the the nasal cavity through the foramen orbitale magnum (De Beer, 1937). In *Crocodilus biporcatus* (De Beer, 1937), the ramus lateralis nasi does not enter the nasal capsule and so the foramen epiphaniale is absent.

In the present study, the ramus medialis nasi enters the nasal capsule through the fenestra olfactoria advehens and gets its exit from the nasal capsule through the foramen apicale. This is the usual condition among lacertilian species (Soliman and Hegazy, 1969; Soliman and Mostafa, 1984; Mostafa, 1990a; Dakrory, 1994). In *Calotes versicolor* (Ramaswami, 1964) the two apical foramina are fused, conseqeuently, a single foramen is present through which the right and left rami medialis nasi pass. In *Varanus monitor* (Bellairs, 1949) and in *Ptydactylus hasselquistii* (Abdel-Kader, 1990), there is no distinct foramen apicale, and the ramus medialis nasi passes between the cupole anterior of the nasal capsule and the rostral process of the nasal septum. However, in *Chalcides ocellatus*, El-Toubi and Kamal (1959) described that the presence of a short channel for the emersion of the ramus medialis nasi and the external opening of which is regarded as the foramen apicale.

Among Ophidia, the absence of the foramen apicale is a common character in ophidian chondrocranium (Pringle, 1954; El-Toubi *et al*., 1973; Hegazy, 1976; Mostafa, 1990b). Pringle (1954) explained the lacking of the foramen apicale in snakes considering that it may be confluent with the fenestra narina.

In this study, the ramus maxillaris gives off immediately after its origin and while passing in the postorbital region and before entering the orbit as infraorbital nerve, two rami; temporalis, lacrimalis. On the othere hand, a third ramus palpebralis inferioris posterioris was desecribed in *Chalcides ocellatus* (Soliman and Hegazy, 1969) and in *Acanthodactylus ophedunus* (Mostafa, 1990a). However, the ramus lacrimalis is absent in *Agama pallid* (Soliman *et al*., 1984; Abdel-Kader, 1990). The ramus lacrimalis was found to be lacking in the ophidians studied by Hegazy (1976), Mostafa (1990b), Abdel-Kader (2005) and Dakrory and Mahgoub (2005). It is also absent in *Tarentora mauritanica* (Soliman and Mostafa, 1984), in *Ptydactylus hasselquistii* (Abdel-Kader, 1990).

Among Ophidia, the ramus maxillaris fuses with the ramus palatines of the nervus facialis before entering the orbit as found in *Psammophis sibilans, Eryx jaculus* (Hegazy, 1976), *Natrix tessellata* (Dakrory and Mahgoub, 2005) and in *Leptotyphlops cairi* (Abdel-Kader, 2005). This fusion is not observed in the scincid species studied, as well as in any other lacertilians so far described.

In the present study, the infraorbital nerve while passing in the orbital region fuses with the lateral palatine ramus and receives an anastomsing branch from the medial palatine ramus. In the orbitonasal region, it fuses for a short distance with the intermediate palatine ramus. The anastomosis of the infraorbital nerve with the ramus palatinus and its branches, before the former leaves the orbit, was mentioned in *Varanus monitor* (Bellairs, 1949), *Tarentola mauritanica* (Soliman and Mostafa, 1984), *Agama pallida* (Soliman *et al*., 1984; Abdel-Kader, 1990, *Acanthodactylus opheodurus* (Mostafa, 1990a), *Diplometopon zarudnyi* (Dakrory, 1994) and in *Acanthodactylus boskianus* (El-Ghareeb, 1997).

In Ophidia, the infraorbital nerve anastomosis with the ramus palatinus of the nervus facialis in *Psammophis sibilans*, *Eryx jaculus* (Hegazy, 1976), *Elaphe obsolete*, *Thamnophis ordinoides* (Auen and Langebartel, 1977) and in *Natrix tessellata* (Dakrory and Mahgoub, 2005), while in *Spalerosophis diadema* (Mostafa, 1990b) this anastomosis was absent.

In the studied *Mabuya quinquetaeniata*, the infraorbital nerve leaves the orbit through the superior alveolar foramen to enter the maxillary bone as the superior alveolar nerve. This is the case mentioned in most lizards and snakes and may be a common character among Squamata (Hegazy, 1976; Soliman *et al*., 1984; Abdel-Kader, 1990; Dakrory, 1994, 2011; Ramadan, 2009).

In *Mabuya quinquetaeniata* studied, the ramus mandibularis carries both motor and sensory fibres. It receives its motor component from the ventromedial division of the trigeminal root. This condition was also found in *Chalcides ocellatus* (Soiman and Hegazy, 1969), in *Tarentola mauritanica* (Soliman and Mostafa, 1984), in *Acanthodactylus opheodurus* (Mostafa, 1990a) and in *Diplometopon zarudnyi* (Dakrory, 1994).

In Ophidia, the ramus mandibularis connected with the nervus facialis, directly after its origin from the Gasserian ganglion. The ramus mandibularis anastomoses with both the ramus palatinus and the ramus hyomandibularis in *Psammophis sibilans* (Hegazy, 1976), with the ramus hyomandibularis in *Eryx jaculus and Spalerosophis diadema* (Hegazy, 1976; Mostafa, 1990b, respectively) and with the geniculate ganglion in *Cerastes vipera* (Hegazy, 1976). This condition is not found in lacertilians so far described, since no mention of such connection was recorded. However, such connection was found in mammals, as in gorilla (Raven, 1950), in certain mammals (Bowden *et al*., 1960), and in the baboon embryos (Gasser and Wise, 1972).

In this study, the ramus cutaneous recurrens arises as a single nerve from the ramus mandibularis before the latter enters the primordial canal. It seems to be a common character among Lacertilia as mentioned in *Ophisaurus* and *Chameleo* by Poglayen-Neuwall (1954), in *Agama pallida* by Soliman *et al.* (1984) and Abdel-Kader (1990), in *Agama siniata* by Ramadan (2009) and in *Uromastyx aegyptius* (Dakrory, 2011).

In Ophidia, the condition differs from that found in Lacertilia, as the ramus cutaneous recurrens arises from the inferior alveolar nerve with the ramus cutaneous externus as a single nerve, then they separate outside the primordial canal as it was mentioned in *Psammophis sibilans and Eryx jaculus* (Hegazy, 1976). However, the ramus recurrens is not present in both *Cerastes vipera* (Hegazy, 1976) and *Natrix tessellata* (Dakrory and Mahgoub, 2005).

In the present study, the ramus cutaneous recurrens passes through a special foramen in the supra-angular bone. This is a common character among Lacertilia, as mentioned by several authors (Poglayen-Neuwall, 1953a; Soliman and Hagazy, 1969; Soliman and Mostafa, 1984; Soliman *et al*., 1984; Abdel-Kader, 1990; Mostafa, 1990a; Dakrory, 1994). However, Fuchs (1931) showed that this ramus passes between the supra-angular and articular bones in *Podocnemis expansa* and between the supra-angular and dentary bones in *Hatteria*.

In this study, the ramus cutaneous recurrens is entirely sensory, as it carries somatic sensory fibres. This was also found in all reptiles so far described. On the other hand, this ramus carries motor fibres beside the somatic sensory fibres to the adductor posterior muscle in *Tupinambis* and *Amphibolurua* (Poglayen-Neuwall, 1954), and to the adductor externus muscle in the *Psammophis sibilans* (Hegazy, 1976).

In the present study, ganglionic cells are detected at the point of fusion of the ramus alveolaris inferior (the continuation of the ramus mandibularis within the primordial canal) and the chorda tympani. Lubosch (1933) found a ganglion at the place, where the chorda tympani fuses with the ramus alveolaris inferior in Sauropsida. Such condition was mentioned in other lacertilians by Willard (1915), Soliman and Hegazy (1969), Soliman *et al.* (1984) and Abdel-Kader (1990), Mostafa (1990a) and by Dakrory (2011) and in the ophidians *Psamophis sibilants* and *Cerastes vibra* (Hegazy, 1976) and *Splaerosophis diadema* (Mostafa, 1990b).

On the other hand, this ganglion is represented by a few ganglionic cells found in the mixed nerve (the inferior alveolar nerve + chorda tympani) at the origin of the intermandibularis medius or the ramus paralingualis in *Tarentola mauritanica* (Soliman and Mostafa, 1984), *Ptyodactulus hasselquistii* (Abdel-Kader, 1990) and in *Diplometopon zarudnyi* (Dakrory, 1994).

In *Mabuya quinquetaeniata* studied, it is clear that, the fibres of the chorda tympani carried by the inferior alveolar nerve are more or less divided into two portions; one portion incorporates with the intermandibularis oralis, while the other combines with the intermandibularis medius or the ramus paralingualis. From the anatomical point of view, it seems that the ramus lingulis of the nervus hypoglossus receives the majority of the fibres of the chorda tympani carried by the ramus intermandibularis medius. This seems to be very common among the reptiles so far described, except in the chelonians. In the turtles *Chelydra serprntina* and *Chelone imbricate* (Soliman, 1964), such an anastomosis is not present.

In the present study, the motor components of the ramus mandibularis innervate the pterygomandibularis, the pseudotemporalis and the intermandibualris muscles. Similar to the preset study, the adductor mandibularis externus muscle receives an additional branch from the anguli oris nerve in *Podoenemis expania* (Fuchs, 1931), all the lizards studied by Pogalen-Neuwall (1954), *Chalcides ocellatus* (Soliman and Hegazy, 1969), *Tarentola mauritanica* (Soliman and Mostafa, 1984), *Agama pallid* and *Ptyodactulus hasselquistii* (Soliman *et al.,* 1984; Abdel-Kader, 1990) and in *Acanthodactylus opheodurus* (Mostafa, 1990a).

In the present study, the intermanidbularis muscle is innervated by the ramus mandibularis (the intermandibularis caudalis nerve). The intermandibularis caudalis nerve carries, in addition to its motor componants, somatic sensory fibres to the skin of the mandible. This was also the case found in *Tarentola mauritanica* (Soliman and Mostafa, 1984), *Agama pallida* (Soliman *et al*., 1984; Abdel-kader, 1990), *Ptyodactylus hasselqustii*

(Abdel-Kader, 1990) and in *Acanthodactylus opheodurus* (Mostafa, 1990a).

In Ophidia, the condition is different, where the intermadibularis muscle is doubly innervated. This is the case found in the snakes studied by Hegazy (1976) and Mostafa (1990b). In this respect, Edgeworth (1935) said that the intermadibularis muscle of Sauropsida is innervated by the ramus mandibularis, and in some Lacertilia, its posterior part is innervated by the ramus hyoideus (N.VII). On the contrary, Brock (1938) found that the intermandibularis muscle is entirely innervated by the trigeminal nerve in amniotes.

The nervus trigminus carries somatic sensory and visceral motor fibres is a matter of no doubt, as it is reported by several authors (Romer, 1962; Soliman and Hegazy, 1969; Soliman and Mostafa, 1984; Soliman *et al*. 1984; Abdel-Kader, 1990; Mostafa, 1990a & b). Kappers *et al*. (1960), on the other hand, mentioned that the nervus trigeminus does not supply the mucous epithelium and does not contain visceral sensory fibres. They added that the sensory fibres carried by the nervus trigeminus are purely somatic afferent. Goodrich (1930) stated that the visceral sensory fibres, when present in the trigeminal branches, are generally supposed to have been derived from the facial nerve.

It is clear from the previously detailed anatomical study of the serial sections of *Mabuya quinquteaniata* that the trigeminal branches carry, in addition to the somatic sensory and visceral motor fibres, visceral sensory and vegetative fibres. The visceral sensory fibres, which are mentioned here, are of general type and have nothing to do with the taste. The vegetative fibres are carried to the nervus trigeminus by means of the ramus palatines of the nervus facialis and the lateral cranial sympathetic ramus. To answer the question, whether all visceral sensory fibres are transmitted to the trigeminal branches from the nervus facialis, as it is the view which has been advanced, or some of them are developed from the trigeminal ganglion, the following may throw some light in solving this problem. In the present study, the anastomosing branches, which are supposed to carry the visceral sensory and vegetative fibres to the trigeminal branches, are too fine, if compared with the rami given by the trigeminal branches to the glands and the mucous epithelium. Example to this is the chorda tympani which carries the visceral sensory and the sympathetic fibres from the nervus facialis to the ramus mandibularis, this nerve is small to carry all sensory fibres given by the ramus mandibularis to the mucous epithelium and glands found at the floor of the mouth.

According to these anatomical observations, it can be said that the trigeminal rami probably derive some of their visceral sensory fibres from the trigeminal ganglion. These fibres are added to the visceral sensory fibres transmitted to the rami from the nervus facialis and nervus hypoglossus.

Corresponding author
Tharwat G. Abdel-Kader
Department of Zoology, Faculty of Science, Helwan University
tgabdelkader@yahoo.com

References

1. **Abdel-Kader, I.Y. (1990):** Anatomical studies on the cranial nerves of the lizards *Agama pallida* and *Ptyodactulus hasselquistii*. Ph.D. Thesis, Fac. Sci. Cairo Univ. Egypt.
2. **Abdel-Kader, I.Y. (2000):** The cranial nerves of *Gallinula chloropus* (Rallidae Gruiformes). The nervus trigeminus. Egypt. J. Zool., 343: 141-163.
3. **Abdel-Kader, I.Y. (2006):** The cranial nerves of the cat snake *Telescopus dhara* (Colubridae, Ophidia): II. The nervus trigeminus. J. Egypt. Ger. Soc. Zool., 50(B): 17-34.
4. **Abdel-Kader, I.Y and Fathy, S.M. (2002):** The cranial nerves of the bee eater, white-throated *Merops albicollis* (Meropidae, Coraciiformes): The Nervus Trigeminus. J. Egypt. Ger. Soc. Zool., 38: 21-29.
5. **Abdel-kader, T.G. (2005):** Anatomical studies on the blind snake Leptotyphlops cairi (Family: Leptotyphlopidae). PHD. Thesis, Fac. Sci., Helwan Univ., Egypt.
6. **Auen, E.D. and Langebartel, D.A. (1977):** The cranial nerves of the colubrid snakes *Elaphe* and *Thamnophis*. J. Morph., 154: 205-222.
7. **Augustine, J.R.; Vidic, B. and Young, P.A. (1971):** The intermediate root of the trigeminal nerve in the dog (*Canis familiaris*). Anat. Rec., 169 (4): 697-704.
8. **Bandy, W.E. (1932):** Certain functions of the roots and ganglia of the cranial sensory nerves. Arch. Neurol. Psychiat. 27: 22-26.
9. **Barry, T.H. (1953):** Contributions of the cranial morphology of *Agama hispida* (Linn.). Ann. Univ. Stellenbosch, 29(A) 2: 55-57.
10. **Bellairs, A.d'A. (1949):** Observation on the snout of varanus and a comparison with that of other lizards and snakes. J. Anat. Lond., 83(2): 116-146.
11. **Bowden, R.E.M.; Mahran, Z.Y. and Godding, M.R. (1960):** Communications between the facial and trigeminal nerves in certain mammals. Proc. Zool. Soc. London, 135: 587-611.
12. **Brock, G.T. (1938):** The cranial muscles of the gecko. A general account, with a comparison of the muscles in other Gnathostomes. Proc. Zool. Soc. Lond., 108: 735.
13. **Dakrory, A.I. (1994):** Anatomical studies on the cranial nerves of the Amphisbaenian (*Diplometopon zarudnyi*). M.Sc. Thesis, Fac. Sci. Cairo Univ. Egypt.
14. **Dakrory, A.I. (2011):** Anatomical study on the cranial nerves of *Uromastyx aegyptius* (Squamata-Lacertilia- Agamidae): I- Nervus Trigeminus. J. Egypt. Zool., 56:175-212.
15. **Dakrory, A.I. and Mahgoub, A.F. (2005):** the cranial nerves of snake Natrix tessellata (Ophidia, Colubridae): The Nervus trigeminus. J. Egypt. Ger. Soc. Zool., 46(B): 17-59.
16. **De Beer, G.R. (1937):** The development of the vertebrate skull. Clarendon Press, Oxford.
17. **Edgeworth, F.H. (1935):** The cranial muscles of the vertebrates. Cambridge Univ. Press.

18. **El-Ghareeb, A.A. (1997):** Anatomical studies on the cranial nerves of the lizard *Acanthodactylus boskianus* (Daud). Ph.D. Thesis, Fac. Sci., Cairo Univ., Egypt.
19. **El-Toubi, M.R. and Kamal, A.M. (1959):** The development of the skull of *Chalcides ocellatus*. II. The fully formed chonorocranium and the osteocranium of a late embryo. J. Morph., 105: 55-104.
20. **El-Toubi, M.R.; Kamal, A.M. and Zaher, M.M. (1973):** The development of the chondrocranium of the snake, *Malpolon monospessulana*. II. The fully formed stage. Acta. Anat., 85: 593-619.
21. **Engelbrecht, D. van Z. (1951):** Contribution to the cranial morphology of the chamaeleon *Microsauna pumila* Daudin. Ann. Univ. Stellenbosch, 47, (A) 1: 5-31.
22. **Eyal-Giladi, H. (1964):** The development of the chondrocranium of *Agama stellio*. Acta Zool., 45: 139-165.
23. **Fischer, J.G. (1852):** Die Gehirnnerven der Saurier anatomisch untersucht. Abhandl. Naturw. Verein in Hamburg. Abt., 2: 109-212.
24. **Frank, G.H. (1951):** The Contribution to the cranial morphology of *Rhampholeon platyceps* Gunther. Ann. Univ. Stellenbosch, 47, (A)2: 35-67.
25. **Fuchs, H. (1931):** Über den Unterkiefer und die Unterkiefernerven (Ramus tertius nervi Trigeminus et Chorda tympani) der Arrauschildkröte (*Podocnemis expansa*). Nebst Bemerkungen zur Kiefergelenkfrage. (Ein Beitrag zure vergleichenden Anatomie des Unterkiefers der Wirbeltiere und des Nervenverlaufs). Zeitschrift f. Anat. U. Entw. Gesch., 94: 206-274.
26. **Gasser, R.F. and Wise, D.M. (1972):** The trigeminal nerve in baboon. Anat. Rec., 172: 511-522.
27. **Goodrich, E.S. (1930):** Studies on the structure and development of vertebrates. Maxmillan and Co. London.
28. **Haas, G. (1964):** Anatomical observations on the head of *Liotyphlops albirostris* (Typhlopidae, Ophidia). *Acta Zool.*, 45: 1-62.
29. **Haas, G. (1968):** Anatomical observations on the head of *Anomalepis aspinosus* (Typhlopidae, Ophidia). *Acta Zool.*, 49: 63-139.
30. **Hegazy, M.A. (1976):** Comparative anatomical studies on the cranial nerves of ophidia. Ph.D. Thesis, Fac. Sci., Cairo Univ., Egypt.
31. **Hoffman, C.K. (1890):** Reptilien, I. Schildkröten. Bronn's Klassen und Ordnungen des Thierreichs. 6, Abt. III.
32. **Jannetta, F.J. and Rand, R.W. (1966):** Transtentorial retrogasserian rhizotomy in trigeminal neurologia by microneurosurgical techniques. Bull. Of Los Angeles Neurol. Soc., 31: 93-99.
33. **Kappers, C.U.A.; Huber, G.C. and Crosby, E.C. (1960) :** The comparative anatomy of the nervous system of vertebrates, including man. 3 volumes. New York.
34. **Lakjer, T. (1926):** Die Trigeminus-versorgte Kaumuskulatur der Sauropsiden. Kopenhagen, C. A. Reitzel.
35. **Lubosch, W. (1933):** Untersuchung über die Visceralmuskulatur der Sauropsiden. (Der Untersuchungen über die Kaumuskulatur der Wirbeltiere 3. Teil.). J. Morph., 72: 584-666.
36. **Malan, M.E. (1946):** Contributions to a comparative anatomy of the nasal capsule and organ of Jacobson of Lacertilia. Ann. Univ. Stellenbosch, 24, (A) 4: 69-137.
37. **Mostafa, R.H. (1990a):** The cranial nerves of *Acanthodactylus opheodurus*. II. The nervus trigeminus. Egypt J. Anat., 13 (1): 67-92.
38. **Mostafa, R.H. (1990b):** The cranial nerves of serpent, *Spalerosophis diadema*. II. The nervus trigeminus. Egypt J. Anat., 13 (2): 75-105.
39. **Oelrich, T.H. (1956):** The anatomy of the head of *Ctenosaura pectinata* (Iguanidae). Misc. Publ. Mus. Zool. Michigan, 94: 9-122.
40. **Pantin, C.F.A. (1946):** Notes on microscopical technique for Zoologists. Cambridge, England: Cambridge, University Press.
41. **Poglayen-Neuwall Ivo (1953a):** Die Besonderheiten der Kiefermuskulatur von *Dermochelys coriacea*. Anat. Anz., 100: 23-32.
42. **Poglayen-Neuwall Ivo (1953b):** Untersuchungen der Kiefermuskulatur und deren Innervation bei Schildkröten. Acta Zool., 34(3): 241-292.
43. **Poglayen-Neuwall Ingeborg (1954):** Die Kiefermuskulatur der Eidechsen und Innervation. Z. f. Wiss. Zool., 158: 70-132.
44. **Pringle, J.A. (1954).** The cranial development of certain South African snakes and the relationship of this group. Proc. Zool. Soc. London, 123**:** 318 – 865.
45. **Ramadan, A.O. (2009):** Comparative anatomical studies on the cranial nerves of (*Agama siniata)*. M.Sc. Thesis, Zool. Dep., Fac. Sci., Cairo Univ., Egypt.
46. **Ramaswami, L.S. (1946):** The chondrocranium of *Calotes versicolor* (Daud.) with a description of the Osteocranium of a just-hatched young. Q.J. Micr. Sci., 87: 237-297.
47. **Raven, H.C. (1950):** The anatomy of the *Gorilla*. Chap. II. W.K. Gregory, ed. Columbia University Press, New York, pp. 15-188.
48. **Romer, A.S. (1962):** The vertebrate body. W.B. Saunders Co. Philadelphia and London.42: 131-139.
49. **Shiino, K. (1914):** Studien zur Kenntnis der Wirbeltierkopfes. I. Das Chondrocranium von *Crocodilus* mit Berruksichtigung der Gehirnnerven und der Kopfgesfasse. Anat. Hefte., 47**:** 1 – 37.
50. **Soliman, M.A. (1964):** Die Kopfnerven der schildkroten Z. F. W. Zool., 169: 215 – 312.
51. **Soliman, M.A. and Hegazy, M.A. (1969):** The cranial nerves of *Chalcides ocellatus*. II. The nervus trigeminus. Bull. Fac. Sci. Cairo Univ., 43: 63-90.
52. **Soliman, M.A. and Mostafa, R.H. (1984):** A detailed study on the cranial nerves of the gecko *Tarentola mauritanica*. II. Nervus trigeminus. Proc. Zool. Soc., A.R.E., VII: 249-287.
53. **Soliman, M.A.; Hegazy, M.A.; Mokhtar, F.M. and Mostafa, R.H. (1986):** The cranial nerves of Birds. III. The nervus trigeminus. Proc. Zool. Soc. A.R.E., 11: 375-406.
54. **Soliman, M.A.; Mostafa, R.H. and Abdel-Kader, I.Y. (1984):** Anatomical studies on the cranial nerves of *Agama pallida* (Reuss). II. The nervus trigeminus. Egypt. J. Anat., 8: 159-190.
55. **Underwood, G. (1970):** The eye. In C. Gans and T. S. Parsons (Eds.), "Biology of the Reptilia", Academic Press, London and New York, pp. 1 – 97.
56. **Van Pletzen, R. (1946):** The cranial morphology of *Cordylus* with special reference to the cranial kinesis. Ann. Univ. Stellenbosch, 24, (A) 4: 41-68.
57. **Vidić, B. and Stefanatus, J. (1969):** The root of the trigeminal nerve and their fibre components. Anat. Rec., 163-330.
58. **Watkinson, G.B. (1906):** The cranial nerves of *Varanus bivittatus*. J. Morph., **35:** 450 – 472.
59. **Weichert, C.K. (1958):** Anatomy of the Chordates. Mc Graw – Hill, New York, Toronto and London.
60. **Willard, W.A. (1915):** The cranial nerves of *Anolis carolinensis*. Bull. Mus. Comp. Zool., **59:** 17 – 116.

11/11/2011

LIST OF ABBREVIATION

AC	:	Auditory capsule.
AG	:	Angular bone.
B	:	Brain.
BSP	:	Basisphenoid bone.
CO.N	:	Common nerve.
CT	:	Chorda tympani.
CT&N.IAV	:	Chorda tympani & inferior alveolar nerve.
D	:	Dentary bone.
DLD.RO.V	:	Dorsolateral division of trigeminal root.
E	:	Eye.
F.APC	:	Foramen apicale.
G.CIL	:	Ciliary ganglion.
G.ET	:	Ethmoidial ganglion.
G.GE	:	Geniculate ganglion.
G.MM	:	Maxillomandinular ganglion.
G.MN	:	Mandibular ganglion.
G.OPH	:	Ophthalmic ganglion.
GC	:	Ganglionic cells.
HDG	:	Hardeŕs gland.
IP	:	Incisura protica.
JO	:	Jacobsońs organ.
LGG	:	Lingual gland.
LP.VMD.RO.V	:	Lateral part of ventromedial division of the trigeminal root.
M.ADME	:	Adductor mandibularis externus muscle.
M.DPI	:	Depressor palpbrea inferioris muscle.
M.IM	:	Intermandibualris muscle.
M.LPT	:	Levator pterygoideus muscle.
M.PPT	:	Protractor pterygoideus muscle.
M.PST	:	Pseudotemporalis muscle.
MC	:	Meckel′s cartilage.
MP.VMD.RO.V	:	Medial part of ventromedial division of the trigeminal root.
MX	:	Maxillary bone.
N.ADME	:	Nerve to adductor mandibularis externus muscle.
N.AO	:	Anguli oris nerve.
N.BV	:	Nerve to blood vessel.
N.CD	:	Constrictor dorsalis nerve.
N.CU	:	Nerve to skin.
N.CU+ILG	:	Nerve to skin and infralabial gland.
N.CU+SLG	:	Nerve to skin and supralabial gland.
N.DPI	:	Nerve to depressor palpbrae inferioris muscle.
N.EP	:	Nerve to epithelium.
N.EP+DE	:	Nerve to epithelium and dental lamina.
N.HDG	:	Nerve to Hardeŕs gland.
N.IM	:	Nerve to intermandibularis muscle.
N.IM+CU	:	Nerve to intermandibularis muscle and skin.
N.IAV	:	Inferior alveolar nerve.
N.ILG	:	Nerve to infralabial gland.
N.IO	:	Infraorbital nerve.
N.LCG	:	Nerve to lacrimal gland.
N.LPT	:	Nerve to levator pterygoideus muscle.
N.MI	:	Mixed nerve.
N.NR	:	Nerve to narial muscle.
N.PPT	:	Nerve to protractor pterygoideus muscle.
N.PST	:	Nerve to pseudotemporalis muscle.
N.PTM	:	Nerve to pterygomandibularis muscle.
N.SAV	:	Superior alveolar nerve.
N.SLG	:	Nerve to supralabial gland.
N.T+VON	:	Nervi terminalis and vomeronasali.
N.TE	:	Nerve to teeth.
NA	:	Nasal bone.
NA.G	:	Nasal gland.
N.IV	:	Nervus trochelaris.
N.V	:	Nervus trigeminus.
N.VI	:	Nervus abducense.
N.XII	:	Nervus hypoglossus.
Nn.BV	:	Nerves to blood vessel.
Nn.CIL	:	Ciliary nerves.
Nn.CU	:	Nerves to skin.

Nn.CU+DE	:	Nerves to skin and dental lamina.
Nn.CU+TE	:	Nerves to skin and teeth.
Nn.EP	:	Nerves to epithelium.
Nn.HDG	:	Nerves to Harderś gland.
Nn.IM	:	Nerves to intermandibularis muscle.
Nn.LCG	:	Nerves to lacrimal gland.
Nn.LGG	:	Nerves to lingual gland.
Nn.ME	:	Nerves to meninges.
Nn.NAG	:	Nerves to nasal gland.
Nn.NR	:	Nerves to narrial muscle.
Nn.SLG	:	Nerves to supralabial gland.
Nn.TB+EP	:	Nerves to taste buds + epithelium.
OL.BU	:	Olfactory bulb.
OL.EP	:	Olfactory epithelium.
PAAMX	:	Palatal process of maxilla.
PAPPA	:	Palatal process of palatine.
PRC	:	Primordial canal.
PRF	:	Primordial fossa.
PTC	:	Parietotectal cartilage.
R.CM.FR+LC	:	Ramus commuincans between the ramus frontalis and the ramus lacrimalis.
R.CM.FR+LCP	:	Ramus commuincans between the ramus frontalis and the lacrimal plexus.
R.CM.IO+PAL	:	Rramus communicans between the ramus intermandibularis oralis and the ramus palatinus lateralis.
R.CM.IO+PAM	:	Ramus communicans between the infraorbital nerve and the medial palatine ramus.
R.CM.LC+LCP	:	Ramus communicans between the ramus lacrimalis and the lacrimal plexus
R.CM.LP.VMD.RO.V+G.MM	:	Ramus communicans between lateral part of ventromedial division (N.V) and maxillomandinular ganglion.
R.CM.NA+G.ET	:	Ramus communicans between the ramus nasalis and the ethmoidal ganglion.
R.CUR	:	Ramus cutaneous recurrens.
R.FR	:	Ramus frontalis.
R.IF.III	:	Ramus inferior.
R.IMC	:	Ramus intermandibularis caudalis.
R.IMM	:	Ramus intermandibularis medius.
R.IMO	:	Ramus intermandibularis oralis.
R.LC	:	Ramus lacrimalis.
R.LCSY	:	Lateral cranial sympathetic ramus.
R.LNA	:	Ramus lateralis nasi.
R.MN	:	Ramus mandibularis.
R.MNA	:	Ramus medialis nasi.
R.MX	:	Ramus maxillaris.
R.NA	:	Ramus nasalis.
R.OPH	:	Ramus ophthalmicus profundus.
R.PA	:	Ramus palatinus.
R.PAI	:	Ramus palatinus intermedialis.
R.PAL	:	Ramus palatinus lateralis.
R.PAM	:	Ramus palatinus medalis.
R.PMXI	:	Ramus premaxillaris inferior.
R.PMXS	:	Ramus premaxillaris superior.
R.TM	:	Ramus temporalis.
RCB	:	Radix ciliaris brevies.
RCL	:	Radix ciliaris longa.
RO.V	:	Nervus trigeminus root.
RO.VII	:	Nervus facialis root.
Rr.IMO+IMM	:	Rami communicans between the ramus intermandibularis oralis and intermandibularis medius.
S.IN	:	Internasal septum.
S.IO	:	Interorbital septum.
VC	:	Vidian canal.
VMD.RO.V	:	Ventromedial division of the trigeminal root

An Integrated Location Inventory Model for Designing a Supply Chain Network under Uncertainty

Mir-Bahador Aryanezhad, Seyed Gholamreza Jalali Naini, Armin Jabbarzadeh

[1.] Department of Industrial Engineering, Iran University of Science and Technology, 16846113114, Tehran, Iran
arminj@iust.ac.ir

Abstract: This paper studies a supply chain design problem with an unreliable supplier and random demand. Due to imperfect performance of the supplier, the quantity of the product received from the supplier may be less than the quantity ordered by distribution centers (DCs). In this system, customers have random demands and the supply chain is flexible in determining which customers to serve. The problem is formulated as a nonlinear integer programming model that simultaneously determines which customers are served, where DCs are located and how DCs are assigned to the customers. The objective of the model is to minimize the total costs including location costs, nonlinear inventory costs, transportation costs, and lost sales costs. In order to solve the model, an effective solution method based on genetic algorithm is developed. Finally, computational results for several instances of the problem are presented to demonstrate the effectiveness of the proposed solution approach.
[Mir-Bahador Aryanezhadl, Seyed Gholamreza Jalali Naini, Armin Jabbarzadeh. **An Integrated Location Inventory Model for Designing a Supply Chain Network under Uncertainty**. Life Science Journal. 2011;8(4):670-679] (ISSN:1097-8135). http://www.lifesciencesite.com.

Keywords: Birth-death process; genetic algorithm; location model; supply chain design model

1. Introduction

In today's increasingly competitive environment, the efficient design of supply chain plays a decisive role in successful performance of companies. Supply chain design models typically treat strategic decisions and tactical decisions separately. Since ignoring the interaction between long term and short term decisions can lead to sub-optimality (Shen and Qi, 2007; Shu et al., 2005; Ozsen, 2004), recently integrated supply chain design models have been developed. These models incorporate the strategic decisions of facility location and tactical decisions of inventory and transportation management. Most of the integrated models in the literature implicitly assume that supplier always performs perfectly. However, in practice a supplier is not always reliable and what is received from the supplier is not equal to what was ordered. In fact, there exist various factors such as random breakdown, raw material shortage, quality rejection, workforce slow down, maintenance duration, transportation damage, and natural disaster leading to unwanted partial yield (Erdem and Ozekici, 2002). Consequently, in many real cases, the amount of yield is random. This highlights the need for supply chain design models that account for uncertain yield.

Also, the majority of the integrated supply chain design models in the literature are based on the assumption that every customer's demands must be fulfilled. In real life world, tough, it may be more beneficial for the company to lose some potential customers, as the cost of maintaining these customers can be inevitably high. In other words, demand choice flexibility can result in cost saving that is significantly important especially for a profit-maximizing business (Shen, 2006). It implies that supply chain design models with demand choice flexibility deserve further attention.

With this background, the present paper discusses supply chain design problem, where yields and demands are uncertain and there is demand choice flexibility. Specifically, a three echelon supply chain comprised of single unreliable supplier, distribution centers (DCs) and customers, is considered. Following the common assumption in the literature, customers are assumed to have independent probabilistic demands with Poisson distribution such that the variance of demand is equal to the mean (Daskin et al., 2002; Shen et al., 2003; Ozsen et al., 2008). The supplier ships one type of product to customers in order to satisfy their demands. It should be noted that there is no requirement for serving all the costumers and the company is flexible in choosing which customers to serve. DCs function as the direct intermediary between the supplier and customers for shipment of the product. That is, DCs combine the orders from different customers and then order to the supplier. A key problem is that the supplier is not always reliable and the quantity of yield received by each DC may be less than what was ordered. In other words, the amount of yield at each DC is not deterministic.

In order to formulate the problem, an integrated supply chain design model is presented. The proposed model simultaneously determines: 1) where DCs are located; 2) which customers are served; 3) which DCs are assigned to which customers; 4) how much and how often to order at

each DC. The objective is to minimize total costs including costs of location, inventory (consisting of working and safety inventory at DCs), shipment, and lost sales. In order to solve the model, a solution approach based on genetic algorithm is developed.

The remainder of the paper is organized as follows. Section 2 discusses some relevant models in the literature. In section 3 the integrated supply chain design model for the problem is proposed. Section 4 develops a solution approach to solve the model. In section 5 the related computational results for testing the effectiveness of the developed solution approach are provided. Finally, section 6 concludes the paper along with directions for future research.

2. Literature review

As this paper investigates the design of a supply chain with random yield, first the literature on integrated supply chain design is reviewed briefly. The reader is referred to Shen (2006) for a thorough review of the integrated supply chain design models. The research by Baumol and Wolfe (1985) is among the earliest works that incorporate inventory costs into location models. They discuss that inventory costs should be considered in the location model with a square root term. After Baumol and Wolfe's work, a number of joint location-inventory models have appeared in the literature. However, in most of these models nonlinear inventory costs either are overlooked, or approximated with linear functions (Ozsen et al., 2008).

In the recent years researchers have focused on the integrated models in which location and nonlinear inventory costs are included in the same model (Shen and Qi, 2007). For instance, Erlebacher and Meller (2000) provide a joint location inventory model with complicated nonlinear objective function. They applied a continuous approximation along with some heuristics techniques to solve the model. Daskin et al. (2002), Shen et al. (2003) and Shen (2000) introduce a location model with risk pooling (LMRP) that incorporates inventory decisions into the location model. LMRP minimizes the sum of fixed facility location costs, linear shipment costs and nonlinear inventory costs. Shen et al. (2003) and Shen (2000) use column generation, while Daskin et al. (2002) present Lagrangian relaxation to solve the LMRP. Another efficient approach to solve the LMRP is presented by Shu et al. (2005).

Shen and Daskin (2005) extend the LMRP to include a customer service element and propose useful techniques for evaluation of cost/service trade-offs. Ozsen (2008) develops LMRP in the condition that each DC has limited capacity. Her capacitated model is noticeably harder to solve than LMRP. Shen and Qi (2007) study an integrated supply chain design model that contains location, inventory, and routing decisions; in fact, they add routing decisions to the LMRP framework. Snyder et al. (2007) propose stochastic version of LMRP (called SLMRP) that handles uncertainty by describing discrete scenarios. The goal of SLMRP is to minimize the expected system cost across all scenarios. The authors argue how to use SLMRP to solve multi-commodity and multi-period problems.

Similar integrated supply chain design models are developed by Shen (2006), Sourirajan et al. (2007; 2008). Sourirajan et al. (2007) study the two-stage supply chain with a production facility where the replenishment lead time at the DCs depends on the volume of flow through the DC. They formulate the relationship between the flows in the network, lead times, and safety stock levels and develop a Lagrangian heuristic to obtain near-optimal solutions for the proposed model. Sourirajan et al. (2008) extend the problem to incorporate arbitrary demand variance at the retailers. They suggest genetic algorithm to solve the model and imply that the genetic algorithm outperforms the Lagrangian heuristic developed in the earlier work in some respects. None of these integrated supply chain design models consider random yield at DCs.

Another issue considered in this paper is random yield which has been discussed several times in the literature (Noori and Keller, 1986; Ehrhardt and Taube, 1987; Gerchak et al., 1988; Erdem and Ozekici, 2002; Qi and Shen, 2007; He and Zhang, 2008; Maddah et al., 2009). Most of these paper use newsboy problem to formulate the inventory problem (Noori and Keller, 1986; Ehrhardt and Taube, 1987; Gerchak et al., 1988; Qi and Shen, 2007). For instance, using newsboy problem, Qi and Shen (2007) provide a profit-maximizing model when the price of the product at each retailer is given and the yield is not deterministic. Parlar and Berkin (1991) and Gurler and Parlar (1997) study the problem where supply is presented only during an interval of random length. Henig and Gerchak (1996), also, examine the inventory policies when the amount of yield is stochastic. Yano and Lee (1995) and Tang (2006) survey the inventory models with random yield and provide general reviews.

The present paper differs from the earlier works in some main directions. First, unlike the most of supply chain design models in the literature, the proposed model of this study takes account of random yields at DCs. Moreover, the presented model dismisses the common restrictive assumption in the literature that demands of all customers must be satisfied necessarily. In fact, the model provides a simple but effective technique for determining the profitable customers. Finally, unlike the most of

supply chain design models in the literature, the presented model consider limited capacities at DCs.

3. Model formulation

This section formulates a model for the problem explained in section 1. The objective of the model is to minimize the expected total cost including: 1) the fixed cost to locate DCs, 2) the working inventory cost at the located DCs (containing order costs, shipment costs from supplier to DCs, and holding costs), 3) safety stock cost at the located DCs, 4) shipment cost from located DCs to customers, and 5) the lost sales cost of not serving some customers. To develop the proposed model, following notations are used throughout the paper. Additional notations will be given out when required.

I : set of customers indexed by i;
J : set of candidate DC locations indexed by j;
D_i : mean of demand at customer i, for each $i \in I$;
f_j : fixed cost of locating a DC at j, for each $j \in J$;
F_j : fixed cost of placing an order at j, for each $j \in J$;
g_j : fixed cost per shipment from the supplier to DC at j, for each $j \in J$;
A_j : per-unit shipment cost from the supplier to DC at j, for each $j \in J$;
h : inventory holding cost per unit of product;
d_{ij} : per-unit cost to ship from distribution center j to customer i, for each $i \in I$ and for each $j \in J$;
C_j : capacity of DC at j, for each $j \in J$;
α : desired percentage of customers orders satisfied;
β: weight factor associated with the shipment cost;
θ : weight factor associated with the inventory cost;
z_α : standard normal deviate such that $P(z \le z_\alpha) = \alpha$;
L: lead time from supplier to DCs, in days;
P: number of DCs which should be located;
u_i : penalty cost of not serving customer i, per unit of demand (it can be interpreted as lost sales cost, or the cost of serving customer i by purchasing product from a competitor).

3.1. Working inventory cost

This subsection details the inventory policy the DCs follow and calculates the resulting expected working inventory cost. As stated in section 1, due to unreliable performance of the supplier, the quantity of yield received by each DC may be different from what was ordered. Specifically, it is assumed that the supplier has two modes for each DC, and each mode is associated with a constant partial yield. In other words, at each mode the supplier can provide only a fraction of the order placed by each DC. For convenience, assume that the supplier can provide a_j % of the order placed by distribution center j at the first mode, whereas it can satisfy b_j % of the order placed by distribution center j at the second mode. It should be noted that a_j and b_j are known given parameters. Also, durations of the first and second modes of the supplier for distribution center j follow exponential distribution with parameters λ_{1j} and λ_{2j}, respectively. Let Q_j denotes the reorder quantity of distribution center j, $Q_{[a_j]}$ indicates integer value of $Q_j \times a_j$ %, $Q_{[b_j]}$ represents integer value of $Q_j \times b_j$ % and μ_j indicates the demand arrival rate to distribution center j in Poisson process. Then, regarding the memoryless property of the exponential distribution, the inventory transition related to distribution center j can be modeled as a birth-death process as Figure 1. In Figure 1, inventory quantities are considered as states of the birth-death process (Ross, 2007). By equating the rate at which the process leaves a state with the rate at which it enters that state, following equations are gained (Wu, 2008):

$$\pi(1) = \pi(2) = \ldots = \pi(Q_{[a_j]}) = \frac{1}{p_{1j} Q_{[a_j]} + p_{2j} Q_{[b_j]}} \quad (1)$$

$$\pi(Q_{[a_j]} + 1) = \pi(Q_{[a_j]} + 2) = \ldots = \pi(Q_{[b_j]}) = \frac{p_{2j}}{p_{1j} Q_{[a_j]} + p_{2j} Q_{[b_j]}} \quad (2)$$

where $\pi(k)$ denotes the limiting probability of state k (for k = 1 to $Q_{[b_j]}$) in Figure 1. In addition, $p_{1j} = \frac{\lambda_{1j}}{\lambda_{1j} + \lambda_{2j}}$ and $p_{2j} = 1 - p_{1j}$. At this stage, the annual working inventory cost at distribution center j can be obtained by:

$$F_j N_j + \beta(g_j N_j + A_j \mu_j) + \theta h \sum_{k=1}^{Q_{[b_j]}} k\, \pi(k) \quad (3)$$

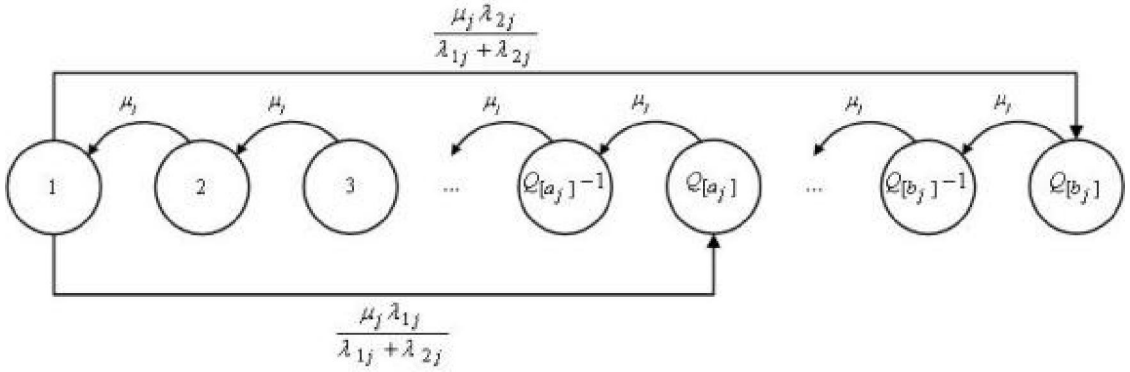

Figure 1. Inventory transition diagram related to distribution center *j*

where N_j denotes the number of orders and is equal to $\frac{(\lambda_{1j}+\lambda_{2j})\mu_j}{\lambda_{1j}Q_{[a_j]}+\lambda_{2j}Q_{[b_j]}}$.

The first term of equation (3) is the annual fixed cost of placing orders. The second term indicates the annual cost of shipping orders, assuming the shipment cost from the supplier to distribution center *j* has a fixed cost g_j and volume dependent cost A_j. The last term represents the cost of holding average of $\sum_{k=1}^{Q_{[b_j]}} k\,\pi(k)$ units of inventory.

Substituting limiting probabilities in (1) and (2) into (3), the annual working inventory cost at distribution center *j* will be:

$$\frac{100(F_j+\beta g_j)\mu_j(\lambda_{1j}+\lambda_{2j})}{a_j\lambda_{1j}Q_j+b_j\lambda_{2j}Q_j}+\beta A_j\mu_j + \frac{\theta h a_j(a_jQ_j+100)}{200(a_jp_{1j}+b_jp_{2j})} + \frac{hp_{2j}(b_jQ_j+a_jQ_j+100)(b_j-a_j)}{200(a_jp_{1j}+b_jp_{2j})} \quad (4)$$

To determine the optimal reorder quantity, we take derivative of (4) respect to Q_j and set the derivative to zero. By this way, the optimal value will be:

$$Q_j = 100\sqrt{\frac{2(F_j+\beta g_j)(\lambda_{1j}+\lambda_{2j})}{\theta h(a_j^{\,2}\lambda_{1j}+b_j^{\,2}\lambda_{2j})}} \quad (5)$$

Plugging (5) into (4), an annual working inventory cost at distribution center *j* can be calculated as following:

$$\frac{1}{a_j\lambda_{1j}+b_j\lambda_{2j}} \times\sqrt{2(F_j+\beta g_j)\mu_j\theta h(a_j^{\,2}\lambda_{1j}+b_j^{\,2}\lambda_{2j})(\lambda_{1j}+\lambda_{2j})} +\beta A_j\mu_j \quad (6)$$

3.2. Shipment cost

Transporting the product from each distribution center *j* to each customer *i* has linear shipment cost. Let S_j be the set of customers assigned to the distribution center *j*. Then, the total demand assigned to distribution center *j* is $\sum_{i\in S_j} D_i$, and the shipment cost from distribution center *j* to the costumers will be:

$$\beta\sum_{i\in S_j} d_{ij}D_i \quad (7)$$

3.3. Lost sales cost

As stated in section 1, in case that the cost of serving a customer is not profitable, the demand of the customer is not provided and the system incurs lost sales cost. This happens when the cost of assigning the customer to any of the DCs is more than u_i. To model the lost sales cost, it is expedient to define a dummy DC with index *u*. Assigning the customer *i* to this dummy DC represents not serving

the customer *i* (Snyder and Daskin, 2005). Regarding distribution center *u*, we assume that it has the shipment cost $d_{ij} = u_i$ to customer $i \in I$ and there is no other cost. Accordingly, when customer $i \in I$ is assigned to distribution center *u* it means that customer *i* is not served and the cost u_i is incurred.

3.4. Safety stock cost

Each DC retains a certain amount of safety stocks to deal with possible stockouts during replenishment lead time. Montgomery et al. (1998) show that a Poisson process with sufficiently large demand values can be approximated by Normal distribution appropriately. Thus, it is assumed that the demands at the customers are normally distributed when calculating the safety stock requirement. Since the customers' demands are assumed to be uncorrelated and normally distributed, the lead time demand variance at distribution center *j* can be gained by $\sqrt{\sum_{i \in S_j} LV_i^2}$, where V_i^2 denotes the variance of demand at customer *i*. Therefore, the needed safety stock to guarantee that the stockouts occur with a probability of α or less is $z_\alpha \sqrt{\sum_{i \in S_j} LV_i^2}$. Given the assumption that the variance and mean are equal, the corresponding holding cost for the safety stock at distribution center *j* is:

$$\theta h z_\alpha \sqrt{\sum_{i \in S_j} LD_i} \tag{8}$$

3.5. Integrated Model

In order to determine the locations of the DCs and assignments of the customers to DCs, two sets of decision variables are defined:

- $X_j = 1$, if *j* is selected as a DC location, and 0, otherwise, for each $j \in J$;
- $Y_{ij} = 1$, if customer *i* is assigned to a DC based at *j*, and 0 otherwise, for each $i \in I$ and $j \in J$.

Now the model can be formulated as follows:

$$\begin{aligned} \text{Min } & \sum_{j \in J} f_j X_j + \left(\beta \sum_{j \in J} \sum_{i \in I} d_{ij} D_i Y_{ij} \right) \\ & + \left(\sum_{j \in J} \sqrt{2(F_j + \beta g_j)\theta h (a_j^2 \lambda_{1j} + b_j^2 \lambda_{2j})(\lambda_{1j} + \lambda_{2j}) \sum_{i \in I} D_i Y_{ij}} \right. \\ & \left. \times \frac{1}{a_j \lambda_{1j} + b_j \lambda_{2j}} + \beta \sum_{j \in J} A_j \sum_{i \in I} D_i Y_{ij} \right) \\ & + \theta h z_\alpha \sum_{j \in J} \sqrt{\sum_{i \in I} LD_i Y_{ij}} \end{aligned} \tag{9}$$

subject to:

$$\sum_{j \in J} Y_{ij} = 1 \qquad \forall i \in I \tag{10}$$

$$\sum_{i \in I} D_i Y_{ij} \le C_j X_j \qquad \forall j \in J \tag{11}$$

$$X_u = 1 \tag{12}$$

$$\sum_{j \in J} X_j = P + 1 \tag{13}$$

$$X_j \in \{0,1\} \qquad \forall j \in J \tag{14}$$

$$Y_{ij} \in \{0,1\} \quad \forall i \in I,\ \forall j \in J \tag{15}$$

The objective function (9) is composed of four components. The first component represents the fixed cost of locating DCs. Considering equation (7), the second part indicates the expected shipment cost from the DCs to customers. Note that we added dummy distribution center *u* to the set *J* to take lost sales cost into account in the model. Also, $\sum_{i \in I} D_i Y_{ij}$ indicates the total annual demand assigned to the distribution center *j*. With regards to equation (6), it is easy to find that the third component represents the working inventory cost where $\mu_j = \sum_{i \in I} D_i Y_{ij}$. Finally, the fourth part indicates the safety stock cost and can be obtained by considering equation (8).

Constraints (10) stipulate that each customer is assigned to a DC. Recall that assigning a customer to dummy distribution center *u* is equivalent to not serving the customer. Constraints (11) state that the mean demand flow through a DC should be less than the capacity of that DC. Constraint (12) requires the dummy distribution center *u* to be located. Constraint (13) assures that the number of located DCs is exactly *P* + 1 (this means that *P* distribution centers must be located in addition to dummy distribution center *u*). Constraints (14) and (15) are binary constraints.

Objective function (9) can easily be reorganized as follows:

$$\begin{aligned}&\text{Min}\sum_{j\in J}f_jX_j+\left(\beta\sum_{j\in J}\sum_{i\in I}(d_{ij}+A_j)D_iY_{ij}\right)\\&+\left(\sum_{j\in J}\sqrt{2(F_j+\beta g_j)\theta h(a_j{}^2\lambda_{1j}+b_j{}^2\lambda_{2j})(\lambda_{1j}+\lambda_{2j})}\sum_{i\in I}D_iY_{ij}\right)\\&\times\frac{1}{a_j\lambda_{1j}+b_j\lambda_{2j}}\\&+\theta hz_\alpha\sum_{j\in J}\sqrt{\sum_{i\in I}LD_iY_{ij}}\\&=\sum_{j\in J}\left\{f_jX_j+\sum_{i\in I}\hat{d}_{ij}Y_{ij}+k_j\sqrt{\sum_{i\in I}D_iY_{ij}}\right\}\end{aligned}\qquad(16)$$

where:

$$\hat{d}_{ij}=\beta(d_{ij}+A_j)D_i$$

$$k_j=\sqrt{2(F_j+\beta g_j)\theta h(a_j{}^2\lambda_{1j}+b_j{}^2\lambda_{2j})(\lambda_{1j}+\lambda_{2j})}\times\frac{1}{a_j\lambda_{1j}+b_j\lambda_{2j}}+\theta hz_\alpha\sqrt{L}$$

4. Solution approach

Meta-heuristic algorithms have been very successful in solving complex mathematical models (Khalilzadeh et al., 2011). In order to solve the model formulated in section 3, a solution approach based on genetic algorithm (GA) is developed. GA is a stochastic search and heuristic optimization technique based on the mechanism of natural genetics which has been successfully applied to various complex problems. It starts with an initial set of random solution called population. Each solution in the population is called chromosome and each component of chromosome is designated by gene. The chromosomes evolve through successive iterations, called generations. During each generation, the chromosomes are evaluated, using some measures of fitness. To create next generation, new chromosomes (called offspring) are formed by crossover or mutation operators. Crossover operator combines two chromosomes from current generation, while mutation operator modifies a chromosome to form offspring. A new generation is created by (a) selecting some of current chromosomes (called parents) and offspring based on the fitness values, (b) rejecting others so as to keep the population size constant. Fitter chromosomes have higher probabilities of being selected. After several generations, the algorithms converge to the best chromosome, which may represent the optimum or suboptimal solution to the problem (Gen and Cheng, 1996). For more details of GA and its application in location problems refer to Sourirajan et al. [(2008), Goldberg (1989) and Jaramillo et al. (2002). In the following subsections, the developed GA for the problem is outlined.

4. 1. Chromosome representation

In this GA-based approach, each chromosome is indicated as a single dimensional array. If *m* is the number of candidate DCs, each chromosome *C* can be demonstrated by:

$C=(X_j,Y_i)=(X_1,X_2...X_m,X_{m+1},Y_1,Y_2..Y_m)$.

Where X_j correspond to the location genes and Y_i correspond to the assignment genes. These genes determine where the DCs are located and how the customers are assigned to the located DCs, respectively. More precisely, if $X_j=1$, it means that candidate site *j* is selected as a DC location, while if $X_j=0$, candidate location *j* is not chosen as a DC site. The gene X_{m+1} corresponds to dummy distribution center *u*; thus, it always takes the value 1. Also, $Y_i=j$ represents that customer *i* is assigned to distribution center *j*. If customer *i* is assigned to a dummy distribution center *u*, the corresponding assignment gene takes the value of *m*+1; in other words, $Y_i=m+1$.

4.2. Generating the first population

Half the chromosomes of the first population are generated from the feasible region randomly. The next half chromosomes are set identical to the obtained lower bound solution. Note that some customers may be allocated to more than one DC in the lower bound solution. In this case, the chromosome is modified to a feasible one, by assigning such customers to the nearest located DCs.

4.3. Chromosomes fitness

The rank-based evaluation function is defined as the objective function (16) for the chromosomes. In fact, we calculate the objective function (16) for each of the chromosomes. Obviously, the chromosome which results in less value of objective function (16) has the better rank.

4.4. Crossover operator

Crossover operator generates offspring by merging parent chromosomes. In order to determine which of chromosomes C_k, *k*=1, 2 … *pop-size* are selected as parents for crossover operation, the following procedure is repeated from *k*=1 to *pop-size*: generating a random number *r* from the interval [0, 1], the chromosome C_k will be selected as a parent provided that $r<P_C$, where the parameter P_C is the probability of crossover. Then randomly we group

the selected parents C_1', C_2', C_3', … to the pairs (C_1', C_2'), (C_3', C_4'),…. Without loss of generality let us explain the crossover operator on each pair by (C_1', C_2').

Crossover operator assigns each customer *i* in offspring chromosome either to the DC which is allocated to customer *i* in parent chromosome C_1', or to the DC which is assigned to customer *i* in parent chromosome C_2'. This occurs randomly and with probability of 0.5. The resulted offspring may be infeasible. If a customer is allocated to an unselected candidate DC site, this infeasibility is removed by locating DC in that candidate location. If the number of located DCs exceeds $P+1$, the number of selected DCs is reduced to $P+1$ by closing some DCs randomly. The customers which are allocated to these closed DCs are allocated randomly to the opened DCs. By this way, the offspring is modified to a feasible chromosome.

4.5. Mutation operator

Mutation operator may modify chromosomes C_k, k = 1, 2 … *Pop-size* to form offspring chromosomes. In order to determine which of chromosomes C_k undergo mutation, the following practice is repeated from k = 1 to *Pop-size*: generating a random number r from the interval [0, 1], the chromosome C_k will be selected as a parent provided that $r < P_M$, where the parameter P_M is the probability of mutation. Each selected chromosome is modified by one of the two following types of mutation several times (each type of mutation is occurred with probability 0.5). The first type of mutation generates offspring by modifying the assignment genes of parent chromosome. Namely, in the first type of mutation two located DCs are selected randomly; let *s* and *t* denote them. Then, if any customer in parent chromosome is assigned to *s*, that customer will be assigned to *t* and if any customer is assigned to *t*, it will be allocated to *s*.

The second type of mutation modifies location genes of parent chromosome to form offspring. Indeed, the second type of mutation randomly selects a location in which no DC is located; let *t* denotes it. Next, a DC is selected randomly from the located DCs and is named *s*. This type of mutation closes distribution center *s* and instead of it locates a DC at *t*. Then, all the customers assigned to distribution center *s*, are allocated to distribution center *t*. Similar to crossover process, if the resulted offspring does not belong to feasible region, it is repaired to become a feasible chromosome.

5. Computational results

This section summarizes the computational experience with the solution approach outlined in the previous section. Also, the performance of the proposed GA is compared with simulated annealing (SA) algorithm developed by Azad and Davoudpour (2010). The solution methods were tested on the 49-node, 88-node, and 150-node data sets described in Daskin (1995). The 49-node data set indicates the capitals of the lower 48 United States plus Washington, DC; the 88-node data set represents the 50 largest cities in the 1990 U.S. census along with the 49-node data set, minus duplicates; and the 150-node data set includes the 150 largest cities in the 1990 U.S. census.

For all three data sets, the mean of demand was obtained by dividing the population data given in Daskin (1995) by 1000. Fixed costs of locating DCs (f_j) were gained by dividing the fixed cost in Daskin (1995) by 10 for the 49-node problem and by 100 for 88-node problem. For the 150-node problem, fixed locating costs were set to 10000 for all the candidate DC locations. We set the per-unit cost to ship from distribution center *j* to customer *i*, d_{ij}, to the great-circle distance between these locations. The fixed ordering F_j and shipping costs g_j were set to 10 and the variable shipping cost A_j was set to 5 for all DCs. The parameters b_j and z_α were set to 100 and 1.96 (corresponding to 97.5% service level), respectively. We set the holding cost *h* and the lead time *L* to 1. For all three data sets, the values of a_j, λ_{1j} and λ_{2j} were set randomly. The other parameters used for the solution method are given in Table 1.

Table 1. Parameters for solution approach

Parameter	Value
Population size of GA	100
Probability of crossover in GA	0.9
Probability of mutation in GA	0.01
The number of generations in GA	500

The developed Solution approach was coded in Visual Basic.Net and executed on Pentium 5 computer with 1.00 GB RAM and 2.00 GHz CPU. Tables 2-4 summarize the results for our computational study on 49-node, 88-node, and 150-node problems with different values for the parameters P, u_i, θ and β, respectively.

Table 2. Computational results for 49-node

	P	u	Θ	β	GA	SA	Percent of Improved Cost
1	5	10	0.01	0.0005	299636	309734	3.37
2	5	10	0.005	0.0001	299525	307133	2.54
3	5	100	0.01	0.0005	299654	308673	3.01
4	5	100	0.005	0.0001	299528	306776	2.42
5	10	10	0.01	0.0005	668011	700543	4.87
6	10	10	0.005	0.0001	667799	695512	4.15
7	10	100	0.01	0.0005	668028	698958	4.63
8	10	100	0.005	0.0001	667801	695315	4.12
9	15	10	0.01	0.0005	1055635	1107889	4.95
10	15	10	0.005	0.0001	1055321	1103760	4.59
11	15	100	0.01	0.0005	1055652	1105373	4.71
12	15	100	0.005	0.0001	667801	696250	4.26
13	20	10	0.01	0.0005	1468258	1545047	5.23
14	20	10	0.005	0.0001	1467843	1541969	5.05
15	20	100	0.01	0.0005	1468275	1544332	5.18
16	20	100	0.005	0.0001	1467846	1539771	4.9

Table 3. Computational results for 88-node

	P	u	Θ	β	GA	SA	Percent of Improved Cost
1	5	10	0.01	0.0005	241015	252632	4.82
2	5	10	0.005	0.0001	240996	250756	4.05
3	5	100	0.01	0.0005	241025	252859	4.91
4	5	100	0.005	0.0001	241000	251267	4.26
5	10	10	0.01	0.0005	547266	581689	6.29
6	10	10	0.005	0.0001	547242	577613	5.55
7	10	100	0.01	0.0005	547276	585749	7.03
8	10	100	0.005	0.0001	547245	572965	4.7
9	15	10	0.01	0.0005	876143	939576	7.24
10	15	10	0.005	0.0001	876113	937528	7.01
11	15	100	0.01	0.0005	876153	932139	6.39
12	15	100	0.005	0.0001	876116	929121	6.05
13	20	10	0.01	0.0005	1223769	1313961	7.37
14	20	10	0.005	0.0001	1223733	1303153	6.49
15	20	100	0.01	0.0005	1223780	1303448	6.51
16	20	100	0.005	0.0001	1223737	1296916	5.98

Table 4. Computational results for 150-node

	P	u	Θ	β	GA	SA	Percent of Improved Cost
1	5	10	0.01	0.0005	625030	661969	5.91
2	5	10	0.005	0.0001	624790	661590	5.89
3	5	100	0.01	0.0005	625065	664632	6.33
4	5	100	0.005	0.0001	624796	663533	6.2
5	10	10	0.01	0.0005	1250039	1346042	7.68
6	10	10	0.005	0.0001	1249579	1344422	7.59
7	10	100	0.01	0.0005	1250074	1351580	8.12
8	10	100	0.005	0.0001	1249584	1349176	7.97
9	20	10	0.01	0.0005	2500055	2768311	10.73
10	20	10	0.005	0.0001	2499159	2760321	10.45
11	20	100	0.01	0.0005	2500084	2772843	10.91
12	20	100	0.005	0.0001	2499164	2762576	10.54
13	30	10	0.01	0.0005	3750068	4241701	13.11
14	30	10	0.005	0.0001	3748739	4235325	12.98
15	30	100	0.01	0.0005	3750099	4269112	13.84
16	30	100	0.005	0.0001	3748744	4238330	13.06

In these tables, the columns marked P , u, θ and β give the parameters P , u_i , θ and β , respectively. The columns labeled GA represent the objective values obtained by GA, whereas the columns marked SA indicate the objective values obtained by SA. The last column in each table indicates the percentage difference between the objective values obtained by GA and SA. In other words, the last column represents the amount of improvement in the objective value when the proposed GA is applied instead of SA, and is obtained by $\frac{(\text{SA-GA})}{\text{GA}} \times 100$.

It follows from Tables 2-4 that the presented solution method based on GA outperforms SA in all the cases. This suggests that the proposed solution approach is effective to solve the model and we can trust it in practice

6. Conclusion

This paper has addressed a stochastic supply chain design problem where a supplier is unreliable. Due to unreliability of the supplier, the yields at DCs are not deterministic. The problem does not assume that all the customers' demands must be satisfied. A nonlinear integer programming model has been presented that minimizes the expected total costs including costs of location, inventory, transportation, and lost sales. The presented model simultaneously determines which customers are served, where DCs are located and how DCs are assigned to the customers. In order to solve the model, a heuristic approach based on genetic algorithm has been proposed. Computational results for different data sets have revealed that the proposed solution approach is quiet effective. In future, it would be interesting to formulate the problem when DCs are unreliable. Furthermore, the model can be extended to consider constraints on the maximum demand that can be provided by a supplier. Finally, incorporating routing decisions in the model makes it more helpful.

Corresponding Author:
Dr. Armin Jabbarzadeh
Department of Industrial Engineering
Iran University of Science and Technology, 16846113114, Tehran, Iran
E-mail: arminj@iust.ac.ir

References

1. Shen ZJ, Qi L. Incorporating inventory and routing costs in strategic location models. European Journal of Operational Research 2007; 179: 372–389.
2. Shu J, Teo CP, Shen ZJ. Stochastic transportation-inventory network design problem. Operations Research 2005;53: 48–60.
3. Ozsen, L. Location-inventory planning models: Capacity issues and solution algorithms, Ph. D. Thesis, Northwestern University, 2004.
4. Erdem AS, Ozekici S. Inventory models with random yield in a random environment. International Journal of Production Economics 2002;78: 239–253.

5. Wu X. (Q; r) Inventory Policies under Uncertain Supply Chain Environment, Ph. D. Thesis, North Carolina State University, 2008.
6. Shen ZJ. A Profit Maximizing Supply Chain Network Design Model with Demand Choice Flexibility. Operations Research Letters 2006; 34: 673–682.
7. Daskin MS, Coullard C, Shen ZJ. An inventory-location model: formulation, solution algorithm and computational results. Annals of Operations Research 2002;110: 83–106.
8. Shen ZJ, Coullard C, Daskin MS. A joint location-inventory model. Transportation Science 2003; 37: 40–55.
9. Ozsen L, Coullard CR, Daskin MS. Capacitated warehouse location model with risk pooling. Naval Research Logistics 2008;55: 295–312.
10. Shen ZJ. Integrated Supply Chain Design Models: A Survey and Future Research Directions. Journal of Industrial and Management Optimization 2007;3: 1–27.
11. Baumol WJ, Wolfe P. A warehouse-location problem. Operations Research 1985;6: 252–263.
12. Erlebacher SJ, Meller RD. The interaction of location and inventory in designing distribution systems. IIE Transactions 2000;32: 155–166.
13. Shen ZJ. Efficient algorithms for various supply chain problems, Ph. D. Thesis, Northwestern University, 2000.
14. Shen ZJ, Daskin M. Trade-offs Between Customer Service and Cost in Integrated Supply Chain Design. M&SOM 2005;7: 188–207.
15. Snyder LV, Daskin MS, Teo CP. The stochastic location model with risk pooling. European Journal of Operational Research 2005;179: 1221–1238.
16. Sourirajan K, Ozsen L, Uzsoy R. A single product network design model with lead time and safety stock considerations. IIE Transactions 2007;39: 411–424.
17. Sourirajan K, Ozsen L, Uzsoy R. A genetic algorithm for a single product network design model with lead time and safety stock considerations. European Journal of Operational Research 2008;197: 599–608.
18. Noori AH, Keller G. One-period order quantity strategy with uncertain match between the amount received and quantity requisitioned. INFOR 1986;24: 1–11.
19. Ehrhardt R, Taube L. An inventory model with random replenishment quantity. International Journal of Production Research 1987;25: 1795–1803.
20. Gerchak Y, Vickson RG, Parlar M. Periodic review production models with variable yield and uncertain demand. IIE Transactions 1988;20: 44–50.
21. Qi L, Shen ZJ. A supply chain design model with unreliable supply. Naval. Research Logistics 2007;54: 829–844.
22. He Y, Zhang J. Random yield risk sharing in a two-level supply chain. International Journal of Production Economics 2008;112: 769–781.
23. Maddah B, Salameh MK, Karame GM. Lot sizing with random yield and different qualities. Applied Mathematical Modelling 2009;33: 1997–2009.
24. Parlar M, Berkin D. Future supply uncertainty in EOQ Models. Naval Research Logistics 1991;38: 107–121.
25. Gurler U, Parlar M. An inventory problem with two randomly available suppliers. Operations Research 1997;45: 904–918.
26. Henig M, Gerchak Y. The structure of periodic review policies in the presence of random yield. Operations Research 1996;38: 634–643.
27. Yano CA, Lee H. Lot sizing with random yields: A review. Operations Research 1995; 43: 311–334.
28. Tang CS. Review Perspectives in supply chain risk management. International Journal of Production Economics 2006;103: 451–488.
29. Ross SM. Introduction to Probability Models. Academic Press, 2007.
30. Snyder LV, Daskin MS. Reliability models for facility location: The expected failure cost case. Transportation Science 2005;39: 400–416.
31. Montgomery DC, Runger GC, Hubele NF. Engineering Statistics. Wiley, New York, 1998.
32. Khalilzadeh M, Kianfar M, Ranjbar M. A Scatter Search Algorithm for the RCPSP with Discounted Weighted Earliness-Tardiness Costs. Life Science Journal 2011;8(2):634-640.
33. Gen M, Cheng R. Genetic algorithms and engineering design. Wiley, New York, 1996.
34. Goldberg DE. Genetic Algorithms in Search, Optimization and Machine Learning. Addison-Wesley, 1989.
35. Jaramillo JH, Bhadury J, Batta R. On the use of genetic algorithms to solve location problems. Computers & Operations Research 2002;29: 761–779.
36. Azad N, Davoudpour H. Designing a Reliable Supply Chain Network Model under Disruption Risks. Journal of American Science 2010;6(12): 1091–1097.
37. Daskin MS. Network and discrete location: models, algorithms, and applications. Wiley, New York, 1995.

10/22/2011

Prognostic Significance of Progenitor Cell Markers in Acute Myeloid Leukemia

Mona Ahmed Ismail[*1] and Sherin Mohamed Hosny[2]

Department of Clinical Pathology[1] and Internal Medicine[2], Faculty of Medicine, Ain Shams University, Cairo, Egypt
[*]monaismail1@Yahoo.com

Abstract: Background: Until now the prognostic significance of flow cytometric immunophenotyping (FCI) in acute myeloid leukemia (AML) has been controversial. The decision whether patients with AML should receive a more intensified therapy has been made according to defined risk categories based mainly on genetic criteria. Unfortunately no specific chromosomal abnormalities are found in about half of the patients. So additional prognostic factors are needed. Aim of work: The aim of the current work was to investigate prognostic value of progenitor cell markers CD34, CD38 and CD90 expression on AML blast cells at initial diagnosis, and to correlate this expression with known prognostic parameters as well as with the clinical outcome. Patients &Methods: This work was conducted on 80 patients with de novo AML meeting World Health Organization criteria for AML, FAB subtype M0-M5 were included. The levels of progenitor markers were determined by FCI, corresponding cytogenetic results were obtained, appropriate follow-up information were analyzed. Results: Sixty one percent, 82.5% and 35% out of 80 patients were positive for CD34, CD38 and CD90 respectively. No differences in expression were found in different FAB subtypes and cytogenetic risk groups. Cut off values were calculated with values ≥38 for CD34, ≥55 for CD38 and ≥52 for CD90. A significant high resistance to induction therapy and poor outcome were observed in patients with increased progenitor cell expressions. Conclusion: Progenitor cell markers are sensitive indicators as regard response to therapy and clinical outcome in patients with de novo AML. Therefore, their determination should be taken into consideration when designing therapeutic regimens.
[Mona Ahmed Ismail and Sherin Mohamed Hosny **Prognostic Significance of Progenitor Cell Markers in Acute Myeloid Leukemia]** Life Science Journal, 2011; 8(4):680-686] (ISSN: 1097-8135). http://www.lifesciencesite.com.

Keywords: Prognostic, CD34, CD38, CD90, Acute Myeloid Leukemia

1. Introduction

Acute myeloid leukemia is an aggressive malignancy characterized by accumulation of immature myeloid progenitor cells in the bone marrow [(1)]. The majority of the adult patients (70-80%) with de novo AML will achieve an initial complete remission after chemotherapy. However, long term free survival remains as low as 30-50% [(2)]. Moreover, there are poor prognostic groups who are less probable to achieve complete remission with induction treatment and for whom the overall survival is less than 1 year [(3)].

The growth and differentiation of the progenitor cells are regulated by specific cytokines and growth factors and their corresponding receptors. By analyzing those receptors it is possible to determine the grade of differentiation and the lineage of the progenitor cells [(4)].

CD34 is expressed on the surface of immature hematopoietic normal progenitor cells that compromise 1-2% of the cells [(5)]. It is not lineage restricted and thus not useful for distinguishing AML from ALL [(6)]. In addition, CD34 is involved in cellular adhesion and mediates resistance to apoptosis [(1)]. CD34 AML blast cells are even more resistant to programmed cell death with increased percentages of CD34 cells [(7)].

CD38 is mostly expressed on the surface of immature cells and different lineages of hematopoietic activated cells like lymphocytes and myelocytes [(8)]. Moreover, CD38 is supposed to mediate signaling pathways that result in cell proliferation, regulation of apoptosis and differentiation. It also serves as a cell adhesion molecule [(9)].

CD90, also known as THY-1, is a 25-35 KDa, glycosylphosphatidyl inositol (GPI) linked surface protein expressed on primitive hemopoietic stem cells in normal BM, cord blood and fetal liver cells. The function of CD90 is not yet clear but possibly it is responsible for hemopoietic cell adhesion and recognition [(10)].

The aim of this study was to investigate prognostic role of progenitor cell markers CD34, CD38 and CD90 expression on AML blast cells at initial diagnosis, and to correlate this expression with known prognostic parameters as well as with the clinical outcome.

2. Subjects and methods

This study included 80 patients with de novo AML presented to Hematology/Oncology Clinic, Ain Shams University Hospitals in the period from January 2009 to March 2011. Their ages ranged from 21-73 years with a mean of 35.28±14.01 years, with a male to female ratio 2:1.

All patients were subjected to thorough history and clinical examination, complete blood picture (using LH 750 Coulter, Beckman) and BM aspiration with examination of Leishmans' stained blood smears, immunophenotyping for estimation of CD34, CD38 and CD90 (using Epics XL flow cytometry, Coulter, Electronics, Hialiah, Fl, USA).

Diagnosis and classification of leukemic cases were based on morphology and cytochemistry according to the French American British (FAB) classification and meeting World Health Organization criteria for AML , immunophenotyping results and corresponding cytogenetic results were obtained, appropriate follow-up information were included.

Flow cytometric immunophenotyping of blast cells was performed using whole blood lysis method. A panel of mouse monoclonal antibodies directly conjugated with fluorescein isothiocyanate (FITC), phycoerythrin (PE0 or tandem Cy 5-PE (PC5) were used. These monoclonal antibodies included myeloid markers (CD13, CD33, CD117, CD14, CD15 and myeloperoxidase), lymphoid markers (CD10, CD19, CD20, CD5, CD2, CD7 and CD3) as well as PE labeled anti CD34, FITC labeled anti CD38, (Beckmann Coulter, Krefeld, Germany), and PC5 labeled anti CD90 (BD Biosciences, Mountain View, CA, USA). An appropriate isotype control IgG1 was used in all cases to assess background fluorescence intensity.

The blast population was gated according to their FS and SS. 5000-10000 cells in the gate were analyzed. If the percentage of positive events was >20%, the leukemic sample was considered as positive for that surface marker [(11)] as well as progenitor cell markers [(12)], except for CD34 and intracellular MPO where expression more than 10% was considered positive [(13)].

Conventional cytogenetic analysis: involves the examination of spontaneously dividing cell populations by blocking cell division at metaphase stage with an inhibitor of spindle formation (colcemid), this is followed by hypotonic wash and fixative then slide making and staining with Giemsa using trypsin to induce G Banding. Analysis of available metaphases were counted and analyzed under microscope and 20 metaphases were captured, analyzed and karyotyped using an image system cytovision/genus application soft ware versus 2.7 (UK).

Statistical analysis:

Data were collected, verified, revised and then edited on PC. Then data were analyzed using IBM SPSS statistics (V.19.0, IBM Corp., USA). Association of categorical data parameters was performed using Chi square test, Fisher exact was performed for value less than 5. Mann-Whitney U test was used for unpaired data The receiving operating characteristic (ROC) was performed to calculate the cutoff values. Kaplan Meier technique was used to estimate the overall survival. A P value <0.05 was considered significant and <0.01 highly significant.

3. Results:

Results of the present study are presented in Tables 1-3 and Figures 1-2.

The study was conducted on 80 patients with de novo AML classified according to the FAB and immunophenotypic criteria. The blast cells were identified according to their forward and side scatter or CD45 expression and side scatter (SS), electronically gated and analyzed by flow cytometry (Figure 1).

According to the age, the patients were divided into 2 groups, patients <60 years and patients >60 years. The frequency of progenitor cell markers were higher in patients who were older than 60 years when compared to patients <60 years. However, these differences were statistically non significant (p >0.05) (Table 1).

Hepatomegaly, splenomegaly, lymphadenopathy, peripheral blood and bone marrow blasts were not significantly associated with progenitor cell markers expression (data not shown).

As regards CD34, fifty two out of 80 patients (61%) were positive and was mostly expressed in immature AML M0 and M1(87.5% and 77% respectively). It was less in other FAB subtypes. However, these differences were statistically non significant with a P value >0.05.

CD38 was positive in 66 out of 80 (82.5%) patients and highly expressed in all FAB subtypes, however this expression was not significant regarding FAB subtypes (P value <0.05).

Twenty eight patients (35%) out of 80 patients with AML were positive for CD90 expression. CD90 showed highest percentage with M3 (55%) but regarding the FAB this difference was statistically non significant.

Successful mitosis was encountered in 74/80 (92.5%) of cases. 29/74 (39%) were classified as favorable group {t(8;21); t(15,17) or inv 16}, 19/74 (26%) were classified as intermediate with normal karyotype or trisomy 8 and 26/74 (35%) were classified as poor cytogenetic risk group with t(9,11) or del11q23.

Studying the association between cytogenetic and progenitor markers revealed that all progenitor markers were higher with adverse risk groups than favorable one, however this difference wasn't

statistically significant (Table 1).

Using the receiver operating characteristic (ROC) study, cut off values of the progenitor cell markers for the most significant separation and differentiation between cases with relapse/death or remission were calculated. Most significant differences between the cases with complete remission and inferior outcome were found in patients with a cut off value more or less than 38% for CD34, 55% for CD38 and 52% for CD90.

There was a highly significant relation between progenitor markers expression and response to chemotherapy ($p<0.01$), where patients with increased expression were mostly non responders to chemotherapy, while most patients with expression less than cut off values responded to chemotherapy (Table 2).

Patients were followed up for 15 months to detect patient outcome. By using Kaplan Meier curves, 76% of patients with CD34 expression <38 showed free survival, while only 25% of the patients with expression >38were still in remission. In addition, 67% of patients with CD38 expression ≥55% and 69% of the patients with CD90 ≥52% relapsed after 12 months follow up (Table 3, Figure 2).

Table 1: Association between CD34, CD38 and CD90 and clinical features in AML patients.

	No of patients	CD34% Positive	CD38% Positive	CD90% Positive	Sig
Age <60years	32	25	25	12	NS
>60years	48	27	41	16	
Sex					
Male	41	24	36	15	
Female	39	28	30	13	NS
Cytogenetic					
Favorable	29	13	19	6	
Intermediate	19	16	21	9	NS
Poor	26	23	26	13	
FAB					
M0	8	7	7	2	
M1	13	10	11	3	
M2	29	19	25	7	NS
M3	18	10	15	10	
M4	8	4	5	4	
M5	4	2	3	2	

Table 2:Association between progenitor markers expression and response to chemotherapy in all studied patients.

	CD34 <38		CD34 ≥38		CD38 <55		CD38 ≥55		CD90 <52		CD90 ≥52	
	No	%	No	%	No	%	No	%	No	%	No	%
Responders	22	76	13	25	23	66	6	9	24	63	11	26
Non responders	7	24	38	75	12	34	25	81	14	37	31	74
Sig.	HS				HS				HS			

Table 3: Association between progenitor markers and patients outcome

Clinical outcome	CD34 <38		CD34 ≥38		CD38 <55		CD38 ≥55		CD90 <52		CD90 ≥52	
	No	%	No	%	No	%	No	%	No	%	No	%
CR	22	76	13	25	19	54	12	39	24	63	11	26
Relapse	6	21	31	61	14	40	18	58	10	26	29	69
Death	1	3	7	14	2	6	1	3	4	11	2	5

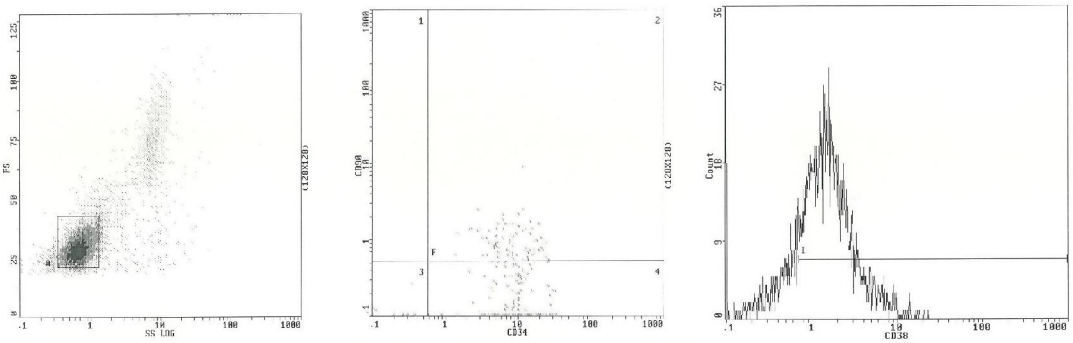

A B C

Figure1: Flow cytometric analysis of an AML case. A: shows gated blasts, B: shows CD34 and CD90 expression and C: shows CD38 expression.

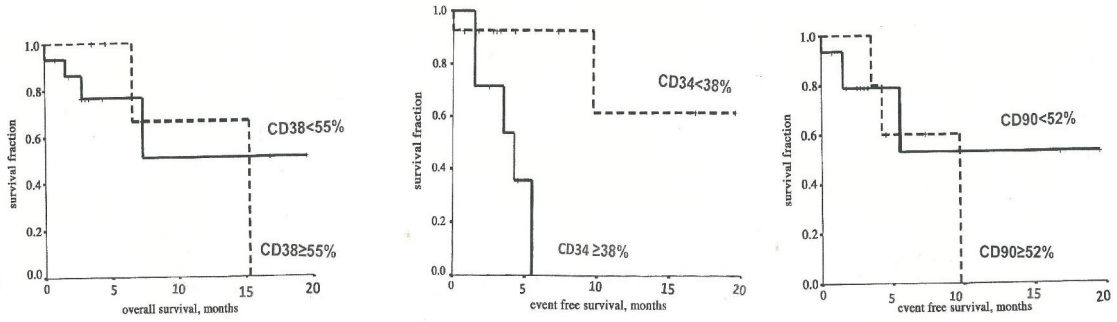

Figure 2: Kaplan –Meier curves for prognostic significance of progenitor cell markers in AML patients.

4. Discussion

The major prognostic parameters with regard to relapse of AML are the response to induction chemotherapy and the genetic abnormalities of the malignant cells[14,15]. It is still not known whether AML cell expressions of progenitor cell markers CD34, CD38 and CD90 represent an additional independent prognostic factor [16].

The present study was carried out on 80 patients with de novo AML, aiming to assess the prognostic value of progenitor cell markers in AML and to establish a relationship between them with the response to chemotherapy and clinical outcome. These markers were established by flow cytometry .

Flow cytometric analysis improves both accuracy and reproducibility of the FAB classification and is considered to be practically useful for the detection of MRD by monitoring AML patients in remission [12].

In this study CD34 was expressed in 61% of the patients with AML, these data were consistent with other studies using the same technique who detected 65% expression of CD34 [17]. This was also in agreement with **Petrovici *et al.*, 2010** [21] and Legrand ***et al.*, 2000** [18] who stated that the expression of CD34 was 57% and 68% respectively. However, wide variation ranging between 25% and 64% [1] was encountered by **Basso *et al.*, 2001** [19] , that could be due to methodological variation in detection of receptor expression (like flurochrome labeling, varying gates in flow cytometric analysis, and different CD34 antibodies recognizing distinct CD34 epitopes).

CD34 expression was highest in M0-M1 FAB subtypes, however this was not statistically significant. This was consistent with other studies [12] who detected no correlation between CD34 expression and FAB subtypes.

Also no significant difference was detected between this progenitor cell marker and age as well as other clinical and laboratory parameters. This was in agreement with other investigators [14,20] who detected no correlation between CD34 expression and clinical data of the patients.

In this study, CD38 expression was expressed in 82.5% of studied AML patients. This expression was lower than that detected by **Keyhani *et al.*, 2000** [21] who detected CD38 expression in >95% of AML cases with 63%-83% positive cells. The different percentages could be due to a lower case number studies as compared to 304 cases studied by them. Furthermore, CD38 is not a specific marker for blasts

being expressed on a variety of cell types (for example lymphocytes and myelocytes) [21].

Our study demonstrated no significant association between CD38 expression with different FAB subtypes or age. This was in agreement with other studies [12] that detected no significant association. On the other hand, **Keyhani *et al.*, 2000** [21] found a significant lower expression of CD38 with M3 FAB subtypes.

Regarding CD90 expression, 28/80(35 %) expressed CD90. This was consistent **Filler *et al.*, 2008** [22] who found coexpression of CD34 and CD90 in 42 out of 120 cases (35%). However, **Buccisano *et al.*, 2004** [23] found an overall frequency of CD90/CD34 positive cases were 17% and that CD90 was always expressed in the CD34 positive cell fraction. On the contrary, other studies [24] found higher percentage than this study which may be explained by their lower reference value e.g. 5% of all positive cells chosen as cut off between CD90+ and CD90- cases.

Again **Petrovici *et al.*, 2010** [12] found the expression of CD90 in 66% of investigated AML case, when measuring CD90+on CD34 + double positive cells (on de novo and secondary AML) using FITC conjugated anti CD90 monoclonal antibody with PE labeled anti CD34 monoclonal antibody.

In our study, the highest CD90 expression was found in AML-M3 (55%), yet no significant difference could be detected between FAB subtypes. This was in agreement with other studies [12] that found the expression of CD90 highest with M3 subtype but still statistically non significant.

There was no statistical significant difference was found between progenitor cell markers and cytogenetic results, although the highest percentages were detected in the poor risk group (88%, 100%, 50% in CD34, CD38 and CD90 respectively) (Table 1). However, the number of patients in this study might still not be sufficient to give a conclusive result.

This was similar to other results [18] that didn't find a correlation between CD34 expression and cytogenetic risk groups. On the contrary other results [23] confirmed a significant correlation between unfavorable karyotypes and high expression of CD34 and CD90.

AML cut off values were identified in order to allow the most significant separation and differentiation between AML cases with remission or relapse/death. In this study patients with more than 38% for CD34, 55% for CD38 and 52 % for CD90 were associated with poor response to chemotherapy while most patients with less expression responded to chemotherapy with a highly significant difference between both groups.

After a 12 month follow up, regarding patients with CD34 more than cutoff value, 61% relapsed, 14% died and only 25% developed remission (Table 3). In addition, patients with CD38 and CD90 more than cutoff values showed 67% and 69% relapse, 2% and 5% died and 31% and 26% developed remission respectively.

This was in agreement with other studies[12] that stated that increased CD34 and CD38 were associated with increased relapse rate. A possible explanation could be that blast cells get more resistant to apoptosis with increasing CD34 proportions resulting in bad prognosis [7]. In contrast, another study proposed that CD34 alone could not be an independent marker for prognosis. It was recommended using a combination of CD34 with other markers [18].

This was also in agreement with **Buccisano *et al.*, 2004** [23] who found that AML patients characterized with poor prognosis (such as elderly AML, de novo AML with unfavorable cytogenetic or drug resistance) were significantly associated with high CD90 expression. On the contrary **Petrovici *et al.*, 2010**[12] found that patients with increased CD90 expression on the blast cells were associated increased remission.

Regarding cytogenetic analysis, our findings support previous reports [25,26] ascribing poor prognosis to AML patients positive for t(9,11) or del11q23, favorable prognosis to AML patients positive for t(8,21), t(15,17) or inv 16.

From this study we can conclude that the expression of progenitor markers CD34, CD38 and CD90 could be used as a predictor of poor therapeutic response and relapse in de novo AML. In this regard, for the consideration of whether patients with high expression of CD34, CD38 and CD90 should get more intensive consolidation therapy or an early bone marrow transplantation due to their poor prognosis, Further studies on wide scale de novo AML patients should be implemented. In addition, in cases with post remission targeted therapies as immunotherapies or in cases with intermediate risk karyotype the prognostic impact of progenitor cell markers could contribute to refine adapt these protocols for individual patients.

Corresponding author
Mona Ahmed Ismail
Department of Clinical Pathology, Faculty of Medicine, Ain Shams University, Cairo, Egypt
monaismail1@Yahoo.com

References

1. Oyan AM, Bo TH, Jonassen I, Ulvestad E, Gjertsen BT, Kalland KH and Bruserud O (2005):

CD34 expression in native human acute myelogenous leukemia blasts: Differences in CD34 membrane molecule expression are associated with different gene expression profiles. Cytometry Part B (Clinical Cytometry); 64B:18-27.
2. Matsunaga T, Fukai F, Miura S, Nakane Y, Owaki T, Kodama H, Tanaka M, Nagaya T, Takimoto R, Takayama T and Niitsu Y (2008): Combination therapy of anticancer drug with the FNIII 4 peptide of fibronectin effectively overcomes cell adhesion mediated drug resistance of acute myelogenous leukemia. Leukemia; 22: 353-360.
3. Bullinger L, Valk PJ (2005): Gene expression profiling in acute myeloid leukemia. J Clin Oncol.; 23: 6296-6305.
4. Sperr W, Hauswirth A, Florian S, Ohler O, Geissler K and Valent P (2004): Human leukemic stem cells: a novel target or therapy. Eur J Clin Invest.; 34 (suppl 2): 31-40.
5. Katz FE, Tindle R, Sutherland DR and Greaves MF (1985): Identification of a membrane glycoprotein associated with hematopoietic progenitor cells. Leuk Res.; 9:191-198.
6. Bene MC, Castoldi G and Knapp W (1995): Proposal for the immunological classification of acute leukemias. European Group for the Immunological Characterization of Leukemias (EGIL). Leukemia; 9:1783-1786.
7. Van Stijn A, van der Pol MA Kok A, Bontje P, Roemen G, Beelen R, Ossenkoppele G and Schuurhuis G (2003): Difference between CD34+ and CD34- blast compartments in apoptosis resistance in acute myeloid leukemia. Hematologica; 88: 497-508.
8. Mehta K, Umar S and Malavasi M (1996): Human CD38, a cell surface protein with multiple functions. FASEB J., 10: 1408-1417.
9. Deaglio S, Dianzani U, Horenstein AL, Fernandez JE, van Kooten C, Bragardo M, Funaro A, Garbarono G, Di Virgilio F, Banchereau J and Malavasi F (1996): Human CD38 ligand. A 120-KDA protein predominantly expressed on endothelial cells. J Immunol.; 156: 727-734.
10. Zucchini A, Del Zotto G, Brando B and Canonico B (2001): CD90. J Biol Regul Homeost Agents; 15: 82-85.
11. Rothe G and Schmitz G (1996): Consensus protocol for flow cytometric immunophenotyping of hematopoietic malignancies. Leukemia; 10: 877-895.
12. Petrovici K, Graf M, Reif S, Hecht K and Schmetzer (2010): Expression profile of the progenitor cell markers CD34, CD38 and CD90 in acute myeloid leukemia and their prognostic significance. Journal of Cancer Molecules; 5(3): 79-86.
13. Jaff E, Harris N and Stein H (2001): World Health Organization Classification of tumours: Pathology and genetics of tumors of hematopoietic and lymphoid tissues. Lyon, France: IARC Press; 3:14-21.
14. Kottaridis PD, Gale RE, Frew ME, Harrison G Langabeer SE, Belton AA, Walker H, Wheatley K, Bowen DT and Burnett AK (2001): The presence of a FLT3 internal tandam duplication in patients with acute myeloid leukemia (AML) adds important prognostic information to cytogenetic risk group and response to the first cycle of chemotherapy: analysis of 854 patients from the United Kingdom Medical Research Council AML 10 and 12 trials. Blood; 98: 1752-1759.
15. Wheatley K, Burnett AK, Goldstone AH, Gray RG, Hann IM, Harrison CJ, Rees JK, Stevens RF and Walker H (1999): A simple robust, validated and highly predictive index for the determination of risk directed therapy in acute myeloid leukemia derived from the MRC AML 10 trial. Br J Hematol.; 107; 69-79.
16. Kanda Y, Hamaki T, Yamamoto R, Chizuka A, Suguro M, Matsuyama T, Takezako N, Miwa A, Kami M and Hirai H (2000): The clinical significance of CD34 expression in response to therapy in patients with acute myeloid leukemia: an overview of 2483 patients from 22 studies. Cancer; 88: 2529-2533.
17. Chang H, Salma F, yi Q, Patterson B, Brien B and Minden M (2004): Prognostic relevant immunophenotyping in 379 patients with acute myeloid leukemia. Leuk Res.; 28: 43-48.
18. Legrand O, Perrot JY, Baudard M, Cordier A, Lautier R, Simonin G, Zittoun R, Casadevall N and Marie JP (2000): The immunophenotype of 117 adults with acute myeloid leukemia: proposal of a prognostic score. Blood; 96: 870-877.
19. Basso G, Lanza F, Orfao A, Moretti S and Castaidi G (2001): Clinical and biological significance of CD34 expression in acute leukemia. J Biol Regul Homeost Agents; 15: 68-78.
20. Bruserud O, Hovland R, Wergeland L, Huang T and Gjertse (2003):Flt3 mediated signaling in human acute myelogenous leukemia (AML) blasts; a functional characterization of Flt3 ligands effects in AML cell populations with and without genetic Flt3 abnormalities. Hematologica; 88: 416-428.
21. Keyhani A, Yang H, Jendibora D, Pagliaro L, Cortez J and Pierce S (2000): Increased CD38

expression is associated with favorable prognosis in adult acute leukemia. Leuk Res.; 24: 153-159.
22. Feller N, Kelder A, Westra G, Ossenkoppele GJ and Schuurhuis GJ (2008): Positive selection for CD90 as a purging option in acute myeloid leukemia stem cell transplants. Cytometry Part B (Clinical Cytometry); 74B: 9-16.
23. Buccisano F, Rossi FM, Venditti A, Del Poeta G, Cox MC, Abbruzzese E, Rupolo M, Berretta M, Degan M, Russo S, Tamburini A, Maurillo L, Del Principe MI, Postorino M, Amadori S and Gattei V (2004): CD90/Thy-1 is preferentially expressed on blast cells of high risk acute myeloid leukemias. British Journal of Hematology; 125: 203-212.
24. Kozii R, Persichetti J, Phelps V, Ball SE and Ball ED (1997): Thy-1 expression on blast cells from adult patients with acute myeloid leukemia. Leukemia Research; 21: 381-385.
25. Chen C, Yang F, Lee K, Kwang W, Yu J, Tzeng C aand Gau P (2005): Pretreatment prognostic factors and treatment outcome in elderly patients with de novo acute myeloid leukemia. Ann Oncol; 16(8): 1366-1373.
26. Cheson B, Peter L, John M, Lowenberg B, Pierre W, Stephen D, Pinto A, Beran M, Richard M, Steven D and Charles A (2006): Clinical application and proposal for modification of the International Working Group (IWG) response criteria in myelodysplasis. Blood; 108(2): 418-425.

11/20/2011

Palynology Of Six Species Of *Solanum* (Solanaceae)

Gamal M. A. Lashin

Department of Botany, Faculty of Sciences, Zagazig University, Zagazig, Egypt.
gamasabaa@yahoo.com

Abstract: This paper presents the palynology of six species of genus *Solanum* (family: Solanaceae) from Saudi Arabia. The species has been investigated by Light microscopy, Scanning and Transmission electron microscopy. Pollen grains are generally radialy symmetrical, isopolar tricolporates zono-aperturates, prolate, subprolate or spheroidal with tectate and columellate exine. Sexine echinates or punctuates. On the basis of amb axis, three distinct pollen types are recognized, viz.; *Solanum* sp.aff. *anguivi* (16-24 µm) type-1, *S. gracileps* (20-26 µm), *S. incanum* (21-26 µm) and *S. villosum* (22-26 µm) type -2 and *S. nigrum* (20-32 µm) and *S. carense* (23-37 µm)) type-3. On the basis of pollen shape class, four distinct pollen types are recognized, viz.; type -1, *S. incanum* (prolate), type-2 *Solanum* sp.aff. *anguivi* (prolate-subprolate), type- 3, *Solanum carens*e (subprolate) and type -4, *S. villosum, S. nigrum* and *S. gracileps* (prolate- spheroidal). On the basis of exine sculptures, five distinct pollen types are recognized, viz.; type-1, echinate-verrucate exine in *S. villosum* and *S. nigrum*, type-2, regulate pislate in *S. incanum* but type-3, *S. gracileps* is crenate, type-4 *Solanum* sp.aff. *anguivi* is regulate scabrates and type-5, *Solanum carens*e is perforate echinates. From the results, the Solanaceae is considering of an europalynous family. The importance of exine sculpture in taxonomy is detailed underlined. The morphological and palynological results obtained above and other taxonomic differences can be used to enhance proper understanding of the species in particular and the genus *Solanum* in general.
[Gamal M. A. Lashin **Palynology of six species of *Solanum* (Solanaceae)** Life Science Journal, 2011; 8(4): 687-697] (ISSN: 1097-8135). http://www.lifesciencesite.com.

Keyword: Palynology, *Solanum*, LM, SEM, TEM, Saudi Arabia.

1. Introduction

The family Solanaceae is one of the most important families of flowering plants economically, floristically, ethnobotanically and scientifically (Olmstead *et al.,* 1992). *Solanum* is a genus of annuals, perennials, sub-shrubs, shrubs and climbers. It's often had attractive fruit and flowers. Most they are poisonous, but several bear edible fruit or other parts, such as the common foods tomato, potato and eggplant. Synonyms and common names: Nightshade, as well as referring to the related genus *Atropa*, is also used for many members of the genus *Solanum*. The name is also extended to the family Solanaceae. *Solanum, Physalis,* and *Lycium* are widely distributed across both the Eastern and Western Hemisphere (D"Arcy, 1991). The Solanaceae family is composed of 98 genera and about 2300 species belonging to 14 tribes grouped in three subfamilies (Wettstein, 1895; Hunziker, 1979 & D"Arcy 1991). Solanoideae eight tribes, 60 genera and about 1746 species. The subfamily Solanoideae has curved embryos contained in flattened discoid seed and the subfamily Cestoideae with straight or slightly bent embryos in prismatic- subglobose seeds, (Hunziker, 1979 and D"Arcy, 1991). According to Mabberly (1997) the family consists of 94 genera and 2950 species. While, Judd *et al.* (1999) report that the number of the genera in the Solanaceae sense lato (including Nolanaceae) is about 147 genera occurring world wide of which 7 genera and 33 species occur in Saudi Arabia (Migahid, 1978 & Collenette, 1985; 1998). Each of these studies was a certain source of taxonomic criteria. Pollen characters have received more attention in taxonomic and pollen morphology. However, the ultra-structure of the pollen wall, its stratification and internal structure can hardly be studied by light microscope (Zavada, 1990). Therefore Scanning and Transmission Electron microscopy become necessary in examining these characters, El- Ghazaly (1990) and Harky, *et al.,* (2000) reported on the morphology of pollen grains of many plant species. So far, no previous ultra-structural studies of pollen grains of family Solanaceae have been reported in Saudi Arabia except Al-Wadai (2000), he studied the pollen morphology and ultra-structures of *Withania sommnifera*, Al-Wadei (2002), studied the cytomorphology of three species of *Solanum* and Al-Wadei and Lashin (2007), they studied also the palynological and cytological characters of some taxa of *Solanum.* In the other Arabic regions El-Ghazaly (1993, 1999) studied some species of family Solanaceae. The taxonomic significance of pollen morphology in Solanaceae is more or less obscure. Sometimes, different tribes or subtribes have similar type of pollen or vice versa the genera referred to the same tribe or subtribe may have different type of pollen (Erdtman, 1952). However,

in the present work a palynological analysis of a combination of different parameter is believed to serve in a better understanding and evaluation of the relationships between the different taxa of the genus *Solanum.* For this aim the data derived from palynological analysis of the pollen grains by LM, SEM and TEM will serve for contribution to the palynology and taxonomy of the family Solanaceae.

2. Materials and Methods

The pollen from mature anthers was collected from Herbarium specimens deposited at the Department of Biological Sciences, Faculty of Sciences, King Khalid University, Abha, Saudi Arabia (SA.) (Table, I). The exine sculpture as well as shape and size of pollen grains were examined by high resolution Scanning and Transmission electron microscope (Jeol T. 100) pollen grains for each species were measured. The length of polar axis (P) and equatorial axis (E) and length ratio (P/E) were assigned in Table 2. The pollen specimens are investigated under Light microscopy and Scanning and Transmission electron microscope as follow:

Processing of pollen grains for Light microscope (LM): The materials are placed in glacial acetic acid for three minutes acetolysed according the method of Erdtman (1960) and Moor *et al.*, (1991) then mounted in glycerin gel for investigation and photographed by light microscopy using a CH2 Olympus microscope, in the Department of Biological Sciences, Faculty of Sciences King Khalid University, Abha, Saudi Arabia.

Processing of pollen grains for scanning electron microscopy (SEM): The dried materials are attached to stubs with double-faced selotape. The stubs are gold- coated in B sputter coater for one minute, and examined. The representative pollen grains are photographed at various magnifications in a Jeol T 100. SEM operated at an accelerating voltage of 15KV. The investigated taxa are illustrated in figures 1-6 and Table, 1- 2. Processing of pollen grains for Transmission electron microscopy (TEM): The materials are fixed for 3 h. in 2.5% glutaraldehyde with 0.05m Cacoldylate buffer at pH 7.4 for 24 h. and post fixed in 1% OsO4 (Osmum tetraoxids) in the same buffer for 2 h. (Cresti *et al.*, 1985). The pollen then dehydrated in graded series of ethanol and embedded in Spurr"s resin (Spurr, 1969) Ultra thin sections are cut using a Diamond Knife on Ultra-microtome, stained with Uranyl acetate followed by lead citrate (Reynolds, 1963). The stained grids are examined and Photographed with a Jeol-Tem 100 B TEM. in the Department of Pathology Faculty of Medicine King Khalid University, Abha, Saudi Arabia. The terminology used for pollen description follow, Faegri, *et al.*, 1989.

Table (1): Sites of collection of the examined species of *Solanum.* Identification of the studied species according to, Migahid (1978) and Collenette (1985-1998)

Herbarium No.	*Species*	Sites of collection
1	*Solanum incanum* L.	Sudd- Samallagi
2	*Solanum nigrum* L.	N.W.Jebel Sawdah
3	*Solanum villosum* (L.) Lam.	N.W.Jebel Sawdah
4	*Solanum carense* Dun. inDc.	Sudd- Samallagi
5	*Solanum* sp.aff. *anguivi* Lam.	Sudd- Samallagi
6	*Solanum gracileps* L.	Abha-Asier

Table (2): Pollen morphology: Dimensions, shape classes and shape (LM, SEM, TEM) among the species of the genus *Solanum*.

Species Characters	Dimensions (LM)			Shape Class		Pollen Class	Sexine sculptures
	Polar axis P (µm)	Equatorial axis E (µm)	P/E	(E view)	P view (Amb)		(IN SEM)
1- *Solanum incanum* L.	32(34)36	21(23)26	1.38-1.52	Prolate	angular	Trizonocolporate	Regulate-scabrate
2-*S. nigrum* L.	20(23)32	20(24)29	1.00-1.10	prolate-spheroidal	angular	Trizonocolporate	Echinate
3-*S. villosum* (L.) Mill.	22(24)26	20(22)25	1.04-1.10	prolate-spheroidal	circular	Trizonocolporate	Echinate
4-*S. carense Dun*. inDc.	23(28)37	20(25)30	1.15-1.23	Subprolate	Rectangular	Trizonocolporate	Perforate-echinate
5-*S.* sp.aff. *anguivi* Lam.	16(17)24	12(15)23	1.04-1.33	prolate-subprolate	circular	Trizonocolporate	Regulate-scabrate
6-*S. gracileps* L.	20(23)26	18(20)25	1.04-1.11	prolate-spheroidal	Semi-angular	Trizonocolporate	Spinulose

3. Results

Pollen grains are generally radialy symmetrical, isopolar tricolporates zono-aperturates, prolate, subprolate or spheroidal with tectate and columellate exine. Sexine echinates or punctuates.

Palynological Description

1- ***Solanum incanum*** L. (Fig. 1, A-I)

LM. (Figs. A-C); Pollen is prolate; P/E: 1.45 (1.38-1.52); pollen axis 27 µm (32(34)36 µm); tricolporate; exine 1.3 µm thick; columella regularly distributed, Pollen grain in different foci is angular rhomboidal with broad ends in equatorial view and angular in polar view. Sculpture is microreticulate and homobrochate.

SEM (Figs. D-F); colpus margins irregular with margo; Ora distinct, lalongate, 2.5 µm.wide; sexine with regulate -scabrate sculptures and faintly perforate; Colpi with tapering ends equatorially constricted.

TEM (Figs G-I); Apertures: pore structures fastigium-like cavity formed by ectoapertural margins. Exine: sexine echinate and thicker than nexine near apertures. columella irregularly distributed and exine tectate.

Comment: Is native to northwestern Africa and the Middle East . Sub-tropical N Africa and SW savanna and *S. incanum L.* sense stricto Asia semi-desert (A common plant in SA. and endemic). The pollen grains are distinguished by their comparatively long polar axis (32(34)36 µm) and rounded amb.

2- *Solanum nigrum* L. (Fig. 2, A-I)

Sy. :S. nodiflorum Jacq.

LM. (Figs. A-C); Pollen prolate-spheroidal; P/E: 1.05 (1.00-1.10); pollen axis 27 µm (20(23)32 µm); tricolporate, exine 1.4 µm thick. Pollen grain in different foci is angular with broad ends equatorial view and angular in polar view. Colpi with tapering ends equatorially constricted.

SEM (Figs. D-F); colpus margins irregular with indistinct margo; pore lolongate (4x5 µm); sexine is microreticulate; homobrochate and echinate.

TEM (Figs. G-I); Apertures: Ora lolongate, 4.5 µm wide, Exine: sexine thick as well as nexine and echinate; columella regularly distributed.

Comment: A common endemic plant in SA. The pollen grains are distinguished by their comparatively long polar axis (20(23)32 µm) and rounded wide pore. The distinct protrusion of the colpi margin in polar view fuse to form a bridge-like structure over the ora. Amb very small and mesocolpium very wide.

3- *Solanum villosum* (L.) Mill. (Fig.3, A-H)

LM. (Figs. A-C); Pollen prolate-spheroidal; P/E: 1.07 (1.04-1.10); pollen axis 27 µm (22(24)26µm); tricolporate; exine 1.3um thick; Pollen grain in different foci is circular with tapered ends. Equatorial view is rounded and circular in polar view. Colpi with tapering ends and equatorially constricted.

SEM. (Figs. D-F); colpus margins irregular with granular margo; pore lalongate (4x5 µm); microreticulate; homobrochate and baculate are visible. sexine thicker than nexine and micro-perforate; columella irregularly distributed.

TEM. (Figs. G-H); Apertures: nexine is thicker than sexine near aperture and Ora, 2.7 µm wide. Exine: sexine tectate, irregular columellate and pore distinct , 2.2 µm wide. Exine: 1.7um thick. sexine is thicker than nexine and verrucate sculptures.

Comment: A common in weed plants in SA. and endemic. The pollen grains are distinguished by their comparatively long polar axis (22(24)26 µm) and rounded ends and intine is thicker than exine –margo is granulate and very small apocolpium.

4- *Solanum carense* Dun. inDc. (Fig.4, A-H)

LM. (Figs. A-C); Pollen subprolate; P/E: 1.19 (1.15-1.23); pollen axis 27 µm (23(28)37µm); tricolporate; pore lalongate (4x5 µm); microreticulate; homobrochate. Pollen grain in different foci quadrangular with broad ends and equatorial view is rectangular in polar view. Colpi are with tapering ends.

SEM (Figs. D-F); exine 1.3 µm thick, perforate and columella regularly distributed. colpus margins regular with indistinct margo. microreticulate. Reticulation is heterobrochate.

TEM (Figs. G-H); Apertures: ora indistinct and exine echinates. sexine thicker than nexine.

Comment: A common plant in SA. and endemic. The pollen grains are distinguished by their comparatively long polar axis (23(28)37 µm), perforate tectum, straight colpus and pore indistinct by SEM.

5- *Solanum* sp.aff. *anguivi* Lam. (Fig. 5, A-G)

LM. (Figs. A-C); Pollen prolate-subprolate; P/E: 1.19 (1.04-1.33); pollen axis 27 µm (16(17) 24 µm); tricolporate; colpus margins irregular Pollen grain in different foci is elliptic with broad ends, in equatorial view, rounded and circular in polar view. Colpi with tapering ends equatorially constricted and Ora lolongates, 1.5 µm.

SEM. (Figs. D-E); exine 1.3 µm thick; sexine thicker than nexine and faintly perforate; columella regularly distributed. with indistinct margo; pore lolongate (4x5µm); microreticulate; homobrochate.

TEM. (Figs. F-G); Apertures: pore distinct 1.5 µm wide. Exine: 2µm thick. Sexine thicker than nexine, microreticulate, columella regularly distributed.

Comment: A common plant in SA. but non-endemic (Collenette, 1998). The pollen grains are distinguished by their comparatively short polar axis (16(17)24 µm) and tapering ends the pollen is shed from the anther singly (monads or in multiples

of four (polyads)-Pollinium or massula.

6-*Solanum gracileps* L. (Fig. 6, A-E)

LM. (Figs. A-C); Pollen prolate-spheroidal; P/E: 1.075 (1.04-1.11); pollen axis 27 µm (20(23) 26µm); tricolporate; colpus margins irregular; pore lalongate (4x5 µm); microreticulate; homobrochate nanoverrucae are visible; exine 1.3µm thick; Pollen grain in different foci is elliptic with broad ends equatorial view and semi-angular in polar view. Colpi with tapering ends equatorially constricted.

SEM; (Figs. E-F); sexine thicker than nexine; columella regularly distributed, tectate faintly perforate and pore indistinct. TEM, (Figs. D-E); Exine: 1.4 µm thick. sexine is thicker than nexine and is creinate sculptures. Comment: A common plant in SA. and endemic. The pollen grains are distinguished by their comparatively long polar axis (20(23)26 µm) and rounded amb.

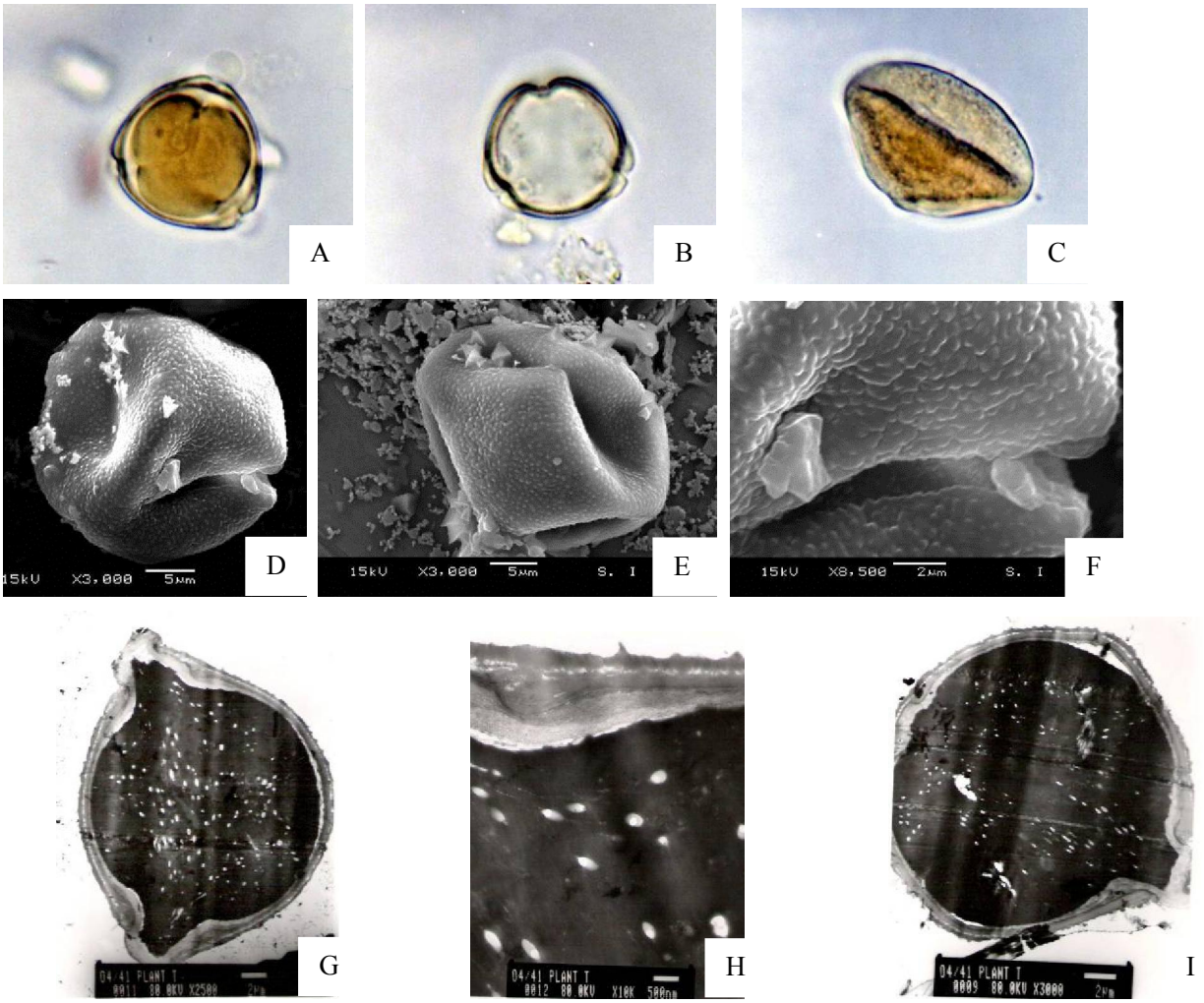

Figure (1): *Solanum incanum;* (L.M. A-Cx1000) A- polar view showing pores structure. B-polar view showing thick exine. C-equatorial view, showing colporate pollen and micro-ornamentation. (SEM, D-F), D- polar view showing tricolporate pollen, x 3000. E-equatorial view showing large mesocolpium of tricolporate pollen, x3000. F-polar view showing lalongate pore and regulate Sexine sculptures, x8500. (TEM, G-I), G- L.S., in pollen grain, showing finely echinate ektexine, pore structures, and fastigium-like cavity formed by ectoapertural margins, x2500. H-L.S., in pollen grains showing echinate Sexine, thick nexine and irregular columella, x10000. I-L.S., in pollen grains showing pore and fastigium-like cavity formed by ectoapertural margins, x3000.

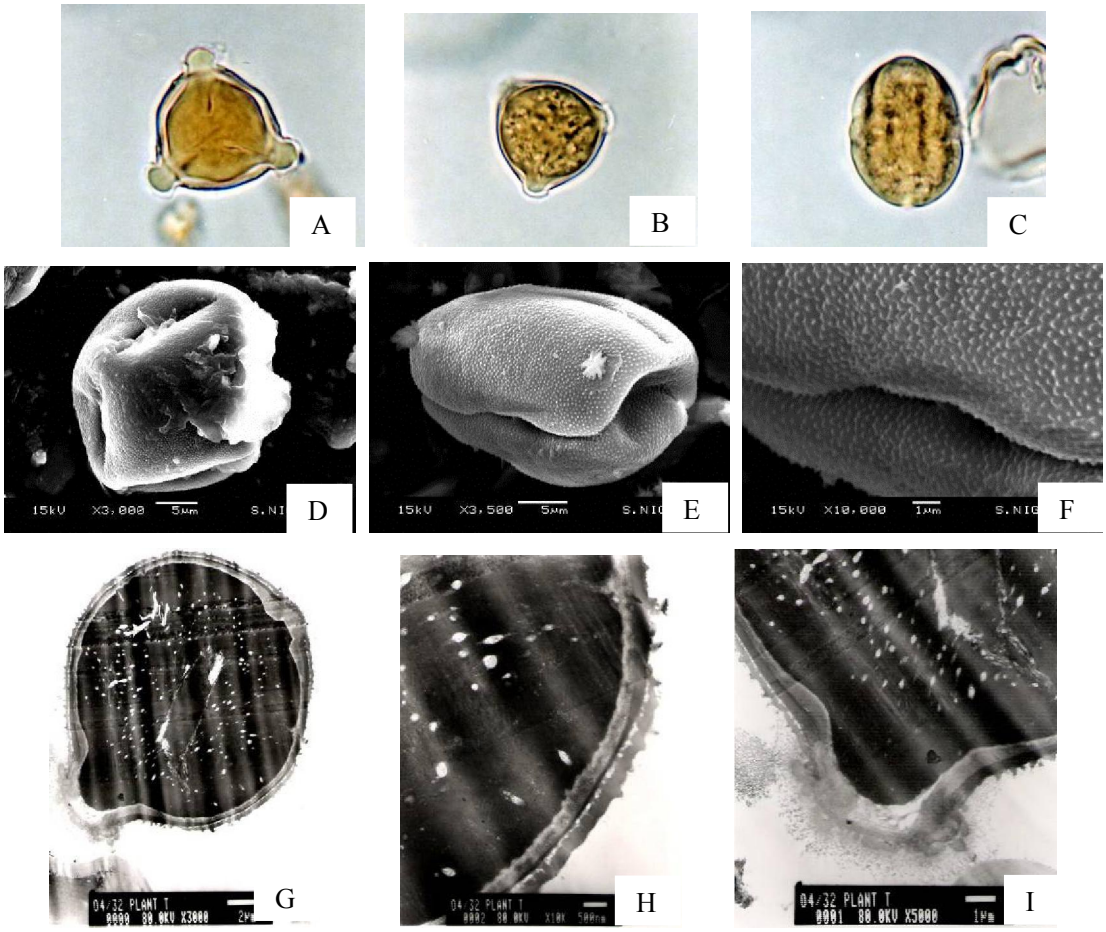

Figure (2): *Solanum nigrum*; (L.M., A-Cx1000), A- polar view showing pores structure, and thick exine. B-polar view showing thick exine and micro-ornamentation. C- equatorial view, showing tricolporate pollen. (SEM, D-F), D- polar view showing colporates pollen, large mesocolpium and small amb, x3000. E-equatorial view showing surfaced furrow and abnormal amb, x3500. F- equatorial view showing colpus margo with the same sculpture of mesocolpium, x10000. (TEM,G-I), G-L.S., in pollen grain, showing pores and exine thickness, x3000. H-L.S., in pollen grains showing spinulose tectum, similar thickness of sexine and nexine with regular columella, x10000. I-L.S., in pollen grains showing circular lalongate pore and fastigium-like cavity formed by ectoapertural margins and very thin sexine near the apertures, x5000.

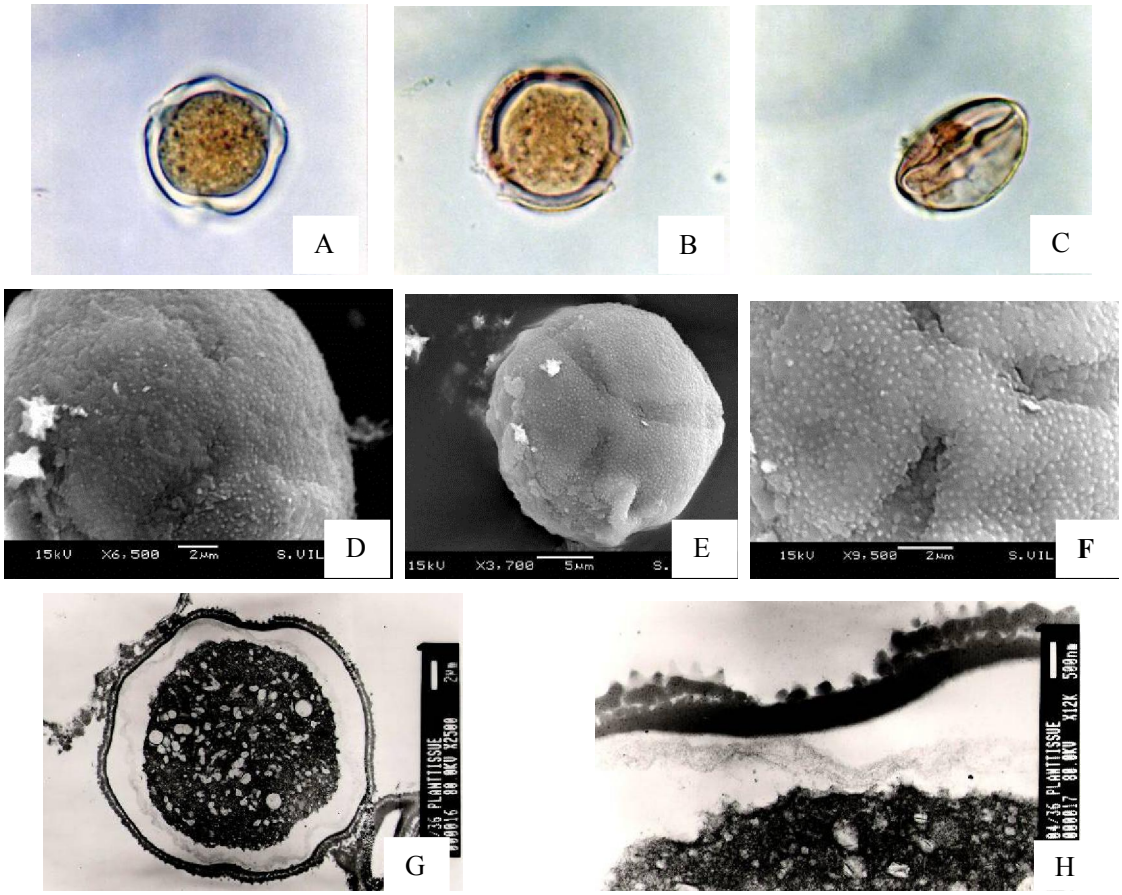

Figure (3): *Solanum villosum*; (L.M. A-Cx1000), A- polar view showing thick exine and pores structure. B-polar view showing micro-ornamentation. C-equatorial view, showing tricolporate pollen. (SEM,D-F), D- polar view, showing surfaced and granulate furrow of colporate pollen,x6500. E-polar view, showing wide mesocolpium, x3700. F-polar view showing very small amb and verrucate margo, x9500. (TEM, G-H), G-L.S., in pollen grain, showing spinulose tectum and thick intine,x2500. H-L.S., in pollen grains showing no tectum and columella at the pore region and verrucate sexine, x12000.

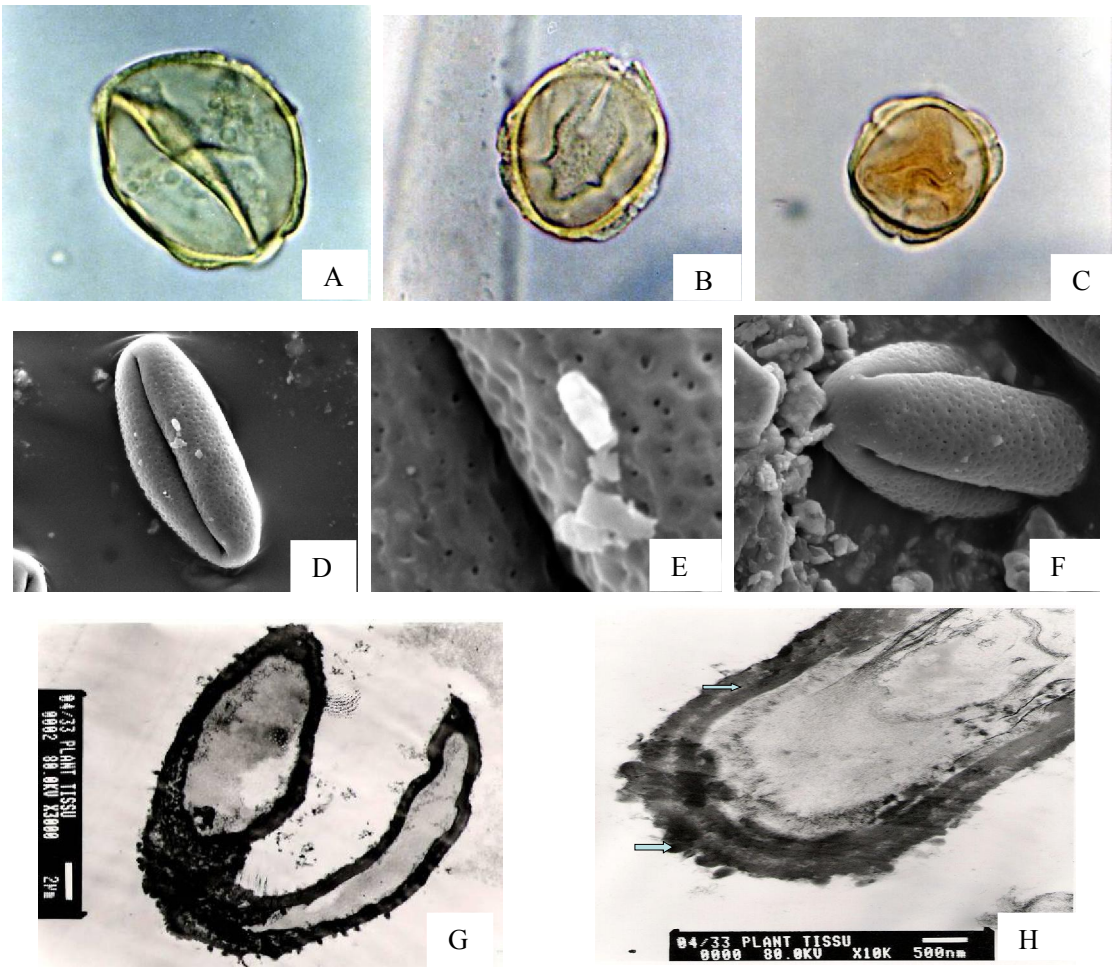

Figure (4): *Solanum carense;* (L.M., A-Cx1000), A-equatorial view, showing large colpus and thick exine of the pollen. B-polar view, showing micro-ornamentation of the exine. C-polar view showing pores structure. (SEM, D-F),D-equatorial view showing straight colpus and mesocolpium, x3300.E-polar view, showing furrow and margo in the same sculpture, x20000. F-equatorial view, showing amb and mesocolpium, x5000. (TEM,G-H),G-L.S., in pollen grain, showing indistinct pore and spinulose tectum, x3000. H-L.S., in pollen grains, showing exine and tectum, x5000.

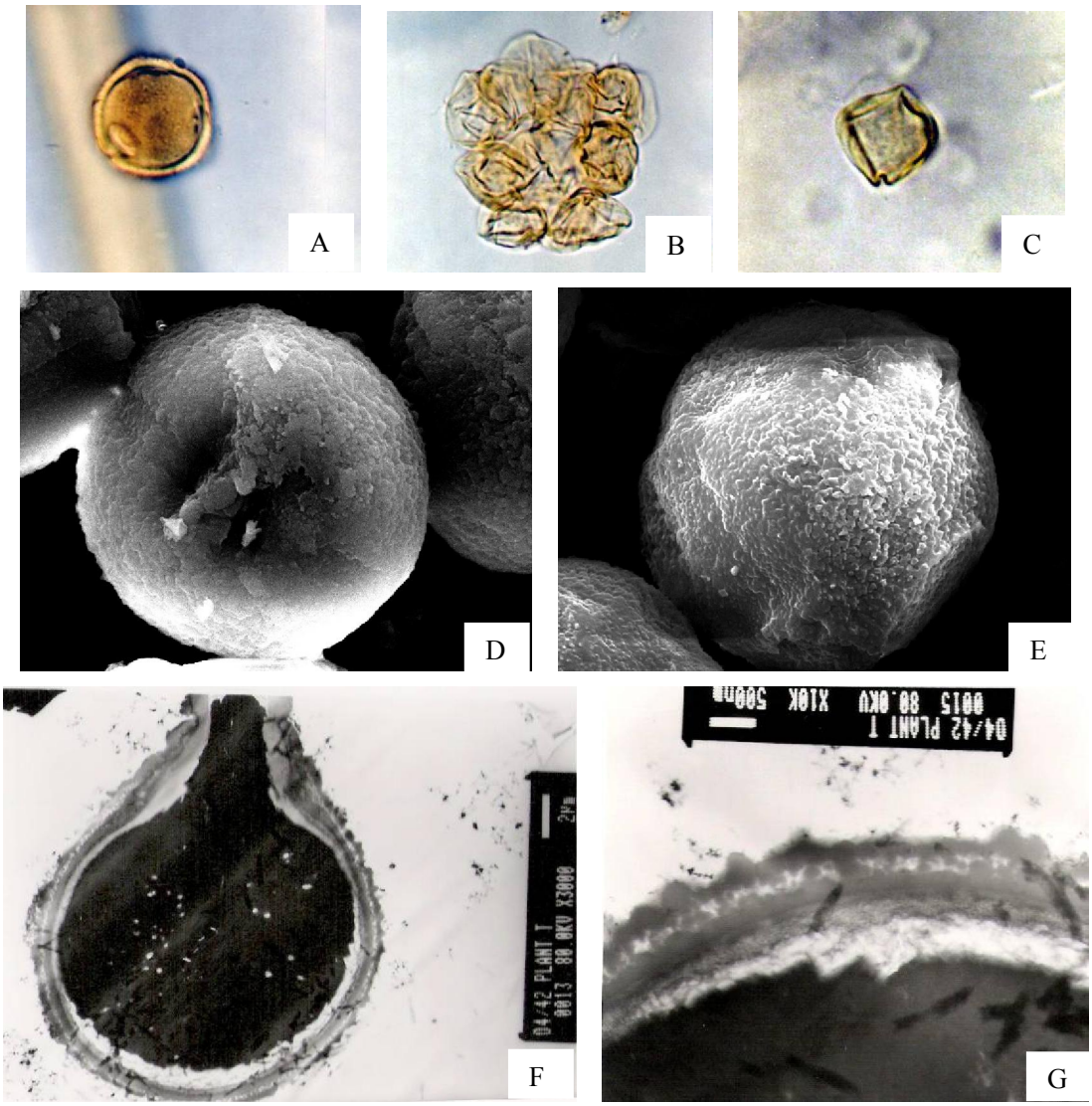

Figure (5): *Solanum* sp.aff. *anguivi*; (L.M., A-Cx1000), A-polar view showing thick exine and micro-ornamentation. B-polyads view, showing tricolporate pollen, x400. C-equatorial view showing of monad, pores structure, x1000. (SEM, D-E), D-equatorial view showing pore bridge and indistinct colpi, x4500. E-polar view, showing surfaced furrow and scabrate sexine, x4300. (TEM, F-G), F-showing aperturate lalongate pore, x3000. G-L.S., in pollen grain, showing crenate sexine and thick nexine, x10000.

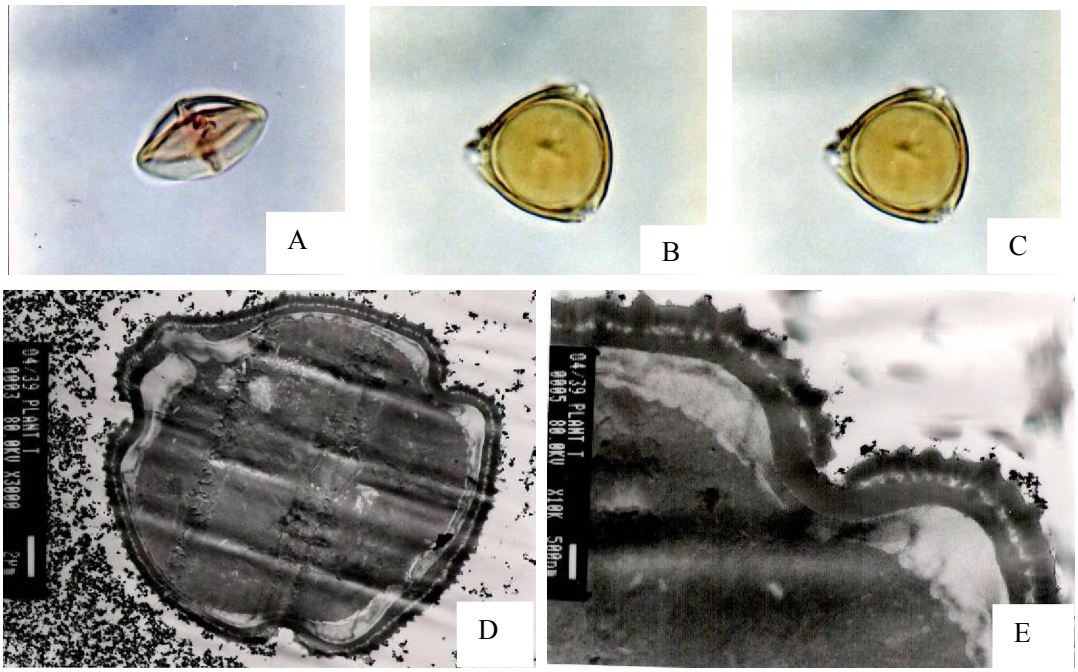

Figure (6): *Solanum gracileps*; (L.M.A-Cx1000), A-equatorial view, showing tricolporate pollen.x1000. B-polar view showing thick exine and psilate-ornamentation. X1000.C- polar view showing pores structure. x1000. (TEM, D-E), D-L.S., in pollen grain, showing crenate tectum, x3000. E-L.S., in pollen grains showing serrate -like, thick ektexine, regular columellae, and the pore intectates, x10000.

4. Discussion and Conclusion

The pollen morphology of the family is quite heterogeneous (Erdtman, 1952). However, tricolporate grains are universally present. Pollen grains are usually radialy symmetrical, isopolar, prolate-spheroidal to sub-prolate or prolate rarely oblate-spheroidal. The work investigates the ultra-structures and comparative structures of the pollen grains in six species of the genus *Solanum*. Palynological data of the species of *Solanum* indicated that all the pollen morphology is isopolar, symmetrical trizoncolporates. While the size measurement of the six species showed an overlapped in most cases. The pollen grains of *Solanum* sp.aff. *anguivi* are the smallest and are classified according to Erdtman, 1952 as (sporae minutae, M1) while spores of the three species *S. carense*, *S. incanum* and *S. nigrum* are similar size and classified as large (sporae Long, M2). However, the two other species *S. gracileps* and *S. villosum* are of similar size classified as medium (sporae mediae, M3). This variation in size may be due to indiscriminate mating leading to hybridization which may be operating in this complex. This is not surprising since previous workers have made similar observations in other groups of angiosperm (Moore & Webb, 1978; Bonnefille & Riollet, 1980; Agwu & Beug, 1982 Agwu & Osibe, 1992; Luna–Cavazos & Gara- Moy, 2002).

The pollen shape expressed as the ratio of the length of polar axis to that of equatorial dimension (Erdtman, 1952), is found to be more or less quinquangular in polar view and elliptic in equatorial view in both species. According to the estimated P/E ratio, pollen grains of *S. incanum* classified as prolate and the other three species of *S. gracileps, S. villosum* and *S. nigrum* as prolate- spheroidal. While the other two species, *S. carense* and *S.* sp.aff. *anguivi* as subprolate (most often prolate-subprolate). The observed differences in pollen morphology between the studied species agree with the observations of Gbile & Sowunmi (1979) that conducted a palynological study in *Solanum* species and found highly significant differences in pollen size and shape within the studied groups (Shrma, 1974; Bonnefille & Riollet; 1980 & El-Ghazali, 1993). However, tricolporate pollen with scabrate tectum is more commonly found within the family. The exine sculpturing provided features for taxonomic distinction. *S. carense* is distinct from the

species by its perforate sexine patterns. Both *S. villosum* and *S. nigrum* are characterized sexine patterns with clearly echinate at *S. nigrum* and verrucate *in S. villosum*. However, the genera and species of this pollen grains type are easily separated on the basis of pollen shape class. Pollen grains of *Solanum nigrum* is recognized by its scabrate sexine. The *S. incanum* pollen had regulated -scabrate sexine and non perforates exine. Although there is much overlap in exine sculptures types, pollen grains size may be significant in delimiting some taxa within the family (Hesse, 1981& Meltsov *et al.,* 2008). The data derived from palynological and characters of the examined taxa could contribute to the taxonomy of Solanaceae and it is found that the Solanaceae is an europalynose family and not stenopalynous as previous authors reported (Erdtman, 1952; Gbile & Sowunmi, 1979; El-Ghazaly, 1991; Moore *et al.*, 1991 & Al-Wadei & Lashin, 2007;). Moreover, *S.* sp.aff. *anguivi* characteristics by poylads pollen dispersal, that character supported by Guinet & Ferguosen (1989) who's suggested that the higher polyads pollen grains number increases the reproductive capacity of the species. The results of the morphology and palynology of the species of *Solanum* studied have proved to be of immense assistance in interpreting problems related to plant taxonomy. The results could therefore be utilized with information from other discipline in clarifying taxonomic relationships of these taxa with other genera and species or subspecies.

Key of the Species:

1-Tricolporates pollen grains, sexine crenate and columella is distinct in SEM and pollen shape is prolate –spheroidal ----------*Solanum gracileps* L.

2-Densly columellate, verrucate sexine and granulate margo……..*S. villosum* (L.) Mill.

3-Columella distinct and wide mesocolpium and ora lolongate .....……..... *S. nigrum* L.

4-Columella distinct, short echinates or scabrate sexine and prolate shape…….. *S. incanum* L.

5-Columella indistinct, perforates tectum and subprolate shape ……*S. carense* Dun. inDc.

6-Columella indistinct, scabrate or regulate sexine and prolate – subprolate ….*S.* sp.aff. *anguivi* Lam.

Acknowledgments

The author thank the stuff members of the Department of Biological Sciences, Faculty of Sciences, King Khalid University, Abha, Saudi Arabia, for their help to collect the herbarium materials and photographs by light microscope, SEM and TEM.

Corresponding author

Gamal M. A. Lashin

Department of Botany, Faculty of Sciences, Zagazig University, Zagazig, Egypt

gamasabaa@yahoo.com

References

Al-Wadei, H.M., 2000. Ultrastructure of the pollen grains of *Withania sommnifera* (L.) Dunal. (Solanaceae *Taeckholmia,* 22(1):115-119.

Al-Wadei, H.M., 2002. Cyto-morphology of three *Solanum* species of Aseer region South West Saudi Arabia. *Online J. Biol. Sci*., 2(2): 106-108.

Al-Wadei, H.M. & G.M.A. Lashin, 2007. Palynological and cytological characters of three species of genus *Solanum* (Family: Solanaceae) from Saudi Arabia. *J. Biol. Sci.,* 7(4): 626-631.

Agwu, C.O. & Beug, H.J., 1982. Palynological studies of marine sediment of the West African. *Coast.Palaeoecol.Africa.16:37-39*

Agwu, C.O. & Osibe, E.E., 1992. Air borne Palynomorphs of Nsukka during the months of February- April (1990). *Nigerian Journal of Botany, 5:117-185*

Bonnefill, P. & Riollet, K., 1980. Pollens des savanes d'afrique arientale. *Cent. Nat. Rech. Sci.,Paris,* 140pp.

Collenette, S., 1985. An illustrated guide to the flora of Saudi Arabia MEPA Flora. Pub. I. Scorptiori. Pupl. Ltd., London.

Collenette, S., 1998. Wild flora in Saudi Arabia. International Asclepiad Society.

Cresti, M., Clampolini, F., Mulcahy, D.L. & Mulcahy, G., 1985. Ultrastructure of *Nicotiana alata* pollen, its germination and early tube formation. *Amer. J. Bot*. 72:719- 727.

D'Arcy, W.G., 1991. The Solanaceae since 1976 with a review of its biography. In: J.G. Hawkes R. N. Lester, M. Nee & N. Estrada (eds) Solanaceae III. *Taxonomy Chemistry and Evolution:75-137 Royal, Bot. Gov. Kew.*

El-Ghazaly, G., 1990. An illustrated key to endoaperture morphology. *Review of Palaeobotany and Palynology,* 63:227-231.

El-Ghazaly, G., 1993. A study on the pollen flora of Sudan. *Review of Palaeobotany and Palynology*,6:99-345.

El-Ghazaly, G., 1999. Pollen flora of Qatar. *Scientific and Applied Research Center, Univ. of Qatar.* pp.429.

Erdtman, G., 1952. Pollen Morphology and Plant Taxonomy, Angiosperms. Chronica Botanica Co., Waltham, Massachusettes, 1952.

Erdtman, G., 1960. The acetolysis method revised description. *Seven. Bot. Taisr*. 54: 651-564.

Faegri, K., Kaland, PE. & Krzywinski, K., 1989.

Textbook of pollen analysis, by K. Faegri and J.Iversen; 4th edition, John wiley and Sons, New York, 328p.

Gbile, Z.O. & Sowunmi M.A., 1979. The pollen morphology of Nigerian *Solanum* species. In: Hawkes JG, Lester RN, Skelding AD, eds. The biology and Taxonomy of the Solanaceae . London: Academic Press,335-342.

Guinet, P. & Ferguson, K., 1989. Structures, evolution and biology of pollen in Leguminosae. *Monogr. Syst. Bot. Missouri. Bot.Garden*, 29:77-103.

Harky, M.; Morton, C. & Bl-ickinore, S., 2000. Pollen and spore morphology and biology. Royal Botanic Garden, Kew, London.

Hesse K., 1981. The fine structure of the exine in relation to the stickiness of angiosperm pollen, *Review of Palaeobotany and Palynology*, 35:81-92.

Hunziker, A.T., 1979. The Solanaceae in the neotropics, a critical appraisal, In: K. Larsen and L. B. Holin- Nielsen (eds) Tropical Botany: 355-364. London.

Judd,W. S.; Campbell, C.S; Kellog, E.A. & Stevens, P.F., 1999. *Plant Systematic*, a phylogenetic approach sinauer Associates Inc. publishers Sander and massachusetts. U.S.A.

Luna –Cavazos, M. & Gara- Moya E., 2002. Morphological and pollen differentiation in *Solanum cardiophyllum ssp. cardiophyllum and S. cardiophyllum ssp. ehernbergii*. *Bot. J. Linn. Soci.,* 140: 415-426.

Mabberley, D. J., 1997. The plant book, Aportable Dictionary of the vascular plants: Cambridge University press. 668-669.

Meltsov V, Poska A. & Saar M., 2008. Pollen size in *Carex*. The effect of different chemical treatments and mounting media. *Grana,* 47: 220–233.

Migahid, A. M., 1978. Flora of Saudi Arabia of the Vascular plants 2nd. Ed.-Cambridge University, press.

Moore, P.D. & Webb, J.A., 1978. An illustrated guide to pollen analysis. Hoaer and Stroueghton, London, Sydney, Aukiad, Toronto.

Moore, P.D., Webb, J.A. & Collinson, M.E., 1991. Pollen analysis 2th ed. –Oxford, London.

Olmstead, R.G., J.A. Sweere, R.E. Spangler, L. Bohs & J. Palmer., 1992. Phylogeny and provisional classification of the Solanaceae based on chloroplast Dna. In: (Eds.): M. Nee, D.E.

Reynolds, E.S., 1963. The use of lead Citrate at high pH as an electron- opaque scaning electrone microscopy. *J. of Cell Biology*,17 : 208-212.

Sharma, B.D., 1974. Contribution of the palyotaxonomy of the genus *solanum* L. *J.Palynol.*,10(1):51-68.

Spurr, A.R., 1969. A Low viscosity epoxy resin embedding medium for electronmicroscopy. *J. of Ultrastructure Research*, 26: 31-43.

Wettstein, R. Van., 1895. Solanaceae. In: A Engler and K. Prantel (eds.), Die *Naturlichen flanzenamilien*.

Zavada, M.S., 1990. A Contribution to the study of pollen wall Ultrastructure of pollinia, Annules, *Mo. Botanical Garden, st. Louis*, 77:785-801.

11/20/2011

Prevalence of cancers in the National Oil Company employees referred to Ahwaz health and industrial medicine in 5 years (Ministry of oil)

Kalantari Farhad[1], Sarami Abdollah[2], Shahba Nariman[3], Marashi seyed Kamal [4]Reza Shafiezadeh[5]

1- Anesthesiologist 2- Infectious & MPH specialist 3- Dermatologist4-pharmacist 5- occupational medicine Department of health and great oil hospital

Abstract: 13% of cancer deaths are, According to Association of America 7. 6 Million People died of cancer in 2007. Cancer is not only a special man and all animals and plants, a cell may also be suffering from cancer. In 2000, six million to ten million new cases of cancer and cancer-related deaths in the world was registered. In America every year for the first time in nearly a half million people are realizing that somehow have been affected by cancer. According cancer kills 556,000 people in 2003 was 1,500 times the daily death and only death from cardiovascular disease with its prevalence is over. In the study (14,957 people) between 2007 to 2011 employees working in the oil industry in Ahwaz on cancer registration in great oil hospital and public health medicine and the oil industry before 5 years were 121 cancer cases were reported from .The commonest cancers are adenocarcinomas, 36 body parts (29.7%),basal cell skin cancer, 26 patients (21.4%), bladder transitional cell carcinoma 12 (9.9%) and squamous cell carcinoma of the number 7 (5.7%) and 2 cases of renal cell carcinoma were reported. 121 cases of cancer reported in eight cases (6.6%) women and 113 (93.3%) were male.

[Kalantari Farhad, Sarami Abdollah, Shahba Nariman, Marashi seyed Kamal, Reza Shafiezadeh. **Prevalence of cancers in the National Oil Company employees referred to Ahwaz health and industrial medicine in 5 years (Ministry of oil)**. Life Science Journal. 2011;8(4):698-700] (ISSN:1097-8135). http://www.lifesciencesite.com.

Key words: cancers, Prevalence, industrial medicine

1. Introduction

Abnormal growth of malignant cancer cells, it also called to say that the proliferation of abnormal cells or cancer occurs when cells die, they lost. All body tissues such as cancers of the lung-colon - breast - skin - are the source of the bone and nerve tissue. Among the causes of cancer can be contacted with benzene, viruses, radiation, sunlight, and tobacco and food toxins aflatoxin and named. Human of cancer at different ages, but there is a high risk of cancer increases with age. 13% of cancer deaths are.

In 2007 died 7. 6 Million People of cancer (According to America health Forum). Cancer is not only a special man and all animals and plants, a cell may also be suffering from cancer. In 2000, six million to ten million new cases of cancer and cancer-related deaths in the world was registered. In America every year for the first time in nearly a half million people are realizing that somehow have been affected by cancer. According cancer kills 556,000 people in 2003 was 1,500 times the daily death and only death from cardiovascular disease with its prevalence is more than. The most common tumors in men with prostate cancer, lung and colon and in women are breast, lung and large intestine.

Cancers of the lung, breast, prostate and colorectal cancers diagnosed as the cause of more than 50 percent of cancer deaths in America are included. Over the past 50 years, the overall death rate from cancer is significantly associated with age in men increased while the proportion of women has decreased slightly. Most of this increase due to lung cancer in men than in women, but this improvement can be clearly reduced mortality from cancers of the uterus, stomach, liver and cervical cancer in women above all linked.

Significant differences were in incidence and mortality from cancer in the world there. For example, the death rate from gastric cancer in Japan 7 to 8 against America.

1.1. Types of cancers

Lung cancer is the most common cause of death from cancer in the world of the most common cancers, including prostate cancer in men - lung and colon adenocarcinoma in different parts of the digestive tract, most notably made up 12 of them were related to colon (33.3%) and Gastric 9 cases (25%) and prostate (6) (6 / 16%) is included. Only one case of lung cancer was included.In women most common cancers, breast cancer - colon and lung is. In this study, 5 cases of breast cancer were reported by colleagues working in the hospital and its 4 Invasive ductal carcinoma is the most common pathology.

A case of uterine cancer (leiomyosarcoma) and 2 cases of BCC skin were reported. Lowest among patients with Hodgkin lymphoma aged 34 years and maximum age was 87 years old colon adenocarcinoma. and both of which were reported in men

The aim of the study

Identify the most common types of cancer and risk factors in decisions to reduce the cause are.

2. Result

The study found that gastrointestinal cancers as colon and gasteric adenocarcinoma accounted for most of that is very similar to Japan and may be involved in that type of diet is more knew that I needed studies. These cancers are reported rarely in the United States.

Papillary carcinoma of thyroid and other cancers have been reported in 4 cases (3.3%) - 12 cases of bladder transitional cell carcinoma (9.9%) - mesothelioma 3 (2.4%) - 7 cases of squamous cell carcinoma (5.7%)

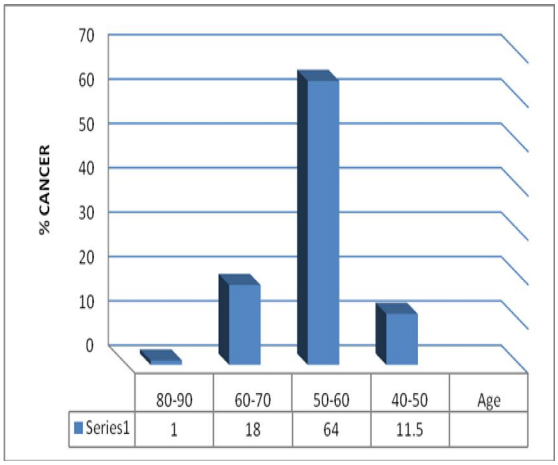

Fig1. The most common age at which the cancers reported.

Unfortunately, cancer patients who have advanced stage and this led to poor results achieved in spite of drug therapy is expensive and advanced nursing care. Therefore recommended screening tests according to international standards Cancer Society is a necessary and inevitable.

3. Discussion

Increasing age increases the likelihood of developing certain cancers. Most cancers occur in aged about 55 years or more. The main cause of cancer death among women 40 and men 60 to 79 years To 76years. Cancer in children less than 15 years will also suffer. More than 10 percent of cancer deaths in this age group are in America.

The issue is power, and now many patients who have used this method and compliance with health issues and healthy eating have been able to recover, but also because of avoiding bad and wrong ways to live with this disease, the procedures again return to health have regained their.

Results show that 59.1% of patients with esophageal cancer in Iran were male and mean age of patients was 62.2 years. In both sexes the prevalence of esophageal cancer in the age group 69-60 years was higher than other age groups. 1 and 5-year survival rate in patients were have seen with esophageal cancer by 42 percent and 8 percent respectively. The survival rates according to age and sex, there was a statistically significant difference (P = 0.01, p = 0.02). So that female patients, with less than 50 years of age had significantly better survival. 1 to 5-year survival rates according to histological type, anatomic location, and treatment did not show significant differences.

The most common site of breast cancer in women is related to the first cause of cancer deaths in America is the same cancer. This type of death from cancer, aged 40 to 44 years is more than deaths from other causes. In the United States every nine women will develop breast cancer in her lifetime and one in 31 women die of the disease, i.e., the women in America each year, more than 44 thousand people die of this cancer. Due to the high death rates in the diagnosis and treatment of this disease is more precise. Rapid and early detection of breast cancer death rate is dramatically reduced. However, a death rate from cancer of the body part that is easily accessible for examination and diagnosis is a pathetic and sad and irreparable damage to the corpus of the family and society. If you aspects of the breast cancer the family aside, the rest of this disease rarely occurs before age 25, but with increasing age, the incidence of cancer is also increased.

The influence of environmental factors on breast cancer studies has been the geographic differences in the genetic groups identified in this cancer has been effective, the risk of the disease in immigrants to America's increased attention to the historically occurrence of breast cancer in the United States and other countries of the West 7 4. Radiation is another environmental factor that is mainly used for the upper parts of the waste treatment and complications of cancer patients from radiation are radioactive materials.

Considering that breast cancer has a variety of different races tends to be different and specific stages of the disease have. Although the overall incidence of breast cancer in black than white race, but usually referring to black women in more advanced stages and higher mortality rates than whites are. Part of this difference relates to the exclusion of blacks and their lack of access to health care and lack of diagnostic facilities such as a mammogram is important, but genetic factors also can be effective, however, there is clearly a genetic predisposition.

4. Conclusion

The results of this study indicate that esophageal cancer is not a good prognosis and a 5-year survival rate of esophageal cancer in this study with studies in North America and European countries have agreed, but the studies made in China and Japan is weaker than the survival rates (Hajian and Sadeghi, 2000).

The relative frequency of colon and rectum Cancers were 62% and 38%, respectively. Ninety percent of Cancers were adenocarcinoma while 7% were lymphoma and 3% were carcinoid tumor. Sixty one percent of patients were male and 39% were female. The prevalence of colorectal Cancer in general population was 7 / 100000 during 1995-1999. The most common age of colorectal Cancer was above 60 years old. The mean age of the patients was 50 years old. The range of patient `s age was between 4 to 93 years. Most patients were diagnosed in 1999 (30 cases). Colorectal Cancer had relatively high incidence rate in Kurdistan province in our study. We recommend detecting risk factors for colorectal Canecrs here Further Evaluation (Dr Najmedin Molanaie, Dr Ezatollah Rahimi and Dr Soada Aiobi).

Reference

1. Vinay Kumar, Abul K. Abbas, Nelson Fausto, Nelson Fausto. Robbins & Cotran Pathologic Basis of Disease. the seventh chapter, 7th edit ISBN-the thirteenth: the 9,780,721,673,356 th
2. Kinzler KW, Vogelstein B (2002) Genetic Basis of Human Cancer.McGraw-Hill.
3. Kurzrock R, Talpaz M (1999) Molecular Biology in Cancer Medicine.Pearson education, Harlow
4. Lakshmi MS, Sherbet GV (1997) Genetics of Cancer: Genes Associated With Cancer Invasion, Metastasis and Cell Proliferation. Academic Press, London.
5. McDonald F, Ford CHG (1997) Molecular Biology of Cancer.Springer-Verlag New York, Incorporated
6. Epidemialogy of Colorectal Cancer in Kurdistan province during 1995-1999
7. Journal of Babol University of Medical Sciences, Winter 2000, 3 (1 (9)) :21-28.
8. Schwartz seysmour L, and et al. Principles of surgery. McGRAW - Hill, INC. 6th Edition, 1994: 1259-1300.
9. Sabiston David C. Text book of surgery. W.B.Saunders compony.14 th ed. 1993: 944-957.
10. Nelson RL, Persky V, Turyk M.Tuneatrebds in distal colorectal cancer subsite location relered toage and how it appears choice of screening madolity. J Surgery oncl. 1998 Dec, 69(4): 235-8
11. Small w, Ray WA, Dougherty j, et al. Use of NSAID and incidence of colorectal cancer. Arch Intern Med. 1999 jan 25, 159(2): 161-6
12. Nelson RL, Dikkear T, Freds S. et al. The relation of age, race and gender to the subsite location of colorectal carcinoma. Cancer. 1997 jul 15, 80(2): 193-7
13. Soliman As, Bondy ML, Levin B, etal. Colorctal cancer in Egyption patients under 40 years of age. Int J cancer. 1997 Mar 28, 71(1): 26-30
14. Bell Jc, Mc cried M, Coats Ms, et al. Trends in colorectal cancer incidence and mortality in new sough woles. Med J Aust. 1997 Feb 17, 166 (4): 178-8

11/20/2011

Evaluations of needle stick people working in great oil hospital of Ahvaz for 4 years (2008-2011)

Kalantari Farhad[1], Salamanzadeh.Shokrollah [2], Sarami Abdollah[3], Salehi Seyedparviz[4], Mooresh. Fariba[5]

Anesthesiologist 2- Infectious specialist 3- Infectious disease MPH specialist 4- General physician 5- Infection control Nurse, Department of health and great oil hospital

Abstract: Needle stick injury, a wound that pierced the skin with a needle tip is caused by common tools. It may also be caused by sharp tools. The common people who have had contact with the needle in the treatment works is like a wound that the medical community. This happened because the risk of disease transmission are concerned lies in the blood such as hepatitis B virus (HBV), hepatitis C virus (HIC), the AIDS virus (HIV). Despite the importance of the event, but the needle stick injuries have been neglected, and often not reported.In a study on 650 nurses and midwifery personnel services were 50 cases (7%) were reported needle stick. Mostly in the age group 29-47 years. 17 cases (34%) men and 33 cases (66%) were women between people. The most common causes of needle stick in people under the cover of this pricing needle in 37 cases (74%) and non use of personal protective equipment and spill into the conjunctively secretions of infected people, medical personnel in 5 cases (10%) cases and in 8 cases (16 %) was caused by rupture with a scalpel.

[**Kalantari Farhad, Salamanzadeh.Shokrollah, Sarami Abdollah, Salehi Seyedparviz, Mooresh. Fariba. Evaluations of needle stick people working in great oil hospital of Ahvaz for 4 years (2008-2011)**. Life Science Journal. 2011; 8(4):701-703] (ISSN: 1097-8135). http://www.lifesciencesite.com.

Key words: Recap, Needle stick, great oil hospital

1. Introduction

Medical personnel have the potential risks of needle stick contaminated medical personnel is. More than 20 diseases through contaminated needles and other sharp instruments contaminated with blood contaminated surgical blade can cause the disease to medical personnel. Transmission is a concern of people employed in these professions. The main diseases transmitted through tears and with a blade or a needle dipped in the blood of people infected with hepatitis B and C and AIDS are.

Transmission of blood-borne viruses such as HIV and hepatitis are individuals exposed to the immune system.

Transmission through hollow needles, using IVlines - phlebotomy needles - Butterfly needles carries the highest risk.

High percentage of needle stick Failure to follow standard precautions needle occurs. In this study, most cases of needle stick through the lid re-investment and non useof personnal protection and spill discharge medical personnel in the conjunctiva of the eye.

The aim of the study

A. *Being employed to identify the causes of needle stick.*
B. *Decisions necessary to prevent its occurrence. (These incidents are preventable.)*

2. Results

Unfortunately, all therapeutic categories, including doctors, nurses and operating room personnel and ... Re-pricing of caps and splashing into the conjunctively secretions were exposed. The non use of personal protective equipment such as (Shield) is also one of the other important causes.

http://www.dentalorg.com/needle-stick-injuries.html

95% of personnel trained and familiar with personal protective equipment are available to them.

The interview was needle stick (fatigue, crowding emergency, and in many cases where the rash exposed to the agent should have.)

All groups that have been in contact with the infection: full vaccination coverage was..Incomplete vaccination one of the laboratory personnel and the level of antibodies was over 20.

Operating room personnel and physicians with a suture needle or have emergency contact with needle, catheters and re-cap investments; particularly in emergency patients during CPR has been a call agent.

http://www.dentalorg.com/needle-stick-injuries.html

To prevent the risk of potential infection control committee with the chairman of the hospital were the following:

- *Instructions for safe injections, according to national guidelines*
- *Poster and administrative measures to deal with cases of infected*
- *Profile of patients documented to record all needle stick.*

Needle stick injury, a wound that pierced the skin with a needle tip is caused by common tools. It may also be caused by sharp tools. The common people who have had contact with the needle in the treatment works is like a wound that the medical community. This happened because the risk of disease transmission are concerned lies in the blood such as hepatitis B virus (HBV), hepatitis C virus (HIC), the AIDS virus (HIV). Despite the importance of the event, but the needle stick injuries have been neglected, and often not reported.

A. Event

In the treatment of wounds events needle stick. This makes the transmission of viruses from one carrier to the recipient. This usually happens when they finally put in a container lid for needles and sharp objects occur. During surgery, the surgical needle may inadvertently penetrate the gloves and a surgical team in the skin. The influence of surgical and utility knives or other sharp instruments in the surgeon's skin, except for needle stick injuries are classified.

Surgical knife wound care requires more than a needle stick. The medical community is not limited just to needle stick injuries and possible exposure to risk in any environment tools, exist.

This happened in 1999 in the United States is estimated at 800 thousand cases. In another study, about 3.5 million cases worldwide statistics are mentioned. The caring staff of nurses and doctors in their training period includes most of all. Within the field about the main difference is the risk of needle stick injury rate: the surgical, anesthesia, ear, nose and throat, internal medicine and dermatology, radiology and pediatrics and a relatively high and are relatively low.

http://www.dentalorg.com/needle-stick-injuries.html

Wounds from needle stick not only May the primary tools sharp spread, but they may after a period with needles that carried the dried blood has also spread to occur. The power of HIV and HCV in hours reduced, but HBV is resistant to drying and for more than a week can cause infection.

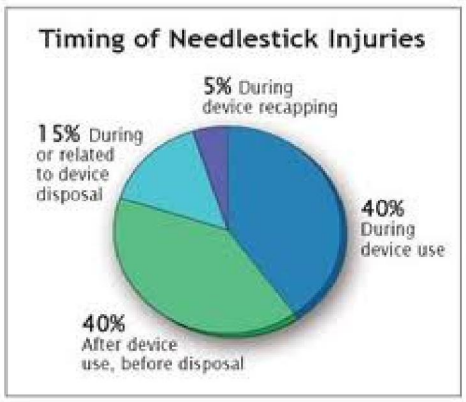

When wounds needle stick handling of the potential for such as bacteria, single cells, viruses (HIV, HBV, HCV) be important that once a year is estimated at 66,000 infected with HBV and 16,000 cases with HCV, 1000 and by of HIV. In addition to needle stick injuries may be a major stress or anxiety can lead to personal injury. Care and treatment of needle stick injuries are expensive and nearly $ 2,500 in a short time in the United States has been estimated.

In most cases of needle stick injury occurs when a person is not carrying any virus, so no risk of any infection. Despite the stress and anxiety caused the symptoms to prevent the separation takes place.

http://www.dentalorg.com/needle-stick-injuries.html

B. Prevention & Management

In the latter involves the use of tools to get the needle (instead of fingers), the performance of surgical utility knives, sharp tools to prevent hands to carry. Engineering advances - including the development of safe and away about safe needle shedding. There is a

surgical suture to the thick edge of needles; needle stick may be used to reduce ulcers.

After the needle stick must injury the important procedures that must be done to reduce the risk of recipient infection. Is that the damage should be washed with soap and water. The operation of the affected area to push more blood to leak out is wrong and by the Centers for Disease Control (CDC) has been commissioned. Laboratory tests for a basic account of the damage can be attributed to HIV and hepatitis, acute HAV IgM, HBsAg, and HB core IgM, HCV, and for safety, surface antibodies. Unless the situation should be known before the tests HBsAG, anti-HCV antibodies should be carried HIV.

http://www.speedsmedical.co.uk/product/81197f5f-7042-47d5-9e22-456951cdf368.aspx

Reference

1- Advisory Committee on Genetic Modification: Compendium of guidance Report HSE Books 2000 ISBN 0 7176 1763 7, available online at:www.hse.gov.uk/biosafety/gmo/acgm/acgmcomp/index.htm

2- Accommodation for Pathology Services NHS Estates Health building note 15The Stationery Office 1991 ISBN 0 11 321401 4 (under revision).

3- Guidance for Clinical Health Care Workers: Protection Against Infection with Blood-borne Viruses Department of Health 1998 available online at: www.advisorybodies.doh.gov.uk

4- Hospital Infection Control Department of Health 1995 HSG(95)10 available online at: www.dh.gov.uk

5- The prevention and control of tuberculosis in the United Kingdom: UK Guidance on the Prevention and Control of Transmission of HIV-related Tuberculosis and Drug-resistant, Including Multiple Drug-resistant, Tuberculosis Department of Health 1998 available online at: www.dh.gov.uk

6- Infection control in the built environment NHS Estates The Stationery Office 2002 ISBN 0 11 322086 3

7- Infection at work: controlling the risks Advisory Committee on Dangerous Pathogens 2003 available online at: www.hse.gov.uk/pubns/infection.pdf

8- 'Directive 2000/54/EC on the protection of workers form risks related to exposure to biological agents at work' Official Journal of the European Communities 2000 45 L262 21-45 ISSN 0378 6978

9- The Approved List of biological agents HSE/HSC 2004 available onlineat:www.hse.gov.uk/pubns/misc208.pdf

10- Anti-terrorism, Crime and Security Act 2001 Ch24 The Stationery Office 2002 ISBN 0 10 542401 3

11- A guide to the Genetically Modified Organisms (Contained Use) Regulations2000 L29 (Third edition) HSE Books 2000 ISBN 0 7176 1758 0

12- A guide to the Reporting of Injuries, Diseases and Dangerous Occurrences Regulations 1995 L73 (Second edition) HSE Books 1999 ISBN 0 7176 2431 5

13- Advisory Committee on Dangerous Pathogens Protection against blood-borneinfections in the workplace: HIV and hepatitis The Stationery Office 1995 ISBN 978 0 11 321953 7

14- Consulting employees on health and safety: A guide to the law Leaflet INDG232 HSE Books 1996 (single copy free or priced packs of 15 ISBN 978 0 7176 1615 2(Web version: www.hse.gov.uk/pubns/indg232.pdf

15- Five steps to risk assessment Leaflet INDG163(rev2) HSE Books 2006 single copy free or priced packs of 10 ISBN 978 0 7176 6189 3) Web version:www.hse.gov.uk/pubns/indg163.pdf

16- Control of substances hazardous to health (Firfth edition). The Control ofSubstances Hazardous to Health Regulations 2002 (as amended). Approved Codeof Practice and guidance L5 (Fifth edition) HSE Books 2005 ISBN 978 0 7176 2981 7

17- Management of health and safety at work. Management of Health and Safety at Work Regulations 1999. Approved Code of Practice and guidance L21 (Second edition) HSE Books 2000 ISBN 978 0 7176 2488 1

18- Health and Safety at Work etc Act 1974 (c.37) The Stationery Office 1974 ISBN 978 0 10 543774 1

19- The Reporting of Injuries, Diseases and Dangerous Occurrences Regulations 1995:Guidance for employers in the healthcare sector Health Services Information SheetHSIS1 HSE Books 1998 www.hse.gov.uk/healthservices/information.htm

20- UK Health Departments Guidance for clinical health care workers: Protectionagainst infection with blood-borne viruses Department of Health 1998Department of Health Immunisation against infectious disease 2006 The Stationery Office 2006 ISBN 978 0 11 322528 6

21- EXTERA LINKS :
http://www.speedsmedical.co.uk/product/81197f5f-7042-47d5-9e22-456951cdf368.aspx
http://www.dentalorg.com/needle-stick-injuries.html

11/20/2011

The Relationship of the Self-Focused Attention, Body Image Concern and Generalized Self-Efficacy with Social Anxiety in Students

Saeed Bakhtiarpoor[1], Alireza Heidarie[1], Shahla Alipoor Khodadadi[2]

1- Assistant professor of of department of human sciences in Ahvaz Branch, Islamic Azad University, IRAN
2- M. A. graduated in psychology of department of human sciences in Ahvaz Branch, Islamic Azad University, IRAN.
(Extracted from M. A. Dissertation in Psychology)
Corresponding Author: S.Alipoor@yahoo.com

Abstract: The aim of this study was to examine The Relationship of the Self-Focused Attention, Body Image Concern and Generalized Self-Efficacy with Social Anxiety in Students of Islamic Azad University of Ahvaz Branch. The research sample was 151 students (61 males, 90 females) which randomly selected for present study. The research sampling was cluster type. To collect data some scales like, social anxiety (FNE. SAD), Focus of attention (FAQ), Body Image concern (Littleton, Axsom & Pury) and generalized self-efficacy (GSE-10) were used. The research design was correlation type. The results by using Pearson correlation and multiple regressions showed that self-focused attention and body image concern had a positive correlation with social anxiety and generalized self-efficacy had a negative correlation with social anxiety. Also a multiple correlation between self-focused attention, body image concern and generalized self-efficacy with social anxiety was showed.

[Saeed Bakhtiarpoor, Alireza Heidarie, Shahla Alipoor Khodadadi. **The Relationship of the Self-Focused Attention, Body Image Concern and Generalized Self-Efficacy with Social Anxiety in Students**. Life Science Journal. 2011;8(4):704-713] (ISSN:1097-8135). http://www.lifesciencesite.com.

Keywords: *Self-Focused Attention, Body Image Concern, Generalized Self-Efficacy, Social Anxiety*

1. Introduction

Social anxiety, known as a disturbing experience at others presence, is one of the factors disordering the individuals` growth and social perfection trends and preventing their talents and proves of existence. This phenomenon, which is relatively prevalent in youth, can have intercepting effects on the adolescence efficacy and dynamism and destruct their personal and social performance in various fields (Mehrabi zadeh, Najarian, and Baharloee, 1999). Kessler, McGonagle, Zhao, Nelson, Hughes, Eshleman & Wittchen (1994) found that the female adolescences with social anxiety are not probably able to finish the high school and both sexes are not able to enter the university and graduate (Mancini, 2001). In addition, this disorder is one of the most current problems of the female university students specially the female ones (17-19 percent of outbreak), and the recovery is not possible but with remedy (Muris & Oosten, 2002).

In the recent decades, several theoretical models have been provided to explain the infrastructural basis of the social anxiety from which mostly emphasized on the cognitive processes (e. g. Beck, Emery & Greenberg, 1985, Foa & kozak, 1986, and Clark & Wells, 1995). Evaluations based on Clark & Wells (1995) theory were concentrated on effect of self–focused attention on social anxiety showing that in the socially anxious individuals facing frightening situations, the self–attention and access to negative thoughts and feelings are increased or interfered with their performance.

Findings showed that the fear of body malformation is related to the dissatisfaction of physical appearance or psychiatric disorders (social panic, anxiety, depression, and etc). Men and women with a fear of physical appearance often suffer from negative mood (anxiety and depression) and do not like to have social relationships with others (Bosak nejad and Ghafari, 2007). since individuals` perception of their body affects their personality and behavior, negative image of body causes psychological complications which inevitably affect the individual`s interpersonal mentality, states, and relationships. One of these disorders is anxiety (Biby, 1998).

Researchers believe that self-efficacy plays an important role in social phobia. Hurrelmann & Losel (1990) showed that the social phobia is affected by negative psychological tendencies especially low self-efficacy and self-esteem.

Many scientific studies concerning the this study`s variables were carried out:

Khayer, Ostovar, Taghavi, and Samani (2008) evaluated the psychic effect of the self focused attention on the relation between social anxiety and judgmental biases. Results showed that there is a

significant correlation between social anxiety and self-focused attention.

Voncken, Dijk, Jong, and Roelofs (2010) evaluated the performance of socially anxious individuals. Results showed that social anxiety has a relationship with the high levels of self-focused attention and negative thoughts.

Higa & Daleiden (2008) evaluated the anxiety and cognitive biases. Results showed that social anxiety is able to forecast the self-focused attention and biases to the threat.

Zue, Hudson, and Rapee (2007), Beidel, Turner, and Morris (1999), and Woody (1996) resulted that socially anxious individuals facing frightening situations, the self–attention and access to negative thoughts and feelings are increased or interfered with their performance.

Mansell (2007) evaluated the social anxiety, self-focused attention, and the effect of nonverbal behaviors of the negative, neutral, and positive auditors. Results showed that socially anxious individuals think that their weakness of social environment processing causes the negative evaluation of others, but they are not able to analyze their judgments. In addition, self–focused attention is increase in the socially anxious individuals.

Etu & Gray (2009) evaluated the relationship between rumination, body image concern, and anxiety. Results showed that the style of rumination especially in the field of body image can forecast the anxiety and body image concern. This study was based on Clark and Wilson`s (2005) showing that rumination can provisionally cause and extend the body image anxiety.

Harth and Hermes (2007) evaluated the body disorders of shape and cosmetic surgery. Results showed that the problems accompanied by body deformity disorder are anxiety, depression, social phobia, and even psychotic disorders.

Taherifar, Fati, and Gharaee (2010) evaluated the model of university students `social panic forecast based on the behavioral cognitive components. Results showed that variable of social self-efficacy can forecast the social panic.

Masoudnia (2008) evaluated the social phobia and generalized self-efficacy. Findings showed the validity and ability of Bandura social–cognitive model as a theoretical model for explaining and predictive the social phobia. Self-efficacy structure, as the main structure in the Bandura social - cognitive theory, could completely explain the changes of the university students` social phobia.

Khayer et al (2008) resulted that there is significant correlation between the social anxiety and social self-efficacy.

Gholami, Kajbaf, Nehat doost, and moradi (2007) studied the effect of self-efficacy`s group education on the rate of self-efficacy in the social situations of the female university students `social panic. Results showed that the self-efficacy belief in the social situations increases the courage and reduce the rate of sadness during the social activities and, consequently, reduces their sensitivity toward the focus of others on their performance. Supportive atmosphere of the group educational courses, in which individuals with similar problems are participated, and techniques such as guest speech pattern and *theological convincing* help the respondents to correct their wrong thoughts about the focus of others` rate on their performance and their kind of evaluation in addition to reduce their sensitivity concerning this kind of being under observation, so their social panic would be reduced.

Rodebaugh (2006) evaluated the self-efficacy and social behavior. Results of his study showed that there is an inverse and significant relationship between self-efficacy and avoidance behaviors in the socially anxious individuals. Respondents with low self-efficacy have more avoidance of group talk than the other respondents.

Thus, according to the issues discussed above, this study was aimed to evaluate the events and factors causing the social anxiety so that the relationship between variable such as self-focused attention, body image concern, and generalized self-efficacy with social anxiety are cleared , this question is aimed to be answered that is there any significant relationship between social anxiety of the students of Azad university–Ahwaz branch and the self-focused attention, body image concern, and generalized self-efficacy.

2. Material and Method

2.1. Statistical population and sampling method

Statistical population of this study is the whole students educating in the Azad University –Ahwaz branch in 2010-11. Cluster multistage sampling method was used for sampling. Three faculties were selected from the faculties, one field of study was selected from the selected faculties, of which five classes were selected, and 12 students were finally selected from each class. 155 questionnaires were filled at last. After scouring the questionnaire, data was analyzed by SPSS. Volume sample, because the test ability was more than 80 percent, was enough.

2.2. Measurement tools

Following tools were used to measure the variables:

- ***A.*** *Social anxiety FNE –SAD (Fear of negative evaluation and social avoidance and distress) questionnaire*
- ***B.*** *FAQ (focus of attention questionnaire*
- ***C.*** *Body image concern questionnaire (Littleton, Axsom, and Pury, 2005)*

D. *10-GSE (Generalized self-efficacy) questionnaire*

A. *Social anxiety FNE –SAD (Fear of negative evaluation and social avoidance and distress) questionnaire*

This questionnaire was prepared by Watson & Friend (1969). This test had two small-scales of social avoidance and fear of negative evaluation including 58 items, 28 ones related to the social avoidance and 30 ones related to the fear of negative evaluation. In the first small-scale (social avoidance), 15 and 13 items had positive and negative answers, respectively, which the higher score indicated a social avoidance and distress, but in the second one (fear of negative evaluation), 17 and 13 items had positive and negative answers, respectively, which the higher score indicated a more fear of negative evaluation. Total score is gained through adding the sum of incorrect answers for the rest items. Continuum of the answers was zero and one designated for each answer (Watson and Friend, 1969).

Reliability of the questionnaire has been calculated between 0.60 and 0.83 in the previous studies (Watson and Friend, 1969). In this study, the questionnaire reliability and its subscales were calculated by Alpha Cornbach`s method, which was 0.83 for whole scale, 0.74 for the small-scale of social avoidance and distress and 0.81 for small-scale of fear of negative avoidance indicating an acceptable reliability for the questionnaire. Validity coefficient of the questionnaire have been calculated by Concurrent criterion validity (0.54 - 0.68) in the previous studies (Watson and Friend, 1969).

B. Focus of attention questionnaire

Focus of attention questionnaire (Woody, Chambless, and Glass, 1997) was created for measuring the socially anxious individuals` focus of attention in the social interactions. This questionnaire has 2 subscales (self-focused attention and external focus of attention) of 5 items. Respondents answered to the items of questionnaire based on the previous imagination of social interaction. Each item is scored on a 5-degree scale from completely incorrect (1) to completely correct (5). Scores of each subscale are calculated by the 5-items mean.

Woody et al (1997) reported that the Alpha Cornbach`s Coefficient for the subscales of Self-focused attention and external attention questionnaires are 0.76 and 0.72, respectively. In this study, reliability coefficients of the focus of attention and its subscales were calculated by the Alpha Cornbach`s method, which were 0.74, 0.68, and 0.51 for whole scale, subscale of self–focused attention, and subscale of external focus of attention, respectively, indicating an acceptable reliability for the mentioned questionnaire. Results of this analysis showed two items, which are 55.85 percent of the focus of attention scores` variance. Consequently, item analysis showed that the first item with special value of 3.47 explains 31.81 percent of the variance including five items (3, 4, 7, 9, 10) and second item with special value of 2.12 explains 21.18 percent of the variance including 5 items (1, 2, 5, 6, 8). Extracted factors were named based on the study of Woody ea at (1997) and their infrastructural structure (factor 1: self-focused attention and factor 2: out-focused attention).

C. Body image concern questionnaire (Littleton, Axsom, and Pury, 2005)

This questionnaire has 19 items evaluating the dissatisfaction and concern of individuals toward their appearance. Respondents were asked to score (on a scale from 1 to 5) each item showing the amount of their feelings or behavior. in this scale, 1 means that I have never had this feeling or I have not ever done such thing, and 5 means that I always have this feeling and do this thing. the questionnaire`s total score was between 19 and 95, higher scores indicate the rate of dissatisfaction of body image. Littleton et al (2005) evaluated the factor structure of the questionnaire, too. Results showed two important and significant factors, including 11 items (1, 3, 5, 8, 9, 14, 15, 16, 17, 18, 19), first on was dissatisfaction and embarrassment of the individuals related to their appearance in addition to evaluate and hide the perceived deficiencies. the second one, including 8 items (2, 4, 6, 7, 10, 11, 12, 13), was the rate of appearance concern interfered with the individual`s social performance.

Littleton et al (2005) evaluated this questionnaire`s reliability by the internal consistency and gained an Alpha Cornbach`s coefficient of 0.93. Correlation coefficient of each question with the questionnaire`s total score was from 0.32 and 0.73 (mean =0.62). In addition, first and second factors` Alpha Cornbach`s coefficients were 0.92 and 0.76, respectively, and the correlation coefficient of them was 0.69. In this study, reliability of the body image concern questionnaire and its subscales were calculated by Alpha Cornbach`s method, which was 0.86 for the whole questionnaire. First little factor (dissatisfaction of appearance) was 0.84 and the second one (involve in the performance) was 0.71 indicating the acceptability of this questionnaire`s reliability. In the study of Bosak nejad and Ghafari (2007), correlation coefficient between the scale of body image concern and fear of negative evaluation of the body appearance was 0.55 and the correlation coefficient between body image concern and fear of negative evaluation was 0.43, which was significant at $p \leq 0.001$ level.

D. Generalized self-efficacy (GSE-10) questionnaire

This scale was created by Schwarzer and Jerusalem (1995). It has 20 items with two small-scalesof generalized self–efficacy and social self-efficacy, which was reduced to a 10-item scale in 1981 in which the generalized self-efficacy is evaluated. Perceived Structure of the self-efficacy illustrates the optimistic view of the individuals toward themselves.

Schwarzer, Bäßler, Kwiatek, SchrÖder, and Zhang (1997) calculated the Alpha Cornbach`s coefficients of the generalized self-efficacy scale for the university students of Germany (0.84), Coasta Rica and Spain (0.81), and China (0.91). Rajabi (2006) gained the Alpha Cornbach`s coefficient for all students (0.82), Shahid Chamran`s (0.84) and Azad university of Marvdasht`s (0.80). In this study, reliability of the generalized self-efficacy questionnaire was calculated by Alpha Cornbach`s maethod, which was 0.85 for the whole questionnaire indicating the accessibility of the questionnaire`s reliability. Schwarzer, Schmitz, & Tang (2000) gained the validity coefficient of generalized self efficacy scale through optimistic attributional style, which was 0.49 in a group of students, 0.45 for challenge perception at stressful situations, and 0.58 for teachers with self-regularity, all coefficients were significant. In Rajabi`s study (2006), Hamgera validity coefficients between the generalized self-efficacy scale and self-esteem scale was 0.30 ($p \leq 0.0001$) for 318 individuals, 0.20 ($p \leq 0.0001$) for 476 students of Shahid Chamran university, and 0.23 ($p \leq 0.001$) for 208 students of Marvdasht Azad university.

3. Findings

Findings of this study are indicated in two sections

A: descriptive findings

Descriptive findings of this study include statistical indexes such as mean, standard deviation, max, min, and the number of sample respondents illustrated in table 1 for all study`s variables.

B: Findings related to the study`s hypotheses

This study includes the following hypothesis, each one, with the results of analysis, is indicated in this section.

Hypothesis 1

There is a relationship between self–focused attention and social anxiety of the male and female university students.

As it is seen in table 2, there is a positive and significant relationship between self–focused attention and social anxiety of the male and female university students ($p \leq 0.006$ and r=0.22). So, this hypothesis was confirmed for all students. There was not any positive and significant relationship between self–focused attention and social anxiety of the male students ($p \leq 0.34$ and r=0.12). So, the hypothesis was not confirmed for the male students. There was a positive and significant relationship between self–focused attention and social anxiety of the female students ($p \leq 0.004$ and r=0.29). So, the hypothesis was confirmed for the male students.

Hypothesis 2

There is a relationship between body image concern and social anxiety of the male and female university students.

As it is seen in table 2, there is a positive and significant relationship between body image concern and social anxiety of the male and female university students ($p \leq 0.0001$ and r=0.44). So, this hypothesis was confirmed for all students. There was positive and significant relationship between body image concern and social anxiety of the male students ($p \leq 0.0001$ and r=0.44). So, the hypothesis was confirmed for the male students. There was a positive and significant relationship between body image concern and social anxiety of the female students ($p \leq 0.0001$ and r=0.44). So, the hypothesis was confirmed for the male students.

Hypothesis 3

There is a relationship between generalized self-efficacy and social anxiety of the male and female university students.

As it is seen in table 2, there is a negative and significant relationship between generalized self-efficacy and social anxiety of the male and female university students ($p \leq 0.001$ and r=-0.27). So, this hypothesis was confirmed for all students. There was not any negative and significant relationship between generalized self-efficacy and social anxiety of the male students ($p \leq 0.15$ and r=-0.18). So, the hypothesis was not confirmed for the male students. There was a negative and significant relationship between generalized self - efficacy and social anxiety of the female students ($p \leq 0.002$ and r=-0.31). So, the hypothesis was confirmed for the male students.

Hypothesis 4

There is a relationship between social anxiety of the male and female university students and self–focused attention, body image concern, and generalized self-efficacy.

As it is seen in table 3, according to the results of regression with the enter method, multiple correlation coefficients for linear integration of the self-focused attention, body

image concern, and generalized self-efficacy variables with the social anxiety in all students were MR =0.49 and RS=0.23, which were significant at a p≤0.0001 level. So, this hypothesis was confirmed for all students. Based on the amount of RS coefficient of determination, 23 percent of the social anxiety`s variance was explained by the predictive variables. Results for the male students were MR=0.47 and RS=0.18, which were significant at a p≤ 0.002. So, this hypothesis was confirmed for the male students. Based on the amount of RS coefficient of determination, 18 percent of the social anxiety`s variance was explained by the predictive variables. Results for the female students were MR=0.51 and RS=0.23, which were significant at a p ≤ 0.0001. So, this hypothesis was confirmed for the male students. Based on the amount of RS coefficient of determination, 23 percent of the social anxiety`s variance was explained by the predictive variables.

4. Conclusion and discussion

4.1. ***Hypothesis 1***

results of this study for all students and the female ones are in accordance with the results of Khaier et al (2008), Voncken, Dijk, Jong, and Roelofs (2010), Higa & Daleiden (2008), Zue, Hudson, and Rapee (2007), Beidel, Turner, and Morris (1999), Woody (1996), Mansell (2002), Bogels & Lamers (2002), Hofmann (2000), mellings and Alden (2000), Rapee & Heimberg (1997), Clark and Wells (1995), Winton, Clark and Edelman (1995), and Rapee & Lim (1992). Explaining the findings of this hypothesis, it can be concluded that:

The second process activated after the social threat understanding is the self–focused attention. Based on the model of Clark and Wells (1995), when socially anxious individuals feel that they are negatively evaluated by others, they change their attention to revise and observe themselves, so their accessibility to the negative feelings and thoughts is increase and involved with their performance.

Individuals with social anxiety don't use others` reaction to get the clues of how they are evaluated, but they wait for the negative sententious evaluation about themselves not the others` judgments, so they automatically suppose that this information is related to that how others evaluate them. Consequently, instead of observing others` reactions, individuals with social anxiety focus their attention on the inner side and only on themselves (Clark and Wells, 1995).

Clark and Wells (1995) emphasized on the biases in attention, change of events, and its key importance, and believed that this kind of biases is created through the wrong activated assumptions about the person`s self and social world followed by the negative evaluation of the social situations, so the anxiety program is activated and this disorder`s cognitive, behavioral, and physical signs are continued.

In addition, there is not any positive and significant relationship between self–focused attention and social anxiety of the male students. There was not any related study, too. Explaining this:

A successful social interaction needs a suitable balance of self–focused attention and outside – focused attention , because of the attention biases of individuals with social panic, this balance become disordered (Wells & Mathews, 1994). It seems that the individuals with social panic increase their self-focused attention and reduce their outer one in the social situations (Mellings & Alden, 2000).

There is a probability in explaining the findings of this study which by considering the limitations of this study, use of experimental methods to measure the attention biases was not possible. Two known cognitive-tentative approaches, Dot-probe paradigm and Stoop task, in most evaluations, were used to measure the attentional processes. Thus, attention biases measurement by a questionnaire is not an ideal method. It can be said that the findings are affected by measurement method.

4.2. ***Hypothesis 2***

results of the second hypothesis (for all respondents) are in accordance with Harth and Hermes (2007), Freda and Gamez (2004), Biby (1998), Thompson (1990), Keeton, Cassh, and Brown (1990), Annis, Cash, and Hrabosky (2004), Cash and Hicks (1990), and Nye and Cash (2006).

Studies showed that individuals more sensitive in their social interactions have more fear of physical appearance and others' evaluation related to this issue. In fact, body image concern, as a cognitive process, can cause social anxiety. Individuals with social anxiety often perceive negative images from themselves during the social situations affecting their social performance.

Based on the self-supply model (a perception which individuals prefer to create in others based on their beliefs toward themselves), individual`s goal is to have a positive effect on others. If individuals conclude this based on their self–confidence, there would not be any efficient effect on others, probably; they will experience a fear of negative evaluation in the social and performance situations.

Individuals with social anxiety think that the other people are naturally critics and negatively evaluating they so, when facing the others, create a mental representation from their own appearance and behavior as they think they are watched by others. This mental representation is created based on several inputs such as the previous experiences, real-self image, and feedbacks of others, which is

usually negative and they focus their simultaneous attention on both this mental representation of themselves and any perceived threat from the environment. Then, they enter the comparison process and start processing the others` expected performance standard and the mental representation of their own appearance and behavior, and have a negative judgment about the probability of being negatively evaluated by others. These negative judgments cause the physical, cognitive, and behavioral signs of anxiety, which affect the individual`s mental representation through an interpretation of internal anxiety signs and external indices of negative evaluation, again, the anxiety`s incomplete cycle would be continued (Rapee and Heimberg, 199).

So, in ones having no positive body image of themselves or low self-esteem, some cognitive, emotional, perceiving , and behavioral inconsistencies related to body`s weight or form are created which cause the signs of anxiety.

4.3. ***Hypothesis 3***

results of third hypothesis in all and female students are in accordance with Taheri Far et al (2010), Masoudnia (2008), Khaier et al (2008), Gholami et al (2007), Gaudianio and Herbert (2003), Muris (2002), Muris et al (2001), Pajares (1997), Clark and Wells (1995), Schwarzer and Jerusalem (1992), Hurrelmann and Losel (1990), Maddux et al (1988), Pearl (1993), and Moe and Zeiss (1982).

Explaining the findings of hypothesis 3:

According to Bandura, perceived inefficiency has an important role in the anxiety, stress, mental irritation, and other emotional states. Individuals become anxious when find themselves unable to counter the threatening stimulus (Muris, 2002). Individuals with weak self-efficacy find the tasks and work difficult and this increases their anxiety. in contrast, powerful beliefs of self-efficacy cause relaxation and closeness to carry out the difficult tasks (Pajares & Schunk, 2002).

These results are logical because Bandura believed that self-efficacy is a cognitive mediator affecting the cognition, thoughts, and sensations of the individuals. When the students face negative or stressful situations, sense of self-efficacy help them to control and organize those events and situation and secure themselves from many psychological problems. In the other hand, sense of low self-efficacy prevents an effective counter to the stress situations and increases the illness signs.

Individuals with high social anxiety often feel that they haven`t the specific skills and the necessary abilities for inter personal behavior, and have a low expectation of success in the social situations; this causes more and contentious anxiety in them. In fact, when individuals have correct judgments from their abilities, they can resolve the problems by a correct analysis so that those problems won't cause any disorders or trauma.

Findings of this study related to the male students are not in accordance with those of the mentioned studies (there was not any negative relationship between the generalized self-efficacy and social anxiety of the male students). Explaining that:

Studies showed that the self-efficacy is different in the two sexes. It seemed that self-efficacy is different based on the age and sex. Males are averagely more self-efficient than females; the sexual differences in this field reach its climax in the age of 20 and start to reduce in the next years. Results` lack of accordance is mostly related to the cultural, family, incorrect perception of abilities, perception of roles, and sexual model-finding factors. Factors such as incorrect perception of abilities, skills, differences in the methods and educational models, low or great expectations, society`s attitude, and social organizations affect the sexual differences (Najafi and Foladchang, 2007).

4.4. ***Hypothesis 4***

Explaining the fourth hypothesis:

Anxiety is an emotional state and is created after evaluating the information related to the threatening event or personal ability perception to counter it (Gaudiano and Herbert, 2003). If an event is perceived beyond the individual`s ability of counter, accidental disability of counter can be effectively followed by anxiety (Bandura, 1997).

Individuals with social anxiety, in the threatening situations, perceive the environmental threats out of their control, so they, intemperately, focus their attention toward themselves. As thinking that they are negatively judged by others, they focus their attention to check and supervise themselves, so the accessibility to negative thoughts is increased in them, which increase the negative biases toward the social facts (Clark and Wells, 1995).

In addition, body image disorder is occurred when an individual has a distortion in perception, behavior, cognition, and emotion related to the body`s weight and form (Rayegan et al, 2006).

Body image is a basic element of the personality and each individual`s self-concept affecting the psychological life and attitudes. this image can be positive or negative, affect the psychological well-being of the individual, and become a resource for positive and negative emotions and, through this, affect the individual`s social relations. If the individual`s body image is too inconsistence, the social relations and interpersonal communications would be highly affected. Intensive concern of the others` negative evaluation causes body image dissatisfaction for the person. If individuals experience a negative

evaluation or being ridiculed by the others, a negative body image is created in them which act as a schema. A special motivating situation, such as situations in which the individual has to show his.her body to the others, activates this schema. This issue, by itself, causes intensive care, negative interpretation of others` behavior, avoidance behavior, effort for covering and hiding the body, seeking- to -ensure, and compensatory actions. These behaviors provide the ground for the creation of negative cognitive and emotional experiences about the body form and its related concern. This issue cause the concern to continue and get worst providing the field for psychological disorder formation and, finally, would have terrible effects on the different aspects of the individual`s life.

In the other hand, cognitive factors such as beliefs of inefficiency and illogical thoughts have an important role in the cause and continuity of the anxiety disorders. Perceived self–efficacy is to counter the perceived social threat. Individuals` beliefs of their ability to counter related to that how much anxiety they can experience at the threatening situations and beliefs of self–efficacy has a key role in motivating the anxiety to control the stressful situation. Individuals who think that they can control the environmental events don`t remember the anxious though method in their mind and don`t be anxious by them, but they believe that they can`t control the potential environmental threats and experience a high level of anxiety at the threatening situations (Clark and Wells, 1995).

In addition, results of studies showed that the self-focused attention activates the individual`s self-concept and increases it in different cognitive processes. Consequently, in these situations, accessibility and processing the self-related information is facilitated and the rate of thoughts and perception negativity would be increased.

Thus, it can be concluded that all mentioned variables are related to the cognitive factors and it is logical to have reciprocal effects on each other. Totally, results of this study showed that self–focused attention, body image concern, and self–efficacy have an important relationship with the cognitive activities of the socially anxious individuals. So, looking for methods, in accordance with our culture, able to focus the attention of socially anxious individuals to the outside of themselves and reduce their negative self-concept activity cause the modification of body image and increase of self-efficacy beliefs.

Table1. Mean standard deviation, min, and max of the students` scores

number	max	min	Standard deviation	mean	variable	respondents
151	44	4	8.12	22.17	Social anxiety	All students
151	24	5	3.79	16.35	Self-focused attention	
151	84	19	13.10	39.74	Body image concern	
151	40	13	5.45	30.03	Generalized self-efficacy	
61	40	7	7.77	21.45	Social anxiety	Male students
61	24	7	3.84	16.70	Self-focused attention	
61	68	19	13.09	39.81	Body image concern	
61	40	17	5.16	30.44	Generalized self-efficacy	
90	44	4	8.36	22.65	Social anxiety	Female students
90	23	5	3.76	16.12	Self-focused attention	
90	84	19	13.19	39.70	Body image concern	
90	40	13	5.64	29.75	Generalized self-efficacy	

Table2. Simple correlation coefficients between the social anxiety of the students and self-focused attention, body image concern, and generalized self -efficacy

Number of samples (n)	Level of significance (p)	Correlation coefficient (r)	respondents	criterion variable	Predictive variables
151	0.006	0.22	All students	social anxiety	self–focused attention
60	0.34	0.12	Male students		
90	0.004	0.29	Female students		
151	0.0001	0.44	All students	social anxiety	Body image concern
60	0.0001	0.44	Male students		
90	0.0001	0.44	Female students		
151	0.001	-0.27	All students	social anxiety	Generalized self-efficacy
60	0.15	-0.18	Male students		
90	0.002	-0.31	Female students		

Table3. Multiple* correlations with simultaneous method for analyzing the relationship of social anxiety of the students and self-focused attention, body *image concern, and generalized self-efficacy

Level of significance (P)	amount (T)	Regression coefficients (B)	Ratio F probability	Consistent coefficient of determination (RS)	Multiple correlation (MR)	Predictive variables	Criterion variable	responden ts
0.049	1.98	0.14	F=15.93 P≤ 0.0001	0.23	0.49	self-focused attention	Social anxiety	All students
0.0001	4.77	0.36				body image concern		
0.010	-2.61	-0.19				Generalized self-efficacy		
0.24	1.18	0.14	F=5.46 P≤ 0.002	0.18	0.47	self-focused attention	Social anxiety	Male students
0.001	3.38	0.40				body image concern		
0.32	-1.001	-0.12				Generalized self-efficacy		
0.14	1.48	0.14	F=10.26 P≤ 0.0001	0.23	0.51	self-focused attention	Social anxiety	Female students
0.001	3.33	0.33				body image concern		
0.02	-2.33	-0.22				Generalized self-efficacy		

REFRENCE

1. Bosak nejad, S and Ghafari, M (2007), relationship between the fear of body malformation and psychological disorders of the university students, Journal of behavioral sciences, 1(2), 179-187.

2. Kaier, M, Ostovar, S, Latifiyan, M, Taghavi, M, and Samani, S (2008*),* immediacy effect of the self-focused attention and social self-efficacy on the relationship between social anxiety and judgment biases Iranian Journal of psychiatry and clinical psychology, 14(1), 24-32.

3. Rayegan, N, Shaeiri M, and Asghari Moghadam, M (2006), evaluation of the effectiveness of cognitive-behavioral therapy based on the cash 8-stages model on the negative body image of the female students. Scientific- research bimonthly of knowledge and behavior, Shahed university, 13(19), 11-22.

4. Rajabi, Gh (2006), evaluation of the reliability and validity of the generalized self-efficacy beliefs, journal of new thoughts of education, 2(2), 111-122.

5. Taheri Far, Z, Fati, L, and Gharaee, B (2010), predictive model of social panic in the student based on the cognitive –behavioral items, Iranian Journal of psychiatry and clinical psychology, 16(1), 34-45.

6. Gholami Ranani, F, Kajbaf, M, Neshat Dost, H, and Moradi, A (2007). Effectiveness of group education of self–efficacy on the reduction of social panic, journal of psychology, 11(2), 216-232.

7. Masoudnia. E (2008), generalized self efficacy and social phobia: evaluation of the Bandura social cognitive model. Journal of psychological studies. 4(3), 115-127.

8. Mehrabizadeh Honarmand, M, Najarian, B, and Baharloee, R (1999), relationship of Perfectionism and social anxiety. Scientific and research journal of psychology, 3(3), 231-248.

9. Najafi, M and Foladchang, M (2007), relationship of self-efficacy and mental health of the high school students, scientific- research bimonthly of knowledge and behavior, Shahed university, 14(22).

10. Annis, N. M., Cash, T. F., & Hrabosky, J. I. (2004). Body image and psychosocial differences among stable average weight, currently overweight, and formerly overweight women: The role of stigmatizing experiences. Body Image, 1 (1), 155–167.

11. Bandura, A. (1997). Self-efficacy:The exercise of control. New York: W. H. Freemam.

12. Beck, A. T., Emery, G., & Greenberg, R. L. (1985). Anxiety disorders and phobias: A cognitive perspective. New York: Basic Books.

13. - Beidel, D. C., Turner, S. M., & Morris, T. L. (1999). Psychopathology of childhood social phobia. Journal of the American Academy of Child and Adolescent Psychiatry, 38, 643-650.

14. Biby, E. L. (1998). The relationship between body dysmorphic disorder and depression, selfesteem, somatization and obsessive compulsive disorder. Journal of Clinical Psychology, 54 (1), 489-499.

15. Bogels, S. M., & Lamers, C. T. J. (2002). The causal role of self-awareness in blushing-anxious, socially-anxious and social phobics individuals. Behaviour Research and Therapy, 40, 1367–1384

16. Cash, T. F., & Hicks, K. L. (1990). Being fat versus thinking fat: Relationships with body image, eating behaviors, and well-being. Cognitive Therapy and Research, 14 (3), 327-341.

17. Clark, D. M., & Wells, A. (1995). Acognitive model of social phobia. In R. G. Heimberg, M. R. Liebowitz, D. A. Hope, & F. R. Schneier (Eds.), Social Phobia: Diagnosis, assessment, and treatment, (69–93). New York: Guilford Press.
18. Etu, S. F., & Gray, j. j. (2009). A preliminary investigation of the relationship between induced rumination and state body image dissatisfaction and anxiety. Journal Body Image, 7, 82–85.
19. Foa, E. B., & Kozak, M. J. (1986). Emotional processing of fear: Exposure to corrective information. Psychological Bulletin, 99, 20-35.
20. Freda, I., & Gamze, A. (2004). Social phobia among university students and its relation to self-esteem and body-image. Canadian Journal of Psychiatry, 49 (9), 630-635.
21. Gaudiano, B. A., & Herbert, J. D. (2003). Preliminary psychometric evaluation of new self-efficacy scale and its relationship to treatment outcome in social anxiety disorder. Cognitive Therapy and Research, 27 (5), 537-555.
22. Harth, W., Hermes, B. (2007). Psychosomatic disturbances and cosmetic surgery. Journal Dtsch Dermatol Ges, 5, 736-743.
23. Heinrichs, N., & Hofmann, S. G. (2001). Information processing in social phobia: Critical review. Clinical Psychology Review, 21, 751-770.
24. Higa, C. K., & Daleiden, E. L. (2008). Social anxiety and cognitive biases in non-referred children: The interaction of self-focused attention and threat interpretation biases. Journal of Anxiety Disorders, 22, 441-452.
25. Hofmann, S. G., & Barlow, D. H. (2002). Social phobia (social anxiety disorder). In D. H. Barlow (Ed.), Anxiety and its disorders: The Nature and Teatment of Anxiety and Panic (2nd. ed., 454-477). New York: The Guilford Press.
26. Hofmann, S. G. (2000). Self-focused attention before and after treatment of social Phobia. Behaviour Research and Therapy, 38, 717-725.
27. Hurrelmann, K., & Losel, F. (1990). Health Hazards In Adolescence. De Gruyter: Berlin.
28. Keeton, W. P., Cash, T. F., & Brown, T. A. (1990). Body image or body images: Comparative multidimensional assessment among college students. Journal of Personality Assessments, 54, 213-230.
29. Kessler, R. C., McGonagle, K. A., Zhao, S., Nelson, C. B., Hughes, M., Eshleman, S., & Wittchen, H. U. (1994). Lifetime and 12-month prevalence of DSM-III-R psychiatric disorders in the United States: Results from the National Comorbidity Survey. Archives of General Psychiatry, 51, 8-19.
30. Littleton, H. L., Axsom, D. S., & Pury, C. L. (2005). Development of the body image concern inventor. Behavior Research and Therapy, 43, 229 -241.
31. Maddux, J. E., Norton, L., & Leary, M. R. (1988). Cognitive components of social anxiety: An integration of self-presentational theory and self-efficacy theory. Journal of Social and Clinical Psychology, 6, 180-190.
32. Mancini, S. (2001). Social phobia and children. International Journal of Social Psychiatry, 34, 18–23
33. Mansell, W. (2002). Social anxiety, self-focused attention, and the discrimination of negative, neutral and positive audience members by their non-verbal behaviours. Behavioural and Cognitive Psychotherapy, 30, 11–23
34. - Mellings, T. M. B., & Alden, L. E. (2000). Cognitive process in social anxiety: the effect of self-focus, ruminatin and anticipatory processing. Behaviour Research and Therapy, 38, 243-257.
35. Moe, K. O., & Zeiss, A. M. (1982). Measuring self-efficacy expectations for social skills: A methodological inquiry. Journal of Cognitive Therapy and Research, 6, 191-205.
36. Muris, P. (2002). Relationships between self-efficacy and symptoms of anxiety disorders and depression in a normal adolescent sample. Journal of Personality and Individual Differences, 32, 337–348.
37. Muris, P., & Oosten, A. V. (2002). Social anxiety in college students. Journal of Behavior Therapy, 3, 203-220.
38. Muris, P., Bogie, N., & Hoogsteader, A. (2001). Effects of an early intervention group program for anxious and depressed adolescents: a pilot study. Psychological Report, 88 (2), 481–482.
39. Muris, P., Bogie, N., & Hoogsteader, A. (2001). Protective and vulnerability factors of depression in normal adolescents. Behavioral Research and Therapy, 39 (5), 555–565.
40. Nye, S., & Cash, T. F. (2006). Outcomes of mineralization cognitive-behavioral body image therapy with eating disordered women treated in a private clinical practice. International Journal of Eating Disorders, 39 (1), 31-40.
41. Pajares, F. (1997). Current direction in self-efficacy research. Advances in Motivation and Achievement, 10, 1-49.
42. Pajares, F., & Schunk, D. H. (2002). Self and self-belif in psychology and Education: An historical perspective. Psychology of Education, Newyork: Academic perss.
43. Pearl, L. (1993). The differential roles of attributions, self-efficacy expectations, and outcome expectations within a self-presentational model of social anxiety. Unpublished doctoral dissertation, State University of New York, Albany.
44. Rapee, R. M., & Heimberg, R. G. (1997). A cognitive-behavioral model of anxiety in social phobia. Behaviour Research and Therapy, 35, 741-756.
45. Rapee, R. M., & Lim, L. (1992). Discrepancy between self and observer rating of performance in

social phobics. Journal of Abnormal Psychology, 101, 728-731.
46. Rodebaugh, T. L. (2006). Self-efficacy and social behaviour. Journal of Behaviour Research and Therapy, 44, 1831-1838.
47. Schwarzer, R., & Jerusalem, M. (1995). Generalized self-efficacy scale. In S. Wright, & M. Johnston, & J. Weinman, (Eds.), Measures in Health Psychology: A User's Portfolio. Causal and Control Beliefs (35–37). Windsor, UK: nferNelson.
48. Schwarzer, R., & Jerrusalem, M. (1992). Advances in anxiety theory: A Cognitive process approach. Advances in Test Anxiety Research, 7, 2-17.
49. Schwarzer, R., Schmitz, G. S., & Tang, C. (2000). Teacher burnout in Hong Kong and Germany: A crosscultural validation of the Maslach Burnout Inventory. Anxiety, Stress, and Coping, 13 (3), 309–326.
50. Schwarzer, R., Babler, J., Kwiatek, P., Schroder, K., & Zhang, J. X. (1997). The assessment of optimistic self-beliefs: Comparison of the German, Spanish, and Chinese versions of the general selfefficacy scale. Applied Psychology, 46 (1), 69–88.
51. Thompson, J. K. (1990). Body image disturbance, assessment and treatment. University of South Florida: Pergamon press.
52. Voncken, M. J., Dijk, C., De jong, P. J., & Roelofs, J. (2010). Not self-focused attention but negative beliefs affect poor social performance in social anxiety: An investigation of pathways in the social anxietyesocial rejection relationship. Behaviour Research and Therapy, 48, 984-991.
53. Watson, D., & Friend, R. (1969). Measurment of social-evaluative anxiety. Journal of Consulting and Clinical Psychology, 33 (4), 448-457.
54. Wells, A., & Mathews, G. (1994). Attention and emotion: A clinical perspective. Hove: Lawrence Erlbaum. In K. Mogg, B. P. Bradley (1998). A cognitive-motivational analysis of anxiety. Behaviour Research and Therapy, 36, 809-848.
55. Winton, E. C., Clark, D. M., & Edelman, R. J. (1995). Social anxiety, fear of negative evaluation and the detection of negative emotion in others. Behaviour Research and Therapy, 33, 193-196.
56. -Woody, S. R., Chambless, D. L., & Glass, C. R., (1997). Self-focused attention in treatment of social social phobia. Behavior Research and Therapy, 35, 117-129.
57. Woody, S. R. (1996). Effects of focus of attention on anxiety levels and social performance of individuals with social phobia. Journal of Abnormal Psychology, 105, 61-69.
58. Zue, J. B., Hudson, J. L., & Rapee, R. M. (2007). The effect of attentional focus on social anxiety. Behaviour Research and Therapy, 45, 2326-2333.

11/20/2011

Electric Characterization of Gallium Resquitelluride Monocrystals

F. S. Bahabri

Physics Department, Science Faculty for Girls, King Abdul Aziz University – KSA
f_s_bahabri@hotmail.com

Abstract: Electronic transport measurements were made on single crystal samples of Ga_2Te_3. The crystals were prepared by a special design based on Bridgman technique. The influence of temperature on the electrical conductivity, hall effect, hall mobility and carrier concentration was investigated in the temperature range 160K to 440K. The study was carried out with the current following parallel to the c-axis and the magnetic field direction perpendicular to the c-axis. The crystal obtained had n-type conductivity with electron concentration of 3.79 $x10^{13}$ cm^{-3} at room temperature. The conductivity and hall mobility at 300K were evaluated as 1.479 x $10^{-3}\Omega^{-1}cm^{-1}$ and 239.88 cm^2/V. sec, respectively. The energy gap width and the depth of donor centre was found to be 1.588 eV and 0.20 eV respectively. The scattering mechanism of the charge carrier was discussed in the same range of temperature.

[F. S. Bahabri **Electric Characterization of Gallium Resquitelluride Monocrystals** Life Science Journal, 2011; 8(4): 714-718] (ISSN: 1097-8135). http://www.lifesciencesite.com.

Keywords: |Gallium resquitelluride, single crystal, electrical conductivity, Hall effect.

1. Introduction

M_2X_3 compounds (where M = Al, Ga or In and X = S, Se or Te) are the simplest examples of materials [1] whose structure is based on the tetrahedral atomic coordination as in the Zinc blende (ZB) structure but in which some atomic sites are empty. In the case of M_2X_3 compounds, one-third of the cation sites of the ZB or wurtzite structures available to group III atoms is vacant. It is apparent from the chemical formula that the valencies are satisfied. In some of these compounds, the vacancies can be ordered to form a superlattice bellow a certain temperature.

Although many recent papers have dealt with $M_2^{III}X_3^{VI}$ – type compounds, their properties remain rather confusing. The reason for this the compounds of this type are defective [2] in respect of their metal atoms : only two-third of all cationic positions are occupied and every third site in the cation sublattice remains vacant. Consequently, the presence of this large number of intrinsic defects strongly affects the motion and scattering of current carriers and phonons, causing their thermal and electrical properties.

Ga_2Te_3 is a member of the above family in the past three decades, significant interest in chalcogenide [3] compounds has been shown by various workers because of their interesting physical properties and well as their wide technological application.

In gallium – tellurium system various stoichiometric compositions have been reported [4-6] three phases are present in the Ga–Te system, GaTe,Ga_2Te_3 and Ga_2Te_5 .Among these compounds Ga_2Te_3 seemed to be the less studied[7]. Many investigations have dealt with this compound while results were reported for the resistivity and thermoelectric power of Ga_2Te_3 binary alloy system in the liquid state [8,9]. Some other authors have investigated Ga_2Te_3 in the form of thin films [10]. Few papers have been published dealing with the solid Ga_2Te_3 such as structure[11] , resistivity under high pressures[12], mass spectrometric[13], *Mössbauer* spectroscopy[14], Dielectric and photoconductivity[15,16], optical properties[17], switching effect[18,19], heat capacity[20] ferroelectric properties[21].

2. Sample preparation and measurements:

High quality of Ga_2Te_3 single crystal have been grown from melt by a modification of Bridgman technique. The growth method and the experimental apparatus have been described in detail elsewhere[22]. The purity of the materials used was a follows Ga, 99.9999% and Te, 99.999%. Stoichiometric quantities of the constituent elements, 13.3523 g Ga and 36.6477 g Te, representing 26.705% gallium and 73.295% tellurium were used as starting materials. The appropriate amounts were first sealed in quartz ampoules at a pressure of 10^{-5}Torr. The lower end of the ampoule was trapered in order to favor crystal growth at a single point. The silica ampoule, coated internally with a thin layer of carbon to prevent contamination of the charge the usual precautions were taken throughout this investigation to prevent oxide formation on the ingot material. In the first procedure the tube was placed in a three – stage tube furnace in which a controlled temperature gradient was maintained the mixture was heated above the melting point according to the phase diagram and

maintained for several hours with periodic agitation to ensure through mixing of the constituents. The ampoule was allowed to move slowly from the high temperature zone towards the low temperature zone with a rate of 1.7 mmh^{-1} through the stationary furnace. As the ampoule continuously enters the low temperature zone, crystallization proceeds until all the contents solidify. A prolonged period of time is necessary for the growth of Ga_2Te_3 single crystals. At least two weeks growth are needed to obtain gallium resquitelluride monocrystals. Then, the obtained dark layered silvery crystals were investigated with x-ray analysis. The analysis confirmed the presence of the crystalline phase without any secondary phases.

For studying electrical conductivity and Hall effect, the sample was prepared in a rectangular shape. The specimens were ground and polished thoroughly with the use of diamond pastes to obtain mirror-like surface. Typical dimensions for the rectangular sample were 9.7 x 3.2 x 2.0 mm^3.In this way the length of the sample was three times of its width to avoid Hall voltage drop.

The d.c Hall measurements were carried out as recommended in ASTM-F 67 and quite similar to those described earlier[23]. Electrical conductivity and Hall effect were measured under vacuum of ~10^{-3}Torr. Measurements above room temperatures were performed with the help of an electrical insulated heater, which was supplied with required voltage, gradually and slowly, from a varic transformer. Liquid nitrogen was used for achieving the low temperature measurements. Calibrated thermocouple, made of copper-constantan, was used for measuring the temperature of the sample. Silver paste contact was used as ohmic contact. The ohmic nature of the contacts was verified by recording the current-voltage characteristics. The conductivity σ and Hall efficient were measured by a compensation method in a special cryostat with a conventional d.c. type measurement system. The designed cryostat allows measurements in a wide range of temperature. For Hall measurements, the magnetic field was perpendicular to the crystallographic c-direction with intensity of 0.5 Tesla. The Hall voltages were measured by reversing the current and the magnetic field directions and taking the appropriate averages.

3. Results and Discussion:

Measurement of the effect of temperature on electric conductivity σ was done from 160K to 440K.**Fig.1** represents the temperature dependence of the electrical conductivity σ of Ga_2Te_3 single crystal.

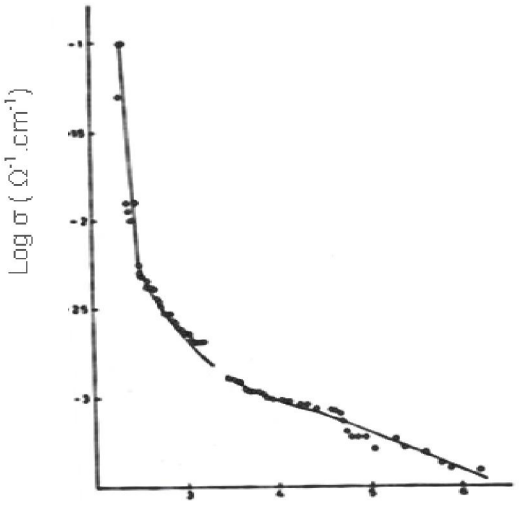

Fig. 1 Electrical conductivity of Ga_2Te_3 single crystal as a function of temperature

The curve shows a typical semiconductor behaviour. As illustrated in the figure, a much less rapid increase in conductivity is observed in the low temperature range with a linear relation up to 240K. After this region the electrical conductivity exponentially increases with a relatively speed rate in the temperature range extending from 240K up to 400K. a rapid increase in the conductivity with linearity is observed in the high temperature range above 400K. It can be stated that the room temperature conductivity reaches a value of σ =1.479 x 10^{-3} Ω^{-1} cm^{-1}. In the extrinsic region σ increases slowly as a result of liberation of the ionized donors and their transition from the impurity level. In the low temperature region the relation between the temperature and electrical conductivity σ can be given as:

$$\sigma = \sigma_o \exp(-\Delta E_d / 2KT) \quad (1)$$

Where σ_o is the pre-exponential factor and ΔE_d is the ionization energy of donor atoms. This is observed in the temperature interval 160-240K and ΔE_d was found to be 0.20 eV. It is also seen from the curve that as the temperature rises the conductivity rises rapidly because of the increase in the total current density (electrons plus holes). The width of the forbidden gap was evaluated from the high temperature slope of the conductivity curve, to be 1.588 eV. This value contrasts with data of other author[20]. The calculated energy gap width in the present work is larger than that reported in the literature. We may attribute the discrepancy between the values of ΔE_g partially to the presence of the

large number of intrinsic defects that affects strongly the motion of scattering of current carriers and phonons. On the other hand it is thought that the technology used to grow these crystals may influence its physical properties. In this paper, we tried to elucidate this confusion but more experimental data were necessary to explain this contradiction. Since Hall effect is important and helpful for the determination of many physical parameter, this work was extended to cover the effect of temperature on the Hall coefficient R_H. This was done in a wide range of temperature (160K-440K). **Fig. 2** shows the dependence of R_H on temperature.

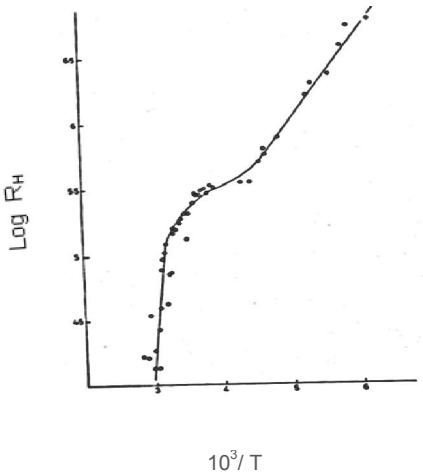

Fig. 2:Effect of temperature the Hall coefficient for Ga_2Te_3 single crystal

It is obvious that the sign of the Hall coefficient indicates that the compound Ga_2Te_3 is a brilliant n-type semiconductor which is in reasonable agreement with the results[20] obtained by the other author. The Hall coefficient R_H at room temperature was evaluated as 16 x $10^4 cm^3/C$. Determination of the energy gap and ionization energy from Hall data is possible by plotting the relation between $R_H T^{3/2}$ and $10^3/T$. **Fig.3** was constructed and the relation between $R_H T^3$ and $10^3/T$ is presented on the basis of the following relationship:

$$R_H T^{3/2} \alpha \exp\left(-\Delta E_g / 2KT\right) \qquad (2)$$

In the temperature region in which the conductivity σ is predominantly intrinsic, the forbidden band width was estimated to be 1.588 eV from the above relationship. The depth of the donner level was determined from the region in which the conductivity is predominantly due to impurity atoms and was found to be 0.20 eV. These values are in good agreement with the values obtained from the temperature dependence of electrical conductivity the curve shows the following facts.

1-The values of R_H are negative over the entirely temperature range of investigation indicating that Ga_2Te_3 is a n-type semiconductor.

2-The three regions of the curve support that extrinsic conduction appears from 160 to 240Kand intrinsic one begins from 400 to 440K while the transition region lies between 240K and 400K as observed in fig. 1.As for the importance of the mobility data in the field of solids, especially semiconductors, the present work has dealt with an investigation of the effect of temperature on Hall mobility σ, as shown in **Fig.3**.

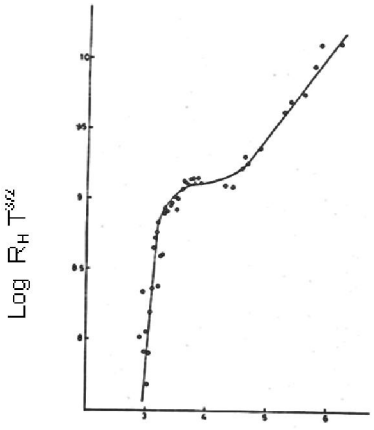

Fig. 3: The relation l $T^{3/2}$and $10^3 / T$ of $Ga_2 Te_3$monocrystal.

The reason for this is to spot some light on the scattering mechanism of the charge carriers. This was done as a result of availability of both and R_H data. **Fig.4** illustrates this dependence for Ga_2Te_3 sample.

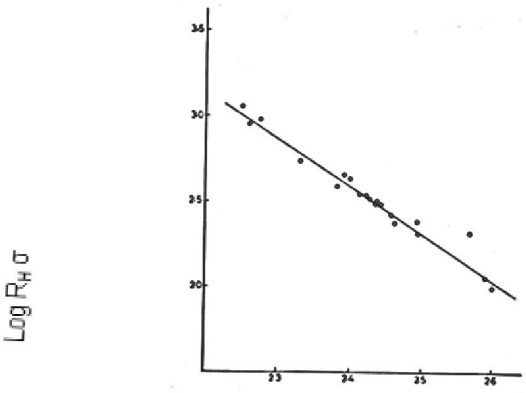

Fig. 4: Temperature dependence of charge carrier mobility's of $Ga_2 Te_3$.

This plot results in a straight line, the slope of which allows the determination of the

exponent. In the temperature range of investigation it was found that the exponent n in the relation $\mu_H \sim T^n$ is – 1.46, which is closely near to the – 3/2 power law. It may be concluded that the charge carriers are scattered by acoustic lattice vibration. The most striking feature of the Hall mobility σ is its temperature dependence as illustrated in fig 4. The mobility is always seen to decrease with increasing temperature and appears to be unaffected by impurity scattering effects. At room temperature the electron mobility of 239.88 cm^2/V. sec, was obtained in these measurements for Ga_2Te_3 sample. Calculation of the diffusion coefficient for electrons gave a value of 6.15 cm^2/sec. Assuming that the effective mass for electrons m^*_n is equal to the rest mass and using the value for the electron mobility at room temperature, the mean free time could be determined and its value was equal to 1.365 x10^{-13} sec. Also the diffusion length of electrons in the Ga_2Te_3specimen was evaluated as 0.916 x 10^{-6} cm. The electron concentration for our investigated sample plotted as a function of inverse temperature is shown in fig.5.

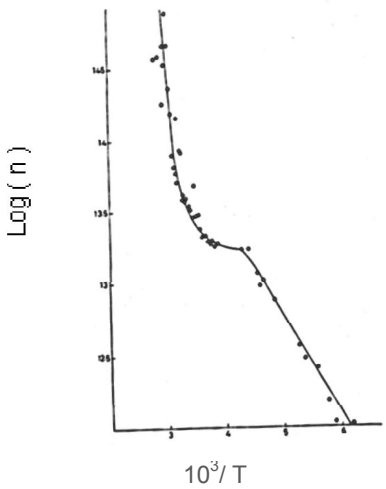

Fig.5: Dependence of carrier concentration of gallium sesquitelluride on temperature

It can be stated that at room temperature the concentration reaches a value of 3.79x10^{13} cm^{-3}. The variation of the carrier density with temperature appears to be nearly linear, except in the temperature range 235-320K which represents the region of transition to intrinsic conduction. At low temperature and indeed (160-235K) in Ga_2Te_3 the carrier concentration is determined by the number of ionized donors. The variation of the carrier concentration is quite slow in the transition region. Since Ga_2Te_3 sample is exhibiting an intrinsic behavior above 400K, then the expected value for the intrinsic concentration n_i will be given as:

$$n_i = 2\left(\frac{2\pi K}{h^2}\right)^{3/2}\left(m_n^* m_p^*\right)^{3/4} T^{3/2} \exp(-\Delta Eg / 2KT) \quad \text{.....(3)}$$

Where "m^*_n and m^*_p :the effective mass for electrons and holes" and another symbol refers to their usual significance and the energy gap width as deduced from this relation is 1.588 eV.

4. Conclusion:

In the present paper, measurements of the electrical conductivity and Hall coefficient in a wide range of temperature extending from 160– 440K was reported. The main conclusions were:-

Ga_2Te_3 crystal is a promising n-type semiconductor.

The energy gap for the compound is 1.588 eV, while the activation energy of donors is 0.20 eV.

The scattering mechanism for Ga_2Te_3 was checked.

The diffusion coefficient for majority carrier and free time between collision as well as the diffusion length was determined.

The conductivity σ , Hall mobility μ_H and carrier concentration n_i at room temperature was evaluated to be 1.479✕$10^{-3}\Omega^{-1}$ cm^{-1}, 239.88 cm^2/V.sec , and 3.79✕1013 cm^{-3} respectively.

This study is a timely one in view of the recent interest in this compound. The important parameters deduced from this study leads to better application in electronic devices and techniques.

Corresponding author
F. S. Bahabri
Physics Department, Science Faculty for Girls, King Abdul Aziz University – KSA
f_s_bahabri@hotmail.com

References

1. Nagat A. T., M. M. Nassary and H. A. El-Shaikh(1991). Semicond. Sci-Technol., 8: 979.
2. Julien C., M. Eddrilf, M. Balkanski, E. Hatzikraniotis and K. Kambas (1985)…… Phys. Stat. Sol., 88:687.
3. Mehta N., K. Singh and A. Kumar(2009)……., Phys. B., 404 :1835.
4. Alapini F., J. Flahaut, M. Guittard, S. Jaulmes and M. Julien – Pouzol (1979)……. J. Sol. Stat. Chem., 28:309.
5. Oh C.S and D. N. Lee(1992)……., Calphad., 16:317.
6. Blachnuk R. and E. Klose(2000)……., J. Alloy Compound, 305:144.
7. Balitskii O. A. and V. P. Savchyn(2007)…… Mat. Sciin Semicond. Processing, 10:124.

8. Valiante J. C. and T. E. Faber(1974)……, Philos. Mag., 29:571.
9. Tschirner H. U., K. Uhlig and M. Wobst(1984)…….. Philos. Mag., B50:645.
10. Bekheet A. E. (2001)…….., European Phys. J. Appl. Phys., 16:187.
11. Singh D. P., D. K. Suri, U. Dhawan and K. D. Kundra(1996)……., J. Mat. Sci., 25:2160.
12. Bose D. N., S. Sen, D. K. Joshi and S. N. Vaidya(1982)……. Matt. Lett. 1 :61.
13. Uy O. M., D. W. Muenow, P. J. Ficalora and J. L. Margrave. (1968)……., Trans. Faraday Soc., 64:2998.
14. Wuyts K., J. Watte, G. Langouche and R. E. Silverans, G. Zégbé and J. C.
15. Jumas(1992) …….. , J. Appl. Phys., 71:744.
16. Bose D. N. and S. De Purkayastha(1981)……., Mat. Res. Bull., 16:635.
17. Seki Y., M. Kusakabe and S. Kashida(2010)……, Phys Stat Sol., (a) 207:203
18. Julien C., I. Ivanov, C. Ecrepont and M. Guittard(1994)……. Phys. Stat. Sol., (a) 145:207.
19. Aliev A., G. M. Niftiev, F. I. Pliev and B. G. Tagiev(1979)…….. Sov. Phys. Semicond., 13:340.
20. Aydogan S., T. Karacali and Y. K. Yogurtca(2005)……, J. Cryst. Growth, 279:110.
21. Tyurin A., K. Gavaichev, V. Zlomanov and T. Bykova(2006)……. Inorganic Mat. ,4:954.
22. Gamal G. A., M. M. Abdalrahman, M. I. Ashraf and H. J. Eman(2005) …… J. Phys. Chem. Sol., 66:1.
23. Hussein S. A. and A. T. Nagat(1989)……..Cryst. Rest Technol. ,24:283.
24. Nagat A. T., G. A. Gamal and S. A. Hussein(1990)……. Phys, Stat. Sol., (a) 120 : 163.

11/20/2011

Screening Of Acute And Chronic Diabetic Complications Among A Cohort Of Diabetic Patients Admitted To Intensive Care Unit

Fathy Z. El-Sewy[1], Abla A. Abou-Zeid[2], Tamer A. Helmy[3], Amr F. Abou-Alkhair[4] and Soha S. A. El baz[3]

[1]Internal Medicine Dept., [2]Clinical and Chemical Pathology Dept., [3]Critical Care Medicine Dept., [4]Opthalmolgy Dept.
Tamer270103@hotmail.com

Abstract: Background: The present study included two hundreds and fifty patients admitted to intensive care units of the main University Hospital of Alexandria. All patients had diabetes mellitus whether diabetes is the primary or secondary cause for admission. There are 148 females (59.2%) and 102 (40.8%) male patients. The age of these patients varies from 9 to 85 years with a mean 49.55 ± 17.46 years. 80.4% of the patients were type 2 DM and 19.6% were type 1 DM. **Aim of the work**: was to determine the prevalence of acute and chronic diabetic complications among 250 diabetic patients admitted to the Intensive Care units of the Alexandria main University Hospital. **Subjects and methods:** All patients were subjected to thorough clinical examination including: Complete history taking, laying stress on the duration of diabetes, treatment given to control diabetes and the occurrence of the different complications of diabetes. Complete general examination, laying stress on the cardiovascular system, chest examination, abdominal examination, and examination of peripheral nervous system. Laboratory investigation especially: Random blood glucose. Serum creatinine, blood urea nitrogen. Serum cholesterol, serum TG. urinary albumin excretion rate. Electrocardiogram. Fundus examination by direct ophthalmoscope. **Result**: The result of the present study can be summarized as follow: 95.6% of patients are suffering from one or more of the diabetic complications. Either acute in 30.8% or chronic in 81.2% DKA was the most frequent acute complication accounting 23.6% of these complications. It occurred mostly in type 1 diabetes and to lesser extend in type 2 diabetes. Diabetic neuropathy was the most common chronic complications accounting for 56% of complications; somatic peripheral neuropathy is the commonest type of diabetic neuropathy, in our study the incidence of somatic neuropathy was 52.8% and autonomic neuropathy was 10%, most of patients suffering from autonomic neuropathy were having in the same time somatic neuropathy. Followed by diabetic nephropathy (41.2%), cardiovascular complications (34.8%), diabetic retinopathy (32.8%), diabetic foot (25.2%), 59 cases have DKA (23.6%), 37 cases have CVS (14.8%). There was positive correlation between BMI and increase in serum cholesterol and serum TG. DKA was significantly higher in patients with type 1 diabetes than those with type 2 diabetes. Diabetic neuropathy, nephropathy, retinopathy, cardiovascular and diabetic complications were significantly higher in type 2 diabetes than type 1 diabetes. There was negative correlation between DKA and duration of diabetes. But, there was positive correlations between duration of diabetes and retinopathy, neuropathy, foot complications, cardiovascular and cerebrovascular complications. There was significant impact present of some metabolic variants like hyperglycemia, HTN and hyperlipidemia on the development of different complications. Also the effect of the body weight (BMI) and its positive correlation with these variables. There is positive correlations between all diabetic complications and blood pressure, RBG, serum cholesterol, and serum TG.

[Fathy Z. El-Sewy[1], Abla A. Abou-Zeid[2], Tamer A. Helmy[3], Amr F. Abou-Alkhair[4] and Soha S. A. El baz. **Screening Of Acute And Chronic Diabetic Complications Among A Cohort Of Diabetic Patients Admitted To Intensive Care Unit.** Life Science Journal, 2011; 8(4):719-732] (ISSN: 1097-8135). http://www.lifesciencesite.com.

Key word: Diabetes mellitus, Incidence, Complications, ICU Admission.

1. Introduction

The term diabetes mellitus describes a metabolic disorder of multiple etiologies characterized by chronic hyperglycemia with disturbances of carbohydrate, fat and protein metabolism resulting from defects in insulin secretion, insulin action, or both [(1-4)] .

The classification of DM is based on etiology, not on treatment The terms juvenile-onset, adult-onset, insulin-dependent and non-insulin-dependent are no longer used since they are not helpful for differentiating etiology of the DM. Current classifications based on etiology utilize the terms type 1, type 2 and gestational diabetes to depict the three most common forms[(4,5).]

Patients may be asymptomatic – discovered on routine examination/lab test. Classic symptoms include: Polyuria, polydipsia, Loss of weight, Fatigue, Blurred vision and Recurrent vaginal infections or recurrent UTIs.

Patients with type 1 diabetes usually present with classic symptoms which may culminate in the

development of DKA which considered to be an acute complication.

Patients with type 2 diabetes may be asymptomatic or present with classic symptoms. Sometimes patients present with complications of diabetes: a) Micro vascular complications: neuropathy, retinopathy, nephropathy and b) Macro vascular complications: cardiovascular and, cerebrovascular disease.

Note that up to 20% of newly diagnosed patients with type 2 diabetes may have micro vascular complications at the time of diagnosis.

- Hyperosomolar non ketatic coma (acute).

In people with type 1 diabetes, the cornerstone of treatment remains insulin injections.

In type 2 diabetes, some individuals will initially obtain control of blood sugar with diet modification, weight loss and exercise.

Unfortunately, many people are unable to meet the dietary and exercise recommendations. In addition, the natural history of type 2 diabetes shows that less insulin is made over time. For most patients, medications are generally required early, and often multiple medications with different mechanisms of action are utilized.

But in significant change in the paradigm of treatment of type2 diabetes, early insulin therapy holds place in the management. Recent studies have shown that if insulin therapy is initiated early it prevents further beta cell destruction[(1)] Insulin should be the initial therapy in type2 diabetic particularly in: Lean individual or those with severe weight loss, In individuals with renal or hepatic disease that precludes the use of oral glucose lowering agents, In hospitalized or acutely ill patients, In pregnant patient and Severe hyperglycemia at presentation 250 – 300mg/dl

The aim of this study was to determine the prevalence of acute and chronic diabetic complications among 250 diabetic patients admitted to the Intensive Care units of the Alexandria main University Hospital.

2. Patients and Methods:

Two hundred and fifty diabetic patients who were admitted to the Intensive Care Units of the Alexandria main University Hospital were included in the present study whether diabetes is the primary or secondary cause for admission. All patients, all ages, different types of diabetes, known or newly diagnosed diabetes were included in the study.

Methods:

All patients were subjected to the following:

1. Complete history taking including: Age, sex, smoking. Duration of diabetes in years and type of diabetes. History of current treatment of hypertension, cerebrovascular disease, cardiovascular, renal, thyroid or other endocrinal diseases. Family history of diabetes: father, mother, brother and sisters and history of consanguinity. Present history of acute symptoms of DM. Symptoms of complications: Ophthalmologic: eg. diplopia, visual loss.Neurological: numbness, hypothesia or anesthesia. Renal: edema, dysuria, and pruritis vulvae. Cerebrovascular events: eg. Stroke. Cardiovascular events: angina or MI.Peripheral vascular disease: intermittent claudication, gangrene or amputation. Autonomic: GIT symptoms, postural hypotension and impotence. History of acute complications: DKA hyperosmolar nonketotic coma and hypoglycemia, and frequency of attacks. History of hospitalization for diabetes related complications and for diseases other than diabetes. Current treatment modalities :Oral drugs (total dose/day). Insulin therapy (type, total dose u/day, number of injections/day) Other ant diabetic treatment. History of discontinuing any treatment for adverse effects. Diet compliance: strict, moderate, or weak.Thorough clinical examination including: Pulse, blood pressure. Body Mass Index (BMI) Body mass index is defined as the individual's body weight divided by the square of his or her height. The formulae universally used in medicine produce a unit of measure of kg/m^2. Head and neck , examination of the extremities for colour changes, fungus infection, coldness, ulcers, gangrene, and amputation. Complete physical examination: with especial stress on chest, cardiac, and nervous system.
2. Laboratory work up: Complete blood picture [(6)]. Random blood glucose level[(7)] . Complete urine analysis including detecting of glucose, and ketones. BUN and serum creatinine[(8)]. Liver function(ALT, AST) [(9)]. Lipid profile including: serum cholesterol, TG [(10)]. Urinary albumin excretion rate[(7)]: normoalbuminuria <30 mg/24h. microalbuminuria 30-300 mg/24h and macroalbuminuria>300 mg/24 h.
3. Direct ophthalmoscopy with pupil dilated by pupil mydriasis (tropicamide 0.5 %). The degree of retinopathy for each patient will be determined. A useful clinical classification according to the types of lesions detected on fundoscopy is as follows:

- **Mild non-proliferative diabetic retinopathy:** Micro aneurysms, Dot, blot hemorrhages and Hard (intra-retinal) exudates.

- **Moderate-to-severe non-proliferative diabetic retinopathy** The above lesions, usually with exacerbation, plus: Cotton-wool spots, Venous beading, loops and Intra retinal micro vascular abnormalities (IRMA)
- **Proliferative diabetic retinopathy**: Neovascularization of the retina, optic disc or iris, Fibrous tissue adherent to vitreous face of retina, Retinal detachment, Vitreous hemorrhage and Pre retinal hemorrhage.
- **Maculopathy**:(difficult to be detected with direct ophthalmoscope), Clinically significant macular edema (CSME) and Ischemic Maculopathy.

4. Autonomic nerve functions: ECG changes (resting tachycardia and variations in PR interval) and orthostatic hypotension.
5. 12 lead Electrocardiogram.
6. Plain X ray chest for detection of chest infection.

3. Results:

Table 1 shows the characteristic features of the studied cases: of the 250 diabetic patients admitted to intensive care units of Alex. University hospitals, 102 were males and 148 females. Their ages ranged from 9.0 to 85.0 years with a mean age 49.55±17.46 SD. 80.4% were type 2 diabetes and 19.6% were type 1. Among type 2 diabetics 10% were newly diagnosed. 31.2% of patients were smokers. Out of the total number of patients 34.8% were receiving insulin, either as mono-therapy or combined with oral agents while 55.2% were receiving only oral hypoglycemic agents. Table (1a) also shows that the duration of diabetes ranged from 0 to 45 years with a mean of 9.46 ±7.84 years. The body mass index (BMI) ranged from 19.10 to 40 with a mean of 24.84 ±4.04 kg/m^2.

Table (1a): Demographic data of studied population

	No.	%
Sex		
Male	102	40.8
Female	148	59.2
Age(years)		
<20	15	6.0
20 - <40	45	18.0
40- <60	110	44.0
60+	80	32.0
Range	9.00-85.00	
Mean ± SD	49.55 ± 17.46	
BMI (kg/m^2)		
Range	19.10-40.00	
Mean ± SD	24.84 ± 4.04	
Smoking		
Non smoker	172	68.8
Smokers	78	31.2
Type of diabetes		
Type I	49	19.6
Type II:	201	80.4
Newly diagnosed	25	10.0
Known diabetic	176	70.4
Treatment of diabetes		
Newly diagnosis	25	10.0
Insulin	87	34.8
OHD (oral hypoglycemic drugs)	138	55.2
Duration of diabetes (years)		
Range	0.00-45.00	
Mean ± SD	9.46 ± 7.84	

Table (1b): Distribution of the studied cases according to BMI:

BMI(kg/m^2)	No.	%
< 25	116	46.4
25 – 29	114	45.6
≥ 30	20	8.0

Table (2) shows past history of the studied cases. Past history of HTN was found in 44.8%, CVS in 4.0%, hyperthyroidism in 1.2%, hypothyroidism in 6%, IHD in 20.0%, bronchial asthma in 5.6%, and pituitary disorders in 0.8%.

Laboratory findings:

Table (3a) shows the results of some of laboratory finding in studied cases:

1. Serum lipids:

19.2% of all diabetic patients had serum cholesterol level above the cut point of 200 mg/dl, 80.8% had serum cholesterol level < 200mg/dl. 16.4% of studied cases had triglyceride level ≥ 150 mg/dl, 83.6% had TG < 150 mg/dl.

2. Glycaemic levels:

Table (3b), shows that 78.4 % of the diabetic patients had random blood glucose (RBG) ≥ 200 mg/dl which considered as inadequate glycemic control.

Table (2): Distribution of the studied cases according to past history

	No.	%
HTN	112	44.8
CVS	10	4.0
History of hyperthyroidism	3	1.2
History of hypothyroidism	15	6.0
IHD	50	20.0
Bronchial asthma	14	5.6
Pituitary disorders	2	0.8

HTN: hypertension CVS: cerebrovascular stroke IHD: ischemic heart disease

Table (3a): Distribution of the studied cases according to different laboratory findings:

	Range	Mean ± SD
Temp	36.00-40.00	37.34 ± 0.54
Hb (g/dl)	4.00-18.00	11.38 ± 2.39
WBCs ($\times 10^3/\mu l$)	4.20-51.10	12.46 ± 6.24
Normal	124 (49.6%)	
Leucocytosis	126 (50.4%)	
BUN(mg/dl)	5.00-270.00	44.53 ± 42.68
Serum Cr(mg/dl)	0.4-12.00	1.83 ± 1.94
Cholesterol(mg/dl)	90.00-300.00	137.18 ± 61.86
< 200	202 (80.8%)	
≥ 200	48 (19.2%)	
TG(mg/dl)	55.00-398.00	96.40 ± 53.07
< 150	209 (83.6%)	
≥ 150	41 (16.4%)	
ALT(u/l)	10.00-939.00	51.80 ± 93.09
AST(u/l)	8.00-853.00	44.95 ± 87.08

Table (3b): Distribution of the studied cases according to random blood glucose

	Controlled (<200mg/dl)		Uncontrolled (≥ 200mg/dl)	
	No.	%	No.	%
RBG	54	21.6	196	78.4
Range	31.00 – 190.00		200.00 – 1136.00	
Mean ± SD	137.40 ± 43.12		405.76 ± 179.65	

Blood pressure levels:

Table (4) shows that 24.8% of the diabetic patients had systolic hypertension (systolic B.P ≥140 mm Hg) and 27.2% had diastolic hypertension (diastolic B.P ≥90 mm Hg).

Table (4): Distribution of the studied cases according to systolic and diastolic blood pressure:

	No.	%
Systolic BP(mmHg)		
Range	60.00-230.00	
Mean ± SD	127.02 ± 30.72	
Systolic HTN (≥140mmHg)	62	24.8
Diastolic BP(mmHg)		
Range	20.00-140.00	
Mean ± SD	76.73 ± 16.72	
Diastolic HTN (≥90mmHg)	68	27.2

Clinical examination and investigations:

Table (5) shows that 59.2% of patients had normal electrocardiogram (ECG) while the remaining had positive finding either new or old ischemic changes or arrhythmia.

Table (6) shows that 67.2% had normal fundus examination while 20.8% of diabetic patients had non proliferative or background diabetic retinopathy and 12% had proliferative retinopathy.

Table (7) shows the result of neurological examination among studied cases, 52.8% had positive neurological signs ranging from glove and stock parathaesia, loss of ankle reflex and loss of vibration sense, while 47.2% had normal neurological examination.

Urinary albumin excretion:

Table (8a) show that 58.8% of patients had normal level of urinary albumin excretion (<30 mg/24 hour urine), 35.6% had microalbuminuria (30 -300 mg/24 hour urine) and 5.6% had macroalbuminuria (≥ 300 mg/24 hour urine).

Table (8b) shows that 52.4% of patients who had microalbuminuria had end stage renal disease, 38.8% were chronic renal failure with regular renal dialysis and 13.6% were acute renal failure , only 1.9% of them had dialysis .The rest of patients had normal renal function .

Table (9) show that interdigital fungus infection was the most common finding (14.4%). Foot ulcers of different sizes and depths were found in 1.6% and evidences of ischemic changes in 3.2%. Amputations ranging from one toe amputation to complete foot amputation or more extensive limb amputation were found in 6% of cases.

Table (5): Distribution of the studied cases according to ECG finding

	No.	%
Arrhythmia	24	9.6
STEMI	29	11.6
NSTEMI	12	4.8
Old ischemia	39	15.6
Normal ECG	148	59.2

STEMI: ST segment elevation myocardial infraction
NSTEMI: Non ST segment elevation myocardial infraction

Table (6): Distribution of the studied cases according to fundus examination.

	No.	%
Fundus examination		
Normal	168	67.2
Non proliferative	52	20.8
Proliferative	30	12.0

Table (7): Distribution of the studied cases according to examination of peripheral neuropathy

	No.	%
Neurological		
Free	118	47.2
+ve	132	52.8

Table (8a): Distribution of the studied cases according to urinary albumin excretion rate

	NO.	%
Albuminuria (mg/24hour urine)		
Range	6.00-984.00	
Mean ± SD	78.01 ± 120.77	
Normal <30mg/24hour urine	147	58.8
Micro30-300 mg/24hour urine	89	35.6
Macro ≥300mg/24hour urine	14	5.6

Table (8b):Distribution of studied cases with albuminuria (n= 103) according to the presence of renal impairment

	No.	%
With RF	**54**	**52.4**
Acute	**14**	**13.6**

On dialysis	2	1.9
No dialysis	12	11.7
chronic	**40**	**38.8**
On dialysis	40	38.8
No dialysis	0	0.0
Without RF	**49**	**47.6**
Microalbuminuria	47	45.6
Macroalbuminuria	2	1.9

Table (9): Distribution of the studied cases according to foot examination.

	No.	%
Foot complication		
Foot infection	36	14.4
Foot amputation	15	6.0
Foot ulcers	4	1.6
Ischemic changes	8	3.2

Complication of DM:

In the present study 4.4% of diabetic patients had no complications and 95.6% had complications, 14.4% had single acute complications, 10.8% had single chronic complications , 54% had multiple chronic complications and 16.4% had combinations of acute and chronic complications (Table 11).

Acute complications:

Diabetic ketoacidosis:

Ketoacidosis ranging from mild short ketonuria to severe ketoacidosis associated with coma was found in 23.6% of patients(Table 10) . 15.2% were type 1 and 8.4% were type 2 DM (Table 16).

Hypoglycemia:

Table (10) shows 3.2% of patients had hypoglycemia. All hypoglycemic patients were type 2 table (16).

Non ketotic hyperosmelar hyperglycemia (NKHH):

Table (10) shows that 4% of studied patients admitted with NKHH , All patients were type 2 diabetes (16).

Chest infection:

Table (10) shows that 5.2% of the patient had chest infection, 4.8% were type2 and 0.4% were type1 DM (Table 16).

Chronic complications:

Macrovascular complications:

Cardiovascular complications:

34.8% of patients had cardiovascular complications in the form of heart failure ,acute coronary syndromes and , or arrhythmia (Table 10) , 33.2% were type 2 DM and 1.6% were type 1 DM (Table 16) .

Cerebrovascular complications:

Table (10) shows that 14.8% of studied cases had one attack of cerebrovascular stroke (CVS) , 13.2% were type 2 DM and 1.6% were type 1 DM (Table 16).

Microvascular complications:

Table 10 shows the distribution of studied cases according to the presence of chronic microvascular complications.

Neuropathy:

56% of patients had neuropathy, 52.8% of them had somatic neuropathy and10% had autonomic neuropathy. 52% of this cases were type 2 DM and 4% were type 1 DM (Table 16).

Nephropathy:

The results revealed that 41.2% of patients had urinary albumin excretion more than 30 mg/24 hour urine table (10) , 35.6% were type 2 DM and 5.6% were type 2 DM (Table 16).

Table (12) ,and fig.(14) show that serum creatinine in patients with normal albumin excretion rate ranged from 0.5- 2.70 mg/dl with a mean of 0.94±0.43 mg/dl, in patients with microalbuminuria 0.4- 9.60 mg/dl with a mean of 2.51±2.05 mg/dl and in patients with macroalbuminuria 0.4- 12.0 mg/dl with a mean of 5.34±3.03 mg/dl. Table (12) also shows that there was significant relation between serum creatinine and urinary albumin excretion rate in detecting renal function integrity.

Retinopathy:

Table (10) shows that 32.8% of cases had diabetic retinopathy, 24.4% were type 2 DM and 8.4% were type 1 DM (Table 16).

Other complications:

Diabetic foot: 25.2% of patients had diabetic foot (Table 10) either fungal infection, ulcers , ischemic

changes and amputations. 22.8% were type 2 DM and 2.4% were type 1 DM (Table 16).

Relation between BMI and different metabolic parameters:

Table (13) and show the relation between the BMI and some risk factors as systolic HTN, diastolic HTN, hyperglycemia, hyperlipidemia. There was positive correlation between BMI and increase in serum cholesterol and TG. But there was no significant correlation between BMI and systolic HTN, diastolic HTN, and hyperglycemia.

Relation between microvascular complications and different metabolic parameters:

Table (14a) show that there is significant association (P≤0.05) between microvascular complications and systolic HTN, diastolic HTN, hyperglycemia, S. cholesterol ≥ 200mg/dl, and S. TG ≥150mg/dl.

Table (14b) shows the correlation between microvascular complications and these metabolic parameters. There is positive correlations between retinopathy and blood pressure (P≤0.05). Also retinopathy is positively correlated with RBG, S. cholesterol, and S.TG.

Diabetic neuropathy is positively correlated with blood pressure, RBG, S. cholesterol, and S.TG.

Diabetic nephropathy is positively correlated with blood pressure, RBG, S. cholesterol, and S. TG.

Table (10): Distribution of the studied cases according to complications

	No.	%
Acute complications	77	30.8
DKA	59	23.6
Hypoglycemia	8	3.2
NKHH	10	4.0
Chronic complications	203	81.2
Microvascular	186	74.4
Retinopathy	82	32.8
Neuropathy	140	56.0
Somatic neuropathy	132	52.8
Autonomic neuropathy	25	10.0
Nephropathy	103	41.2
Macrovascular	139	55.6
Cardiovascular	87	34.8
CVS	37	14.8
Other		
Diabetic foot	63	25.2
Chest infection	13	5.2

Table (11): Distribution of the studied cases according to single and multiple complications

	No.	%
Acute (n=77)		
Single	77	100.0
Chronic (n=203)		
Single	52	25.6
Multi	151	74.4
Complications		
No complications	11	4.4
Single (acute)	36	14.4
Single (chronic)	27	10.8
Multi (chronic)	135	54.0
Multi (acute + chronic)	41	16.4

Relation between macrovascular complications and different metabolic parameters:

Table (15), and show that there is significant association (P≤0.05) between macrovascular complications and systolic HTN, diastolic HTN, hyperglycemia, S. cholesterol ≥200mg/dl, and S. TG ≥150mg/dl.

Table (15b) shows the correlation between macrovascular complications and these metabolic parameters. There is positive correlations between cardiovascular complications and blood pressure. Also cardiovascular complications are positively correlated with RBG, S. cholesterol, and S.TG.

CVS is positively correlated with blood pressure, RBG, S. cholesterol, and S.TG.

Relation between diabetic foot complications and different metabolic parameters:

Table (15), show that there is significant association between diabetic foot complications and systolic HTN, diastolic HTN, hyperglycemia, S. cholesterol ≥200mg/dl, and S. TG ≥150mg/dl.

Table (15b) shows that there is positive correlations between diabetic foot complications and blood pressure, RBG, S. cholesterol, and S.TG.

Table (12): Relation between serum creatinine and urinary albumin excretion rate

	Normal	Micro	Macro
Serum creatinine Range	0.5-2.70	0.4-9.60	0.4-12.00
Mean ± SD	0.94 ± 0.43	2.51 ± 2.05	5.34 ± 3.03
χ^2 (p)	82.401* (<0.001)		
Z_1 (p)		7.414* (<0.001)	6.301* (<0.001)
Z_2 (p)			4.001* (<0.001)

χ: Chi square for Kruskal Wallis test
Z_1 : Z for Mann Whitney test between normal with micro and macroalbuminuria
Z_2 : Z for Mann Whitney test between micro and macroalbuminuria

- : Statistically significant at $p \leq 0.05$
-

Table (13): Correlation between BMI with systolic HTN, diastolic HTN, hyperglycemia, and hyperlipidemia

	R	P
Systolic HTN	0.007	0.910
Diastolic HTN	0.060	0.345
RBG	-0.027	0.667
Cholesterol	0.380*	<0.001
TG	0.276*	<0.001

r: Pearson coefficient * : Statistically significant at $p \leq 0.05$

Table (14a): Relation between retinopathy, neuropathy, nephropathy with systolic HTN, diastolic HTN, hyperglycemia, hyperlipidemia

	Retinopathy		Neuropathy		Nephropathy	
	No.	%	No.	%	No.	%
Systolic HTN	18	7.2	48	18.0	35	14.0
p	0.001*		0.002*		0.005*	
Diastolic HTN	19	7.6	49	19.6	38	15.2
p	0.002*		0.002*		0.004*	
RBG(>200mg/dl)	25	10.0	99	39.6	90	36.0
p	0.008*		0.001*		0.004*	
Cholesterol (>200mg/dl)	14	5.6	37	14.8	26	10.4
p	0.006*		0.001*		0.042*	
TG(>150mg/dl)	11	4.4	32	12.8	23	9.2
p	0.039*		0.002*		0.034*	

p: p value Chi square test * : Statistically significant at $p \leq 0.05$

Table (14b): Correlation between systolic BP, Diastolic BP, RBG, S. cholesterol and S. TG with retinopathy, neuropathy and nephropathy:

		Retinopathy	Neuropathy	Nephropathy
Systolic BP (mmHg)	**r**	0.289*	0.268*	0.265*
	p	<0.001	<0.001	<0.001
Diastolic BP (mmHg)	**r**	0.295*	0.244*	0.158*
	p	<0.001	<0.001	0.012
RBG (mg/ dl)	**r**	0.242*	0.134*	0.264*
	p	<0.001	0.035	<0.001
S. cholesterol (mg/ dl)	**r**	0.306*	0.203*	0.192*
	p	<0.001	0.001	0.002
S. TG (mg/ dl)	**r**	0.275*	0.226*	0.145*
	p	<0.001	<0.001	0.022

r: Pearson coefficient * : Statistically significant at $p \leq 0.05$

Table (15a): Relation between foot, cardiovascular and CVS with systolic HTN, diastolic HTN, hyperglycemia, hyperlipidemia

	Foot		cardiovascular		CVS	
	No.	%	No.	%	No.	%
Systolic HTN	19	7.6	36	14.4	20	8.0
p	0.255		<0.001*		<0.001*	
Diastolic HTN	21	8.4	35	14.0	17	6.8
p	0.206		0.001*		0.006*	
RBG(>200mg/dl)	54	21.6	62	24.8	24	9.6
p	0.103		0.045*		0.030*	
Cholesterol (>200mg/dl)	18	7.2	27	10.8	12	4.8
p	0.029*		0.001*		0.029*	
TG(>150mg/dl)	15	6.0	24	9.6	11	4.4
p	0.066		<0.001*		0.018*	

p: p value Chi square test * : Statistically significant at $p \leq 0.05$

Table (15b): Correlation between systolic BP, Diastolic BP, RBG, S. cholesterol and S. TG with foot, cardiovascular and CVS

		Foot complications	Cardiovascular complications	CVS
Systolic BP (mmHg)	**r**	0.163*	0.228*	0.169*
	p	0.010	<0.001	0.007
Diastolic BP (mmHg)	**r**	0.213*	0.173*	0.135*
	p	0.001	0.006	0.032
RBG (mg/ dl)	**r**	0.196*	0.136*	0.259*
	p	0.002	0.031	<0.001
S. cholesterol (mg/ dl)	**r**	0.165*	0.323*	0.182*
	p	0.009	<0.001	0.004
S. TG (mg/ dl)	**r**	0.140*	0.304*	0.205*
	p	0.027	<0.001	0.001

r: Pearson coefficient * : Statistically significant at $p \leq 0.05$

Relation between type of diabetes and development of diabetic complications:

DKA was significantly higher in patients with type 1 diabetes than those with type 2 diabetes. Diabetic retinopathy, nephropathy, neuropathy, foot complications, and cardiovascular complications were significantly higher in patients with type 2 diabetes than those with type 1 diabetes. There is no significant difference in hypoglycemia, NKHH, chest infection, and CVS between type 1 and type 2 diabetes (Table 16).

Relation between duration of diabetes and development of different complications:

There was negative correlation between DKA and duration of diabetes,. But, there was positive correlations between duration of diabetes and retinopathy,; neuropathy; foot complications,; cardiovascular; and cerebrovascular complications, , (Table 17). There was no significant correlations between duration of DM and nephropathy.

Table (18), show that all studied cases who had diabetes for more than 10 years had complications, and when the duration increased there were increase risk to develop more than one chronic complications as 41.3% of patients who had diabetes for less than 10 years had multiple chronic complications, 15.4% had single chronic complication. And those who had diabetes for more than 20 years no one had single chronic complication, and all patients had multiple complications either multiple chronic 84.2% or multiple acute and chronic 15.8%.

Table (19), show that hyperglycemia was significantly high ($p<0.05$) between patients with single acute, single chronic, multiple acute, and multiple chronic complications and patients with no complications. however hyperglycemia had no significant difference on development single or multiple chronic complications.

Table (16): Relation between type of diabetes and development of diabetic complications :

	Type of diabetes				Test of sig.
	Type I		Type II		
	No.	%	No.	%	
DKA	38	15.2	21	8.4	χ^2= 98.386* p <0.001
Hypoglycemia	0	0.0	8	3.2	FEp= 0.361
NKHHG	1	0.4	9	3.6	FEp= 0.692
Retinopathy	21	8.4	61	24.4	χ^2= 23.340* p <0.001
Neuropathy	10	4.0	130	52.0	χ^2= 31.333* p <0.001
Nephropathy	14	5.6	89	35.6	χ^2= 4.012* p= 0.045
Chest infection	1	0.4	12	4.8	FEp= 0.473
Foot	6	2.4	57	22.8	χ^2= 5.426* p= 0.020
Cardiovascular	4	1.6	83	33.2	FEp <0.001*
CVS	4	1.6	33	13.2	FEp= 0.181

χ^2: Chi square test FEp : p value for Fisher Exact test * : Statistically significant at $p \leq 0.05$

Table (17): Correlation between duration of diabetes with complication

	R	P
DKA	-0.177*	0.005
Hypoglycemia	0.101	0.110
NKHHG	-0.084	0.186
Retinopathy	0.487*	<0.001
Neuropathy	0.512*	<0.001
Nephropathy	0.056	0.376
Chest infection	-0.115	0.069
Foot	0.392*	<0.001
Cardiovascular	0.194*	0.002
CVS	0.178*	0.005

r: Pearson coefficient * : Statistically significant at $p \leq 0.05$

Table (18): Relation between complications with duration and type of diabetes

	Complications									
	No complications		Single (acute)		Single (chronic)		Multi (chronic)		Multi (acute + chronic	
Duration										
<10 (n= 143)	11	7.7	26	18.2	22	15.4	59	41.3	25	17.5
10-20 (n= 88)	0	0.0	10	11.4	5	5.7	60	68.2	13	14.8
>20 (n= 19)	0	0.0	0	0.0	0	0.0	16	84.2	3	15.8
MCp	<0.001*									
Type of diabetes										
Type I (n= 49)	2	4.1	26	53.1	1	2.0	7	14.3	13	26.5
Type II (n=201)	9	4.5	10	5.0	26	12.9	128	63.7	28	13.9
MCp	<0.001*									

MCp: p for Monte Carlo test * : Statistically significant at $p \leq 0.05$

Table (19): Relation between RBG and complications

	No complications	Single (acute)	Single (chronic)	Multi (chronic)	Multi (acute + chronic)
Range(mg/dl	110.00-500.00	58.60-1122.00	110.00-576.00	60.00-594.00	31.00-1136.00
Mean ± SD	253.18 ± 111.85	484.49 ± 222.06	298.41 ± 102.86	298.45 ± 133.08	473.25 ± 283.93
Median	253.00	487.00	274.00	275.00	463.50
χ^2 (p)	38.765* (<0.001)				
Z_1 (p)		3.447* (0.001)	1.288 (0.198)	1.071 (0.284)	2.680* (0.007)
Z_2 (p)			3.957* (<0.001)	4.924* (<0.001)	0.271 (0.786)
Z_3 (p)				0.378 (0.706)	3.010* (0.003)
Z_4 (p)					3.980* (<0.001)

χ: Chi square for Kruskal Wallis test

Z_1 : Z for Mann Whitney test between no complications with single (acute), single (chronic), multi (chronic) and multi (acute + chronic)

Z_2 : Z for Mann Whitney test between single (acute) with single (chronic), multi (chronic) and multi (acute + chronic)

Z_3 : Z for Mann Whitney test between single (chronic) with multi (chronic) and multi (acute + chronic)

Z_4 : Z for Mann Whitney test between multi (chronic) and multi (acute + chronic)

* : Statistically significant at $p \leq 0.05$

4. Discussion:

In the present study,78.4% of patients were uncontrolled and there was positive correlation between RBG and all diabetic complications, and significant association between hyperglycemia and these complications which denotes the great impact of glycemic level and the development and the progress of diabetic complications.

Glycaemic control is fundamental for the management of diabetes, and its improvement is associated with decrease of the rate of several diabetes complications. This was proved by the Diabetes Control and Complication Trial DCCT)[11] and the UK Prospective Diabetes Study (UKPDS)[12] studies.

In the present study, the glycaemic control was assessed from the latest random blood sugar values at the time of admission as in intensive care patients it was difficult to measure fasting and post prandial blood glucose values. It was demonstrated that high number 78.4% of our patients had random blood glucose ≥ 200 mg/dl which considered as inadequate glycaemic control. these findings are consistent with the results of anther study done on the epidemiology of diabetic complications in Egypt, as they found the frequency of patients exceeding the adequate levels were: fasting blood glucose 80.2%, and post prandial glucose 78.6%.[13]

Measuring glycsalated heamoglobin (Hb A1c) level is the perfect way to judge the state of glycaemic control, because it measures the average glycaemic level over a preceding period of 2-3 months and it avoids the misleading impressions from accidental high or low blood glucose values . However, we did not use this parameter because the test is somewhat costly and is not largely requested by the diabetes caring physicians.

Our study revealed that 27.2% of the patients exceeded the diastolic level of 80 mmHg and about 24.8% exceeded the systolic level of 130 mmHg. There are 44.8% of patients had past history of HTN. The great impact of HTN on developing different complications was observed by the significant positive correlation between BP and different complications ($P \leq 0.05$).

The association of hypertension with diabetes is an essential factor known to increase the risk of several complications of diabetes, including specifically cardiovascular complications ,retinopathy, and nephropathy. The recommended target level for adequate blood pressure control among diabetic patients by the ADA (American Diabetic Association) is < 130/80 mm HG [14] ,which was also our cut point for adequate control.

Hypertension is a highly co-morbid condition in diabetic patients. In a study conducted in Punjab, 53.8% of patients with diabetes had hypertension as compared to17.3% in non-diabetic counterparts[15]. Almost the same proportion of hypertension (52%) prevailed in study conducted in Islamabad in which upper limit of blood pressure for diagnosis was taken as 130/80 instead of 140/90 in the former [16] .

Control of body weight is a principal target in diabetes care. Obesity is recognized risk factor, not only for increasing the prevalence of diabetes in the community at large, but also for predisposing diabetic patients to failure of metabolic control and to an increased risk for development of various complications. In this study, more than half of the tested cases (53.6%) were overweight (BMI more than 25), the results of this study also confirm the close relation between obesity and both of hypertension and lack of metabolic control. We found among the very obese group (BMI>30) significantly higher percentages of diabetic patients who exceeded the adequate control cut points (in all

parameters: systolic B.P. 25%, diastolic B.P. 40% ,RBG 65%, total cholesterol 60%, and triglyceride 55%) than among the less obese or normal weight groups. We therefore should consider that in order to improve the overall control and to reduce the risk of complications , we should spare no efforts, through patient education, to keep body weights under closer control.

The present study 239 (95.6%) patients have developed complications either acute or chronic, single or multiple complications , 31.6% from type 1 DM and 65% from type 2 DM . The 2007 report released by the American Association of Clinical Endocrinologists (AACE), showed an estimated three out of five Americans with type 2 diabetes (57.9 percent) have one or more diabetes complications [17] .

In the present study, the most frequent complication is diabetic neuropathy, nephropathy followed by cardiovascular complications. There is an important age effect in the occurrence of diabetic complications. Diabetic ketoacidosis is the most common complication in the early years of life.

Diabetes itself is a risk factor for heart disease and stroke. In this study the incidence of cardiovascular complications was 34.8% and cerebrovascular complications was 14.8%. Also, many people with diabetes have other conditions that increase their chance of developing heart disease and stroke. One risk factor for heart disease and stroke is having abnormal blood fat (cholesterol , triglyceride) levels , having high blood pressure , and smoking.

In our study 44.8% of the patients have history of hypertension,31.2% are smokers. There was positive correlation between cardiovascular, cerebrovascular complications and blood pressure, RBG, serum TG, and serum cholesterol.

The analysis of possible risk factors revealed a significant association between the presence of macrovascular disease and presence of hypertension among the surveyed diabetic population ($p < 0.005$). This is consistent with results from studies in other settings elsewhere. For example, in Spain, a large multicenter, outpatient clinics cross sectional population study, on hypertensive and type 2 DM patients, evaluating the risk of cardiovascular disease and renal damage using ECG-LVH, GFR and/or urinary albumin excretion, was able to establish an increased prevalence of cardiovascular disease in patients with hypertension and type 2 DM [17]

Both in type 1 and type 2 DM it has become increasingly clear that multiple risk factors may be as important as hyperglycemia. A study, comprising two extreme groups, *i.e.* patients with early onset(microangiopathy within 5 years duration) and those with late protection (without microangiopathy even after 14 years) showed that the former group had higher prevalence of associated conditions like hypertension, hyperlipidemia, poor glycemic control, obesity, and smoking indicating their positive correlation with development of micro vascular complications [18] .

In our study the incidence of diabetic neuropathy was 56.0%. In a report on the epidemiology of diabetic neuropathy[19] ,it was noted that the inconsistency in the selection of diagnostic procedures makes it difficult to compare results of different studies. In our study as all our patient were intensive care units patients and their general conditions varies from fully conscious , to comatose patients the results of our neurological examinations may carry false negative results. In fact the precise prevalence of diabetic neuropathy has been always very difficult to determine. A prevalence of as high as 50% was reported from a US population study[20,21] and a prevalence of 30% in European and African populations[22,23].

People with diabetes can develop nerve problems at any time, but risk rises with age and longer duration of diabetes. The highest rates of neuropathy are among people who have had diabetes for at least 25 years. In our study 94.7% of patients who had diabetes for more than 20 years had neuropathy, there is positive correlation between duration of diabetes and development of diabetic neuropathy.

Diabetic neuropathies also appear to be more common in people who have problems controlling their blood glucose, as well as those with high levels of blood fat and blood pressure and those who are overweight. In our study we found 39.6% of patients who had neuropathy had uncontrolled hyperglycemia. Also we found positive correlation between neuropathy and RBG, The relation between hyperglycaemia and development of severity of neuropathy has been shown in retrospective and prospective studies, a classic study on 440 diabetic patients who were followed up over 25 years, showed an increase in clinically detectable diabetic neuropathy from 12% at the time of diagnosis of diabetes to about 50% after 25 years and those with poorest diabetic control had the highest prevalence [24]. Also in the present study we found positive correlation between diabetic neuropathy and blood pressure, and significant association between them, Previous observational studies have investigated the link between hypertension and sensorimotor peripheral neuropathy (SMPN) in type 2 diabetes **Valensi *et al*.**[25] showed that the presence SMPN correlated with the presence of retinopathy, hypertension, and macroangiopathy. Logistic regression analysis showed that age, diabetes duration, presence of retinopathy, body mass index, metabolic control, and duration of hypertension were independently associated with SMPN[26] .

Somatic peripheral neuropathy is the commonest type of diabetic neuropathy, in our study

the incidence of somatic neuropathy was 52.8%, and autonomic neuropathy was 10%, most of the patients suffering from autonomic neuropathy were having in the same time somatic neuropathy.

Data from 12 countries in the Asian Pacific region, including Australia and New Zealand, showed an increase in both incidence and prevalence of diabetic nephropathy between1998 and 2000 [27]. The prevalence of diabetic nephropathy as a cause of ESRD in Egypt has previously been examined in 2 small cross-sectional studies with conflicting results[28,29]. Other reports on prevalence of diabetic nephropathy also produced the following widely divergent figures: 8.4% [30], 13.7%[31], 20.1% [32] and 8.9% [33].

In our study the incidence of nephropathy was 41.2%, 35.6% had microalbuminuria , and 5.6% had macroalbuminuria.

Diabetes is the most common cause of kidney failure, accounting for nearly 44 % of new cases [34]. Even when diabetes is controlled, the disease can lead to CKD and kidney failure. Nearly 24 million people in the United States have diabetes,[35] and nearly 180,000 people are living with kidney failure as a result of diabetes [34] .Diabetic kidney disease takes many years to develop. In some people, the filtering function of the kidneys is actually higher than normal in the first few years of their diabetes.

In our study 52.4% of patients who had albuminuria were having renal failure, 13.6% of them had acute renal failure and 38.8% had chronic renal failure.

Overall, kidney damage rarely occurs in the first 10 years of diabetes, and usually 15 to 25 years will pass before kidney failure occurs. For people who live with diabetes for more than 25 years without any signs of kidney failure, the risk of ever developing it decreases. In this study 46.6% of patients had diabetes for 10 to 20 years had diabetic nephropathy, and 52.6% of patients had diabetes for more than 20 years had nephropathy. this clearly proves that the incidence of nephropathy increase with long duration of diabetes. As we found positive correlation between diabetic nephropathy and duration of DM, blood pressure, RBG, and serum lipids.

In our study 35.6% of diabetic nephropathy were type 2 DM, and 5.6% were type 1 DM.

Almost everyone with diabetes develops this complication, but the first to feel its impact are people with type I diabetes, who frequently develop a mild form of this condition within five years of diagnosis of diabetes. In fact, there's a strong correlation between duration of diabetes and the development of retinopathy. the longer the duration of diabetes, the greater the chance of developing retinopathy. This is proved in the present study as we found positive correlation between duration and developing retinopathy and the stage of retinopathy. In our study 32.8% of diabetic patients had retinopathy , 20.8% had non proliferative retinopathy, 12% had proliferative retinopathy.

Hyperglycemia, and hypertension are important risk factors to develop diabetic retinopathy. In our study we found significant association and positive correlations between these risk factors and retinopathy, which confirm that good control to these metabolic variants reduce the development of diabetic retinopathy. Earlier studies have suggested that there is a positive relationship between hypertension and the incidence or progression of diabetic retinopathy [36-38]. Also several studies have shown that normalizing blood glucose over time can significantly reduce one's risk of developing advanced stages of retinopathy [39].

Our study shows that there is positive correlations between serum cholesterol and diabetic retinopathy. The WESDR (Wisconsin Epidemiologic Study of Diabetic Retinopathy) also demonstrated a correlation between serum cholesterol and risk of retinopathy in the diabetic population generally[40].

Better glycaemic control has been established by the DCCT and by UK PDS to reduce the risk of development and progress of diabetic retinopathy[14,32]. Tight blood pressure control has been also shown to reduce effectively the progression of retinopathy.

In a pilot study conducted in Karachi on 3000 diabetic patients, it was shown that 780 (26%) of the patients were affected with retinopathy[41]. Similarly, Ramachandra studied 3010 type 2 diabetic patients noted a prevalence of 23.7% retinopathy, 19.7 % nephropathy, and 27.5% peripheral neuropathy. Duration of diabetes, poor glycemic control and hypertension were shown significantly associated with the complications in his study[42,43]. In contrast our study has demonstrated significantly high frequency of each complication

In the present study the prevalence of diabetic foot is 25.2%. 6% of studied patients had foot amputations,14.4% had foot infection, 1.6% had foot ulcer, and 3.2% had ischemic changes. Compared to a cross-sectional study done in 4 general practitioner practices in the Netherlands showed that the prevalence of an infected foot lesion or ulcer in patients with diabetes was 3% [44]. An other study showed that 5% had an ulcer or had undergone an amputation [45].

References

1. American Diabetes Association. (2005). Diagnosis and Classification of Diabetes Mellitus. Diabetes Care; 28:S37-42.
2. National Diabetes Fact Sheet. (2005). National Center for Disease Prevention and Health Promotion. Available at: http://www.cdc.gov/ diabetes/ pubs/ factsheet. htm. Accessed January 4, 2005.
3. Smith, D. (2000). Report of the expert committee on the diagnosis and classification of diabetes mellitus," 1183-97.
4. Tuomilehto J, Lindström J, Eriksson JG, *et al.* (2001)."Prevention of type 2 diabetes mellitus by changes in lifestyle among subjects with impaired glucose tolerance," The New England Journal of Medicine; 344:1343-50.
5. Fishbein H, Palumbo PJ(1995). Acute metabolic complications in diabetes. In: National Diabetes Data Group. Diabetes in America. Bethesda (MD): National Institutes of Health, National Institute of Diabetes and Digestive and Kidney Diseases; 283-91.
6. Pain DJ, Lewis SA, Pates I. Basic hematological technique. (2006). In: Dacie J , Lewis SM, editors. Practical hematology. Tenth edition. Philadelphia, Churchill Livingstone; 25-57.
7. Freeman VS. Carbohydrate. (2005). In: Bishop ML, Fody EP, Schoeff L, ed. Clinical Chemistry: principles, procedures, correlations. Fifth edition. Philadelphia: Lippincott Williams and Wilkins.; 226-80.
8. Frank EL. Nonprotein nitrogen compounds. (2005). In: Bishop ML, Fody EP, Schoeff L, ed. Clinical Chemistry: principles, procedures, correlations. Fifth edition. Philadelphia: Lippincott Williams and Wilkins.; 219-35.
9. Shumann G, Bonora R, Ceriotti F. (2002). Primary reference procedures for the measurement of catalytic activity concentrations of alanine aminotransferase and aspartate aminotransferase. Clin Chem Lab Med; 40:718-33.
10. Rifai N, Dominiczak M, Warnick GR. (2000). Handbook of lipoprotein testing. 2nd edition. Washington AACC Press.
11. Diabetes Control and Complications Trial Research Group(1993). The effect of intensive treatment of diabetes on the development and progression of long term complications in insulin dependant diabetes mellitus. N Eng. J. Med.; 329:997-86.
12. UK Prospective Diabetes Study (UK PDS) Group(1998). Intensive blood glucose control with sulphonylureas or insulin compared with conventional treatment and risk of complications with type 2 diabetes. Lancet.; 352:837-53.
13. Arab M, El kafrawy N, Rifaie MR, Shahwan MM, Kamel M, Abou Bakr F(2002). Epidemiology of diabetes complications in Egypt. The Egyptian Journal of Diabetes.7 (2):50 -53.
14. American Diabetes Association Standards of Medical Care for patients with Diabetes Mellitus. Diabetes Care 2003; 26 (suppl. I):S33-S50.
15. Raza M, Mehboob A and Qais MS(2000). Prevalence of hypertension in Punjab. *PJMR*; 39 (3): 103-6.
16. Shafiqur-Rahman, Irfan Zia(2004). Prevalence of micro vascular complications among diabetic patients. Pakistan J.Med. Res.; 4: 43.
17. Cea-Calvo L, Conthe P, Gomez-Fernandez P, de Alvaro F, Fernandez-Perez C(2006). Target organ damage and **cardiovascular** complications in patients with hypertension and type 2 diabetes in Spain : a cross-sectional study. *Cardiovasc Diabetol.*; **5:**23.
18. American Association of Clinical Endocrinologists. AACE (2007). Medical Guidelines for Clinical Practice for the Management of Diabetes Mellitus .
19. Shaw JE, Zimmet(1999). The epidemiology of diabetic neuropathy Diabetic Reviews; 7:245-52.
20. Adler AL, Boyko EJ, Ahroni JH, Stensel V, Forsberg RC, Smith DG(1997). Risk factors for diabetes peripheral sensory neuropathy. Results of the Seattle prospective diabetic foot study, Diabetes Care; 20: 1162-7.
21. Forrest KY, Maser RE, Pambianco G, Becker DJ, Orchard JJ(1997). Hypertension as a risk factor for diabetic neuropathy. A prospective study. Diabetes; 46:665-70.
22. Young MJ, Breddy JL, Veves A, Boultin AJ(1994). The prediction of diabetic neuropathic foot ulceration using perception thresholds: A prospective study. Diabetes Care; 17:557-60.
23. Fedele D, Comi G, Coscelli C, Cucinotta D, Feldman EL, Ghirlanda G(1997). Amulticenter study on the prevalence of diabetic neuropathy in Italy. Italian Diabetic Neuropathy Committee. Diabetes Care; 20:836-43.
24. Pirart J(1977). Diabetes mellitus and its degenerative complications: a prospective study of 4400 patients observed between 1947 and 1973 (third and last part). *Diabetes Metab.*, 3245–256.
25. Valensi P, Giroux C, Seeboth-Ghalayini B, Attali JR(1997). Diabetic peripheral neuropathy: effects of age, duration of diabetes, glycemic control, and vascular factors. J Diabetes Complications; 11: 27–34.

26. Cohen JA, Jeffers BW, Faldut D, Marcoux M, Schrier RW(1998). Risks for sensorimotor peripheral neuropathy and autonomic neuropathy in non-insulin-dependent diabetes mellitus. Muscle Nerve; 21: 72–80.
27. Lee G(2003). End-stage renal disease in the Asian-Pacific region. *Seminars in nephrology*, , 23(1):107–14
28. Arab M(1992). Diabetes mellitus in Egypt. *World health statistics quarterly*, 45(4): 334–7.
29. Herman WH Ali MA, Aubert RE, Engelgau MM, *et al (*1995). Diabetes mellitus in Egypt: risk factors and prevalence. Diabetic medicine, , 12(12):1126–31.
30. El-Sharkawi M(1996). Changing pattern of etiology of chronic renal failure among dialysis patients [thesis]. Cairo, Ain Shams University.
31. Ibrahim T(1998). Etiology of chronic renal failure among a sample of Egyptian population [thesis]. Cairo, Ain Shams University.
32. Ahmed T(1991). Clinical and laboratory features of patients with chronic renal failure at the start of dialysis [thesis]. Cairo, Ain Shams University.
33. Afifi A, Karim MA(1996). Renal replacement therapy in Egypt: first annual report of the Egyptian Society of Nephrology,.
34. United States Renal Data System. USRDS (2007). Annual Data Report. Bethesda, MD: National Institute of Diabetes and Digestive and Kidney Diseases, National Institutes of Health, U.S. Department of Health and Human Services; 2007.
35. National Institute of Diabetes and Digestive and Kidney Diseases. National Diabetes Statistics, 2007. Bethesda, MD(2008): National Institutes of Health, U.S. Department of Health and Human Services.
36. Knowler WC, Bennett PH, Ballantine EJ(1980). Increased incidence of retinopathy in diabetes with elevated blood pressure. *N Engl J Med.*; 301:645–50.
37. Chahal P, Inglesby DV, Sleightholm M, Kohner EM(1985). Blood pressure and the progression of mild background diabetic retinopathy. *Hypertension* 7 (Suppl. 2):79–83,.
38. Klein BEK, Klein R, Moss SE, Palta M(1995). A cohort study of the relationship of diabetic retinopathy to blood pressure. Arch Ophthalmol 113:601–606,.
39. Javitt JC. (1996). Cost-effectiveness of detecting and treating diabetic retinopathy. *Annals of Internal Medicine*; 124(1): 164-9.
40. Klein BEK, Moss SE, Klein R, Surawics TS(1992). Serum cholesterol in the Wisconsin epidemiologic study of diabetic retinopathy. Diabetes Care, 15:282-7.
41. Khan AJ(1991). Prevalence of diabetic retinopathy in Pakistani subjects- a pilot study. *JPMA*; 41: 49-50.
42. Ramachandra A, Snehaletrha C, Sathyavani K, Latha E and Vijay V(1999). Prevalence of vascular complications and their risk factors in type 2 DM. *J* Assoc Physicians *India*; 47 (12): 1152-6.
43. Karamanos B, Porta M, Songini M and EURODIAB IDDDM complication study group(2000). Different risk factors of microangiopathy in patients with type 1 DM of short vs. long duration. *Diabetologia*; 43: 348-55.
44. Crebolder HFJM(1985). De huisarts en de diabetische voet. In: Consensus bijeenkomst diabetische voet. Utrecht: CBO,: 2-11.
45. Verhoeven S, Ballegooije E van, Casparie AT(1991). Impact of late complications in type II diabetes in a dutch population. Diabet Med.; 8: 435-8.

11/20/2011

Using potato processing waste in sheep rations

Hamed A.A. Omer[1], Soha S. Abdel-Magid[1], Fatma M. Salman[1], Sawsan M. Ahmed[1], Mamdouh I. Mohamed[1], Ibrahim M. Awadalla[1] and Mona S. Zaki[2]

[1]Animal Production Department, National Research Center, Dokki, Giza, Egypt
[2]Hydrobiology Department, National Research Center, Dokki, Giza, Egypt
dr_mona_zaki@yhaoo.co.uk

Abstract: Twenty-seven male growing Rahmani lambs aged 6 months with an average weight 27.17 ± 0.31 kg were used to determine the effects of inclusion potato processing waste (PPW) on performance of Rahmani lambs. Animals divided into three equal groups and assigned for control and two experimental diets containing PPW which was at 0% PPW (TMR_1), 7% PPW (TMR_2), and 14% PPW (TMR_3), respectively. The results showed that dietary treatments had no significant effect on feed intake, while water intake insignificantly (P>0.05) increased. Digestibility coefficients of organic matter, crude protein and nitrogen-free extract significantly (P<0.05) improved. However, dietary treatment had no significant effect on dry matter and ether extract digestibilities. Values of total digestible nutrient significantly (P<0.05) increased while, digestible crude protein insignificantly (P<0.05) increased. Nitrogen retention was positive for all groups. Inclusion PPW in sheep rations had no significant effect on ruminal pH, ammonia nitrogen and total volatile fatty acid concentrations. Both ruminal NH_3-N and TVFAS concentrations were significantly (P<0.05) increased, while ruminal pH was significantly (P<0.05) decreased after 3 hours post feeding compared with before feeding. Molar proportion of volatile fatty acids and all blood plasma constituents insignificant affected. Final weight, body weight gain, and average daily gain were significantly (P<0.05) decreased, while feed conversion ratio insignificantly decreased. Total daily feeding costs of experimental rations were decreased. It could be concluded that potato processing waste can be successfully fed to lambs without any adverse effect on digestibility coefficients, ruminal fermentation, blood plasma constituents and performance. Also, PPW can be used economically in formulation of sheep rations.

[Hamed A.A. Omer, Soha S. Abdel-Magid[1], Fatma M. Salman, Sawsan M. Ahmed, Mamdouh I. Mohamed, Ibrahim M. Awadalla[1] and Mona S. Zaki**. Using potato processing waste in sheep rations]** Life Science Journal. 2011;8(4):733-742] (ISSN:1097-8135). http://www.lifesciencesite.com

Keywords: Potato processing waste, Sheep, Digestibility, Ruminal fermentation, Performance, Blood plasma constituents, Economical evaluation**.**

1. Introduction:

The total world potato waste production is estimated to 12 million tons per year (El-Boushy and Van der Poel 1994).

In Egypt, the yield of potatoes crop was two million tons (A.E.S.I. 2008). Smith and Huxsoll (1987) estimated the peeling losses of the potato chips industry which used abrasion peeling extensively to be 10%. Also, in Egypt, potato processing industry produced several by-products all the time of the year. In addition to the obtaining on potato by-products and transportation is easy and economical, but it needs to be dried to use it all the time of the year.

Potato waste is an excellent energy source for feedlot cattle. It has energy values similar to corn and barley while being low in protein and calcium. The biggest problem that has to be managed with potato waste is the water, where moisture content in potatoes are reach to 80 percent. In most feedlot rations silage is being used which could contain from 45 - 65 percent water as well. The water content of potato waste is not constant and it ranged from 72 to 83% (Murphy**,** 1997).

The starch in potato waste is fermented rapidly, limiting inclusion levels due to problems such as acidosis and bloat. Due to the wet nature of the product, spoilage can be a concern, especially during the summer (Radunz et al. 2003).

Potato waste is the product remaining after potatoes have been processed to produce frozen potato products for human consumption. The product can include peelings, cull potatoes, and other potato products. Potatoes have a feeding value similar to cereal grain but lower in CP. Potatoes are high in energy and low in protein and vitamin A. (Lardy and Anderson 2009).

Potatoes are primarily a source of energy, on a 100% dry matter (DM) basis, it has 81–82% total digestible nutrient (TDN) and only about 10% protein. The crude protein is in the form of non-protein nitrogen, and only 60% of the total may be digestible (Boyles, 2006). Because of potatoes' very low fiber content, it should not be considered a forage substitute but rather should be thought of as a

high moisture source of starch. Potatoes are quite low in protein content and, when given in high amounts without protein supplementation, will not give good animal performance or feed efficiency.

Toxic components of potato called glycoalkaloids (usually solanine and chaconine). Glycoalkaloids are normally found at low levels in the tuber, and occur in the greatest concentrations just beneath the skin (FAO, 2008).

Gado et al. (1998) reported that replacement of concentrate feed mixture by potato waste at level 25% of DM significantly increased digestibility of DM and nitrogen balance. Using potato by-product in growing goat ration saved 50% of yellow corn, which is used in the ration and used at 60% of the control ration without any adverse effect on goat performance (Omer and Tawila 2008). Potato products can be an economical substitute for grains (Murphy 1997 and Omer et al. 2010).

The main objectives of this study was to make a good cheap ration for growing Rahmani lambs and to investigate the effect of inclusion sun-dried potato processing waste on performance, digestion coefficients, rumen fermentation, blood plasma constituents and economical evaluation.

2. Materials and Methods

The present experiment was carried out at the Sheep and Goats' Units in El-Bostan area in Nubaria, which belongs to the Animal Production Department, National Research Center, Dokki, Giza, Egypt.

Experimental animals and feeds

Twenty-seven growing male Rahmani lambs, aged at approximately 6 months with average live weight of 27.17 ± 0.31 kg, were divided randomly into three equal groups (nine animals in each) and used to evaluate the effect of inclusion potato processing waste (PPW) at 0%, 7% and 14% of total mixed ration (TMR). The composition of different total mixed rations are presented in Table 1 The animals were individually fed with the experimental rations that cover the requirements for total digestible nutrients and protein for growing sheep according to the NRC (1985), and feed allowance was adjusted every 2 weeks according to their body weight changes. Animals were housed in individual semi-open pens. Experimental animals received one of the three experimental rations of PPW. The feeding trial lasted for 105 days, diets were offered twice daily (0700 and 1300 hours) while feed residues (if any) were removed and weighed once daily before morning feeding. Fresh water was available all the time in plastic containers. Water intake was recorded weekly. Live body weights were recorded weekly before morning feeding and after fasting overnight (feed and water). Potato processing waste was obtained from potato chips factory, Borg El-Arab city, Alexandria governorate, this potato processing waste composed of peel potatoes only.

Digestibility trials

At the end of the feeding experiment, five animals from each group were selected randomly and used to determine digestion coefficients and nutritive values of the experimental rations. The nutritive values expressed as the total digestible nutrients (TDN) and digestible crude protein (DCP) of the experimental rations were calculated according to Abou-Raya (1967).

Rumen fluid

Rumen fluid samples were collected from 15 animals (five animals for each treatment) at the end of the digestibility trial before feeding and 3 h post feeding via stomach tube and strained through four layers of cheesecloth to study the effect of dietary treatments on ruminal fermentations, ruminal pH, ammonia nitrogen (NH_3–N), total volatile fatty acid (TVFA) concentrations, and molar proportion of volatile fatty acids.

Blood plasma constituents

Blood samples were collected from the same lambs at the end of digestibility trials from the left jugular vein in heparinized test tubes at about 3 hours post feeding and centrifuged at 5.000 rpm for 15 minuets. Plasma were kept frozen at –20 °C for subsequent analysis of glucose, total proteins, albumin, urea, triglycerides and cholesterol.

Analytical procedures

Representative samples of ingredients, experimental rations, feces, and ruminal NH_3–N concentrations were analyzed according to A.O.A.C (1995) methods. Neutral detergent fiber (NDF), acid detergent fiber (ADF), and acid detergent lignin (ADL) were also determined in the ingredients and experimental rations according to Goering and Van Soest (1970) and Van Soest et al. (1991). NDF and ADF were expressed, inclusive of residual ash. Ruminal pH was immediately determined using digital pH meter. Ruminal TVFA concentrations were determined by steam distillation according to Kromann et al. (1967). Molar proportions of volatile fatty acids were determined according to Erwin et al. (1961). Plasma total proteins were determined as described (Armstrong and Carr, 1964); albumin (Doumas et al., 1971); urea (Patton and Crouch, 1977); triglycerides (Fossati and Principe, 1982); cholesterol (Allain et al., 1974) and Plasma glucose was measured using the enzymatic glucose oxidase

method (Bauer et al., 1974). Globulin and albumin: globulin ratio (A: G ratio) were calculated. Gross energy (mega calories per kilogram DM) was calculated according to Blaxter (1968), where, each gram of crude protein (CP) = 5.65 kcal, each gram of ether extract (EE) = 9.40 kcal, and each gram crude fiber (CF) and nitrogen-free extract (NFE) = 4.15 kcal.

Economic evaluation

The relation between feed costs and gain was calculated for the different experimental groups. The general equation by which the costs of 1 kg of live body weight gain was calculated as follows:
The cost for 1-kg gain = total cost (Egyptian pound (LE)) of feed intake/total gain (kilogram).

Statistical analysis

The analysis of variance for completely randomized design experiments using SAS (1998) examined the effects of dietary treatments. Differences among means were evaluated using Tukey's test.

3. Results and Discussion

Composition, chemical analysis, and cell wall constituents of feed ingredients and experimental rations

Results of chemical analysis and cell wall constituents of feed ingredients are presented in Table 1. The results showed that yellow corn recorded the highest values of organic matter (OM) and nitrogen-free extract (NFE) while wheat bran showed the lowest value of OM. On the other hand, undecorticated cotton seed meal showed the highest values of CP and the lowest value of NFE. While, pea straw (PS) showed the highest value of Neutral detergent fiber (NDF) and Acid detergent fiber (ADF), however PPW showed the highest values of hemi cellulose and lowest value of cellulose. Gross energy of potato processing waste (PPW) was nearly from yellow corn (4.274 vs. 4.423 Mcal/kg dry matter. These results were within the ranges obtained by Omer and Tawila (2008), Tawila et al. (2008) and Omer et al. (2010) who recorded that chemical composition of potato waste ranged from 40 to 146 g/kg DM for CP, 16 to 175 g/kg DM for CF, 780 to 820 g/kg DM for TDN, 400 to 415 g/kg DM for NDF, 58 to 64 g/kg DM for ADF, 36 to 42 g/kg DM for ADL, 323 to 347 g/kg DM for hemicellulose, and 25 to 43 g/kg DM for cellulose, respectively.

Composition, chemical analysis, and cell wall constituents of the experimental rations are presented in Table 2. Experimental rations were in the same trend of gross energy (GE). Hemicellulose content was increased while cellulose content was decreased by adding PPW in the diet. These results in agreement with those obtained by Omer et al. (2010).

Table 1 Chemical analysis and cell wall constituents of feed ingredients (g/ kg DM)

Item	Feed ingredients				
	PPW	UDCSM	YC	WB	PS
Dry matter (DM; g/kg)	941.1	878.8	913.0	902.0	942.9
Chemical analysis on DM basis					
Organic matter	965.4	942.0	988.0	883.0	885.6
Crude protein	129.2	248.2	93.0	140.0	115.1
Crude fiber	30.6	277.5	23.0	112.2	297.6
Ether extract	14.0	27.1	35.0	30.0	25.3
Ash	34.6	58.0	12.0	117.0	114.4
Nitrogen-free extract	791.6	389.2	837.0	600.8	447.6
Gross energy (Mcal/kg dry matter)	4.274	4.424	4.423	4.032	3.981
Cell wall constituents					
Neutral detergent fiber (NDF)	410.0	506.3	326.3	442.1	546.0
Acid detergent fiber (ADF)	63.0	361.8	224.5	321.6	425.0
Acid detergent lignin (ADL)	38.0	204.6	21.3	40.5	134.0
Hemi cellulose	347.0	144.5	101.8	120.5	121.0
Cellulose	25.0	157.2	203.2	281.1	291.0

Hemicellulose = NDF – ADF, Cellulose = ADF – ADL
PPW potato processing waste, *UDCSM* undecorticated cotton seed meal, *YC* Yellow corn, *WB* wheat bran, *PS* pea straw

Table 2 Composition (fresh kilogram per ton), chemical analysis and cell wall constituents (g/ kg DM) of the experimental rations

Item	Experimental rations		
	TMR_1	TMR_2	TMR_3
Composition (fresh kg/ton)			
Potato processing waste	000	70	140
Undecorticated cotton seed meal	240	205	168
Yellow corn	280	280	280
Wheat bran	150	135	122
Pea straw	300	280	260
Lime stone	20	20	20
Sodium chloride	7	7	7
Vit. and mineral mixture[a]	3	3	3
Price of ton (LE)	1,220	1,090	0,995
Chemical analysis (g/kg DM)			
Dry matter	913.8	916.6	920.5
Organic matter	933.8	934.6	938.1
Crude protein	141.1	137.0	132.8
Crude fiber	179.1	163.8	148.5
Ether extract	28.4	27.6	26.7
Nitrogen-free extract	585.2	606.2	630.1
Ash	66.2	55.4	61.9
GE (Mcal/ kg DM)	4.236	4.229	4.232
Cell wall constituents			
Neutral detergent fiber (NDF)	443.0	436.5	430.2
Acid detergent fiber (ADF)	325.4	303.9	282.2
Acid detergent lignin (ADL)	101.4	93.6	85.4
Hemi cellulose	117.6	132.6	148.0
Cellulose	224.0	210.3	196.8

LE= Egyptian pound equals 0.18 USS approximately, TMR_1 = control ration contained 0%potato processing waste, TMR_2 = second experimental ration contained 7% potato processing waste of total mixed ration, TMR_3 = third experimental ration contained 14% potato processing waste of total mixed ration.

[a] Each 3 kg vitamins and mineral mixture contains: vitamin A 12,000,000 IU, vitamin D3 2,200,000 IU, vitamin E 10,000 mg, vitamin K_3 2,000 mg, vitamin B_1 1,000 mg, vitamin B_2 5,000 mg, vitamin B_6 1,500 mg, vitamin B_{12} 10 mg, pantothenic acid 10 mg, niacin 30,000 mg, folic acid 1,000 mg, biotin 50 mg, choline 300,000 mg, manganese 6,0000 mg, zinc 50,000 mg, copper 10,000 mg, iron 30,000 mg, iodine 100 mg, selenium 100 mg, cobalt 100 mg, CaCo3 to 3,000 g.

Feed and water intakes, nutrient digestibility coefficients and nitrogen utilization by the experimental group lambs

Feed and water intakes, nutrient digestibility coefficients, and nitrogen utilization by the experimental group lambs are presented in Table 3. The results showed that inclusion PPW in the diet insignificant decreased (P>0.05) feed intake. Dry matter, total digestible nutrient and crude protein intakes were decreased gradually with increasing quantity of PPW in the TMR. The present results might indicate that the PPW had adverse effect on palatability. These results were in agreement with those obtained by Omer and Tawila (2008) and Omer et al. (2010) found no significant effect on feed intake when Baladi goats or Ossimi sheep fed diets replaced yellow corn by 25% and 50% PPW. Sugimoto et al. (2006) noted that dry matter intake increased (linear; P<0.01) as the feeding level increased and was not affected by the diet. Onwubuemeli et al. (1985) fed lactating Holstein cows for 12 wk rations contained, on a dry matter basis, 0, 10, 15, and 20% potato waste and were substituted for high moisture corn in diets. They noticed that substituting potato waste for corn did not significantly affect dry matter intake.

Increasing level of PPW in the diets leads to insignificantly increasing (P>0.05) water intake as ml/h/d or L/kg dry mater intake, whoever, it significantly increased (P<0.05) water intake as L/100 kg body weight. These results were in agreement with those obtained by Omer and Tawila (2008) who noted that replacement of yellow corn (60% of control diet) by PPW at 25% and 50% in Baladi goats insignificantly increased water intake. On contrast Omer et al. (2010) noted that increasing level of PPW in sheep diets leads to insignificantly decreasing (P>0.05) water intake.

Inclusion of PPW in the diet insignificantly (P<0.05) improved digestibility coefficients of DM and EE, however, it significantly improved (P<0.05) OM, CP and NFE digestibility coefficients. On the

other hand, except for OM digestibility increasing quantity of PPW in the diet from 7% to 14% had no significant effect on the other nutrients digestibility coefficients. Omer et al. (2010) reported that instead of 25% or 50% of yellow corn with PPW in sheep diets significantly (P<0.05) improved digestibility coefficients of (DM, OM and CP), while, dietary treatment had no significant effect on CF and NFE digestibilities. Tawila et al. (2008) found no significant differences among rations which were detected for DM, OM, CF, EE, and NFE digestibilities when yellow corn was replaced with PPW in Baladi goat diets at 0%, 25%, and 50%. However, the digestibility of CP was significantly lower (P< 0.05) in R_3 (50%) than in R_1 (0%) and R_2 (25%). Also, Radunz et al. (2003) noted that decrease in total apparent nitrogen disappearance was occurred with increasing potato waste levels in beef finishing diets to a less digestible protein with potatoes or more bacterial fermentation in the large intestine which would lead to greater fecal nitrogen extraction. Sugimoto et al. (2006) noticed that digestibility was not affected by any treatments when steers fed diets contained 0.2, 0.4 and 0.6% of Body weight (BW) on a dry matter basis potato pulp silage-based diet (PPS). Szasz et al. (2005) examined the main effects and interactions of pasteurization (54.4° C for 2 h) of potato slurry (PS) and grain type on total tract digestion of beef finishing diets. They recorded that steers fed barley-based diets had greater (*P*=0.02) DMI and lesser (*P*<0.05) total tract digestibility of DM and ADF compared with steers fed corn diets. Pasteurization increased (*P*=0.10) total tract starch digestibility. Onwubuemeli et al. (1985) tested digestibility and nitrogen utilization of potato waste substituted for corn at 0, 10, and 20% of the ration dry matter in steers diets. Potato waste did not significantly affect digestibility of crude protein or dry matter, but at 20% substitution digestibility of acid detergent fiber decreased.

Table 3 Feed intake (gram), water intake (milliliter), nutrient digestibilities coefficient (g/ kg DM) and nitrogen utilization (gram) by the experimental group lambs

Item	Experimental rations			SEM
	TMR_1	TMR_2	TMR_3	
Feed intake, gram as				
Dry matter (DM)	1,448	1,373	1,336	59.0
Total digestible nutrient (TDN)	1,093	1,048	1,044	44.7
Crude protein (CP)	204	188	177	8.3
Digestible crude protein (DCP)	132	132	124	5.5
Average body weight[a]	39.65a	37.95ab	36.65b	0.42
Water intake				
ml/h/day	4259	4330	4285	51.0
L/100 kg body weight (BW)	10.74b	11.41a	11.69a	0.13
L/ kg dry mater intake	2.94	3.15	3.21	0.14
Nutrient digestibilities coefficient				
Dry matter	792.2	801.7	796.4	0.23
Organic matter	779.7 c	789.8 b	805.0 a	0.32
Crude protein	646.5 b	701.2 a	700.3 a	0.92
Crude fiber	679.4 a	649.9 b	662.1 ab	0.44
Ether extract	748.6	735.6	754.0	0.70
Nitrogen-free extract	844.1 b	850.1 ab	864.2 a	0.38
Nutritive values (%)				
Total digestible nutrient (TDN)	754.7 b	763.6 b	781.1 a	0.34
Digestible crude protein (DCP)	91.2	96.1	93.0	0.10
Nitrogen utilization (g)				
Nitrogen intake	33.34	33.13	32.56	0.51
Fecal nitrogen	8.80	8.31	8.02	0.17
Digested nitrogen	24.54	24.82	24.54	0.45
Urinary nitrogen	8.02	8.36	8.61	0.16
Total nitrogen losses	16.82	16.67	16.63	0.23
Nitrogen retention	16.52	16.46	15.93	0.43

a, b and c = means in the same row having different letters differ significantly (P<0.05)
SEM = standard error of the mean
[a]Average body weight = (Initial weight + Final weight/2)

Inclusion PPW in the rations significantly (P<0.05) improved TDN and insignificantly (P>0.05) DCP, which is mainly due to the increase in CP and NFE digestibilities. The TMR_3 had the highest TDN while, TMR_2 had the highest DCP value. Tawila et al. (2008) noted that replacement concentrate feed mixture with PPW at 50% decreased TDN by 7.52% and by 29.09% for DCP, respectively, compared to the control ration. Diets containing PPW significantly increased (P < 0.05) nitrogen retention. Omer et al. (2010) noted that Instead yellow corn with PPW at 0%, 25% and 50% in sheep rations significantly (P<0.05) increased TDN and DCP values. The diet replaced 25% of corn with PPW (R_2) improved TDN by 1.85% and by 21.90% for DCP, respectively, compared to the control diet (R_1). While, diet replaced 50% of corn with PPW R_3 improved TDN by 2.06% and by 29.65% for DCP, respectively, with respect to the control diet (R_1).

Nitrogen retention was insignificant decreased (P>0.05) when PPW introduced in the diet at 7% or 14 for TMR_2 and TMR_3 compared to the control diet (TMR_1). In contrast, Omer et al. (2010) and Tawila et al. (2008) observed that nitrogen retention was improved when sheep fed diets replaced 25% or 50% of corn with PPW.

Rumen fluid parameters of the experimental group lambs

Results of mean effects of rumen fluid parameter of the experimental rations (Table 4) indicated that dietary treatment had no significant effect on ruminal pH, NH_3–N and TVFAS concentrations. Ammonia nitrogen was insignificant (P>0.05) decreased with inclusion PPW in the diet. However, pH value and total volatile fatty acids were in significant increased. These results are in agreement with those obtained by Omer and Tawila (2008) with Baladi goats and Tawila et al.(2008) and Omer et al. (2010) with Ossimi sheep. The reduction of ammonia–N in the rumen liquor appears to be the result of increased incorporation of ammonia–N into microbial protein, and it was considered as a direct result to stimulated microbial activity while increasing TVFAS might be related to the more utilization of dietary energy and positive fermentation in the rumen. Feeding Baladi goats on diets replaced by 0%, 25%, 50%, or 100% of concentrate feed mixture by potato waste had no significant effect on ruminal pH, TVFAS, and ammonia–N concentrations (Gado et al. 1998). The rate of VFAS production may in this situation exceed the rate of VFAS absorption through the rumen epithelium, and VFAS concentration in the rumen juice is increased (Van't Klooster 1986). Also, Radunz et al. (2003) found that increasing levels of PW lead to increased ruminal TVFAS concentration (linear, P < 0.01; quadratic, P = 0.03). It should be noted that TVFAS concentration in the rumen is governed by several factors such as dry matter digestibility, rate of absorption, rumen pH, transportation of the digesta from the rumen to the other parts of the digestive tract, and the microbial population in the rumen and their activities (Allam et al. 1984). Onwubuemeli et al. (1985) substituted corn with 0, 10, 20, and 30% potato waste in steers diet. They reported that rumen ammonia, acetate, acetate to propionate ratios, and total volatile fatty acids were lower at high intakes of potato waste and pH was increased. The shift in rumen fermentation when large amounts of potatoes were fed explains the depressed butter fat on these rations. Sugimoto et al. (2006) fed steers at 0.2, 0.4 and 0.6% of BW, potato pulp silage-based diet (PPS) and a grain-based diet (GRAIN).They reported that steers fed the grain diet had a lower (P<0.1) ruminal pH compared with steers fed the PPS diet. Ruminal pH was not significantly affected by feeding level; however, it was numerically higher for steers supplemented at 0.2% per BW than that for the steers supplemented above 0.4% per BW due probably to the higher starch intake.

Sampling time has a significant effect on rumen fluid parameters. Inclusion Potato processing waste in the sheep diets significantly decreased (P<0.05) ruminal pH at 3 hours post feeding compared with before feeding. However, it significantly increased (P<0.05) NH_3–N and TVFS concentrations at 3 hours post feeding compared with before feeding. These results are in agreement with those found by Omer and Tawila (2008) and Omer et al. (2010). In contrast, these results were not in agreement with those found by Onwubuemeli et al. (1985) who studied the effect of sampling time at 0, 2, 4, and 8 hours on rumen fermentation of diets containing 0%, 10%, 20%, and 30% PPW fed to dairy cattle. They suggested that the higher percentages of dietary PPW decreased (P<0.05) rumen ammonia concentrations, which peaked 2 hours post feeding. Also, the same authors observed that TVFAS concentration was decreased while pH value was increased at 4 hours post feeding.

Inclusion PPW in sheep diets had no significant effect on molar proportion of volatile fatty acids. Omer et al (2010) with sheep and Gado et al. (1998) with goat fed diets containing potato processing waste found significant increased (P<0.05) of acetic acid and butyric acid and insignificantly increased (P>0.05) both propionic acid and acetic/ propionic ratio compared to the control diet. Neither diet nor the feeding level had any effects on the proportion of ruminal propionate (Sugimoto et al. 2006).

Table 4 Effect of dietary treatments and sampling time on the basic patterns of rumen fermentation by the experimental group lambs

Item	TMR_1	TMR_2	TMR_3	SEM
pH value	6.22	6.25	6.30	0.02
NH_3-N (mg/dl)	24.69	23.88	23.98	0.41
TVFAs (mEq/dl)	7.47	7.64	7.52	0.21
Sampling time	Before feeding		3 hrs post feeding	
pH value	6.32a		6.16b	0.02
NH_3-N (mg/dl)	23.32b		25.05a	0.41
TVFAs (mEq/dl)	6.42b		8.66a	0.21
Molar proportion of VFAs and acetate/propionate ratio				
Acetic acid (A; %)	42.59	42.93	42.50	0.21
Propionic acid (P; %)	24.53	24.65	24.70	0.18
Butyric acid (%)	18.21	18.34	18.50	0.15
A:P ratio	1.74	1.74	1.72	0.02

a, b and c = means in the same row having different letters differ significantly (P<0.05)
[a] *NH_3-N* ruminal ammonia nitrogen [b] *TVFAs* total volatile fatty acids

Blood plasma constituents by the experimental group lambs

Data of Table 5 showed that inclusion PPW in sheep diets had no significant effect on blood plasma glucose, total protein, albumin, glubulin, albumin: glubulin ratio, urea, triglycerides and cholesterol. These results are inagreement was those obtained by Gado et al (1998) who indicated that partial replacing concentrate by potato processing waste at 0, 25, 50 or 100% in growing Baladi goats had no significant (P>0.05) effect on the serum urea nitrogen.

Table 5 Effect of dietary treatments on blood plasma constituents by the experimental group lambs

Item	Experimental rations			SEM
	TMR_1	TMR_2	TMR_3	
Glucose (mg per100 ml)	63.43	64.25	65.00	0.43
Total protein (g per100 ml)	7.91	7.86	7.84	0.03
Albumin (g per100 ml)	1.81	1.80	1.80	0.004
Globulin (g per100 ml)	6.10	6.06	6.04	0.03
Albumin: Globulin ratio	4.37	4.37	4.36	0.02
Urea (mg per100 ml)	22.51	22.93	23.11	0.19
Triglycerides (mg per100 ml)	30.09	30.11	30.16	0.04
Cholesterol (mg per100 ml	219	221	220	0.76

Growth performance of the experimental group lambs

Growth performance of the experimental group animals is presented in Table 6. The results showed that increasing level of PPW in the experimental rations significantly (P<0.05) decreased final weight, body weight gain, average daily gain (ADG), and relative gain, while feed conversion expressed as kilogram intake of DM per kilogram gain insignificantly decreased. These results were in agreement with those obtained by Omer et al (2010) when sheep fed diets contained PPW replaced 25% or 50% of yellow corn in basal diet. Sauter et al. (1980) recorded a 17% decrease in ADG and 5% decrease in efficiency with inclusion of 50% potato by-product as compared with 25% potato by-product in barley-based diets. Also, Radunz et al. (2003) recorded that increasing PPW decreased ADG and feed efficiency from 0% to 30% and then increased at 40% (quadratic, P < 0.01) when they used PPW from frozen potato products industry in high grain beef cattle finishing diets. In contrast, these results were not in agreement with those found by Omer and Tawila (2008) with Baladi goats and Makkar et al. (1984) with buffalo calves. They found that ADG and feed efficiency were better when potato waste substituted cereal grains in the rations. On the other hand, Duynisveld et al. (2004) attributed that the replacement of corn with potato processing by-product in beef cattle rations did not affect (P>0.05) average daily gain and improved (P<0.05) feed conversion efficiency.

Table 6 Growth performance of the experimental groups

Item	Experimental rations			SEM
	TMR_1	TMR_2	TMR_3	
No. of animals	9	9	9	-
Initial weight (kg)	27.30	27.20	27.00	0.31
Final weight (kg)	52.00 a	48.70 b	46.30 c	0.64
Gain (kg)	24.70 a	21.50 b	19.30 c	0.55
Experimental duration, days	105	105	105	-
ADG (g/day)	235 a	205 b	184 c	5.20
Relative gain (% of initial weight)[a]	90.48 a	79.04 b	71.48 c	2.12
Feed conversion (kg intake /kg gain) of				
Dry matter (DM)	6.16	6.70	7.26	0.29
Total digestible nutrient (TDN)	4.65	5.11	5.67	0.23
Crude protein (CP)	0.87	0.92	0.96	0.04
Digestible crude protein (DCP)	0.56	0.64	0.67	0.03

a, b and c = means in the same row having different letters differ significantly ($P<0.05$)
[a] Relative gain (percent of initial weight)= gain/initial weight x 100

Economic evaluation of the experimental group lambs

Economic efficiency was represented by daily profit over feed cost. The costs were based on average values of year 2010 for feeds and live body weight. Feeding costs and profit above feeding costs are shown in Table 7. Inclusion PPW in sheep diets lead to the decrease of total daily feeding costs of experimental rations by 15.56% for TMR_2 while 25.34% for TMR_3 in comparison with the control diet TMR_1. Meanwhile, average daily gain, daily profit above feeding cost, and relative economical efficiency for TMR_2 and TMR_3 were less compared to the control diet TMR_1. Feed cost LE per kilogram gain was improved by 3.16% and 4.62% for TMR_2 and TMR_3, respectively, compared to control diet TMR_1. These results are in agreement with those found by Omer et al. (2010). Potato by-products or potato waste can be economical substitute for feedlot cattle (Murphy 1997) and for sheep (Omer and Tawila 2008 and Omer et al., 2010).

Table 7 Economic evaluation for the experimental rations

Item	Experimental rations		
	TMR_1	TMR_2	TMR_3
Daily feed intake (fresh; kg)	1.585	1.498	1.451
Value of 1-kg feed (LE)	1.220	1.090	0.995
Daily feeding cost (LE)[a]	1.934	1.633	1.444
Average daily gain (kg)	0.235	0.205	0.184
Value of daily gain (LE)[b]	6.345	5.535	4.968
Daily profit above feeding cost (LE)	4.411	3.902	3.524
Relative economical efficiency[c]	100	88.46	79.89
Feed cost (LE/kg gain)	8.23	7.97	7.85

LE = Egyptian pound equals 0.18 USS approximately
[a] Based on prices of year 2010 [b] Value of 1- kg live body weight equals 27 LE (2010)
[c] Assuming that the relative economic efficiency of control diet equals 100

4. Conclusions

From the results of this study it could be concluded that potato processing waste can be successfully fed to sheep. Quality of the product and dry matter intake must be monitored for maximum performance. Potato processing waste can be an economical substitute for sheep rations. Optimal inclusion of PPW in sheep rations may depend on the cost of transportation and other dietary ingredients used in formulation of rations.

References

Abou-Raya, A.K., 1967. Animal and Poultry Nutrition. 1st Edit. Pub. Dar El-Maarif, Cairo (Arabic text book).

A.E.S.I., 2008. Agriculture Economic and Statistics Institute, Agric., Economics, Pub. By Agric. Res. Center, Egypt.

Allain, C.C., Poon, L.S., Chan, C.S., Richmond, W. and Fu, P.C., 1974. Enzymatic determination of

total serum cholesterol. Clin. Chem., 20: 470 – 475.

Allam, S.M., Abou-Raya, A.K., Gihad E.A. and El-Bedawy T.M., 1984. Nutritional studies by sheep and goats fed NoaH treated straw. 1st Egyptian British conference on Animal and Poultry Production, Zagazig, 11–13 Sep. P. 53.

A.O.A.C., 1995. Association of Official Analytical Chemists: Official Methods of Analysis. 16 th ed. Washington D.C.USA.

Armstrog, W.D.and Carr C.W., 1964. Physiological Chemistry: Laboratory directions 3: 75 Buger Puplishing Co. Minneapolis, Minnesota, U.S.A.

Bauer, T.D., Ackermann, P.G. and Toro, G., 1974. Methods in clinical chemistry. Clinical laboratory methods. The C.V. Mosley Company, Saint Louis, p. 946.

Blaxter, K.L., 1968. The energy metabolism of ruminants. 2nd ed. Charles Thomas Publisher. Spring field. Illinois, U.S.A.

Boyles, S., 2006. Feeding potato processing wastes and culls to cattle. OSU Extension Beef Specialist. http://beef,osu.edu/library/potato. html.

Doumas, B., Wabson, W.W. and Biggs, H., 1971. Albumin standards and measurement of serum with bromocrfsol green. Clin. Chem. Acta, 31: 87.

Duynisveld, J.L., Charmely E., Mandell I. and Aalhus J., 2004. Replacing corn or barley with potato processing by–product in beef finishing diets improves feed conversion efficiency and alters carcass fat distribution. Journal of Animal Science 82, Suppl. 1.

El–Boushy, A.R.Y. and Van der Poel, A.F.B., 1994. Poultry feed from waste processing and use. Chapman and hall (Ed).

Erwin, E.S., Marco, C.J. and Emery, E.M., 1961. Volatile fatty acid analysis of blood and rumen fluid by gas chromatography. Journal of Dairy Science 44: 1768.

F.A.O., 2008. Potatoes, nutrition and diet. International year of the potato, 2008 www.potato 2008.org

Fossati, P and Principe, L., 1982. Clin. Chem. 28, 2077.

Gado, H., Mansour, A.M., Metwally, H.M. and El-Ashry, M.A., 1998. The effect of partial replacing concentrate by potato processing waste on performance of growing Baladi goats. Egyptian Journal of Nutrition and feeds 1 (2): 123–129.

Goering, H.K. and Van Soest, P.J., 1970. Forage fiber analyses (Apparatus, Reagents, Procedures and some applications). USDA, Agr. Hand. Book 379..

Kromann, R.P., Meyer, J.H. and Stielau, W.J., 1967. Steam distillation of volatile fatty acids in rumen digesta. Journal of Dairy Science 50:73.

Lardy, G and Anderson, V., 2009. Alternative feeds for ruminants. NDSU.permission@ndsu.edu. North Dakota State University Agriculture and University Extension Dept. 7070, Morrill 7, P.O. Box 6050, Fargo, ND 58108-6050.

Makkar, G.S., Kakkar, V.K., Bhullar M.S. and Malik, N.S., 1984. Potato waste as a substitute for cereal grains in the rations of buffalo calves. Indian Journal of Animal Science 54: 1060–1061.

Murphy, S., 1997. Feeding potato by-products. Prince Edward Island, Agriculture and Foresty, Fact Sheet, AGDEX 420–68. http://www.gov.pe.ca/af/agweb/library/factsheet/ wastpot. Php3.

N.R.C., 1985. Nutrient requirements of domestic animals. Nutrient requirements of sheep. National Academy of Sciences, Washington. D.C.

Omer, H. A. A., Abdel-Magid, S. S., Ahmed S. M., Mohamed, M. I. and Awadalla, I. M., 2010. Response to partial replacement of yellow corn with potato processing waste as non-traditional source of energy on the productive performance of Ossimi lambs. Trop Anim Health Prod 42:1195–1202.

Omer, H.A.A and Tawila, M.A., 2008. Growth performance of growing Baladi goats fed diets containing different levels of sun dried peel potato waste. Egyptian Journal of Nutrition and feeds 11 (3): 453–468.

Onwubuemeli, C., Huber, J.J., King, K.J. and Johnson, C.O., 1985. Nutritive value of potato processing wastes in total mixed rations for dairy cattle. Journal of Dairy Science 68: 1207–1214.

Patton, C.J. and Crouch, S.R.., 1977. Spectrophotomattic and kinetics investigation of the Berthelot reaction for the determination of ammonia. Anal. Chem. 49: 464.

Radunz, A.E., Lardy, G.P., Bauer, M.L., Marchello, M.J., Loe, F.R. and Berg, P.T., 2003. Influence of steam–peeled potato processing waste inclusion level in beef finishing diets: Effects on digestion, feedlot performance and meat quality. Journal of Animal Science 81:2675–2685.

SAS., 1998. Statistical Analysis System. SAS Users Guide. Version 6. 12 Ed. Basics SAS Institute Inc., Cary, NC, USA.

Sauter, E.A., Hinman, D.D., Bull, R.C., Howes, A.D., Parkinsson, J.F., and Stanhope, D.L., 1980. Studies on the utilization of potato processing waste for cattle feed. University of Idaho Agric. Exp. Sta. Res. Bull 112, Moscow, ID.

Smith, T. J. and Huxsoll, C.C., 1987. Peeling potatoes for processing (Eds W.F. Talburt and O. Smith) AVI – Van Nostrand rein hold Company, New York, PP. 333–369.

Sugimoto, M. Saito W., Ool M., Sato Y., Saito T. and Mori K. 2006. The effects of potato pulp and feeding level of supplements on digestibility, in situ forage degradation and ruminal fermentation in beef steers. Animal Science Journal 77, 587–594.

Szasz, J. I., Hunt, C. W., Turgeon, O. A., Szasz, Jr. P. A. and Johnson, K. A., 2005. Effects of pasteurization of potato slurry by-product fed in corn-or barley based beef finishing diets J. Anim. Science 83: 2806-2814.

Tawila, M.A., Omer, H.A.A and Gad, Sawsan M., 2008. Partial replacing of concentrate feed mixture by potato processing waste in sheep rations. American-Eurasian Journal of Agricultural & Environmental Science 4 (2): 156–164.

Van Soest, P.J., Robertson, J.B. and Lewis, B.A., 1991. Methods for dietary fiber, neutral detergent fiber and non starch polysaccharides in relation to animal performance. Journal of dairy Science 74: 3583–3597.

Van't Klooster, A.T., 1986. Pathological aspects of rumen fermentation. In: New developments and future perspectives in research on rumen function (Neimann–Sorensen, A., Ed). Commission of the European Communities, Luxembourg, 259–276 (C.F Gado et al., 1998).

Abbreviations

ADF	Acid detergent fiber
ADL	Acid detergent lignin
ADG	Average daily gain
BW	Body weight
CF	Crude fiber
CP	Crude protein
DCP	Digestible crude protein
DM	Dry matter
DMI	Dry matter intake
EE	Ether extract
LE	Egyptian pound
Mcal/kg	Megacalories per kilogram
NDF	Neutral detergent fiber
NFE	Nitrogen-free extract
NH_3–N	Ammonia nitrogen
NRC	National Research Center
OM	Organic matter
PS	Pea straw
PPB	Potato processing by-product
PPW	Potato processing waste
TMR	Total mixed ration
TMR_1	Control ration contained 0% potato processing waste
TMR_2	Second experimental ration contained 7% potato processing waste of total mixed ration
TMR_3	Third experimental rations contained 14% potato processing waste of total mixed ration
UDCSM	Undecorticated cotton seed meal
WB	Wheat bran
YC	Yellow corn

11/20/2011

Molecular Detection of *Cucumber Mosaic Virus* Symptoms Diversity on Squash Plants

M.M.M. El-Shamy

Botany Dept., Fac. of Sci. El-Monofia Univ., Egypt.
magdyelshamy@yahoo.com

Abstract: A wide range of severe symptoms were appeared on inoculated squash plants (Cucmus pepo cv. El-Skandrani) with CMV under greenhouse condition. One of the first signs of systemic CMV infection, is vein clearing in the youngest leaves (about 7 days), the veins become translucent and leave produced subsequently showed a mosaic (about 10 days) severe mosaic and mottling (about 15 days). Then changed in leaves growth form i.e. little, malformation and no-Lamina giving shoestring the so-called fern leaf (about 20-25 days). The virus was transferred from each symptom to squash and chenopodium amaranticolor plants by sap mechanical inoculation then conformed by DBIA-assay. The change in chlorophyll contents to ensure that all these symptoms resulted from CMV-s EG. SDS-PAGE, peroxidase isozyme separation and RAPD-PCR to molecular analyze of S-CMV-EG symptoms development on squash plant leaves. SDS-PAGE of protein separation showed variability protein pattern and contents of healthy and S-CMV symptoms infected squash leaves (m-mosaic, S-mosaic, crinkling and malformation) with 24, 26, 28, 25, 20 and 22, 21, 20, 22, 16 soluble and unsoluble polypeptides respectively. As well as. DISC-PAGE isozyme showed 6, 7, 8 and 8 peroxidase isozymes respectively. RAPD-analysis revealed DNA polymorphic among CMV-symptom development on squash plants. RAPD analysis using two random primers revealed 8 polymorphic of total 15 amplified fragments with 53% under CMV infection. Crinkle symptoms revealed the highest number with 18 markers followed by S-mosaic 17 and malformation 16 and mild mosaic with 15 bands. [Life Science Journal. 2011; 8(4):743-752] (ISSN: 1097-8135). http://www.lifesciencesite.com.

Key words: Squash plants, CMV symptoms development, SDS-PAGE, DISC-PAGE, PAPD PCR.

1. Introduction

Cucumber mosaic cucumorius is widely distributed in different crops in Egypt and has been reported as a main problem for squash crop production in open field and protected agriculture besides causing severe losses in cucurbit crops (Staniulus et al., 2000). The virus showed several types of symptoms including, vein clearing, mild and severe mosaic blisters, green vein banding and chlorotic local lesion followed by vein netting, yellow often necrosis and plant death, leaf distortion, crinkle and malformation, and filformshape (Gomaa, 2008). Therefore, it was important to define the etiology of this virus by symptomatology, biology, serology and protein related index tests.

Leal and Lastra (1984) revealed that the reduction in chlorophylls, soluble proteins and nitrogen contents was evident in leaves infected by tomato yellow mosaic virus that causes severe symptoms. The subcelular distraction of virus stimulates the synthesis of soluble proteins which were detected by SDS-PAGE. The most prominent as judged by the intensity of their staining, is the enhancement of 14.3, 20, 39, 58 and 97 kDa proteins (Hadidi, 1988; El-Dougdoug, 1996 and Sherif and El-Habbaa, 2000). Certain host proteins were increased dramatically as part of a general physiological response in infection by viruses and other pathoens (Comacho-Henriquez and Sanger, 1982). Viral infection with yellow leaf carl, leaf roll, mosaic, curl, crinkle and malformation leaves of tomato and squash exhibited higher activity of peroxidase polyphenol oxidase and esterase (Tag El-Din et al., 2006).

The present study aims to the study the chemical and molecular variability of CMV symptoms development in infected squash plants, using, SDS-PAGE, DISC-PAGE and RAPD-PCR.

2. Material and Methods

Virus source:

Cucumber mosaic cucumoviridae CMV-s EG isolate was obtained from the Virology Lab, (Megahed, 2008). Agric. Microbiology Dept., Fac. of Agric., Ain Shams Univ. The virus isolate maintance on Nicotiana glutinosa.

Virus detection : In order to determine the presence of CMV in inoculated and symptoms squash plants, the goat antirabbit immunoglobuline-alkaline phosphtase conjugate (Sigma A 4503) was used by Dot blot immunoassay as described by Lin et al. (1995).

The seeds of squash (Cucurbita pepo cv, Eskandarani) and indicator plants for CMV-s EG detection were kindly provided from Virology Lab., Fac. Agic., Ain Sham Univ., Cairo, Egypt.

The squash plants were grown into steam sterilized soil in pots under greenhouse conditions until the seedling stage (cotyledon leaf). The squash leaves were mechanically inoculated with CMV-s EG

isolate prepared in 0.1 M phosphate buffer pH 7.4. The symptoms were recorded at 2-6 weeks and photographed after mechanical inoculation. The plants showed symptoms were indexed by Chenopodium amaranticolor as indicator host and also by DBIA assay.

Chlorophyll content :

Chlorophyll a, b and carotenoids were extracted and estimated according to Wettstein (1957) as mg/L.

Biochemical analysis :

Protein content was determined by Bradford (1976) using bovine serum albumin as a standard.

SDS-polyacrylamide gel electrophoresis :

S odium dodecyl sulfate polyacrylamide gel electrophoresis (SDS-PAGE) was performed as described by Laemmli (1970). Extraction of soluble and non-soluble proteins were done according to Studier (1973).

Peroxidase (PRX) isozymes electrophoresis: Gel electrophoretic isozymes were performed according to Stegemann et al. (1985) among four symptoms leaves using one enzyme staining systems. Peroxidase revealed the most variables with good determined banding patterns.

Molecular analysis :

DNA extraction was performed by the method of Wulff et al. (2002).

DND amplification:

Random amplified polymorphic DNA (RAPD) analysis was applied according to Williams et al. (1990) using 10 mers of four random oligonucleotide primers obtained from (Metobion AG. Lena Christ Strasse, Martinsried, Deutschland) as shown in Table (1). The gels analysis was applied by programme (UVI geltec version 12.4, 1444-2005 USA).

Table 1. The four random primers used in DNA amplification

Primer name	Sequence (5`-3)
OPD-11	5`AGCGCCATTG3`
OPT-20	5`GACCAATGCC3`
2-19	5`GCACGGCGTT3`
2	5`AACGCGCAAC3`

Agarose gel electrophoresis :

PCR amplified products were analyzed using 1.2% agarose gel electrophoresis staining with ethidium bromate. The amplified DNA bands were visualized under UV light and the sizes of the fragments were estimated based on a DNA ladder of 100 to 2000 bp (manufactured by Bloron).

3. Results

Symptoms development :

Sequency of symptoms development on CMV infected squash plants (Cucurbita pepo cv. Eskandarani) showing signs of viral symptoms a wide range of severe symptoms were appeared on squash plants. One of the first signs of systemic infection is vein clearing in the youngest leaves (at 7 days), the vein become translucent and leaves produced subsequently showed a mosaic (10 days), severe mosaic yellowing, mottling (chlorosis) (20 days). Then changed in leave growth forms i.e. little, blisters, crikle, malformation and no-lamina giving shoestring (at 25-35 days). The so-called fern leaf. The symptoms were than developed into four main features on cultivated plants and thus they were classified into the following four categories:

1- The leaves were mild mosaic (Fig. 1-a); 2- The leaves were severe mosaic and blisters (Fig. 1-B). 3- The leaves were curling and narrow (Fig. 1-C) and 4- leaves showed reduction in blade and filiform or shoestring shapes (Fig. 1-D).

A number of eight plants infected squash plants showing viral different symptoms types were examined by dot blot immunoassays assay using specific polyclonal antibodies by DBIA. A purplish blue color was developed infected plants in positive reaction, whereas extracted from healthy plants remain green in the negative reactions (Fig. 2).

Another assay for viral detection and variability of symptom via local lesion diversity on Ch. amaranticolor by characteristic of morphological local lesions. It was observed variation in local lesions i.e. size, shape, colour without center and halo; chlorotic necrotic, fine and large (Fig. 1B).

Chloropyll and carotenoids :

Data presented in Table (2) showed that chlorophyll a and b were significantly decreased in infected plants showed mild and severe mosaic, where as curling and deformation plants didn't show significantly different from healthy plants. On the other hand carotenoids were not significantly changed.

Protein contents:

Protein contents were determined in squash leaves with individual symptoms elated to BSA (Table 2), it was revealed that, all the symptoms types due to increasing in total protein content with different values compared with healthy squash leaves.

Table 2. chlorophyll; carotenoids and protein contents in squash leaves at different periods of symptoms developments

Symptoms development / Chlorophyll* and protein contents	Symptoms development				
	Healthy	m-Mosaic	S- Mosaic	Crinkling	Malformat-ion
Chlorophyll-a	1.015	0.234	0.095	0.695	0.792
Chlorophyll-b	0.625	0.185	0.047	0.375	0.410
Carotenoids	0.412	0.425	0.445	0.495	0.485
Proteins **	7.87	4.76	5.44	6.37	6.23

* Photopigment : mg/g fresh.
** Protein content: mg/ml

SDS-PAGE proteins analysis :

SDS-PAGE profile of soluble proteins extracted from infected and uninfected squash leaves presented in Table (3) and Fig. (3). SDS-PAGE analysis revealed 32 bands with different molecular weights ranged from 275 to 10 as shown in Fig. (3).

The soluble protein bands of the four plants which revealed different symptom types were varied in number and density of bands, whereas mild mosaic, severe mosaic, crinkle and malformation were revealed the highest total number with 24, 26, 26, 25 respectively bands while healthy displayed the lower number with 20 bands.

The variability analysis of symptoms development showed some proteins bands disappeared in healthy for example 9, 7, 8 and 9 band for mild, severe mosaic, crinkling and malformed respectively (Table 2). The present of variability between symptoms development was 53% related to total bands.

The protein bands were appeared in both healthy and in under all symptoms types with 32 bands. Some other protein 17 bands were appeared under symptoms types and displayed in healthy. Some of these bands were appeared in both healthy and symptoms types such as bands number 15, 19, 18 and 16 protein bands respectively (Table 3).

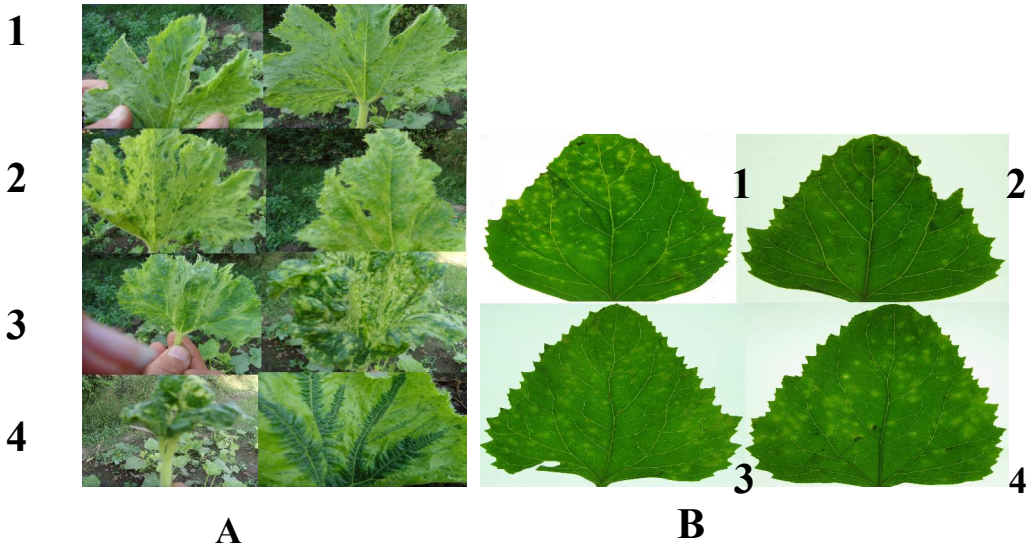

Fig. (1): Symptoms development on infected squash leaves by CMV, A. Systemic symptoms, B. Variability of local lesion on *Ch. amaranticolor* 1- mild mosaic; 2- severe mosaic, 3- crinkle and 4- malformation symptoms.

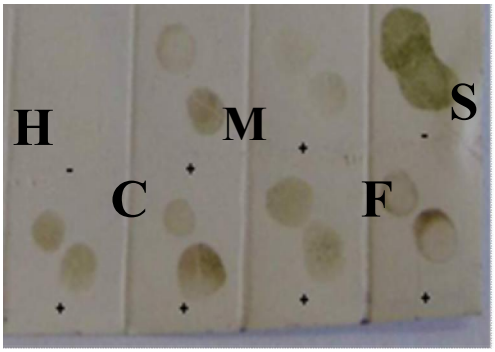

Fig. (2): Dot blot immunoassay for CMV detection in symptoms types on squash leaves against specific IgG-CMV polyclonal, H = healthy leaves, M = mild mosaic, S= severe mosaic, C = crinkle and F = malformation.

Table (3): SDS-PAGE analysis of soluble protein patterns of the variable the symptoms development related to CMV-squash inoculated.

Band no.	Healthy	Mild mosaic	Severe mosaic	crinkling	Malformation
275	-	+	+	-	+
195	-	+	+	-	+
161	-	+	-	-	-
104	+	+	+	+	+
92	+	+	+	+	+
85	+	+	+	+	-
74	-	-	-	+	+
68	-	+	+	+	+
63	+	+	+	+	-
59	+	-	+	+	+
58	+	+	-	-	-
55	+	-	+	+	+
52	+	+	+	+	+
50	-	+	+	+	+
46	+	+	+	+	+
40	-	+	-	+	-
38	+	-	+	+	+
36	+	+	+	+	+
34	+	+	+	+	+
33	-	-	+	+	+
31	+	+	+	+	+
28	+	+	+	+	+
26	-	+	+	-	-
24	+	-	+	+	-
22	+	-	+	+	+
20	+	+	+	-	+
19	+	+	+	+	+
18	+	+	+	+	+
17	-	+	+	+	+
14	-	-	-	+	+
11	+	+	+	+	+
10	-	+	-	+	+
Total bands	20	24	26	26	25

SDS-PAGE analysis revealed 26 bands with different molecular weight ranged from 238 to 20 kDa as shown in Fig. (3). The non-soluble protein of symptoms development were varied in number and density whereas 22, 21, 20, 22 bands of mild mosaic, severe mosaic, crinkling and malformation respectively, while healthy plant displayed the lower 16 bands.

SDS- profile of non-soluble proteins extracted from the infected plants with CMV and non-infected presented in Table (4). They were varied between symptoms types in numbers and density where as symptom types plants revealed increasing in protein profiles their healthy plants. The number increase was 6, 5, 4 and 6 bands for mild mosaic severe mosaic, crinkle and malformation symptom types respectively (Table 4 and Fig. 3).

On the other hand the newly induced bands under CMV infection 9 bands in symptoms types plants where disappeared in healthy plants.

The variability analysis of symptoms showed some bands disappeared in healthy and between symptoms plants. The percent of variability between symptoms plants was 48% related to total bands.

Peroxidase isozymes : Results of peroxidase isozymes are shown in Table (5) and Fig. (4). Each symptom types and healthy plants could be characterized by unique set. of isozymes. The total number of peroxidase isozymes shown in all symptoms types were 11 isozymes while those of each type 7, 8, 8 and 9 for mild mosaic severe mosaic, crinkling and malformation respectively as well as 7 bands for healthy ones. The variability between symptoms types was 60% related total peroxidase isozymes (Table 5).

Peroxidase isozyme (PRX) analysis displayed a total of 11 band whereas 5 of them were variable (polymorphic) and 5 (monomorphic) other bands among the different symptoms types of CMV-squash inoculated. As well as the control as presented in the zymogram (Table 5) and Fig. (4). The effect of CMV-EG strain infection could be observed among of 4 peroxidase bands, whereas bands No. 2, 5, 6 and 7 disappeared in the control (healthy) plants and appeared in some symptom types, on the other hand polymorphic band No. 1 appeared in healthy and symptom type 3; polymorphic band No. 2 appeared in symptoms type 1 and 4; polymorphic band No. 5 appeared in four symptoms types; polymorphic band No. 4 appeared in symptoms types 1, 2 and 4 and polymorphic band No. 6 appeared in symptoms types 3 and 4. However, 7 bands were appeared in healthy plants , 3 polymorphic bands No. 1 with symptom type 3 and No. 7 with symptoms types 3 and 4, as well as 3 monomorphic bands No. 3, 8 and 9 (Table 5 and Fig. 4).

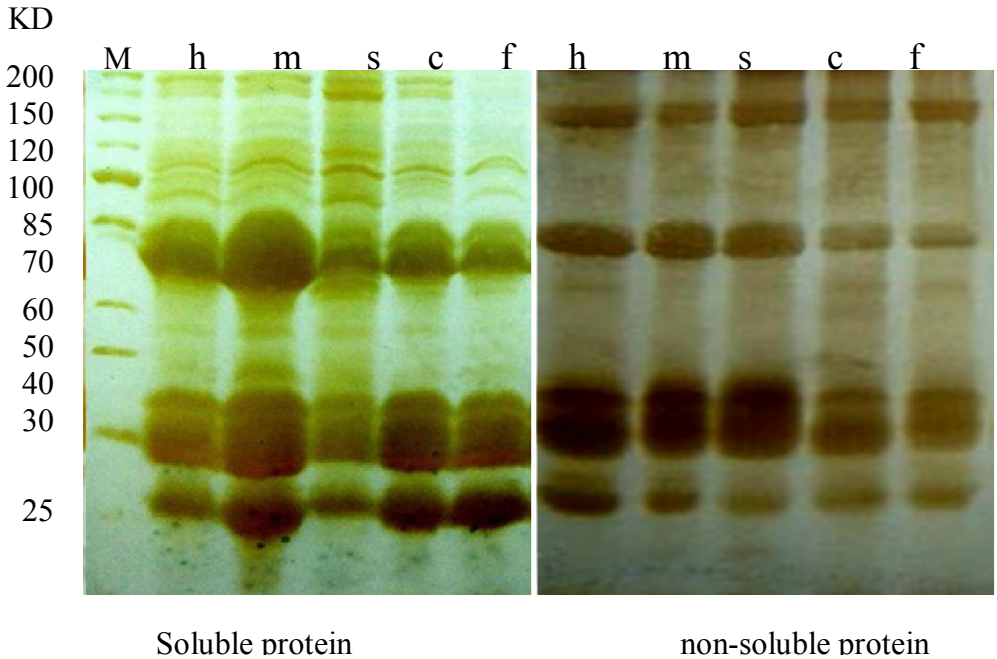

Fig. (3): SDS-PAGE (12%) of soluble protein (a) and non-soluble protein fractions extracted from the infected squash leaves with CMV. H = healthy leaves, m = mild mosaic, s = severe mosaic, c= crinkle and F = malformation.

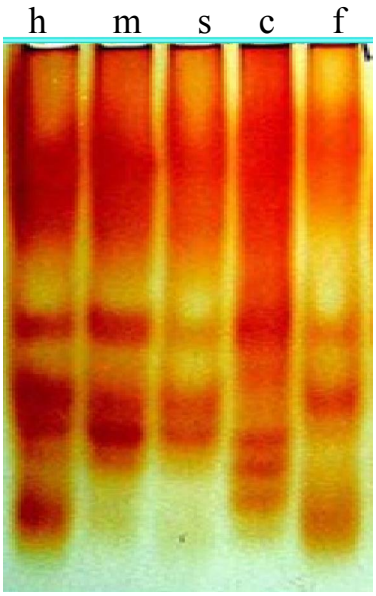

Fig. (4): Peroxidase (PRX) isozyme profiles of squash leaves infected with CMV. H = healthy leaves, m = mild mosaic, s = severe mosaic, c= crinkle and F = malformation.

Table (4):SDS-PAGE analysis of non-soluble proteins patterns of the variable the symptoms development related to CMV squash infection.

Band no.	Healthy	Mild mosaic	Severe mosaic	crinkling	Malformation
238	+	+	+	+	+
161	-	+	+	-	-
109	+	+	+	+	+
92	+	+	+	+	+
85	+	+	+	+	+
74	+	-	-	-	+
68	-	+	-	-	+
63	-	+	+	+	+
51	+	+	+	+	+
58	-	+	+	+	+
57	+	+	+	+	+
55	+	+	+	+	-
52	-	+	+	+	+
50	-	+	+	+	+
46	+	+	+	+	+
40	+	+	+	+	+
38	-	-	-	-	+
36	+	+	+	+	+
34	+	+	+	+	+
33	+	+	+	+	+
31	+	+	+	+	+
28	+	+	+	+	+
26	+	+	-	+	+
24	-	+	-	-	+
22	-	-	+	-	-
20	+	+	+	+	+
Total bands	16	22	21	20	22

Table (5): Peroxidase (PRX) isozymes analysis of the variable bands of the variable the symptoms development related to CMV squash infection

Band no.	Healthy	Symptoms development				Polymorphism
		m-mosaic	s-mosair	Crinkle	malformation	
1	+	-	-	+	-	Polymorphic
2	-	+	-	-	+	polymorphic
3	+	+	+	++	+	monomorphic
4	+	+	+	-	+	polymorphic
5	-	+	+	+	+	polymorphic
6	-	-	+	+	+	polymorphic
7	-	-	+	+	+	monomorphic
8	+	+	+	+	+	monomorphic
9	+	+	+	+	+	monomorphic
10	+	+	+	+	+	monomorphic
11	+	+	-	-	-	Polymorphic
Total bands	7	8	8	8	9	

Such new peroxidase bands may related to CMV infection in mild and severe symptoms types. In general, results in table (5) which represent the peroxidase enzyme polymorphism among the 4 symptoms types could be served as a model for analyzing the gene action and different mild and severe symptoms types.

RAPD analysis of CMV infected squash plants :

Four random primers, OPT-20, OPD-11, 2-19 and 2 were used in random amplified polymorphic DNA (RAPD) analysis in infected squash plants with CMV-s EG.

Primers OPT-20 and OPD-1 revealed 12 amplified fragments with sizes ranged from 690 to 190 bp. Whereas 8 fragments were polymorphic and 4 commonly detected among the symptom type 5 , plants with molecular size 690, 590, 340 and 380 bp. As well as the healthy squash plants revealed 16 amplified fragment (Table 6 and Fig. 5).

The healthy squash plants was varied considerably in the presence of amplified fragments where 14 fragments, thus m-mosaic, s-mosaic crinkle and malformation were 15, 16 and 18 and 16 amplified fragments respectively. On the other hand 4 amplified fragments appeared in healthy plants only and disappeared in infected plants, Table (6).

Table (6): RAPD analysis of symptom development on CMV-infected squash plants using RAPD primers

Molecular weight (bp)	**OPT-20**					OPD-11					Polymorphism
	H	**M**	**S**	**C**	**F**	**H**	**M**	**S**	**C**	**F**	
1045	+										Unique
920	+										Unique
865	+										Unique
765	+										Unique
690	+	+	+	+	+	+	+	+	+	+	Monomorphic
630	+++	+	+	++	++	-	-	-	-	-	Polymorphic
590	-	+	++	+++	+++	+	+	+	+	+	Monomorphic
415	+	-	++	+++	++++	-	-	-	-	-	Polymorphic
440	-	++	+++	+++	++++	-	-	-	+	-	Polymorphic
340	+	++	+++	++++	++++	+	+	+	+	+	Monomorphic
331	-	+++	+++	++++	++++	+	+	-	-	-	Polymorphic
320	-	+++	+++	++	++	-	-	-	-	-	Polymorphic
380	+	+	+	+	+	+	+	+	+	+	Monomorphic
240	-	+	++	+	+	-	-	+	-	-	Polymorphic
210	-	-	-	+	-	-	+	-	+	++	Polymorphic
190	-	-	-	-	-	-	+	+	+	+	Polymorphic
Total bands	9	9	10	11	10	5	6	6	7	6	

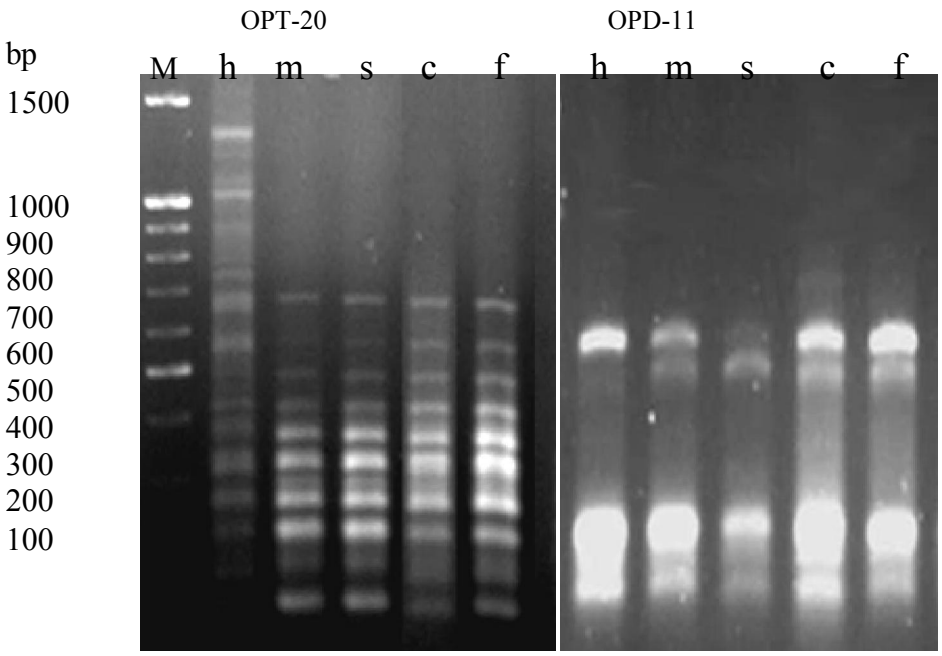

Fig. (5): RAPD amplified products of CMV-infected squash leaves using two primers. OPD-11 and OPT-20. H = healthy leaves, m = mild mosaic, s = severe mosaic, c= crinkle and F = malformation.

Moreover, the numbers of fragments of symptoms types were affected by different behaviour either by increase or by decrease compared with healthy plants. For contrast, the crinkle symptoms increased in 9 bands, S-mosaic (7) and malformation increased in 7 bands and m-mosaic increased 6 bands related healthy plants. Meanwhile, the crinkle symptoms type revealed induced amplified fragment that were nor existed either in the healthy or mild and severe mosaic and malformation symptoms (440 bp) and s-mosaic symptoms with 240 bp in OPD-11 RAPD primer. There bands resulted from RAPD-PCR amplified products could be used as RAPD markers for symptoms types against CMV infection in squash plants.

Table (7): Summarized results of biochemical and molecular variation among symptoms types of CMV-infected squash plants.

CMV symptom types	Photopigments			Proteins				RAPD primers		
	Chl a	Chl b	Carote-noid	Protein content	SP	NSP	PRX	OPD20	OPD11	Total M.M
Healthy plants	1.015	0.625	0.412	7.87	26	16	6	8	5	62
Mild-mosaic	0.234	0.185	0.425	4.76	24	22	7.	9	6	68
Severe mosaic	0.095	0.047	0.445	5.44	26	21	7	10	6	70
Crinkling	0.695	0.375	0.495	6.37	26	20	8	11	7	72
Malformation	0.792	0.410	0.485	6.23	25	22	8	10	6	71

Chl = chlorophyllNSP = non-soluble protein M.M = molecular markers SP = Soluble rotein
PRX = peroxidase isozymes

The results of biochemical and molecular variation for symptom types of CMV-infected squash plants were summarized in Table (7). Consequently the genetic analysis of CMV symptom types showed that crinkle was the highest biochemical and molecular markers (72) followed by malformation (71) severe mosaic (70) and m-mosaic (68) compared healthy with 62 molecular markers.

4. Discussion

The effects of viruses on plants are multifarious, practically and function of a plant may be disturbed. Symptoms will be named and briefly described. They may be grouped according to their effect on overall growth, colour, water content, tissue life span, shape of organs, plant anatomy and plant physiology. Most plant

virus diseases and viruses are named after their main symptoms in a particular host.

More obvious and better known are colour changes, especially of leaves. Mosaic disease has long been synonymous with virus disease. CMV-s EG mosaic of squash is one type of variegation as mentioned of tobacco and abutilon (Bos, 1983 and Mathews, 1991). Diffusely bordered variegation is often called mottling but there are various intermediates. The term vein mosaic (vein clearing) denotes an irregular mosaic along veins and vein-banding a regular one.

Actually decrease in photosynthetic rate of the infected leaves is often associated with development of the symptoms (Plat et al. 1979).

The effects are, of may be, related to changes within organs or entere plants, symptoms are variable and greatly depend on the host plant and how long it has been infected, the virus strain and the environmental conditions. For example, symptoms that are particularly noticeable in plants that have been growing in cool bright conditions since infection may become masked in host poorly-lit conditions. The time after infection before symptoms appear depends on the virus, the plant and the environmental conditions too; it is commonly a few days or weeks in herbaceous plants through it may be one or more years in woody ones.

Under greenhouse conditions the symptoms could be more clear and restricted. It should be independent of the virus and should reflect the host genetics. Symptoms of CMV disease on squash differed depending on the isolates as well as the environmental conditions (Makkouk et al., 1979 and Aref and El-Dougdoug, 1996). By comparing the data presented in this study of the viral symptoms development and mechanically transmitted with the results. CMV-s EG was detected biological and serological in infected squash plaints (Megahed, 2008), Abo El-Nasr et al. (2004), it was concluded that the three viral symptoms had ZYMV viral complex of one or more strains. Similar results were obtained for TYLCV-E (Aref and El-Dougdoug, 1996). Local lesions diversity of CMV produced n Ch. amaranticolor were used CMV identification and variability as well as isolation of CMV strains (Megahed 2008).

Protein isozymes, and DNA analysis should be independent of host genetics under virus inducer. Whereas, amino acid sequence of polypeptides are dependent on nucleotide sequence of their coding genes; therefore on electrophoretic analysis of protein and isozymes of CMV infected leaves which showing different symptoms approximates the analysis of there genetic variation. The variation of CMV symptom types was detected via determination of polypeptides by using SDS-PAGE and peroxidase isozymes using DISC-PAGE. Data presented in Table (2) indicated that the number of protein fractions increased in infected plants as recorded in severe mosaic followed crinkle and malformation than mild mosaic. Also this results indicated the CMV due to increasing protein content or certain protein fraction or both together. For example severe mosaic showed decrease in protein content but increase in protein fractions. This clearing that despite increasing the biodegradation of protein content new protein types were detected due to virus infection. The same observation was reported by (Hadidi 1988 and El-Dougdoug, 1996). The synthesis of new proteins are due to the host-virus interaction previous results also indicated that protein contents could be increased dramatically (Camacho-Henriquez and Sanger 1982) or decreased (Lead and Lastra, 1984).

The enzymatic pools and their metabolic pathways are the most important factors affecting pathogenicity especially with viruses. The results showed that the level of peroxidase in infects leaves of crinkle and severe mosaic were higher than those in healthy leaves. This high level play an important role in the defense mechanism. Increase in this enzyme activity and isozymes has been detected after infection by pathogens in different host pathogen combination (Hammeschmidt et al. 1982 and Sherif and El-Habbaa, 2000).

DNA prepared was found crucial for RAPD-PCR. The yields of DNA were determined of spectrophotometrically as, 11, 14, 15 and 13 µg/0.05 g fresh tissues. The PCR conditions for DNA analysis were optimized by investigated each factor individually, the optimized conditions were detailed in material and methods section. A total of scoroble amplified DNA fragments ranging in size 1045 to 190 bp were observed using the two primers were as polymorphic with 8 and 4 bp monomorphic fragments with detected among symptoms types. Interesting to note that, the four symptoms types were varied in there formed and developed. Where 15, 16, 18 and 16 for m-mosaic, S-mosaic, crinkle and malformed symptom, respectively compared with DNA fragments in healthy leaves. The genetic variability among symptoms types has yet 16 to be established rapid and unambiguous of genetic variability among symptoms types has greatly benefied from recent advances in DNA fragments based on the PCR and random amplified polymorphic DNA (El-Dougdoug et al. 2007 and Sharma, 2003).

5. References

1. Abo El-Nasr, M.A.; Kh. A. El-Dougdoug; M.H. El-Kattan and E.A. Salem (2004). Induction of salicylic acid in cucumber against ZYMV potyvirus by some nutrient chemicals. Egyptian J. Virol. 2: 301-312.

2. Aref, N.M. and Kh.A. El-Dougdoug (1996). Biological and molecular diagnosis of three different symptoms of TYLC-disease in open field. Annals Agric. Sci., Ain Shams Univ., Cairo, Egypt, (41): 173-185 pp.
3. Bos, L. (1983). Introduction to Plant Virology, Longman, London and New York, 160 pp.
4. Bradford, M.M. (1976). A rapid and sensitive method for quantification of microgram quantities of protein utilizing the principle of protein dye binding. Anal. Biochem. 72:248-254.
5. Camacho-Henriquez and H.L. Sanger (1982). Analysis of acid extractable tomato leaf proteins after infection with a viroid two viruses and fungi and purification of the pathogenesis related protein. Arch Virol. 74: 181-193.
6. El-Dougdoug, K.A.; H.M.S. El-Harthi; H.M. Korkar and R.M. Taha (2007). Detection of some nuclear variations in banan tissue culture using isozyme and DNA fingerprint analysis Journal of applied Science Research, 3 (7): 622-627.
7. El-Dougdoug, Kh.A. (1996). Detection of virus and viroid diseases in the sep. of infected potato leaves using gel electrophoresis. Annals Agric. Sci. Ain Shams Univ., Cairo, 41: 635-648.
8. Gomaa, H.A. Hanaa (2008). Effect of Cucumber mosaic virus on anatomical structure of squash leaves. Egyptian J. Virology 5 (2): 101-113.
9. Hadidi, A. (1988). Synthesis of disease associated proteins in viroid infected tomato leaves and binding of viroid to host proteins. Phytopathology, 78: 575-578.
10. Hammeschidt, R.; E.M. Nuckies and J. Kuc (1982). Association of enhanced peroxidase activity with induced systemic resistance to Collelotrichum lagenarium. Physiol. Plant Pathol. 20: 73-82.
11. Laemmli, U.K. (1970). Cleavage of structural protein during the assembly of the head of bacteriophage T4 nature 227: 980-985.
12. Leal, N. and R. Lastra (1984). Altered metabolism of tomato plants infected with tomato yellow mosaic virus. Physiological Plant Pathology 24: 1-7.
13. Lin, L.; J.W. Kloepper and s. Tuzun (1995). Induction of systemic resistance in cucumber plant against Fusarium wilt by plant growth promoting rhizobacteria. Phytopathology. 85: 695-698.
14. Makkouk, M.M.; S. Shehab and S.F. Majdalani (1979). Tomato yellow leaf curl, incidence yield losses and trasmission in Labanon. Phytopathogie. Zeitschrift 96: 263-267.
15. Matthews, R.E.F. (1991). Plant Virology, 3rd Ed., Academic Press, San Diago, p. 33.
16. Megahed, A.A.E. (2008). Effect of antiviral proteins produced by bacterial and fungal isolates on some viruses infected vegetable crops. M.Sc. Fac. of Agric., Ain Shams Univ. 188 pp,
17. Platt, S.G. ; Henriques , F. And Rand , L. (1979). Effects of virus infection on the chlorophyll content, photosynthetic rate and carbon metabolism of tolmiea menziesii physiol. Plantpathol. 16:351–365.
18. Sharma, T.R. (2003). Molecular diagnosis and application of DNA markers in the management of fungal, and bacterial plant disease. Indian Journal of Biotechnology 2: 99-109.
19. Sherif, A.E. and G.M. El-Habbaa (2000). Biochemical changes and specific protein synthesis related to fungal bacterial and viral infection in tomato plants. Annals of Agric., Sci. Moshtohor, 38: 169-177.
20. Staniulus, J.; L. Zitikaite; R. Jomantiene; L. Metspalu (ed.) and S. Mitt (2000). Reverse transcription polymerase transcription polymerase chain reaction (RT-PCR) for detection of Cucumber mosaic virus isolates. Proceedings of the international conference. Development of invironmentally friendly plant protection in the Baltic region, Tortu; Estonia. Transactions of the Estomia Agriculture University Agronomy, 209: 190-193.
21. Stegemann, H.; A Afify and N. Hussein (1985). Cultivar identificaton of dates by protein patterns. 2nd Inter. Sympo. Of Biochem. Approaches to identification of cultivar. J. Mol. Biol. 79: 237-248.
22. Studier, F.W. (1973). Analysis of bacteriophage T, early RNAs and proteins of slab gel. J. Mol. Biol. 79-273-248.
23. Tag El-Din, M.A.; H.A. Sharaf El-Dean and Kh.A. El-Dougdoug (2006). Application of protein related index and isozymes in defining Zucchini yellow mosaic potyvirus in infected squash plants. J. Biol. Chem. Environ. Sci. Vol. 1 (3): 575-594.
24. Wettstein, D. (1957). Chlorophyll-letate and submikroskopishe form vechsel der plastiden. Exp. Cell. Res. 12: 427-506.
25. Williams, J.; M. Hanafy; J. Rafulski and S. Tingey (1990). DNA polymorphisms by arbitrary primers are useful as genetic markers. Nucleic Acids. Res. 18: 6531-6535.
26. Wulff, E.G.; S. Torres and E.G. Vigil (2002). Protocol for DNA extraction fram potato tubers. Plant Mol. Biol. Reporter, 20: 187a-187e.

5/6/2011

Role of Multislice CT in Assessment of Carotid Stenosis

Mohammad S. Hassan and Mohsen G. Hassan

Department of Radiology, Faculty of Medicine, Ain shams University, Cairo, Egypt

Abstract: Objective: the objective of this study is to evaluate the role of multislice CT in evaluation of carotid stenosis. Method: forty five patients who had neurological symptoms suggestive of neurovascular disease and who had 60% stenosis on Doppler study were evaluated by multislice CT and DSA and the results were compared for each of the ninety carotid arteries. Results: Conventional angiograms and CT angiograms were in agreement in 71 arteries (79 %). Disagreement was found in the remaining eighteen arteries were CT angiogram showed the stenosis to be one category less in 13 arteries (14.4%) and one category more sever in 6 arteries (6.66%). No disagreement was found by more than one category. Sensitivity and specifity for detecting sever stenosis or occlusion was 85% and 97 %.

[Mohammad S. Hassan and Mohsen G. Hassan **Role of Multislice CT in Assessment of Carotid Stenosis.** Life Science Journal. 2011; 8(4): 753-756] (ISSN: 1097-8135). http://www.lifesciencesite.com.

Keyword: Role, Multislice CT, Assessment, Carotid Stenosis.

Introduction

Cerebrovascular Stroke is one of the leading causes of morbidity and mortality worldwide. Carotid artery stenosis is a frequent finding in the general population with a prevalence of 75% in men and 62% in women over 64 years as determined by ultrasonography. Atherosclerosis is by far the commonest cause of arterial stenosis and occlusion in clinical practice. Although atherosclerosis may affect the intracranial vessels themselves, 88% of patients with amaurosis fugax or hemispheric transient ischemic attacks have atherosclerotic disease at the carotid bifurcation(6)

Results of the North American Symptomatic Carotid Endoarterectomy Trial (NASCET); the European Carotid Surgery Trial (ECST); and the Asymptomatic Carotid Study (ECACAS) show the effectiveness of carotid endarterectomy for preventing stroke in patients with significant carotid stenosis. More recently, surgery has been suggested for high-grade asymptomatic severe stenosis. (6)

Conventional angiography was considered to be the standard method for evaluating stenosis of the internal carotid artery however, this technique is associated with a risk of thromboembolic event because of the use of an arterial catheter and because angiography outlines the luminal profile in limited angular projections and does not demonstrate the arterial wall or the plaque itself, it is unreliable in depicting ulceration. Furthermore, the results can cause under- or overestimation of the degree of stenosis. Moreover, the invasiveness of the technique adds risk, including stroke, making it impractical for the screening of asymptomatic patients or monitoring of disease progression. (3)

Recently, noninvasive techniques, such as computed tomographic (CT) angiography, have been developed. By using CT angiography, the cross-sectional luminal morphology can be accurately evaluated and the degree of stensis can be assessed .(5)

2. Patients and Methods

The study starts from August 2007 till July 2009 on forty five patient (90 arteries) suffering from stroke, TIA or other neurological symptoms suggestive of neurovascular disease. Those patients were referred from the Neurology Departments in Ain Shams University Specialized Hospital for Doppler sonography and were found to have significant disease in the form of a stenotic lesion causing more than 60% narrowing of lumen at site of stenosis compared to distal normal segment of the affected artery or doubling of velocity at site of stenosis.

Those patints were furtherly evaluated by CT angiograrhy and conventional angiography .CT scanning was performed with 120 kV and 250 mAs. The other imaging parameters were 1.6 mm section thickness, 3 mm collimation, 12-19 cm field of view, 3 mm/sec table feed, and 0.5 second gantry rotation time. Spiral scanning included the volume between the seventh cervical vertebra and the circle of Willis. The patients were asked to breathe evenly and smoothly without swallowing or moving.

The non-ionic iodinated contrast agent used is iopromide (Ultravist) 300 mg of iodine/mL; Bayer Health Care (formerly Schering AG). The volume for CT angiography was 120 mL, with a saline chaser bolus of 30 mL by using a flow rate of 3 mL/s with a 1.3-mm (18 gauge) cannula through the median cubital vein. The bolus-tracking method was used for assessment of the optimal time delay for CT scanning, to optimize contrast material enhancement in carotid arteries; the region-of-interest indicator was placed on a reference image obtained from the aorta.

Fig (1). Sever stenosis of proximal right ICA seen by conventional angiogram and axial source images of CT angiogram.

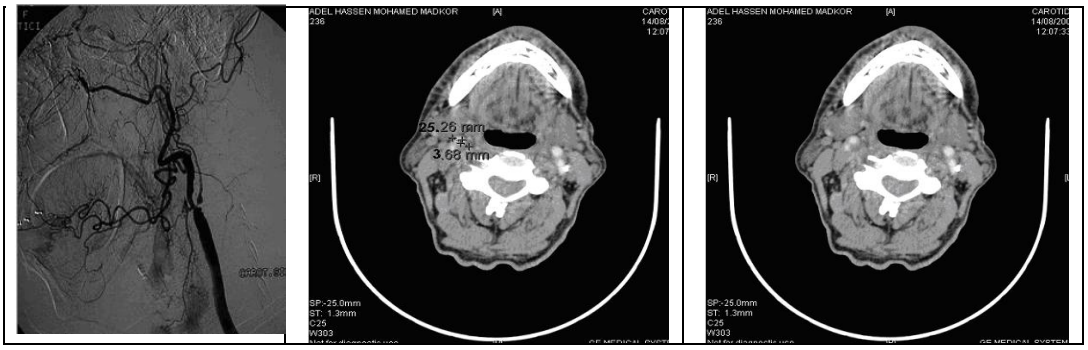

Fig(2): Moderate stenosis of right internal carotid seen by conventional angiogram and axial source images of CT angiogram.

Table (1). Compraison of degree of stenosis on Conventional and CT angiograms

Stenosis category at CT angiographgy				
Stenosis category at conventional angiography	Mild	Moderate	Sever	Occluded
Mild	35	4	0	0
Moderate	8	14	2	0
Sever	0	4	22	0
Occluded	0	0		0

Scanning started 5 seconds after enhancement in the aorta reached 70 HU.

A radiologist, blinded to patient data, interpreted the CTAs. Each artery was evaluated using magnified axial sections at a computer workstation. No three-dimensional reconstructions were used in evaluation. Using magnification, a measure (dmin) was taken of the diameter of the narrowest portion of the cervical internal carotid in the axial plane. This was compared with the maximal diameter (dnorm) of the cervical internal carotid artery distal to the carotid bulb at a location in which the imaging plane was orthogonal to the artery, the arterial walls were parallel, and where there was no arterial disease (figure 1, A and B). The degree of cross-sectional stenosis was calculated in percent as: percent stenosis =(1 - [narrowest ICA diameter/diameter normal distal cervical ICA])x 100%. analogous to the method used in the North American Symptomatic Carotid Endarterectomy Trial (NASCET). The stenosis was graded as mild = 0-19%diameter reduction, moderate = 20-69% sever = 70-99% and occlusion = 100%.

All conventional angiographic procedures were performed in an angiographic interventional room with high resolution C-arm - fluoroscopy, and digital subtraction angiography on GE medical system Advantx LCA Single Plane Angio-Cath Labs.

Angiograms were obtained by using a femoral approach. After arch aortograms with two oblique cervical views were obtained, selective catheterisation

of the common carotid artery was performed to evaluate the degree of common or internal carotid artery stenosis. The carotid artery studies included at least three projections (posteroanterior, lateral, and ipsilateral 45 ° oblique), and two images per second were acquired with a 512 x 512 matrix and a 20 cm field of view. For each projection, an 8 mL bolus of iohexol (Omnipaque 300) was injected at a rate of 4 mL/sec by using a power injector. The contrast material dose for the entire study did not exceed 150 mL.

The degree of stenosis was determined and was defined as the ratio of the perpendicular diameter of the stenosis at its narrowest point to the normal internal carotid artery diameter wall cranial to the stenosis. Percentage of ICA stenosis was calculated by using electronic digital callipers according to the method used in the North American Symptomatic Carotid Endarterectomy Trial (NASCET). With this technique, the single view with the highest degree of stenosis is used, and the minimal diameter of the residual lumen at the site of greatest stenosis is compared with the normal ICA wall beyond the arterial bulb where the arterial walls become parallel. The degree of stenosis on both CT and convetional angiography were compared for each of the 90 carotid artries,(FIG 1,2).

3. Results

Ninety carotid arteries were evaluated in forty five patients in this study .35 arteries were categorized as mildly stenotic on conventional and CT angiograms while 14 arteries were categorized as moderate stenosis on both conventional and CT angiograms and 22 were categorized as severely stenotic by both modalities . 8 arteries with mild stenosis on CT were found to be moderately stenotic on conventional angiogram and 4 arteries with moderate stenosis were found to have sever stenosis on conventional angiography.4 cases of mild stenosis on CT were found to be only midly stenotic on angiograpgy and 2 cases with sever stenosis on CT were only moderately stenotic on conventional angiograpgy. One case of total occlusion on angiography was found to be severly stenotic yet patent on CT. In retrospect, a “string sign” of pseudo-occlusion has been present on the angiography, in which case angiography was falsely positive for occlusion.

Thus conventional angiograms and CT angiograms were in agreement in 71 arteries (79 %). Disagreement was found in the remaining eighteen arteries were CT angiogram showed the stenosis to be one category less in 13 arteries (14.4%) and one category more sever in 6 arteries (6.66%). Sensitivity and specifity for detecting sever stenosis or occlusion was 85% and 97 %.

4. Discussion

Stroke is the third leading cause of severe disability and death in the Western world, creating an enormous economic burden on society. Ischaemic cerebrovascular events are often due to atherosclerotic narrowing at the carotid bifurcation. The severity of atherosclerosis may be determined by assessing both luminal stenosis and lesion morphology.(2)

Digital subtraction angiography (DSA) is the current standard of reference for the evaluation of carotid artery disease. DSA is a relatively expensive technique that uses numerous resources. So because of the costs and risks of this procedure, non-invasive techniques such as computed tomography (CT) have been developed. The importance of a reliable, non-invasive imaging modality is also related to the recent development of less invasive means than carotid endarterectomy to treat carotid artery occlusive disease with angioplasty and stenting. Relevant preoperative information can be achieved with CT. (2)

Although DSA remains the gold standard for assessment of carotid stenosis however, findings in previous reports showed that DSA has limited use for measuring the degree of arterial stenosis. Researchers in ex vivo studies who observed carotid artery specimens that were removed during carotid endarterectomy documented discrepancies between the cross-sectional lumina of the specimens and those depicted at DSA. These discrepancies are probably due to the wide variety of shapes of the lumen, although the morphologic features of the specimens can change during and after surgical removal because of shrinkage and manipulation. Researchers who conducted in vivo studies in which evaluation was performed with colour duplex US showed that DSA has a tendency to underestimate the degree of carotid stenosis .(5)

The introduction of multidetector-row CT (MDCT) scanners further advanced the revolution started by helical CT, and has had its greatest impact on CT angiography, with further decreasing scan time and routine slice thickness, as well as increasing volumetric coverage and improving multiplanar and three-dimensional reconstructions. (9)

MDCT has the advantage of being fast where the entire length of the CCA and ICA can be scanned in under 60 s (the extracranial ICA alone in less than 30 s), minimizing image misregistration from motion and breathing artifacts, and often reducing contrast requirements. Accuracy is also another advantage and CTA provides truly anatomic, non-flow dependent data with regard to length of stenoses and residual lumen diameters.Flow-dependent techniques such as MR angiography (MRA) and ultrasound (US) are not able to provide these data. It also allows the observations of bony structures. MDCT angiography provides excellent results even in pseudo-occlusions, which are difficult to

differentiate from total occlusion. CTA also has a lower rate of patient discomfort and has considerably lower risk of stroke and other vascular complications compared to conventional catheter arteriography.

Cumming and Morrow, in a study performed in 1994 (3) on Thirty-five patients referred for evaluation of carotid artery disease who were studied with conventional angiography followed by CT angiography 4-24 hr later, also found a high degree of correlation with catheter angiography. With CT angiography, all occluded Internal carotid arteries were correctly identified, and no arteries were wrongly classified as occluded. The degree of stenosis was overestimated on CT angiograms by greater than 10% in 16 arteries, especially when calcified atherosclerotic plaque was present. In some of these cases, the severity of the stenosis was underestimated on the conventional angiograms. All arteries, except one, with severe disease seen on conventional angiograms were correctly classified on the basis of the results of CT angiography.

Leclerc et al. in a study performed in 1995 (7) on 20 patients with atherosclerotic stenosis of the internal carotid artery, found a very good correlation between catheter and CT angiography, with correct classification of the degree of stenosis in 95% of the cases by axial sections.

Randoux et al., in 2001(8), performed a more complete study, evaluating several parameters, among which were the degree and length of stenosis, and the presence of plaque irregularities and ulcerations. The sensitivity and specificity of CT angiography for the demonstration of stenosis greater than 70% were, respectively, 100% and 100%, with a very good correlation for what regards the length of the stenosis. CT angiography showed more plaque irregularities and ulcerations than catheter angiography, in consideration of the limited number of views obtained with catheter angiography.

In a study by Bartlett et al., 2006(1), on 268 patients, it was concluded that there is a linear relationship between millimetre carotid artery stenosis diameter and derived percent stenosis as used in NASCET., allowing prediction of NASCET-type percent stenosis from directly millimetre carotid artery stenosis measured on CTA. Threshold values of 1.4 – 2.2 mm can be used to evaluate for moderate stenosis (50-69%) with sensitivity of 75% and specificity pf 93.8%. a carotid diameter measurement of 1.3 mm corresponds to 70% stenosis and can be used as a threshold value to test for sever carotid artery stenosis (> 70%) with a sensitivity of 88.2% and a specificity of 92.4%.

In our study we used the axial source images of CT angiography to measuare the degree of stenosis and the persent wes calculated using NASCET method. In 79 % the CT was similar in categorizing the degree of stenosis to conventional angiography and sensitivity and specifity were 85 and 97 % for detecting severs stenosis or occlusion.

Conclusion:

CT angiography is a reliable non invasive method for detecting and categorizing carotid stenosis with adequate specifity and sensitivity. Axial source images can provide enough data for measuring the stenosis.

Corresponding author
Mohammad S. Hassan
Department of Radiology, Faculty of Medicine, Ain shams University, Cairo, Egypt

References

1- **Bartlett ES., Walters TD., Symons S. and Fox AJ. (2006):**Quantification of carotid stenosis on CT angiography. AJNR Am J Neuroradiol., 27(1) :13-19
2- **Catalano C., Pediconi F., Napoli A., Danti M., Nardis P., and Bertoletti L.(2005):** Multidetector-Row CT Angiography: Carotid arteries. Multidetector-Row CT Angiography, Series: Medical Radiology, Subseries: Diagnostic Imaging, Springer, p: 69-87.
3- **Cumming MJ and Morrow IM (1994):** Carotid artery stenosis: a prospective comparison of CT angiography and conventional angiography. AJR Am J Roentgenol., 163: 517-23.
4- **Harley JD, Haynor DR. Angiography. In: Zeirler REHirai T., Korogi Y., Ono K., Murata Y., Takahashi M. , Suginohara K., and Uemura S., (2001):**Maximum Stenosis of Extracranial Internal Carotid Artery: Effect of Luminal Morphology on Stenosis Measurement by Using CT Angiography and Conventional DSA. Radiology; 221:802-809.
5- **Kono Y, Pinnell SP, Sirlin CB, Sparks SR, Georgy B, Wong W and Mattrey RF (2004):**Carotid arteries: Contrast-enhanced US Angiography-Preliminary Clinical Experience. Radiology, 230:561-568.
6- **Leclerc X, Godefroy O, Pruvo JP and Leys D (1995):** Computed tomography angiography for the evaluation of carotid artery stenosis. Stroke, 26:1577–1581
7- **Randoux B, Marro B, Koskas F, Duyme M, Sahel M, Zouaoui A and Marsault C (2001):** Carotid artery stenosis: prospective comparison of CT, Three-dimensional gadoliniumenhanced MR and conventional angiography. Radiology, 220: 179-85.
8- **Rydberg J, Buckwalter KA, Caldemeyer KS *et al.* (2000):**Multisection CT: scanning techniques and clinical applications. Radiographics 20:1787–1806
9- Surgical management of cerebrovascular disease. New York, NY: McGraw-Hill, 221-236.

11/25/2011

Reliable data delivery and energy efficient aware multi-path routing protocol in wireless sensor network

Amir Masoud Bidgoli [1], Mohammad Pajouhesh [2], Mehdi Ahmadi[3]

1. Department of Computer, North Tehran Branch, Islamic Azad University, Tehran, Iran
am_bidgoli@iau-tub.ac.ir
[2.] Department of Computer, Science and Research Branch, Islamic Azad University, Khuzestan, Iran
mo.pajouhesh@gmail.com
[3.] Islamic Azad University, Shahrekord Branch, Ardal Center, Iran
M_Ahmadi@iaushk.ac.ir

Abstract: Wireless Sensor Networks (WSNs) are generally energy and resource constrained. To provide energy efficiency while enhancing reliable delivery the packets, we propose a reliable data delivery and energy efficient aware multi-path routing protocol. The reliable delivery of the source to sink through the creation of safe routes and send data on these routes is done. The hybrid scheme is used to acknowledge received messages at every hop that larger percentages of packets are received at the sink. To reduce the energy consumption used the load balancing on multipath routs to avoid congestion and decrease delivery delay is given below, Also decreased overhead protocols spent time less for data transfer and increased network lifetime. Our protocol uses the residual energy, node available buffer size, and Signal-to-Noise Ratio (SNR) with influence hop count metric to predict the best next hop through the paths construction phase. We implemented our protocol using simulator for evaluating its performance. Results show that our protocol has significant improvement in packet delivery ratio and energy savings.
[Amir Masoud Bidgoli [1], Mohammad Pajouhesh [2], Mehdi Ahmadi . **Reliable data delivery and energy efficient aware multi-path routing protocol in wireless sensor network.** Life Science Journal. 2011; 8(4): 757-763] (ISSN: 1097-8135). http://www.lifesciencesite.com.

Keywords: Reliable data delivery, Multipath routing, Energy efficiency, Wireless sensor networks.

1. Introduction

Wireless Sensor Networks (WSNs) provide a distributed, sensing and computing platform for monitoring the environments, in which deploying conventional networks is impractical. Nodes in WSN are generally organized in a multi-hop topology and consist of one Base Stations (or sinks) and a very large number of sensor nodes scattered in physical space. Applications of sensor networks is very broad, they can be used to monitor the health, military environments[5], forest fire detection [9], habitat monitoring [10], and inaccessible areas But the very special characteristics of these networks like Limited energy, and bandwidth and topology changes cause difficulties in designing protocols for these networks. Therefore, in order to design a protocol should be considered in these networks than the networks had better performance in data delivery and Energy efficiency and increase network lifetime. One of the ways that energy efficiency is disperses traffic in multiple paths and reducing the overhead transmission of protocol.

In this paper we propose a protocol to balance load by sending data through the nodes in multiple routing and reliable data delivery to sink. Our protocol uses the residual energy, node available buffer size and Signal-to-Noise Ratio (SNR) with influence hop count metric to construction path And gives the priority to this paths and send data to sink uses these paths. The paths with highest priority have high delivery rate and high reliability so this protocol uses retransmission scheme to send data packets. To ensure delivery of packets uses NACK and ACK hybrid method. Using NACK and ACK hybrid method saves energy and reduces the transmission overhead and increases network lifetime.

The remainder of the paper is organized as follow: In Section 2, we describe our proposal. Section 3 presents the performance evaluation. Finally, we conclude the paper in Section 4.

2. Related work

Reliable data delivery and energy efficient in sensor networks is a challenging problem because of the scarce resources of the sensor node. Thus, this problem has received a significant attention from the research community, where many proposals are being made. Some routing proposals are surveyed in [1,8]. In this section we do not give a comprehensive summary of the related work, instead we present and discuss some proposals related to our protocol.

One of the early proposed routing protocols is the Sequential Assignment Routing (SAR) protocol [12].

SAR protocol is a multi-path routing protocol that makes routing decisions based on three factors: energy resources, QoS on each path, and packet's priority level. Multiple paths are created by building a tree rooted at the source to the destination. During construction of paths those nodes which have low QoS and low residual energy are avoided. Upon the construction of the tree, most of the nodes will belong to multiple paths. To transmit data to sink, SAR computes a weighted QoS metric as a product of the additive QoS metric and a weighted coefficient associated with the priority level of the packet to select a path. Employing multiple paths increases fault tolerance, but SAR protocol suffers from the overhead of maintaining routing tables and QoS metrics at each sensor node.

Recently, X. Huang and Y. Fang have proposed a multiconstrained QoS multi-path routing (MCMP) protocol [7] that uses braided routes to deliver packets to the sink node according to reliability and delay. The problem of the end-to-end delay is formulated as an optimization problem, and then an algorithm based on linear integer programming is applied to solve the problem. The protocol objective is to utilize the multiple paths to augment network performance with moderate energy cost. However, the protocol always routes the information over the path that includes minimum number of hops to satisfy the required QoS, which leads in some cases to more energy consumption.

EQSR(Energy efficient and Qos based routing Protocol) protocol has recently been proposed, to send the data real-time and non-real-time applications. EQSR uses the residual energy, node available buffer size, and signal-to-noise ratio to predict the next hop through the paths construction phase. Path with higher priority to send real time data is used. But the protocol suffers from the overhead of transmission. In some cases the paths are long which consume more energy, more delay and inappropriate use of nodes with high reliability.

3. Description of protocol

We assume N identical sensor nodes are distributed randomly in the sensing filed. All nodes have the same transmission range, and have enough battery power to carry their sensing, computing, and communication activities. The network is fully connected and dens (i.e. data can be sent from one node to another in a multihop bases). Each node in the network is assigned a unique ID and all nodes are willing to participate in communication process by forwarding data. Furthermore, we assume that the sensor nodes are stationery for their lifetime. Additionally, at any time, we assume that each sensor node is able to compute its residual energy (the remaining energy level), and its available buffer size (remaining memory space to cache the sensory data while it is waiting for servicing), as well as record the link performance between itself and its neighboring node in terms of signal-to-noise ratio (SNR).

2.1 Link cost function

The link cost function is used by the node to select the next hop during the path discovery phase. We use a cost function such as presented in [8,2] with some changes. Let Nx be the set of neighbors of node x. Then our cost function includes an energy factor, available buffer factor, and interference factor with appropriate weights (γ, β, α):

$$\text{Next hop} = \max \{\alpha E_{resd,y} + \beta B_{buffer,y} + \gamma I_{interference,xy}\} \quad (1)$$

Where, $E_{resd,y}$ is the current residual energy of node y, where $y \in N_x$, $B_{buffer,y}$ is the available buffer size of node y, and $I_{interference,xy}$ is the SNR for the link between x and y. In this cost function, we only consider the residual energy of node y but not x. Because node y consumes energy for data reception and transmission if it is selected as a next hop for node x. We do not consider node x, because whatever node y is, node x still needs to spend the same amount of energy on data transmission [8, 2].

2.2 paths discovery phase

The path discovery procedure is executed according to the following phases:

2.2.1 Hop count calculation and classification of neighbor nodes phase

Source broadcasts the advertisement message with the value of hop count has 0 to all neighbor nodes. On receiving this advertisement message, each node increments the hop count value that is specified in the message and store it in its neighbors table if it is lesser than the previous value. Then every node send advertisement message to all the neighbor nodes. When a node receives an advertisement message, it stores the sender of the packet with hop count as its neighbor. Thus each node maintains a list of its neighboring Nodes and hop count has added a number and if it is lesser than the previous value it is store as new hop count therefore a new advertisement sends to its neighbors. A node classifies its neighbors by comparing its hop count value with that of its neighbors as Follows:

A) If the hop count value of the neighbor node is less the current node, then this neighbor node is placed in a negative set. (Hs^{-})

B) If the hop count value of the neighbor node is greater he current node, then this neighbor node is placed in a positive set. (Hs^+)
C) If the hop count value of the neighbor node is the same, and then this neighbor node is placed in a zero set. (Hs^0)

2.2.2 Collect information of neighbor phase

Each sensor node broadcast a HELLO message to its neighboring nodes in order to have enough information about which of its neighbors can provide it with the highest quality data. Each sensor node maintains and updates its neighboring table during this phase. The neighboring table contains information about the list of neighboring nodes of the sensor node. The link quality field is expressed in terms of signal-to-noise ratio (SNR) for the link between any node and its neighbor. Fig. 1 illustrates the structure of the HELLO message.

Source ID	Residual Energy	Free Buffer	Link Quality

Fig. 1: Hello message structure.

Source ID	Dest . ID	Route ID	Route Cost	Hop Count

Fig. 2:PREQ message structure.

2.2.1 Primary Path discovery phase

After pervious phases each sensor node has enough information to compute the cost function for its neighbouring nodes. The sink node starts the route discovery phase. Sink node locally computes Preferred next hop between nodes that are in Hs^- or Hs^0 using the cost function and sends out a RREQ message to its most preferred next hop. Similarly, the preferred next hop node of the sink computes locally its most preferred next hop between nodes that are in Hs^- or Hs^0 in the direction of the source node, and sends out a RREQ message to its next hop, the operation continues until source node. Fig. 1 illustrates the structure of the RREQ message.

Route Cost field is calculated of sum the output cost function of each node. The Hop Count field specifies the sum of hop in any paths and each node that receives a PREQ, adds it's a unit. When PREQ message for every path received to the source by divided the Route Cost field value on the Hop-Count field value can be achieved a measure of priority for each path. This measure is an average measure of each route.

For example, in Fig.3 after sink send the PREQ message to node 2 as the highest priority, Node 2 between the nodes are in the set Hs^- or Hs^0 as{3,4,5}, selected the Node with higher priority and selected the node 4 And the PREQ message sends for it. Among the node 4 neighbours as {3,5,6,7}, Node 3 sees a higher priority But because it is node in set Hs^+. The node 4 has avoided send the PREQ message and the message send to another node with higher priority, which is located in the Hs^- or Hs^0 that is node 7. With this method the paths will not be long and reduced the delayed and energy consumption further did not prevent the construction of more paths.

2.2.2 Alternative Paths discovery phase

For the second alternate path, similar the Primary Path discovery, sink send out the PREQ message to the next preferred neighbour node which is located in the Hs^- or Hs^0, but to avoid the path of the shared nodes, each node is limited to accepting only one PREQ message. For those nodes that receive more than one RREQ message, only accept the first RREQ message and reject the remaining messages and INUSE message is sent in response.

For example, in Figure 3 the node 6 find the node 7 with higher priorities of sets Hs^- or Hs^0 and Node 6 sends the message PREQ to node 7, But node 7 in the first path is selected then node 7 responds to node 6 with an INUSE message and node 6 sends the PREQ message the next priority node as node 9. Node 9 accepts the message and continues the procedure in the direction of the source node.

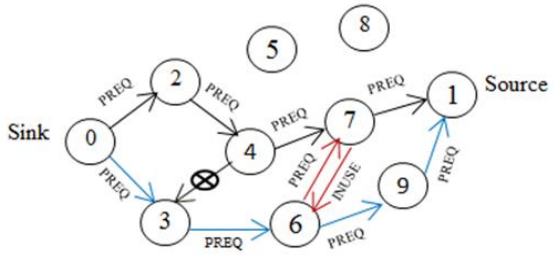

Fig. 3:Example of path discovery.

Primary Path
Alternative Path

ID	MS	Off	SA	DA	Residual Energy	Free Buffer	Link Quality

Fig. 4:ACK message structure.

2.3 Path refreshment

In order to save energy, we reduce the overhead traffic through reducing control messages. Therefore, instead of periodically flooding a KEEPALIVE message to keep multiple paths alive

and update cost function metrics, we append the metrics on the ACK message by attaching the residual energy, remaining buffer size, and link quality to the ACK message. Fig. 4 illustrates the structure of the ACK message.

2.4 Paths selection

Because all paths did not have high reliable delivery and some paths are made in the retransmission probability is very high. We need to select a set of paths from the N available paths to transfer the traffic from the source to the destination with a desired bound of data delivery given by α.

From the N paths didn't use the paths with the lowest priority that the packet retransmission probability is very high. To find the number of required paths, we assume that each path is associated with some rate Pi (i=1, 2… N) that corresponds to the probability of successfully delivering a message to the destination. Following the work done in [6], the number of required paths is calculated as:

$$K=X_{\alpha}\sqrt{\sum_{i=1}^{n} pi(1-pi)}+\sum_{i=1}^{n} pi \qquad (2)$$

Where x_{α} is the corresponding bound from the standard normal distribution for different levels of α. Table 1 lists some values for x_{α}. The best k paths that have higher priority are used to send packets, because the high priority routes are more reliable delivery of data.

TABLE 1. Some values for the bound α [6].

α	95%	90%	85%	80%	50%
x_{α}	-1.65	-1.28	-1.03	-0.85	0

2.5 Data transfer across multiple paths

Data transfer is done through three steps: distributed packets; data transmission; confirmation packet. The details are given below:

2.5.1 distributed packets

The packets distributed among the k paths as the equal number of packets to be assigned to all paths and Additional packets is given to the paths with higher priority. For example, for 78 arrival packets and k = 10 paths, in each paths ⌊ 78 / k ⌋ =7 packets are given and 8 paths ((78 mod k) = 8) of the k = 10 paths have an additional packet. Packets with Sequential ID are assigned to routes. Fig 5 shows the format of the packet.

Off and MS fields of packets have different usage. The Off field in the packets with a value 0 shows the first packet is assigned to each the paths. The MS field shows the last packet assigned to each the paths which In this case is 0. These values together with the ID field in the packet NACK or ACK, confirm or not confirm of each packet shows.

2.5.2 Data transmission

After the selection of a set of multiple paths, the source node can begin sending data to the destination along the paths. The traffic allocation mechanism used deal with how the data is distributed amongst the available paths. After the send data in the path if a node fails and it was not possible to send through that path, the most preferred next hop used for send data and continue through the most preferred next hop when the route updated at the earliest opportunity.

Fig. 5: Packet format

2.5.3 Confirmation packet

For confirmation the packets, we used a NACK and ACK hybrid scheme. In this scheme, the node transmits the packet to the next node, after a certain time if the NACK message with the ID packet received, sender try again to send the same packet, otherwise, it sends the next packet. In this scheme, the packet sent in the between sequence packets that should be send, if it is missing, The receiver nodes with sequence checking of packets received, will inform sender, with a NACK and the ID of lost packets if there was no sequence ID.

For the latest packet or single packets is used an ACK message, because after sending out the packets, there are no another packets that was sent and the packet sequence is compared. Also used to create the more reliability of the ACK message.

Only on the ACK message of hybrid scheme, the amount of energy remaining, the SNR and available buffer nodes give prior nodes. The advantage of this hybrid scheme is that has little overhead, and don't need to send response message for each packet and less energy is consumed. It should be noted that the messages NACK, ACK packets to determine and inform the sender to confirm or not confirm, all the fields ID, MS, Off is used. Fig. 6 illustrates the structure of the NACK message.

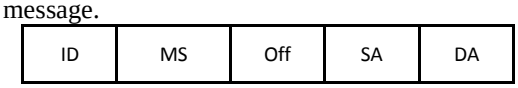

Fig. 6: NACK message structure.

3. PERFORMANCE EVALUATION OF PROTOCOL

We evaluate the performance and validate the effectiveness of our protocol through simulation. In this section, we describe the performance metrics, simulation environment and simulation results. We used NS-2 to implement and conduct a set of simulation experiments for our protocol and do a comparative study with the MCMP protocol [7].

Our simulation environment consists of 200 sensor nodes randomly deployed in a field of 500 m * 500 m. All nodes are identical with a radio transmission range set to 25 m. The sink node is situated at the upper right corner of the simulation field, and the source node is situated on the left bottom corner. Table 2 shows the simulation parameters [2].

We investigate the performance of our protocol in a multichip network topology. The metrics used in the evaluation are the energy consumption, delivery ratio and average delay. The average energy consumption is the average of the energy consumed by the nodes participating in message transfer from source node to the sink node. The delivery ratio is the number of packets generated by the source node to the number of packets received by the sink node. The average delay is the average time required to transfer a data packet from source node to the sink node. We study the impact of packets generation rate on these performance metrics. Simulation results are averaged over several simulation runs.

TABLE 2. Simulation Parameters [2]

Network field	500m*500m
Number of sensors	200
Number of sinks/number of source	1/1
Transmission range	25m
Packet size	1024Bytes
Sub-packet size	256Bytes
Transmit power	15mv
Receive power	13mw
Idle power	12mw
Sleep mode Power	0.015mw
Initial battery power	100J
MAC layer	IEEE 802.11
Max buffer size	256 K-bytes
Buffer threshold	1024byte
Weights(γ, β, α) respectively	3/2/3
Simulation time	1000s

3.1 Impact of packets generation rate

In this experiment, we change the packets arrival rate at the source node from 10 to 100 packets/s. We compare our protocol with the MCMP protocol.

3.2 Packet delivery ratio

Another important metric in evaluating routing protocols is the average delivery ratio. Fig. 7 shows the average delivery ratio of our protocol and MCMP protocol. Obviously, our protocol outperforms the MCMP protocol.

Our protocol for use the ACK, NACK hybrid scheme and assurance of packet delivery in every hop, packets with high delivery rates to destinations delivers. Creating paths with high reliability and distribution packets on the routes to avoid congestion and packet loss is very effective in enhancing the delivery rate.

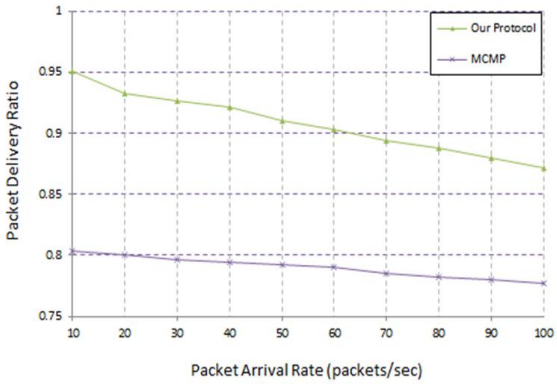

Fig. 7: Packets delivery ratio.

3.3 Average energy consumption

Fig. 8 shows the results of energy consumption. In the figure we see that our protocol has better performance than the other protocol. This is because the overhead of our protocol is lower than the MCMP protocol and also due to the use of load balancing on multi routing and reduce congestion on a route. In also this protocol to send the packet loss from the previous node is performed and energy consumed to reach the node, not wasted.

Using a combination of ACK, NACK is effective in reducing energy consumption. In this hybrid scheme, for each packet is not required to send a response packet. In the protocol because routes have been created with effect the number of hops and shorter routes have been created, packet transmission, consumes less energy.

3.4 Average end-to-end delay

The average packet delay of our protocol and MCMP protocol as the packet arrival rate increases is illustrated in Fig. 9. In this experiment, we change the packet arrival rate at the source node, and measure the delay packets. Due to the construction of paths with effect the hop count, and using a combination of NACK Our protocol delay is less than MCMP protocol.

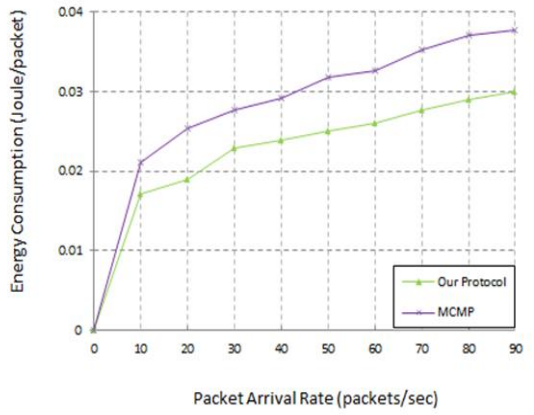

Fig. 8: Average energy consumption

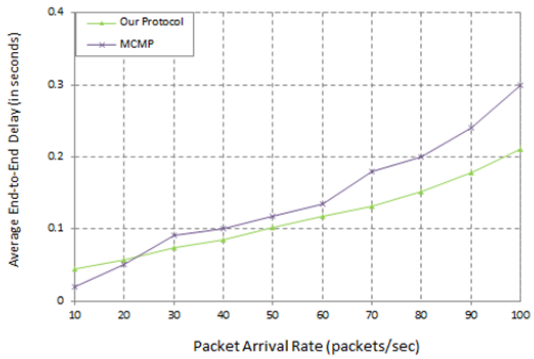

Fig. 9: Average end-to-end delay.

4. Conclusion

In this paper, we have presented our protocol; a reliable data delivery and energy efficient aware multi-path routing protocol designed specifically for wireless sensor networks to provide reliability data delivery and energy efficient. we used a NACK and ACK hybrid scheme. This method is very effective in energy efficiency. Our protocol uses the residual energy, node available buffer size, and signal-to-noise ratio with influence hop count metric to predict the next hop through the paths construction phase. Our protocol distributed packets over multiple paths to reduce overhead transmission.

Through computer simulation, we have evaluated and studied the performance of our routing protocol under different network conditions and compared it with the MCMP protocol. Simulation results have shown that our protocol achieves more energy savings, lower average delay and higher delivery ratio than the MCMP protocol.

As a future work, we are intended to deeply analyses the performance of our protocol and study the impact of the network size, path length, and buffer size on the performance metrics.

Corresponding Author:
Mr. Mohammad Pajouhesh
Department of Computer, Science and Research Branch, Islamic Azad University, Khuzestan, Iran
E-mail: mo.pajouhesh@gmail.com

References

[1] Kemal Akkaya, Mohamed Younis, A survey on routing protocols for wireless sensor networks, Journal of Ad Hoc Networks 3 (3) (2005) 325-349.

[2] J.B. Othman, B. Yahya, Energy efficient and QoS based routing protocol for wireless sensor, Journal of Parallel Distrib. Comput. 70 (2010) 849-857

[3] L.N. Joseph1, G.V.Uma2, Reliability Based Routing in Wireless Sensor Networks, IJCSNS VOL.6 No.12, December 2006

[4] K. Akkaya, M. Younis, An energy aware QoS routing protocol for wireless sensor networks, in: The Proceedings of the 23rd International Conference on Distributed Computing Systems Workshops, Providence, RI, USA, May 19-22, 2003, pp. 710-715.

[5] T. Bokareva, W. Hu, S. Kanhere, B. Ristic, N. Gordon, T. Bessell, M. Rutten, S. Jha, Wireless sensor networks for battlefield surveillance, in: Proceedings of The Land Warfare Conference, LWC Brisbane, Australia, October 24-27, 2006.

[6] S. Dulman, T. Nieberg, J. Wu, P. Havinga, Trade-off between traffic overhead and reliability in multipath routing for wireless sensor networks, in: The Proceedings of IEEE Wireless Communications and Networking Conference, WCNC-2003, vol. 3, New Orleans, Louisiana, USA, March 16-20, 2003, pp. 1918-1922.

[7] X. Huang, Y. Fang, Multiconstrained QoS multipath routing in wireless sensor networks, Journal of Wireless Networks 14 (4) (2008) 465-478.

[8] Ye Ming Lu, Vincent W.S. Wong, An energy efficient multipath routing protocol for wireless sensor networks, International Journal of Communication System 20 (7) (2007) 747-766.

[9] M. Hefeeda, M. Bagheri, Wireless sensor networks for early detection of forest fires, in: The Proceedings of IEEE International Conference on Mobile Adhoc and Sensor Systems, MASS-2007, Pisa, Italy, October 8-11, 2007, pp. 1-6.

[10] A. Mainwaring, J. Polastre, R. Szewczyk, D. Culler, J. Anderson, Wireless sensor networks for habitat monitoring, in: The Proceedings of the 1st ACM International Workshop on Wireless Sensor Networks and Applications, ACMWSNA, Atlanta, Georgia, USA, September 28-28, 2002, pp. 88-97.

[11] D. Chen, P.K. Varshney, QoS support in wireless sensor networks: a survey, in: The Proceedings of the International Conference on Wireless Networks, ICWN-2004, Las Vegas, Nevada, USA, June 2004, pp. 227-233.

[12] K. Sohrabi, J. Pottie, Protocols for self-organization of a wireless sensor network, IEEE Personal Communications 7 (5) (2000) 16-27

[13] Stephen Muller, Rose P. Tsang, Dipak Ghosal, Multipath routing in mobile ad hoc networks; issues and challenges, in: Performance Tools and Applications to Networked Systems, in: Lecture Notes in Computer Science (LNCS), vol. 2965, Springer, 2004, pp. 209-234, ISBN:3540219455.

[14] K. Srinivasan, M. Ndoh, H. Nie, H. Xia, K. Kaluri, D. Ingraham, Wireless technologies for condition-based maintenance (CBM) in petroleum plants, in: The Proceeding of the International Conference on Distributed Computing in Sensor Systems, DCOSS'05, (Poster Session), Marina del Rey, CA, USA, June 30-July 1, 2005, pp. 389-390.

[15] Jack Tsai, Tim Moors, A review of multipath routing protocols: from wireless ad hoc to mesh networks, in: The Proceedings of ACoRN Early Career Researcher Workshop on Wireless Multihop Networking, Sydney, Australia, Jul. 17-18, 2006.

[16] Kui Wu, Janelle Harms, On-demand multipath routing for mobile ad hoc networks, in: Proceedings of 4th European Personal Mobile Communication Conference, EPMCC, Vienna, Austria, Feb 20-22, 2001.

[17] Zhiqiang Xiong, Zongkai Yang, Wei Liu, Zhen Feng, A lightweight FEC algorithm for fault tolerant routing in wireless sensor networks, in: The Proceedings of International Conference on Wireless Communications, Networking and Mobile Computing, WiCOM-2006, Wuhan, China, September 22-24, 2006, pp. 1-4.

[18] N. Xu, S. Rangwala, K. Chintalapudi, D. Ganesan, A. Broad, R. Govindan, D. Estrin, A wireless sensor network for structural monitoring, in: The Proceedings of the 2nd International Conference on Embedded Networked Sensor Systems, Baltimore, MD, USA, November 03-05, 2004, pp. 13-24.

19. Bashir Yahya, Jalel Ben-Othman, Towards a classification of energy aware MAC protocols for wireless sensor networks, Journal of Wireless Communications and Mobile Computing 9 (12) (2009) 1572-1607.

[20] M. Younis, M. Youssef, K. Arisha, Energy aware routing in cluster based sensor networks, in: The Proceedings of the 10th IEEE International Symposium on Modeling, Analysis, and Simulation of Computer and Telecommunication Systems, MASCOTS-2002, Fort Worth, Texas, USA, October 11-16, 2002, pp. 129-136.

[21] Y. Zhang, M. Fromherz, Message-initiated constraint-based routing for wireless adhoc sensor networks, in: The Proceedings of the First IEEE Consumer Communication and Networking Conference, CCNC-2004, Las Vegas, Nevada, USA, Jan 5-8, 2004, pp. 648-650.

[22] Y. Zhang, M. Fromherz, L. Kuhn, Smart routing with learning-based QoS-aware routing strategies. in: The Proceedings of First Workshop on QoS Routing, Barcelona, Spain, October 1st, 2004.

11/25/2011